REPORT DOCUMENTATION PAGE

AFRL-SR-BL-TR-00-

0370

1. REPORT DATE (DD-MM-YYYY)	2. REPORT TYPE	3. DATES COVERED (From - To)
6-30-2000	Unclassified. - Final	10/1/97 - 3/31/00

4. TITLE AND SUBTITLE
Chromatographic Isolation of the Polymer Diazoluminomelanin and Related Components

5a. CONTRACT NUMBER

5b. GRANT NUMBER
F49620-98-1-0071

5c. PROGRAM ELEMENT NUMBER

6. AUTHOR(S)
Joel Timothy Smith, Ph.D.

5d. PROJECT NUMBER

5e. TASK NUMBER

5f. WORK UNIT NUMBER

7. PERFORMING ORGANIZATION NAME(S) AND ADDRESS(ES)
Southeastern Oklahoma State University
Dept. of Physical Science
5th and University St.
Durant, OK 74701

8. PERFORMING ORGANIZATION REPORT NUMBER
USAF/CE

9. SPONSORING / MONITORING AGENCY NAME(S) AND ADDRESS(ES)
AFOSR/NL
801 NORTH RANDOLPH STREET
ARLINGTON, VA 22203-1977

10. SPONSOR/MONITOR'S ACRONYM(S)

11. SPONSOR/MONITOR'S REPORT NUMBER(S)

12. DISTRIBUTION / AVAILABILITY STATEMENT
APPROVED FOR PUBLIC RELEASE: DISTRIBUTION UNLIMITED

13. SUPPLEMENTARY NOTES

14. ABSTRACT
The specific objective of this project has been to provide chemical characterization towards the polymer diazoluminomelanin (DALM) and related products, which have proven to be of significant interest to the USAF. Our method of characterization of the DALM polymer has been focused initially on the sole characterization of the polydiazotized-3-amino-L-tyrosine (p-DAT) polymer. The initial aqueous reaction between 3-amino-L-tyrosine (3-AT) and nitrous acid was studied in detail along with several analogs of 3-AT. The methodologies used to characterize this polymer and related analog polymers included, but was not limited to, CE, CE-MS, HPLC, ESI-MS, APCI-MS, HPLC-ESI-MS, MALDI-TOF-MS, 1H-NMR, 13C-NMR, ESR, DCS,, UV/Vis, IR, Pyrolysis-GC-MS and elemental analysis. Two analog polymers, p-HAHA and p-Tyr, with both show similar properties were characterized also. Our findings indicate that p-DAT is a heterogeneous polymer consisting of multiple modes of polymerization. The polymer is a stable radical even at RT. Based on our current findings, the polymer contains azo-, azoxy, ether, and phenylene linkages. The predominance of each type of linkage was not established.

15. SUBJECT TERMS
Polymer characterization

16. SECURITY CLASSIFICATION OF: Unclassified			17. LIMITATION OF ABSTRACT	18. NUMBER OF PAGES	19a. NAME OF RESPONSIBLE PERSON
a. REPORT	b. ABSTRACT	c. THIS PAGE			Dr. Tim Smith
Unclas	Unclas	Unlcas		155	19b. TELEPHONE NUMBER (include area code) 580 745 2444

Final Technical Report

October, 1997 - March, 2000

Submitted by
Dr. Tim Smith, P.I.

Southeastern Oklahoma State University
Department of Physical Sciences
Durant, OK 74701

Chromatographic Isolation of the Polymer Diazoluminomelanin and Related Components

Grant: F49620-98-1

Objective

The objectives of this project have not changed. The specific objective as stated in the original research proposal is to develop chromatographic methodologies to provide insight towards the polymer diazoluminomelanin (DALM) and related products, which have proven to be of significant interest to the USAF. This project was to be performed in conjunction with Dr. John R. Wright at this institution whom had been characterizing reaction products associated with DALM. With the loss of funding for JRW, our role of the project was expanded to include all efforts to gain further insight into the chemical characterization of the polymer.

Our method of characterization of the DALM polymer has been focused initially on the sole characterization of the polydiazotized-3-amino-L-tyrosine (p-DAT) polymer, and if successful we would proceed to the addition of luminol. There have been many preparation protocols developed for the formation of DALM including biological and synthetic methods. When we submitted the proposal for this project, our group's effort was to be in collaboration with Dr. John Wright's efforts at this institution. We have relied solely on the protocols provided by his previous research for the synthetic production of p-DAT and DALM.

Initial Reaction of 3-AT

Our first studies examining the 3-AT reaction made it clear that this has the potential to be a very complex system of products. Figure 1 is an electropherogram of the reaction products after precipitation with acetone. The polymeric species elute around 8-10 min under these conditions, however CE can resolve more than 40 components of this reaction mixture. In order to fully understand this system, we must know what each of these products identity and secondly determine which ones are active in the formation of the polymer and to what extent. We must consider that not only the aromatic amine is a site for potential polymeric linkage, but also the α-amine can play a critical role as well. If we look at the potential reactions that can occur, we get a complex picture to match our experimental findings. The following reaction schematic shows a number of products that can form under ideal condition, i.e., equal equivalence of nitrite and at a cooled temperature. Our reaction calls for 5.5 equivalences of nitrite and is performed at room temperature.

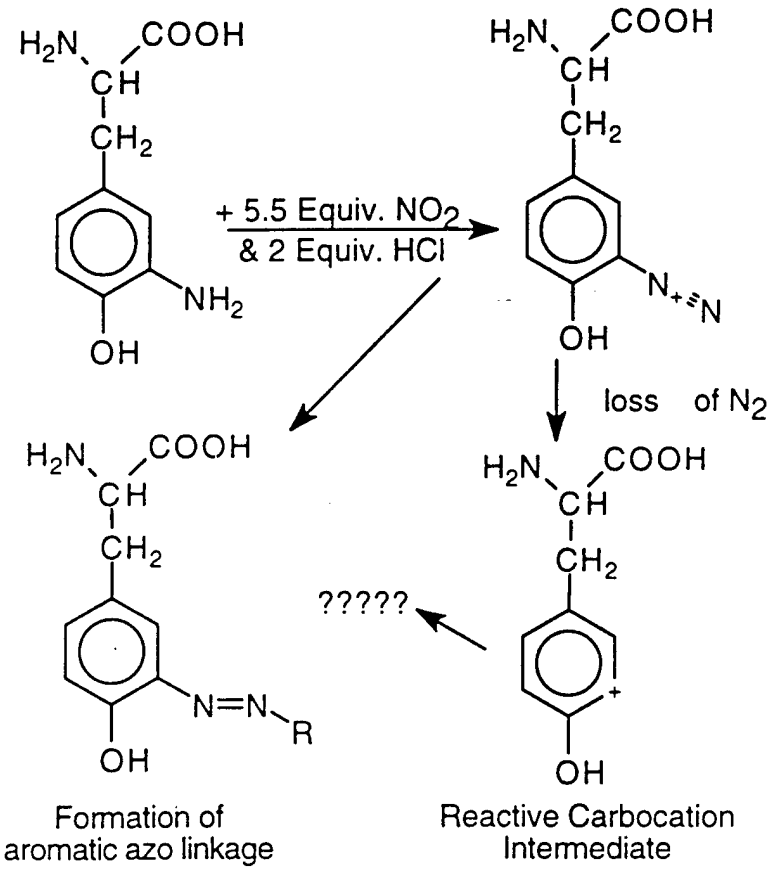

First, only consider the aromatic amine. Upon reaction with nitrous acid, the diazonium intermediate should be formed which is unstable and quite reactive. Conventional uses of such diazonium salts have been to form aromatic azo-type linkages in pigment and dye chemistry. When molecular nitrogen is evolved, the reactive carbocation is formed which is then open for attack by a nucleophile. The literature describing the potential types of products is quite overwhelming. The carbocation could be attached yielding the addition of $-NO_2$, -Cl, -OH, or -NO, which all exist in varying concentration in our reaction matrix. We also know that the aromatic ring itself is subject to nitration as our analog studies have indicated.

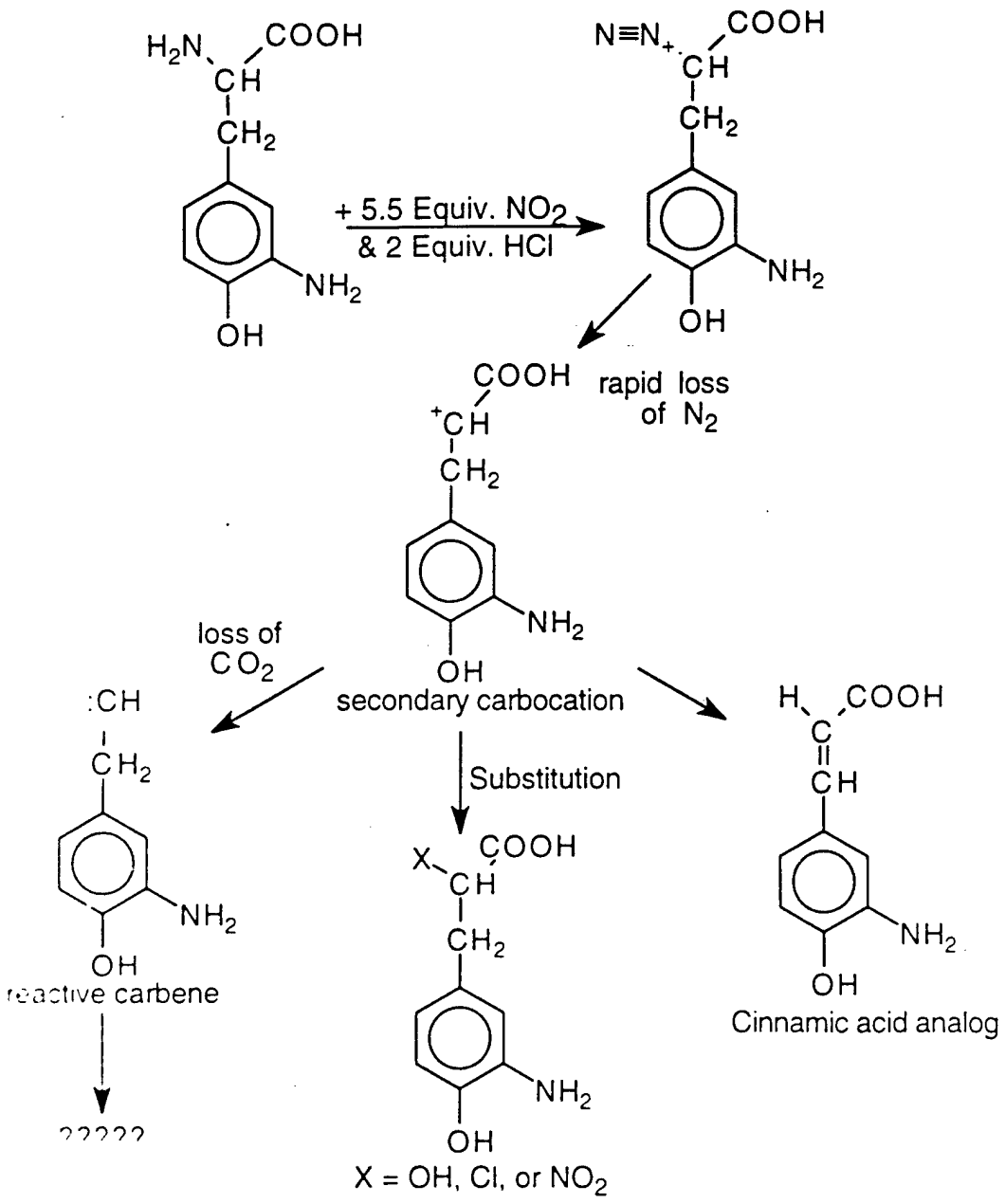

When we consider only the aliphatic amine, the initial product should be the aliphatic diazonium, which will be very unstable at room temperature, decomposing to yield the carbocation. Loss of CO_2 would yield a carbene. Loss of hydrogen would yield a cinnamic acid derivative. We must also consider that any of these potential intermediates could react with other intermediate to form "unusual" species.

To get a better understanding of the potential reactions that occur and attempt to simplify our experimental picture, we examined a large number of analogs. We studied analogs

with only α-amines or aromatic amines. We have limited this report to the analog data that we feel is potentially significant to the formation of the polymeric species of interest.

Alanine

The amino acid alanine was reacted as a model compound to monitor α-amino group activity under identical reaction conditions. Alanine is among the simplest potential model compounds.

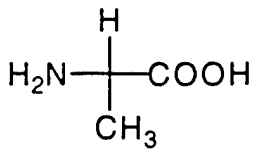

Alanine
MW = 89

The deamination of α-amino acids by nitrous acid has been the basis of the classic Van Slyke determination for the quantification of amino acids developed in the 1910's [1, 2]. This methodology was described by the following equation for glycine:

$$H_3N^+ - CH_2 - COO^- + HNO_2 \rightarrow HO - CH_2 - COOH + N_2 + H_2O$$

Closer examination of this test revealed that "too much" nitrogen was evolved plus the addition of CO_2. The deamination equation given above is an incorrect/incomplete description of the total reactions occurring. Researchers later studied this reaction and suggested the reaction was indeed much more detailed and that a vast array of reaction products may be observed [3]. However, these studies were prior to modern spectroscopic techniques and many of the products were speculation.

We performed the reaction in aqueous solution with 5.5 equivalences of nitrite and 2 equivalences of HCl, similar to that of the 3-AT reaction. The reaction yielded no colored products and appeared much like that of the starting material. A comparison between the ^1H NMR of alanine and the reaction product, Fig 2 and 3, indicates that indeed something did occur. The spectra for alanine indicate the methylene doublet at 2.2 ppm and the α-proton quadruplet at 4.5 ppm. The reaction product indicates that the methyl doublet at 2.2 ppm no longer exist; however, two new doublets at 2.7 and 2.9 ppm

appear. A singlet at 3.2 ppm has appeared. Two new quadruplets have appeared at 5.4 and 5.6 ppm. There are trace indications of other products in the proton spectra as well. The ^{13}C spectra for alanine reveals the methyl at 16.5 ppm, the α-carbon at 51.2 ppm, and the carboxylate carbon at 176 ppm, see Fig. 4. The ^{13}C spectra of the reaction product is more difficult to interpret, see Fig 5. The spectra of the reaction product shows 3 methyl carbons at 21.6, 23.3, and 21.6 ppm. The α-carbons appear at 58.7 and 69.6 ppm (one is potentially lost in the MeOH-d_4 signal). Three carbonyl at appear 177.9, 180.8, and 182.9 ppm. This is consistent with predicted substitutions of different anions upon deamination forming the carbocation. Predicted substitutions include -Cl, -OH, and -NO_2. This data is also in agreement with the three UV absorbing peaks observed in CE.

We also examined the alanine reaction products using HPLC-ESI-MS. Our first attempt was using negative ion mode. Figure 6 illustrates the observed chromatographs for the 214 nm UV signal and MS. Most of the reaction products are very polar and elute at or near the void peak. Extracting the 88 m/z peak reveals that no alanine remains. In addition, the predicted hydroxyl- and chloro- substituted compounds were observed at 89 and 107/109 m/z, respectively. There was no signal detected for the nitro-substituted alanine. A signal for 71 m/z was observed which can be attributed to the formation of a double bond between the α- and β-carbons. The type of elimination is suggested in some text.

Analysis of the reaction products in the positive ion mode surprisingly gave a number of strong signals, see Fig. 7. These species are likely decarboxylated or contain multiple amines in order to yield the positive ions observed. Very weak signals were observed at 91 and 73 m/z which correspond to the hydroxylated and elimination products observed in the negative ion spectra. Much to our surprise, higher mass peaks were also observed at 211, 268, 320, 325, 377, 382, 434, 439, 469, and 491 m/z. Initially, we could see no correlation of an oligomeric series in these peaks. While in the preparation of this report, we recognized that every other signal varies by 57 m/z. Figure 8 illustrates the extracted ion chromatogram for the series at [320 + (57) x n] and Figure 9 is for the series [211 + (57) x n]. This 57 repeat unit was quite puzzling and indicated a significant change in the structure of alanine was occurring in the reaction.

The 57 m/z repeat unit does not contain chlorine as indicated by the lack of isotopes in the mass spectra. This means the repeat unit may contain C, H, N, and/or O. A simple

mass calculator gives the following possible imperial formulas: $C_2H_1O_1$, $C_2H_5N_2$, $C_2H_3N_1O_1$, $C_3H_5O_1$, and $C_3H_7N_1$. Of these possible formulas, only $C_2H_3N_1O_1$ seems to be feasible due to valances. Possible structures would be:

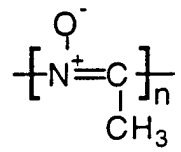

57 repeat unit

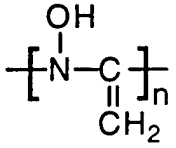

57 repeat unit

A structure similar to the left was proposed by Austin as a polymer product resulting from the deamination of glycine with nitrous acid [3]. However the reaction mechanism proposed by Austin is derived through methylnitrolic acid, which is not feasible from the structure of alanine. The proton NMR indicated the presence of a singlet at 3.2 ppm, which can not be explained by a substitution or elimination reaction. The singlet supports the structure on the left and not the oxime type structure suggested on the right. The repeat unit was not observed below 211 or 320 m/z for the two series and seems to go to higher masses. As indicated by the differences in retention times on the HPLC, these are 2 discrete series of oligomers with 2 different initial head groups but the same repeat unit. The polymers are likely to contain a strongly basic group due to their strong presence in the positive ion spectra and lack of in the negative ion spectra. A brief literature search on such an oligomer yielded no results but a comprehensive search was not performed.

Key questions lie in the fact that since this observed polymer is not a strong UV-absorbing species, is it present at significantly higher concentrations with respect to the other species formed in the alanine reaction? Unfortunately, ESI-MS signal is very structure related to the observed ionization efficiency, and, therefore, it is not a good indicator of product yield unless standards are available.

Phenylalanine

The amino acid phenylalanine (Phe) was also chosen as a model monomer to test this reaction. It adds the aromatic functionality to the reaction without the aromatic amine or hydroxyl group found in 3-AT.

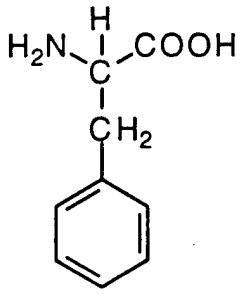

Phenylalanine
MW = 165

Phenylalanine was reacted under the same reaction conditions as 3-AT with 5.5 and 2 equivalence of NO_2^- and HCl, respectively. Once again, the reaction product was largely colorless, and a white precipitate formed that appeared to be the starting material, Phe. We would expect to see the α-hydroxy- and α-chloro-Phe formed as in the alanine reaction. The HPLC chromatogram shows that a complex mixture of reaction components has been formed, which have a good absorbance at 214 nm, see Fig. 10. However, when the products were examined at 405 nm, none produced the 405 nm absorbance associated with many of the 3-AT products. In fact, none of the products had a significant absorbance above 300 nm. By examining the MS signal, we see the peak at 6.6 min in the 214 nm trace contains the elimination product, 147 m/z; the α-hydroxy-Phe, 165 m/z; and the α-chloro-Phe; 183/185 m/z, see Fig. 11.

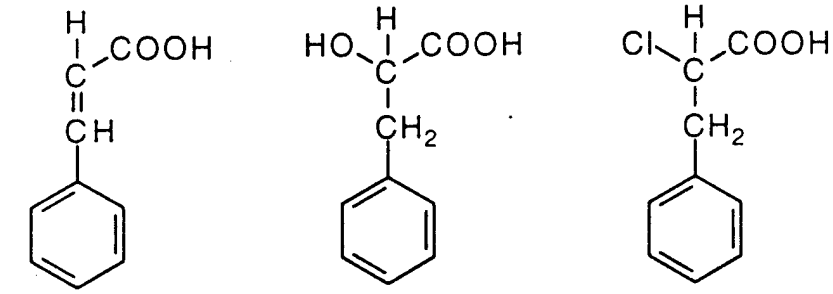

MW = 148 MW = 166 MW = 184 / 186

No signal was observed for the α-nitro-Phe, 194 m/z, or nitrated aromatic products of the hydroxy and chloro substituted species, 210 and 228 m/z. These products much followed the predicted reaction products observed from the alanine system. Addition products are also observed that are more retained on the column. The peak at 15 min corresponds to an unidentified component having a mass of 242, see mass spectra in Fig. 12. This component appears to contain one Cl atom as indicated by the 241/243 isotope pattern.

Four other components eluting in the 16-18 min range also give strong MS signals. Interestingly, these 4 species also have identical mass spectra, suggesting that they may be positional isomers of one type. These species all have a 313 m/z signal, see Fig 13. This corresponds to products with mass of 314 which means it contains either none or two nitrogen atoms. The only reasonable structure that we can assign to such a mass in given below:

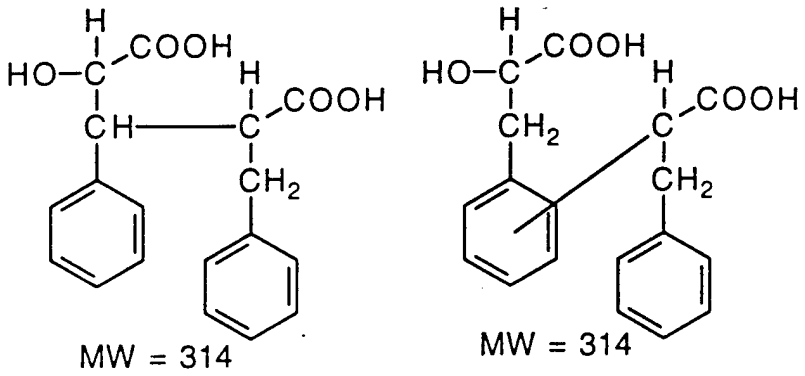

These products could form from the carbocation attacking either the methylene carbons or the *o*-, *m*-, or *p*- positions of the aromatic ring. A mass spectra for the products is shown in Fig. 14. The fragments observed at 165 and 147 are in agreement with the proposed structures.

To attempt to identify additional components and confirm proposed ones, the Phe reaction product was also examined in positive ion mode. The chromatography is identical, however several of the products yielded better signals in the MS in positive mode. Figure 15 shows the 214 nm trace and the TIC. All of the products observed in the (-)-mode were acids so it is doubtful that they will be observed in the (+)-mode as $[M+H]^+$ ions. That was indeed the case. The 7 min peak corresponding to the α-hydroxy-Phe yielded only a 121 m/z peak which would correspond to the loss of CO_2H yielding the cation radical. The signal at 9.0 min yields 91 m/z, due to a benzyl cation, and is likely only a fragment ion. The 314 mass isomers proposed above are also seen in the MS as $[M+H]^+$, $[M+Na]^+$, and $[M-H+2Na]^+$, see Fig. 16.

The Phe reaction also yielded a series of products that could be extracted into CH_2Cl_2. These components were also analyzed using HPLC-MS, but with APCI instead of ESI. The 214 nm trace shows that again a complex mixture of products is observed that seem

unrelated to the aqueous soluble components, see Fig 17 (note that this chromatogram was obtained under different chromatographic conditions and can not be correlated with the aqueous soluble components). The TIC gives peaks for products at 166, 225, 354, 285, and 382 m/z, see Fig 18. Their corresponding spectra are attached, Figure 19a-d, however no further attempt was made to identify these components.

Unfortunately, the Phe reaction demonstrates the complexity of the products that can exist with the addition of the aromatic ring. It is important to note that no repeat unit analogous to that observed with alanine was detected.

Tyrosine

We examined tyrosine (Tyr) as a potential analog as well. It introduces the phenolic group into the reaction, which could potentially be reactive.

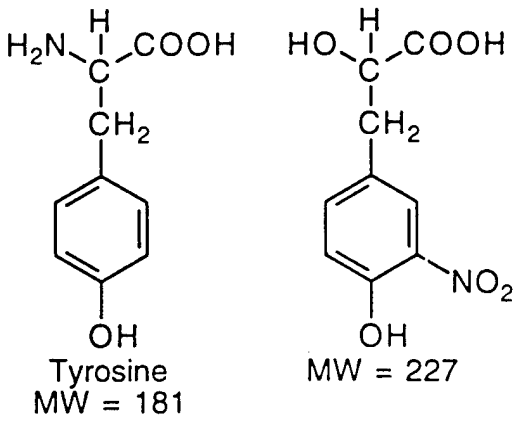

The tyrosine reaction products seem to only add complexity to a complex picture. Figure 20 illustrates a 214 nm CE electropherogram obtained from the tyrosine reaction product after the addition of acetone. There are two predominant species observed, but a large number of others as well. When we attempted to analyze this product with CE-MS, only a small fraction of the components yield MS signals, see Fig. 21. The extracted ion chromatograms (EIC) reveal the α-hydroxy-Tyr at 181 m/z, the elimination product at 165 m/z, and a nitro-substituted-α-hydroxy-Tyr at 226 m/z (see structure above). No signal was observed for the chlorinated species. These species were expected, but no coupling reactions were observed that yielded higher MW species.

When analyzed in the HPLC-MS, the tyrosine reaction products gave a very good separation at 254 nm, however, little signal was observed in the MS, see Fig. 22. This MS signal at 16.5 min corresponds to the nitro-substituted-α-hydroxy-Tyr at 226 m/z. The P.I. feels that incorrect MS parameters are likely the reason for the lack of MS signal.

3-Nitrotyrosine

A similar analog examined was 3-nitrotyrosine. This analog proved to be as reactive as tyrosine. The major reaction product proved to be the α-hydroxy-3-nitrotyrosine. The CE trace revealed that a complex mixture of products is observed, but difficulty remained in producing ions for the MS.

DOPA

DOPA was chosen as an analog because it has similar electron density on the aromatic ring as 3-AT but without the reactive aromatic amine.

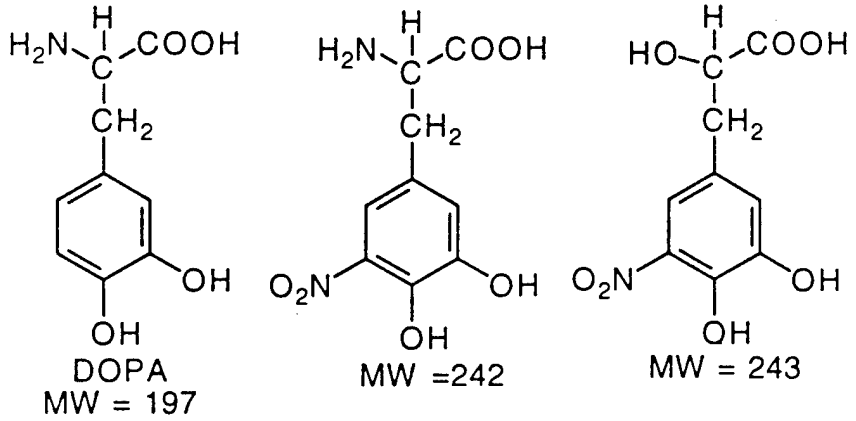

The DOPA reaction yielded only a few products. LC-MS shows a few very products that elute near the void and a large peak at 5 min and one at 9 min, see Fig. 23. The expected α-hydroxy-DOPA ion, which would be at 199 m/z was not observed. The peak at 5 min contains two nitrated forms of DOPA. One is the nitro-DOPA at 243 m/z and the other is α-hydroxy-nitro-DOPA at 244 m/z. It would be possible that the 244 m/z signal is only an isotope of the 243 signal; however, the isotope abundance is much higher than would be expected, and it attributed to the hydroxylated species. Another strong MS signal was

observed at 4 min for 238 m/z, a weak product in the UV signal. However, no structure could be assigned to this product.

Any interesting question is raised to account for the lack of reactivety of the α-amine group as was observed in each of the other amino acid analogs. Perhaps the α-amine is under going strong intramolecular hydrogen bonding with the 3-hydroxy group of tyrosine that is protecting the amine from the nitrous acid and deamination. There is an apparent increase in nitration reactivity for the dihydroxy as well.

HAHA

We synthesized 3-amino-4-hydroxy-hydrocinnamic acid (HAHA) as an analog. HAHA is 3-AT without the α-amino group.

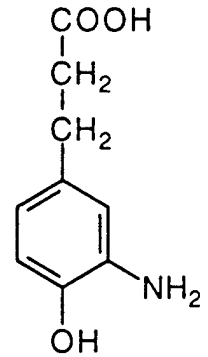

HAHA
MW = 181

This analog was of particular interest to us since it forms a polymeric substance very similar to that of p-DAT. We analyzed this reaction with CE and CE-MS. Figure 24 shows a CE trace at 214 nm of the reaction products. The electropherogram contains a number of peaks that seem to merge into a polymer-like distribution. When this product was examined in CE-MS, 4 peaks could be detected. The EIC for these 4 peaks are given in Fig 25. The signals observed were at 181, 226, 361, and 407 m/z. The PI has made a tentative assignment of the peaks to the following structures:

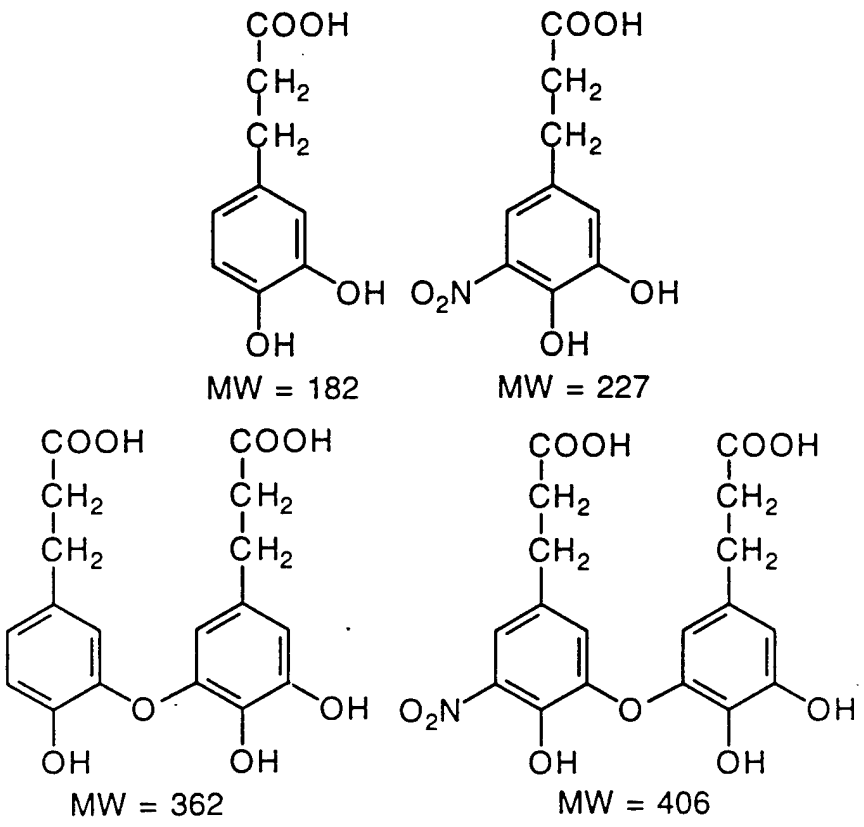

The production of the dihydroxy species would occur the with lost of N_2 from the diazonium yielding the carbocation which could pick up a hydroxy group from the aqueous phase. The nitrated dihydroxy product is consistent with the reactions observed from DOPA. The ether-linked ring systems only makes since according to their mass and are highly speculated by the P.I. We could find no such reaction in the liteature that could explain such products.

2-Aminocresol

As a model analog to access the aromatic amine reactivity, we chose 2-amino-p-cresol (2-AC). It has similar electronic distribution throughout the aromatic ring as 3-AT.

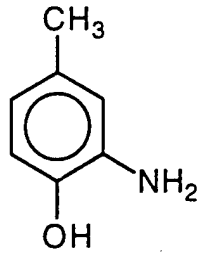

2-Aminocresol
MW =123

The mixture of products produced from the reaction are simple, initially, but grow in complexity with time. Figure 26 shows the UV at 214 nm, the 405 nm Vis, and the MS chromatograms observed. The MS signal was obtained in negative ion APCI mode. Several of the reaction products contain strong visible absorbances characteristic of azo-linked aromatics. The peak eluting near the void (~1.0 min) has a strong MS signal at 226/210 m/z, which suggest it has an odd mass and would contain either 1 or 3 nitrogen atoms. Repeating this experiment using ^{15}N-nitrite revealed, most surprisingly, that it gained 3 ^{15}N atoms from nitrite. Such a mass can not be explained by 3 nitrations or the formation of an azo-oxide or nitro-azo groups. The loss of 16 m/z could be attributed to the loss of oxygen from an azo-oxide type. We could not assign a structure to such mass. The large peak at 3.2 min has a signal at 257 m/z and the ^{15}N experiment showed it gains one nitrogen atom from nitrite. This signal can be attributed to the azo linked to a diol aromatic (on left below) or azoxy linkage between (on right below) the aromatics as shown below.

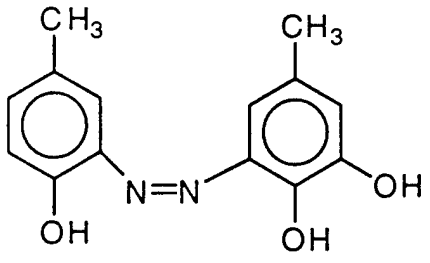

MW = 258

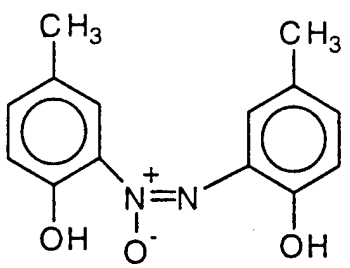

MW = 258

The peak at 10.5 min in the UV also has a 257 m/z signal and gains only one nitrogen from nitrite. We suspect that the 3.2 min peak is the zwitterion azoxy linkage which would be far more polar and elute quicker from the column, and the 10.5 min peak is the azo-linked diol. These would be typical structures of those predicted by the known literature. The signals at 18.2 and 19.0 min have MS at 316 and 271 m/z, respectively.

These species are much more hydrophobic and elute near the end of our gradient. The 18.2 min component gains 2 nitrogens from nitrite and the 19.0 min components only gains 1 nitrogen from nitrite. Their mass spectra are shown in Fig. 27a and b. With a mass difference of 45, it can be assumed the first eluting peak is a nitrated analog of the later eluting peak.

One significant disadvantage of 2-AC is that its reaction products do not precipitate with the addition of acetone like that of the 3-AT products. If the reaction is allowed to remain in solution for a number of days or if the aqueous phase is dried away, the complexity of the products increased greatly. We could separate more than 15 bands on flash chromatography that yielded a wide range of visible colored products, several with extended conjugation like that of p-DAT. However, it attempts to concentrate the components from the flash column so that NMR spectra could be obtained, notable changes in most of the fractions were observed. The color of most products went to a dark green or black, assumed to be oxidation products. Figure 28 shows an HPLC chromatogram of the 2-AC reaction mixture that was allowed to stand for 10 days. More than 30 products are detectable in the 214 nm trace. Most components had absorbance maxima in the 350-450 nm range with absorbance extending in the 600 nm range. The MS gave a much better signal in the positive mode for most of these components. The first eluting peaks at 1.1 min appear to be a mixture of 2-AC and 2-hydroxy-p-cresol. A very weak MS signal is observed for 243 m/z which would correspond to the 2,2'-diazo-p-cresol. A very weak MS signal for 259 m/z is also seen which correspond to a hydroxylated-2,2'-diazo-p-cresol. These are both minor components of the UV trace. Examining the mass spectra reveals some similarities, Fig 29a-h. First, several of the components have isotopic ratios at the molecule ion that can't be explained by natural abundance. For example, in Fig 29b the peak 363 m/z is almost the height of the 362 m/z peak. It can not be attributed to ^{13}C or ^{2}H atoms or $^{35/37}Cl$, which would separate the isotopes by two m/z units instead of the one, observed in this usually isotope pattern. Secondly, all but one spectra show a loss of 123/124 m/z fragment which would support an ether linkage as shown below:

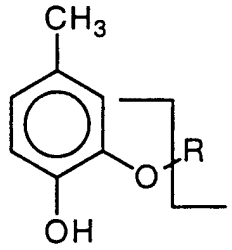

neutral fragment loss of 123 m/z

There appears to be one set of cis/trans or positional isomers at 6.5 and 7.5 min both 488 m/z signals are identical spectra which would strongly support there is an azo linkage. Our attempts to assign structures to these m/z where not successful. This experiment should have been completed using the ^{15}N nitrite to determine the number of nitrogen atoms added to each molecule.

3-AT with 1 equivalence of NO_2^-

We obtained reference spectra of 3-AT in NMR and IR for comparison with later reaction products. The proton NMR of 3-AT in D_2O is fairly simple, see Fig 30. The starting material had four signals for the seven protons: the methylene at 3.2 ppm; the α-proton at 4.2, a singlet at 7.2; and the remaining two aromatic protons between 7.0 and 7.2 ppm. The ^{13}C NMR for 3-AT in D_2O gave 9 clear signals for each of the carbons: 34, 54, 117, 118, 125, 126, 131, 150, and 171 ppm, see Fig. 31. We attempted to assign these carbons based on two articles using compounds similar to 3-AT but with variations of the amino acid head group. However, these references had a disagreement between the assignment of the aromatic carbon shifts, and we did not give an assignment. The IR spectra for 3-AT is given in Fig. 32.

The most reactive amine was thought to be the aromatic amine. Upon diazotization, the diazonium product can under go deprotonation to form diazo as shown below:

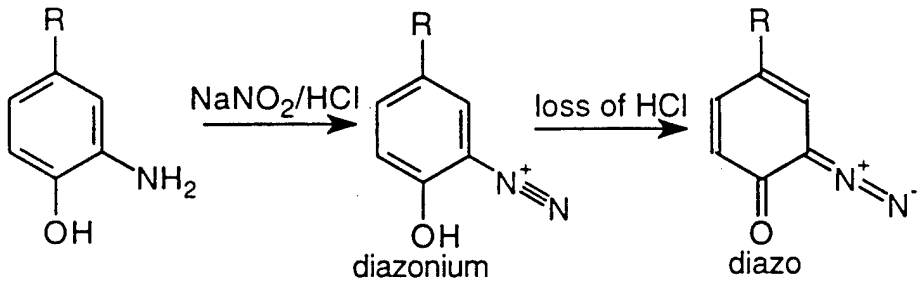

NMR or IR can not distinguish between the diazonium and diazo forms. We reacted 3-AT with one equivalence of nitrite to form the diazonium/diazo species we distinguished as diazonium-3-AT (DAT). DAT is obtained by adding an excess of acetone, which causes the diazo species to precipitate as a yellow solid. This species can be isolated as a BF_4^- or a PF_6^- salt and, when isolated, has a bright red color. Proton NMR reveals that the α- and β-protons of the side chain are still intact and unchanged, see Fig. 33. The three aromatic protons are still present in much of the same pattern as 3-AT; however, one aromatic proton has shifted to 6.6 ppm. The ^{13}C NMR still shows the 9 carbons but has carbonyl shifts at 170's ppm, see Fig. 34. A tentative assignment of the carbons was made based on a reference where the 2-diazonium-p-cresol had been isolated [4]. The IR spectra shows the characteristic 2250 cm^{-1} band associated with diazoniums, see Fig 35

We performed HPLC-MS on this reaction product. Figure 36 illustrates a peak near the void at 1.0 min and two additional peaks at 9 min, which have strong 405 nm absorbances. Examination of the MS at 1.0 min shows the 208 m/z for the diazonium species and its fragment for loss of N_2, see Fig. 37. An additional peak appears at 198 m/z that corresponds to the dihydroxy species. The peaks at 9 min both give identical spectra, see Fig 38, at 405 m/z. Our initial thought was that this component was an azo-linked species (one hydroxy and one dihydroxy), but the fragmentation of MS does not support this structure. We found that if the 1 equivalence reaction is allowed to set over extended periods of time, a red precipitate begins to form, which corresponds to this species. We ran MS-MS on the 404 MW component to confirm if it was the proposed azo linked species, see Fig 39, but it proved not to match the expected fragmentation. Figure 40 shows the proton NMR of this species obtained in D_2O/NaOD. Most importantly, we can see that some change has occurred to the aliphatic protons introducing new shifts in this region. The low solubility of this species prevented us from obtaining a ^{13}C spectra on this material. One critical question that must be addressed before assuming too much from the proton spectra is to know if this product is a pure substance or mixture of components. This component is not observed in 3-AT with 5.5 equivalences of nitrite added so we did not peruse its characterization further.

3-AT with 5.5 equivalence of NO_2^-

When the 3-AT reaction is performed with 5.5 equivalence of nitrite, the aliphatic amine is now attacked by nitrous acid as well. We performed this reaction in D_2O so that we

could examine the reaction products directly without extraction. Figure 41 illustrates the proton NMR observed from this reaction. First, the aromatic region looks basically the same as the reaction preformed with 1 equivalence of nitrous acid. However, the complexity arises in the aliphatic protons. Two additional forms of the α-proton are observed at 4.3 and 3.8 ppm. The methylene protons are divided among a very complex pattern between 2.3 and 2.9 ppm. There also appears to be traces of multiple additional components. Our attempts to obtain a ^{13}C spectra where not successful under these reaction conditions. A precipitate begins to form after a short period of time due to the limited solubility of some products in the acidic media. It was also noted that the aliphatic proton region alters slightly with time, indicating that additional reactions occur in the aqueous phase. We changed the solvent to a mixture of 50:50 D_2O/DMSO-d_6 to attempt to enhance the solubility of the reaction components. The change in solvent shifted the spectra of 3-AT in both ^1H and ^{13}C, see Fig. 42 a and b. Upon examination of the reaction spectra, we see that the aromatic region is much like that observed in the D_2O solvent and is similar to the 1 equivalence reaction but the aliphatic protons appear somewhat broaden, see Fig. 43. The multiple forms of the α-proton are not detected, but instead, there appears to be two singlets at 3.3 and 3.8 ppm. The complexity associated with the β-protons are still apparent. The ^{13}C spectra hints of the complexity as shown in Fig 43. There are 5 clear signals in the carbonyl region at 179 to 184 ppm compared to the two observed with the 1 equivalence nitrous acid reaction (carbons 1 and 7).

The carbon assigned to the diazo group also appears now in 4 or more forms at 93.6 to 94.3 ppm (carbon 8). The remaining 4 ring carbons appear compressed and have 8 separate resonances. Most puzzling is the large shift in the α- and β-carbons to 77.3 and 67.6 ppm, well above the DMSO-d_6 signal, and they each appear as a single signal.

Examination of this reaction by CE revealed that indeed a mixture of components has been made but with 2 major products, see Fig 45. The resolving power of CE has proven quite useful for this project to demonstrate purity and complexity; however, the UV mode of detection provides little structural information. We have struggled to learn the "art" of interfacing CE with ESI-MS. The major problem lies in the fact the mass sensitivity for the MS is near overload capacity of CE and there is little overlapping ground. We have learned some of the parameters necessary to make MS compatible with CE. Figure 46 illustrates the positive ion mode TIC for the CE-MS of the 3-AT reaction product. There are 4 peaks detected. First at 4.5 min is the Na^+ ions which form clusters with the

ammonium acetate electrolyte (note: this peak is not detectable in the UV electropherogram above). The extracted ion chromatograms for 223, 209, and 199 m/z are also shown in Fig 46. The mass spectra of the 209 m/z component is consistent with that of the α-hydroxy-3-diazonium-tyrosine, see Fig 47.

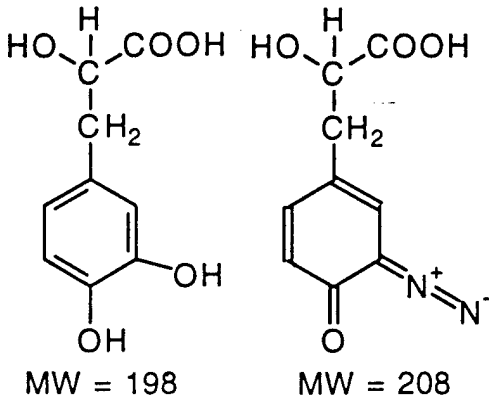

The 199 m/z mass spectra is consistent with the α-hydroxy-3-hydoxytyrosine, see Fig. 48. No structural assignment is given to the 223 m/z spectra shown in Fig. 49. When the same sample was analyzed using CE-MS in negative ion mode, the same two species were observed with m/z of 221 and 207, corresponding to the $[M-H]^-$ peak of the structures given above (data not shown).

The products of the 5.5 equivalence NO_2^- reaction were also analyzed using HPLC-ESI-MS. We have one major concern with the methodology which lies in the fact the some reaction components bind irreversibly to the HPLC column and they never elute. A second problem we faced was the fact that, at neutral pH, most components are so polar they co-elute in void peak and true mass spectra can not be observed for an coeluting species without MS-MS. In order to achieve retention, we where forced to run at lower pH (~3-4). We focus to a great extent using traditional TFA-aqueous-organic gradient typically used in the analysis of proteins and peptides. We found the TFA forms a precipitate when mixed with some reaction components and was not suitable as a mobile phase modifier. Mildly acidic separations were obtained using acetic or formic acids, but the pH frequently had to be changed post-column in order to yield good ions in the negative mode ESI-MS.

Positive ion mode HPLC-ESI-MS gave a good separation of the four major components obtained and is consistent with the separation obtained with CE. Figure 50 illustrates the

254 nm, the 405 nm, and the TIC. Three of the components observed have a strong 405 nm signal indicating they likely possess the diazo group. The peak in the 214 nm trace at 4.3 min produces a very weak positive-ion MS signal. A spectra associated with this peak is given in Fig. 51. It is unlikely that the peak has either an acid or base functional group due to its weak signal. It is likely a decarboxylated and deaminated species of some type. The 12 min peak corresponds to the α-hydroxy-diazo-species observed in the CE-MS, spectra shown in Fig. 52. The first eluting peak at 15 min corresponds to the dihydroxy species also seen in the CE-MS, spectra shown in Fig. 53. The later eluting peak at 15.2 min did not yield a significant MS signal in the positive ion mode. When the sample was examined in negative ion mode, two MS peaks seem to appear, see Fig. 54. The 13 min peak corresponds to the α-hydroxy-diazo-species as observed in the positive ion spectra at 207 m/z, see Fig. 55. Surprisingly the MS signal for the dihydroxy species, which would have had an $[M-H]^-$ ion at 197 m/z, was not observed. Instead, we see a strong signal at 225/227 m/z which indicates a chloride isotope, see Fig. 56. This was quite confusing initially, but considering that the 199 m/z species observed in the positive ion mode is actually a α-chloro-diazo species, then the 199 m/z signal is attributed to the loss of N_2. This theory is further supported by the fact that this peak had a strong 405 absorbance, which would not be characteristic of a dihydroxy species. Thus, we now assign this peak to the α-chloro-diazo species illustrated below:

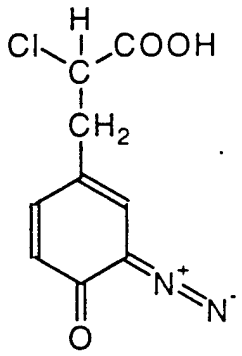

MW = 226/228

The 15.2 min peak yields ions in the negative mode, and its spectra is given in Fig. 57. It $[M-H]^-$ signal appears at 221 m/z, which corresponds to the 223 m/z observed in the positive ion CE-MS of this product.

The addition of the extra equivalences of nitrite seems to yield the predicted α-deamination products observed in the 3-AT analogs. We found it notable that no nitro-

substitution on the aromatic ring appears to occur in the initial aqueous reaction. The 2 major components that we can identify are the α-hydro-diazo and α-chloro-diazo derivatives of 3-AT.

Gas Analysis

A series of experiments were performed to quantify the gas released from the initial reaction of p-DAT. The reactions were allowed to react for 10 minutes after which the evolved gases were analyzed using GC with thermal conductivity detection. The data from this series of experiments is summarized in the table below.

	Percent Area of Component			
Sample	N_2	NO	CO_2	N_2O
Control (1min)	99.81	0	0	0.18
Control (10 min)	61.12	37.58	0	0.28
3-Aminotyrosine	67.56	14.59	12.78	0.75
2-Aminocresol	98.29	0	0	0.79
Phenylalanine	72.90	4.94	20.91	1.20
DOPA	39.58	55.23	2.02	0
3-Nitrotyrosine	80.39	0.15	17.14	2.30
HAHA	93.31	0	5.51	1.18

This data is not calibrated in any way and simply represents the percent area of the total observed for each chromatogram. Since these gases are approximately the same mass we can make a rough approximation that their response to the detection would be equal. In simpler terms, twice the area is approximately twice the concentration of the gas. Our control experiment revealed the N_2, NO, and N_2O are evolved just as predicted. The 3-AT reaction evolves a decreased amount of NO, but there is some CO_2 released. We were somewhat surprised by this, but it would be consistent with loss of the carboxylate following the loss of the α-amino yielding a carbene. The fact the CO_2 percentage is so high is troublesome, and it conflicts with elemental analysis data to be discussed. The ratio of N_2 to CO_2 is around 5.5. The fact that phenylalanine, DOPA, and 3-nitrotyrosine vary significantly among their N_2/CO_2 ratios is disturbing since we feel that these should all have similar behavior in the deamination/decarboxylation at the α-position. The P.I. is unsure if this is due to poor experimental accuracy or that these reactions could vary

this much due to changes in structure of what is assumed to be an unreactive portion of the molecule. From this data, we feel that some decarboxylation is occurring, but we question to what extent.

Formation of p-DAT

As previously stated, our method of characterization of the DALM polymer has been initially focused on the sole characterization of the p-DAT polymer. Then, if successful, we would proceed to the addition of luminol. There have been many preparation protocols developed for the formation of DALM including biological and synthetic methods. When we submitted the proposal for this project, our group's effort was to be in collaboration with Dr. John Wright's efforts at this institution. We have relied solely on the protocols provided by his previous research for the synthetic production of p-DAT and DALM. Briefly, this protocol is given below:

Synthetic Formation of p-DAT

1. 4.14 g of $NaNO_2$ (5.5 equivalences) is added to a breaker containing 20 mL of Milli-Q water.
2. 3.23 g of 3-amino-L-tyrosine•2HCl are added to a second beaker containing 20 mL of Milli-Q water.
3. The solutions are mixed in a large beaker and placed in the dark for 30 min. Note that this procedure should be performed in a hood since a large amount of gas is evolved.
4. Add 800 mL of acetone and allow to set overnight.
5. A reddish-brown precipitate will form. Using a suction filter and #2 Whatman paper, filter the precipitate from the acetone solution. The precipitate is the polymer. Heating the precipitate appears to accelerate the polymer formation, but is not necessary.

   Note: We established that acetone is not necessary to form the polymer and that speed vacuuming the mixture after step 3 results in the same product.

We have attempted a great number of experiments to attempt to characterize this polymeric substance. We have also synthesized a number of analog polymers, which seem to have similar properties. This report will discuss those we feel are significant.

UV/Visible characterization of p-DAT

The UV/Vis analysis of 3-AT, sodium nitrite, and their immediate aqueous phase products are given in Fig. 58. 3-AT has no absorption above 300 nm. Sodium nitrite has an absorbance maxima at 350 nm but quickly diminishes. Solutions of $NaNO_2$ are colorless. Mixing the 3-AT and $NaNO_2$ immediately forms a golden yellow color which appears orange/brown when concentrated corresponding to the absorbance maxima at 404 nm. The 404 nm absorbance is due to the aromatic diazonium/diazo group. When the precipitate from the polymer formation has been dried and dialyzed to remove lower MW components, it has a significantly different appearance than the starting materials, see Fig. 59. The polymer has a fairly strong low UV absorbance, likely due to π to π^* transitions, but also has an extended pigmentation absorbing beyond 650 nm. The nature of the visible absorbance is likely the key to the polymer formation.

IR Analysis of pDAT

The IR spectra of p-DAT obtained from pressure-assisted ultrafiltration (MWCO 10k) is shown is Fig 60. This spectra is quite featureless compared to the 3-AT spectra. Absorptions appear at 3420 (broad), 1600 (strong), 1510 (weak), 1400 (weak), and 1250 cm^{-1} (weak). This is quite surprising considering the complexity believed to be in the polymer. We had a diffuse reflectance spectra obtained to see if any other absorbance might possibly be detectable in this variation of IR, see Fig. 61. The spectra showed all of the same absorbances. The broad 3400 peak is likely due to a bonded-OH and H_2O that is formed as a hydrate with the polymer. The 1600 band is assigned to a carbonyl, likely from a carboxylate salt. The 1500 absorbance could be assigned to a great number of groups, but we feel it is likely a $-NO_2$ group.

DCS of pDAT.

Differential scanning calorimetry was performed on an aged and dialyzed (MWCO 10k) sample of p-DAT, see Fig 62. The plot shows no strong transitions up to 500 degrees. This is quite surprising. There are two weak transitions at 240°C and 410°.

Raman of pDAT

We had hoped that raman spectroscopy could provide us with key functional group information. Raman has recently found rebirth in polymer analysis due to the enhanced sensitivity of FT-Raman. We submitted a sample for analysis at Monsanto's Corporate

Research-Analytical Sciences Center. Dr. Queta Cortez is a senior research scientist and is a specialist in the analysis of polymers with raman. She attempted to analyze the dialyzed p-DAT and was unable to obtain a raman signal. Dr. Cortez believes that is could be due to the near IR absorption associated with the p-DAT causing fluorescence from the 1064 nm Nd/YAG laser used for excitation. A former student who had worked on the DALM project under Dr. Wright's supervision, Kenny Roberts, contacted us to see if we would like to have the polymer analyzed using new raman technology being developed in his research group at Iowa State University. The standard raman of solution sample of pDAT yielded no signal and was consistent with Dr. Cortez's findings. The ISU group was able to get a weak raman spectra by using surface enhanced raman spectroscopy. Basically, the polymer is chemisorbed on a silver substrate and spectra is obtained from the thin film. Figure 63 illustrates the resulting spectra; the top being the raw data spectrum, and the bottom is the subtracted spectra. A number of weak signals were observed. The strongest absorption at 1386 cm^{-1} is characteristic of a diazo linkage (1300-1400), however there are a greater number of other groups that absorb in this region. Most likely it corresponds to the carboxylate group (1440-1340, s) observed in the IR. Despite the great efforts that were put forth to obtain the raman data, there appears little information that can be used to characterize this polymer.

Elemental Analysis

We submitted a number of samples for elemental analysis including two analog polymers that we made, p-HAHA and p-Tyrosine, which form under identical conditions as p-DAT. The table below summarizes the results of element analysis and the conversions to the corresponding C/H and C/N ratios.

Elemental Analysis

Element	p-DAT [1]	p-DAT [2]	p-HAHA	p-Tyr
C	50.10	51.13	47.88	41.58
H	4.23	4.64	4.19	4.17
N	9.02	9.01	8.21	6.21
O	**	32.70	-	-
Cl	-	2.52♦	-	-
Na	-	<0.025%	-	-
C/H	0.99 (0.75)	0.92 (0.74)	0.95 (0.83)	0.83 (0.83)

C/N	6.53 (4.5)	6.66 (4.5)	6.80 (9)	7.86 (9)
C/O	-	2.09 (3)		
C/Cl	-	60 (0)		

p-DAT[1] was a dialyzed sample (MWCO 10k). It contained a significant quantity of Na, which interfered with the O analysis (**). p-DAT[2] was a dialyzed sample that had Na removed by passing across a strong cation exchanger. The Cl percentage was not measured directly, but calculated indirectly since it is the only possible element remaining (♦). The numbers in parenthesis next to the atom ratios represent the ratio for the starting material. The C/H and C/N ratios match well between the two lots of p-DAT and are in agreement with that previously reported by Dr. John Wright in his characterization efforts of the polymer. The desalted p-DAT gave us complete elemental information.

We were not surprised to see the C/N ratio increase as would be expected from the loss of the α-amine. It also indicates that a diazo-type linkage, although it may be present in the polymer, is not the most abundant form of linkage. The loss of hydrogen attached to both the α-amine and aromatic amine is supported by the increase in the C/H ratio. Replacing the α-amine with a hydroxyl group and removing the protons on the aromatic amine would yield a C/H ratio of 1.00 which is closely match to the observed 0.92 in the p-DAT[2] sample. A significant increase in oxygen is indicated by the decrease in theC/O ratio. Most significantly, this suggests that the polymer retain its carboxylate group. The increase can be explained in part by formation of the α-hydroxy but this would only raise the C/O ratio to 2.25. The additional oxygen could be explained from the formation of the dihydroxy species, azo-oxy linkages, or substitution with NO_2. There are many possibilities, but it is likely attributed to several things. The presence of Cl was not surprising since the initial reaction of 3-AT indicated that it is attached in the α-position for one species detected. We confirmed that the Cl is covalently bond by a negative response to repeated AgCl test. Because the increased mass associated with Cl is higher, its C/Cl is only 60. If we assume that all 9 carbons of the 3-AT remain intact in the polymer, then approximately every 7th 3-AT unit will possess a Cl. This crude value is in agreement with the initial 3-AT reaction results.

Another estimation can be made based on the comparison of the desalted versus non-desalted p-DAT. If we assume that all of the Na^+ is bound to a carboxylate group, we can

estimate the C/COOH ratio by looking at the increase in hydrogen from the elemental analysis between the 2 samples. The difference calculates to 0.41% H that corresponds to a C/COOH ratio of 10.39. This is only a crude estimation, but considering that the H% came from different batches of p-DAT and that deviation in the two batches will be maximized by the low weight of H, it matches the C/COOH ratio of 3-AT quite well.

The elemental results from the analog polymers, p-HAHA and p-Tyr, did not provide a great deal of information due to the fact that complete elemental information was not obtained. However, there were some surprises. First the p-HAHA (3-AT analog with only aromatic amine) showed a decrease in the C/N ratio, which suggests that either the polymer is highly nitrated or the polymeric linkage contains multiple nitrogen atoms (e.g., a diazo linkage). We make these statements assuming that the aromatic nitrogen is the source of polymer linkage; however, this is a critical question. The C/N ratio for the p-Tyr also from decreases 9 to 7.86 upon the polymer formation. We expected the ratio to remain constant based on the studies from the tyrosine reaction components as previously discussed. This would be in accordance to the loss of the α-amine and nitration of aromatic ring, which was the major product we observed. It is hard to imagine that these two polymers could possess the same form of linkage. However, the polymers have very similar properties in many aspects and we have learned to take nothing for granted in this project.

High Field NMR

We have analyzed a number of p-DAT and analog polymer samples using NMR. We quickly found that the 200 MHz NMR at our institution was not suited for the complexity of these samples. We have been very fortunate to have a State of Oklahoma Statewide Shared NMR Facility that is based at Oklahoma State University. The centerpiece of this facility is a new 600 MHz NMR. The unique funding of this facility allows our institution to submit samples for analysis at a greatly reduced cost. The 600 MHz NMR is the most powerful within 300 miles of our campus.

We obtained a ^{1}H and ^{13}C 1-D spectra of a higher molecular weight (MWCO 10k) sample of p-DAT that was aged for one month. The sample was a saturated solution in D_2O. Figure 64 is the proton obtained after 30,272 pulses (over two days of acquisition time). This spectra was most disappointing due to the broadness of the peaks and its lack of discrete resonances. There is an aliphatic signal at 2.9 ppm (β-position) and 4.3 ppm (α-

position) and an aromatic signal at around 7.0 ppm. Perhaps most significant are, what appear to be, singlets at 3.4, 3.9, and 4.8 ppm. These are resonances corresponding to protons bonded a sp^3 carbon. The 1-D ^{13}C spectra is shown in Fig. 65. Very surprisingly, this spectra has very little signal that should correspond to the α- and β-carbons. There are 2 small signals at 45 and 79 ppm, but the area is very low. In the aromatic region a broad signal is observed from 90 to 200 ppm. There appear to be peaks at 124, 138, and 186 ppm, but the weakness of the signal makes this somewhat questionable. Dr. Feng Qui, the facility manager, felt that our lack of signal could potentially be attributed to the presence of a free radical, which could explain the overall lack of sensitivity and broadness of the signals.

A preparation of p-DAT was prepared using ^{15}N-$NaNO_3$. In our hopes were to obtain a ^{15}N NMR spectra of the polymer the ^{15}N enriched p-DAT should have given an enhanced signal, assuming the nitrite is somehow consumed into the polymer. This preparation was dialyzed using a lower MWCO (2k) in hopes that the heterogeneity of lower MW material would be less severe. These two samples MW>2k and MW<2k were prepared by saturating a solution in D_2O/NaOD. Increasing the pH to above 10.0 greatly enhances the solubility of this polymer. Figure 66 shows a 1-D proton spectra of the MW<2k sample. This spectra unfortunately reveals the complexity of this polymer system. The same three signal regions appear as observed in the previous sample (α-, β-, and aromatic protons); however, there is a large number of resonances occurring in each position. A host of minor component signals in both the aromatic and aliphatic regions are now visible. The singlets near the α-proton that were observed previously are again present. Dr. Qui was unable to obtain a 1-D ^{13}C spectra in a reasonable time period. Instead, we were able to acquire good spectra using ^{13}C-^{1}H-HETCOR technique. HETCOR is much more sensitive than traditional 1-D ^{13}C and provides us with the correlation between which protons are attached to which carbons. This technique requires that the carbon have a proton attached, which is not the case of carboxylates. Figure 67 provides the HETCOR spectra for p-DAT<2k. The spectra shows the methylene proton of the β-position and its carbon at 25 ppm. The singlet observed in the proton spectra are attached to the α-carbon at 59 ppm. A minimum of 19 aromatic signals are observed in the 100-125 ppm range.

When the pDAT>2k was analyzed, the results were somewhat encouraging in the fact that many of the trace signals apparent in the lower MW fraction have now disappeared

indicating they do not play a significant role in the overall composition of the polymer. Figure 68 is the 1-D proton spectra obtained. It clearly illustrates the many environments present at the β-position between 2.3 and 2.8 ppm. The somewhat surprising feature is the α-proton region, which shows 2 discrete signals at 3.8 and 4.0 ppm that have minimal splitting by the β-protons. The aromatic region is again quite complicated with an array of signals from 6.4 to 7.4 ppm. The HETCOR spectra, see Fig 69, is very similar to that of the lower MW fraction. A key difference is the loss of many signals in the aromatic region. There appear to be 4 discrete aromatic signals at 103, 110, 115, and 121 ppm. In an attempt to simplify the proton spectra, we obtained a ^{1}H-^{1}H COSY spectra for the pDAT>2k, see Fig 70. This yields a correlation between which protons neighbor other protons. The COSY spectra shows the 2 α-protons are coupled to overlapping sets of doublets. The majority of the methylene signal can be assigned to these different environments of the α-proton, which greatly simplifies the 1-D proton spectra. The COSY also indicated that one position of the aromatic ring no longer has its proton as indicated by the missing meta-postion for some splitting patterns. Unfortunately, the hyper-fine splitting observed in such a field NMR can make things seem over-complicated when patterns overlap. This COSY spectra only indicates correlations between strong peaks and we do not feel that the bulk of the higher MW polymer is truly represented in the spectra.

We tried a number of different pulse programs in an attempt to obtain a ^{15}N signal but were not successful. This can be interpreted in a many ways. The elemental analysis confirms the presence of a significant quantity of nitrogen, but the natural abundance of ^{15}N is only 0.37% meaning that if no ^{15}N was consumed from the nitrite that the natural ^{15}N is to low to detect. The sensitivity of ^{15}N is less than 1/10 of ^{13}C, and we couldn't obtain a direct ^{13}C spectra. Dr. Qui suggested that we obtained ^{13}C and ^{15}N enriched 3-AT and that he might then obtain direct spectra using ^{15}N-^{13}C HETCOR. We obtained a bid from Cambridge Isotope for 1 g of enriched 3-AT, and it was in excess of $15,000. Since this value exceeded our supplies and materials budget, we decided against the idea; however, it remains the most promising method to find the true nature of the nitrogen in this polymer, which is almost certainly a critical factor in its pigmentation and linkage.

We also submitted samples of 2 analog polymers, p-Tyr and p-HAHA, both dialyzed to above 2,000 and dissolved in D_2O/NaOD. Figure 71 shows the 1-D proton of p-Tyrosine. Unfortunately, this system seems more complex than that of p-DAT. There is a large

distribution of peaks in both the aliphatic and aromatic regions. The α-protons around 3.9-4.1 ppm seem much like p-DAT. However, the β-protons are divided into a number of regions that range from 2.3-3.4 ppm. The aromatic shows the doublet pattern you would expect for the 2/6 and 3/5 position of tyrosine, but again, there are a great number of other environments present that make of a significant percentage of the total area. Perhaps COSY could simplify this spectra, but time did not allow for this to be completed. Figure 72 shows the HETCOR for p-Tyr. Unlike p-DAT, 2 signals are observed at 40 and 45 ppm for what is assumed as the β-carbon, but this is shifted much further upfield than p-DAT's β-carbons at 25 ppm. The α-carbon appears up at 75 ppm, again shifted 15 ppm above p-DATs. The aromatic carbons show the greatest signals at 120 and 132 ppm, which likely correspond to the symmetrical 2/6 and 3/5 positions of tyrosine. There are a number of other carbons detected that correspond to an asymmetrical structure. The 1-D proton spectra of p-HAHA is shown in Fig. 73. Most surprisingly it possesses a number of signals from 0.7 to 1.6 ppm, which seem much too low to correspond to the α and β-protons (2.4-2.7 for HAHA monomer). There are a number of signals in the 2.3-3 ppm range which match those of the monomer. Most odd are 2 resonances at 3.8 and 4.0 ppm that match those of the α-proton of p-DAT perfectly, but this doesn't seem possible considering the structure of the monomer. HETCOR and COSY spectra would be critical in understanding the nature of these aliphatic signals.

Pyrolysis GC-MS of p-DAT

In an attempt to gain more information about p-DAT we submitted a sample for flash-pyrolysis GC-MS to Chemir/Polytech Laboratories in St. Louis, MO. Chemir specializes in the analysis of polymers and has the state-of-the-art equipment to do such testing. Pyrolysis studies are not ideal for the characterization of unknown systems since structural rearrangements are the norm under high temperatures. Samples of p-DAT were pyrolyzed at 450, 550, and 650°C. The results of these tests are summarized in Fig. 74. The pyrolysis products consist of phenols and benzoxazoles. Figure 75 illustrates the chromatogram obtained at 550°C. There were 15 different components detected; however, 6 of them did not give good matches with the spectral library. The structures of the identifiable components are shown below.

Pyrolysis GC-MS of poly-DAT @ 550 C

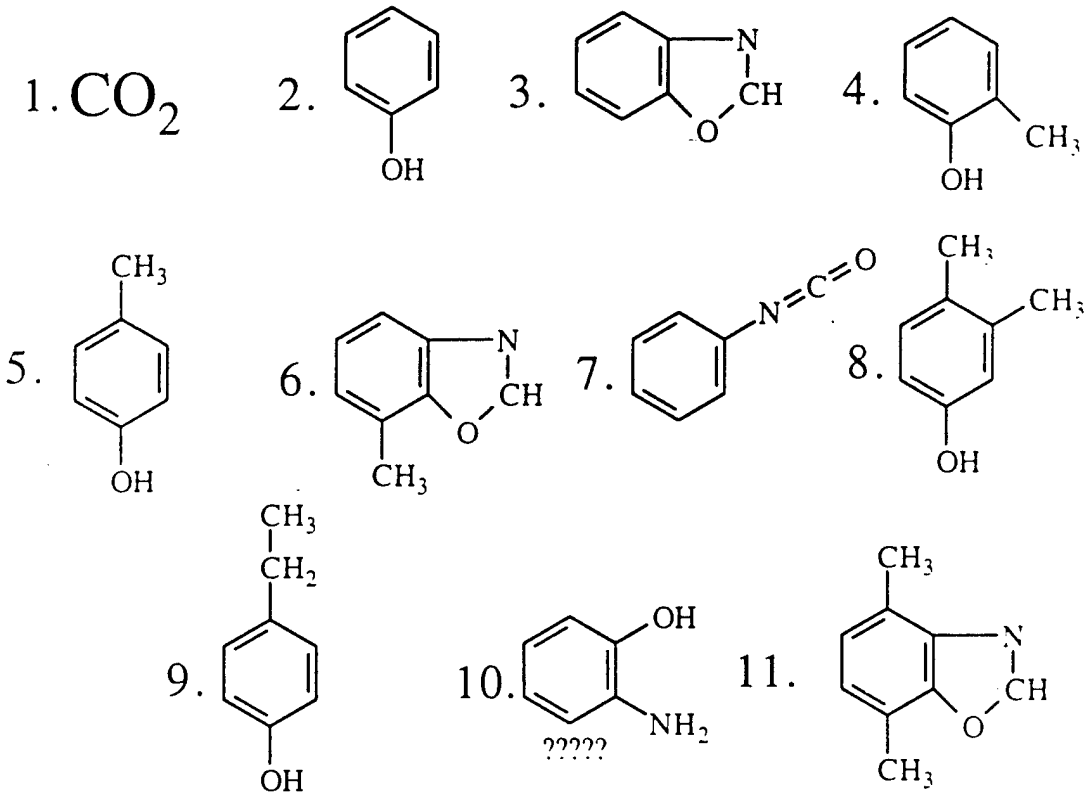

The presence of CO_2 confirms the remaining carboxylate group. The p-phenols would be expected from the conservation of the basic 3-AT structure. The o- and m-phenols are of interest. They could be rearrangement products from the pyrolysis or an indication that the aliphatic chain is somehow attached to the aromatic ring. Another feature of great interest is the presence of the benzoxazole components. Benzoxazole polymers are formed from heating 2-aminophenols with a carboxylate group attached to a side chain with compounds equivalent to α-deaminated 3-AT [5]. The loss of 2 H_2O molecules occur during the formation of the benzoxazole ring. Benzoxazoles have been observed in pyrolysis products from a host of other compounds including nitrophenoxyacetic acids [6] and oxime materials [7]. This data gives us a clear indication that the aromatic ring is conserved; however. it does not provide conclusive evidence about the mode of polymerization. This data needs to be examined more carefully by an expert of pyrolysis

studies. We attempted to contact two such scientists but neither was interested in our project.

We also submitted samples of p-DAT, p-HAHA, and p-Tyr to Dr. Robert White of the University of Oklahoma. Dr. White is exploring new instrumentation that can follow the thermal degradation of a substance by slowly heating it, trapping the volatile degradation component and performing rapid GC-MS analysis on the trapped segments. The results of his analysis are shown in Fig 76, 77, and 78 for p-DAT, p-HAHA, and P-Tyr, respectively. The top signal represents the total ion chromatogram observed and the bottom are the relative signals for CO_2 and phenol as a function of temperature. It was disappointing that these were the only two components readily identifiable; however, this is a new technology still under development. We can see similarities between all the polymers. Each emits phenol in the 440 to 560°C range. Also each emits CO_2 that rapidly decreases in intensity with temperature. It was notable that both p-DAT and p-Tyr are not releasing their maximum CO_2 until 300°C. This could indicate a similarity between the 2 polymers that is difficult to observe otherwise.

High Resolution MALDI-TOF-MS

We analyzed a sample of p-DAT using matrix assisted laser desorption ionization-time of flight-mass spectroscopy (MALDI-TOF-MS). This is the standard methodology used for the analysis of intact proteins and various other biopolymers. MALDI has also proven quite powerful for synthetic polymers and is known for is high sensitivity. Dr. Lloyd Sumner ran our sample at the Noble Foundation's new proteomics laboratory in Ardmore, OK. This is a new facility and Dr. Sumner is the former MS lab director at Texas A&M University in College Station. Figure 79 shows the best spectra that we could obtain. This was a sample of p-DAT dialyzed between 3k and 10k for the purpose of this experiment. Despite attempts using many different matrices, we could not improve the signal in the higher mass region. This MS shown gives a peak at 779 m/z but no repeat unit can be identified due to the lack of signal at higher m/z. These results were most disappointing.

GPC of p-DAT

We attempted fractionation of the p-DAT using a series of size-based LC separations. A variety of separation media were attempted, each with varying success. Media included

Sepharose, Superdex, Sephadex, Sephacryl, and Toyopearl. Separations based on size exclusion rely on differences of molecular volume of the analyte. The difficulty we observed was extensive non-exclusion interactions, which makes estimations of the molecular weight invalid. In fact, with every media we tried a portion of the polymer would bind irreversibly to the head of the column. Attempts to elute these substances with strong acid or base or organics were unsuccessful. The polymer chemically binds to the media. The media that proved to have minimum non-exclusion interactions was Toyopearl. Figure 80 shows a chromatogram of the exclusion markers using HW-55S (1-200k for dextrans) with the void appearing at 67 min and fully retained at 102 min. Figure 81 is a chromatogram of crude p-DAT. The peak at 77 min is of much higher MW than 200k according to our dialysis yet it is retained and appears to be lower MW.

We found that we could separate some of the lower MW fraction of p-DAT using Sephadex. If the 3-AT is left in aqueous solution without the addition of acetone, the polymer begins to form; however, it occurs over an extended period of time. We hoped to use this characteristic to trap and identify lower MW components of the polymer. Figure 82 shows the 254 nm trace and the TIC MS from a 7 day old 3-AT reaction separated on a 1 meter Sephadex G15-120 (MW<1500) column. As the chromatogram shows, we are getting fairly good separation of the lower MW components. Figure 83 is the 3-D chromatogram for the same separation showing the spectra as a function of time. A key feature that we noted from this data was that the extended absorbance associated with p-DAT was observed only in the higher MW fraction eluting at the void and not in any of the lower MW components. We are somewhat unsure how to interpret this information, but it diminishes hopes that lower MW components will yield the secrets to the absorption spectra. We found that some useful information could be obtained in the MS. Figure 84 is the mass spectra of the void region at 38 min. What we see is a vast number of different ions formed and little useful information to extract. This is due, in part, to the acidic nature of p-DAT and the fact the ESI often forms multiple charges in the individual molecules. The spectra averaged from 40 to 45 min shows a number of different ions that are real: 765, 737, 586 m/z, see Fig. 85. The averaged spectra from 45 to 50 min has a predominant peak at 585 m/z with what appears to be a fragment ion at 557 m/z (loss of 28 = N_2?), see Fig. 86. The 50 to 55 min spectra shows a new species at 603/605 m/z appearing to contain a chloride, see Fig. 87. The 55 to 60 min and 60 to 65 min spectra shows a strong 405 m/z signal, see Fig 88. The 65 to 70 min spectra shows a 423 m/z signal, see Fig. 89. The separation of these peaks are more clearly demonstrated in the extracted ion chromatogram shown in Fig. 90. This experiment proved to be quite

expensive in that small particles from the Sephadex column passed through the frit and into the HPLC detector and the electrospray needle. We were required to replace the spray needle and rebuilt the flow-cell due to the damage it caused.

We were quite excited about the separation and MS signals. We attempted to collect the fractions from the column and concentrate them so that NMR, IR, and MS-MS could be performed. We were most disappointed in the results after freeze-drying the aqueous solvent away. The problem we accounted is illustrated in Fig. 91, which is a CE separation of one of the fractions. No longer is there one or two over lapping components, but the species has reacted with itself or other species to yield an array 15 or more products. The products eluting from the GPC are much too dilute to be measured directly by NMR and all attempts to concentrate the eluents results in a host of new products being from. This is the reactive nature of this polymer system that make it so difficult to deal with. Ideally, advanced mass spectroscopic (MS-MS) techniques need to be performed on these species as they are separated so that structural information can be generated of individual m/z peaks can be obtained even in the case of co-elution from the column. We do not have this capability at our facility.

When we examined the MS show above in Fig. 85-89 we noted a few similarities. First, all components seem to have a M-28 fragment ion that is highly characteristic of a diazo group. Secondly, there was a mass difference of 18 between some species and a related species that contained a Cl atom (indicated by the isotope ratios). The different between a ^{35}Cl and an OH group is 18 mass units. Based on these characteristics we were able to give a tentative structural assignment to every signal MS signal we observed. These are purely tentative and no MS-MS has been generated that supports them. All of these structures are polyphenylene based. This type of linkage was proposed by Dr. Wright. It could be generated by a diazonium losing N_2 to form the carbocation which would under go an electrophilic attack on a neighboring ring. Dr. Wright's performed molecule modeling and determined that the most probable position of attack would be the 5-position of the ring based on electron density. Compound A, observed as the 405/407 m/z (see Fig 88), would result from one α-hydroxydiazo linking with one α-chlorodiazo with the loss of N_2 forming phenyl linkag show. Compound B would result from a similar reaction of two α-hydroxydiazo compounds. The dichloro product (Compound C) is also observed, see Fig 89. The addition of α-hydroxydiazo to Compound A would

yield Compound E, see Fig. 86. The addition of α-chlorodiazo to Compound A would yield Compound D, see Fig. 87. And finial the addition of an α-hydroxydiazo to

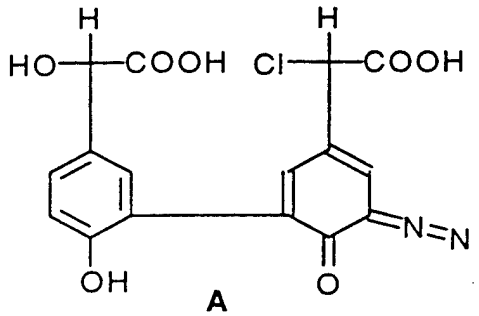

A
MW = 406/408

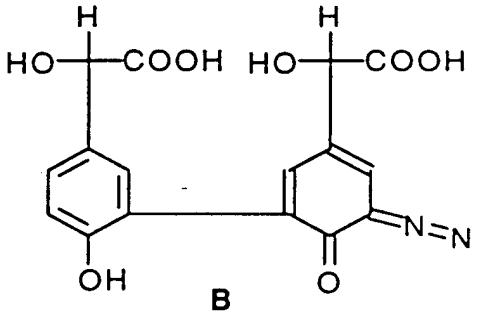

B
MW = 388

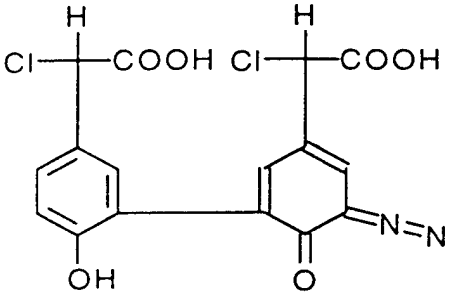

C
MW = 422/424/426

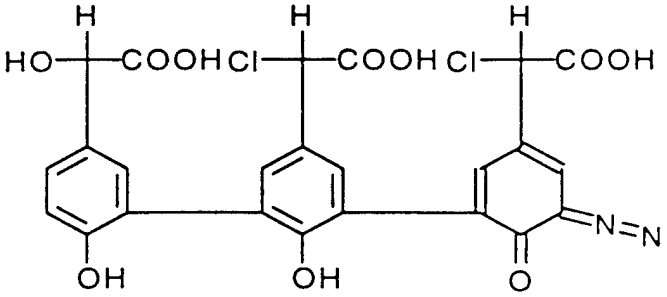

D
MW = 602/604/606

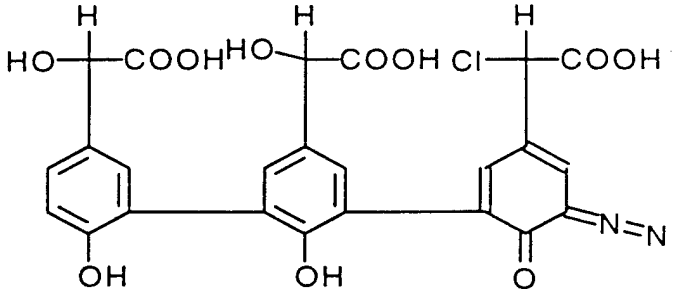

E
MW = 586/588

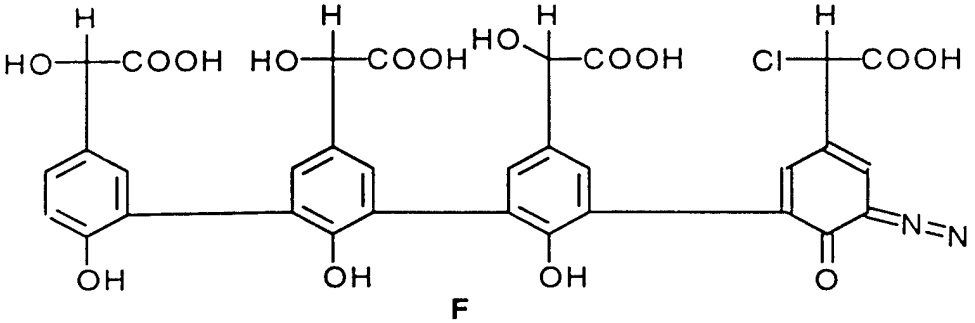

F
MW = 766 / 768

Compound E would yield Compound F. This series of compounds appears to be quite real. What is not well understood is if that are major or minor components of the reaction. This data does not provide that information since there may be major components eluting that are not detected by the MS. MS-MS of this series of compounds seems critical to confirm their identity. However this can explain the continued reactivity upon concentration and the toughest of the polymer to withstand digestion and degradation with a polyphenyl backbone. There a major inconsistency in the loss of N_2 would seem to go against the elemental analysis data.

Degradation of p-DAT

One classic way to characterize a polymer is to cleave the polymer into a number of small units that are more easily identified. We attempted this fundamental procedure on p-DAT using a variety of degradation methods. The degradation methods included treatment with 2 M HCl, 5 M NaOH, $SnCl_2$, $Na_2S_2O_4$, and HI. The possibility of an amide linkage had been discussed several times within our research group. Amides are susceptible to both acid and base cleavage under extreme conditions. Extensive treatment of p-DAT with 2 M HCl or 5 M NaOH at 105 °C for up to one week yields no considerable degradation products. The HCl caused an immediate precipitation of the polymer and that could possibly explain its lack of reactivity. However, the p-DAT remained soluble in the base and no degradation products could be observed by CE. This data makes us believe that an amide linkage does not play a role in the formation of this polymer. $SnCl_2$, $Na_2S_2O_4$, and HI are all reagents that should cleavage azo-type bonds to yield 2 amines. The major problem in the treatment of with these reagents is similar to that of HCl in that all require or are strong acids causing immediate precipitation of the polymer.

When we began examining these degradation products in the MS, we observed two common repeat patterns that appear polymer-like. These repeat patterns occur at 82 and 136 m/z. The appearance and disappearance of these peaks confused us. We attempted to perform labeling experiments and isolate this polymer species to no avail. Proper control experiments have clearly shown that these are adducts of the HPLC buffer, the eluting component, and sodium. For example, the 136 m/z repeat unit we observed when using trifluoroacetic acid (TFA)-modified HPLC mobile phases gave a series of peaks at X+136, X+272, X+408..etc. We now know this is attributed to the component+n(TFA-proton+Na^+). The repeat unit is the TFA-sodium cluster (MW=136). This occurred

when species that were bound to multiple sodiums, i.e., polycarboxylates, elute from the HPLC column into the MS. A similar 82 m/z repeat occurs from acetic acids minus a proton plus sodium. Some lessons are learned hard, and this was a quite disappointing blow.

Our most successful degradation appears to be $SnCl_2$ based on CE. Figure 92 shows a 214 nm electropherogram of a neutralized $SnCl_2$ digest of p-DAT>10k. About 10 peaks are apparent that are new from the dialyzed p-DAT used in the degradation. Despite many repeated efforts to obtain CE-MS data, this did not prove successful. The degradation needs to be performed on a larger scale and degradation components extracted and concentrated for further analysis. At the time this digestion was performed, we only had a limited quantity of dialyzed p-DAT and the yield from the degradation is enormously low. We were able to get some separation and detection of a $SnCl_2$ degradation using HPLC-MS. Figure 93 shows the UV and TIC of such a separation. The MS signal at 7 min and above system peaks associated with the gradient. The first MS peak at 0.7 min has a 227 m/z signal, see Fig. 94. The second peak at 1.0 min has a 453 m/z and its Na adduct at 475 m/z, see 95. The next peak has a strong 340 m/z peak and its dimer at 701 m/z, see Fig. 96. It is difficult to assign structures to these peaks without any other information. A strong possibility for the 227 m/z is given below:

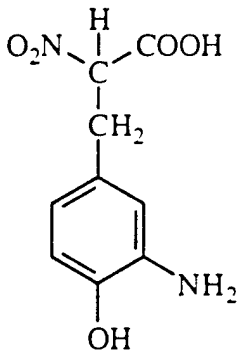

MW = 226

Considering this as a possible structure resulting from the digest of an azo linkage, we looked for the masses of the corresponding α-hydroxy and α-chloro products that would be expected; however, these were not observed.

Electron Spin Resonance Spectroscopy

Due to the weakness of our NMR signals we suspected that p-DAT contained a radical. We hoped that ESR could prove or disprove the presence of a nitroxide linkage in the polymer. Dr. Mark Filiphowaki from the University of Arkansas, Fayettevillle ran our first ESR spectra on the p-DAT polymer. Figure 97 is a spectra of the solid p-DAT powder. The material gave a signal at 3381 G. The ESR spectrometer at UA was apparently quite old and was retried shortly after we obtained this data. We questioned the reference for the g value but were not able to resolve this issue. We contacted Dr. Yashige Kotake with the Free Radical Biology and Aging Research Program at the Oklahoma Medical Research Foundation. Dr. Kotake agreed to attempt to obtain an ESR spectra. Figure 98 illustrates the signal observed of solid p-DAT. The signal was observed at 3483 G (g = 2.002). The data indicated that the radical is at a very low concentration in the polymer (<0.01%). Dr. Kotake suggested that we obtain a spectra at liquid N_2 temperature (77°K) to possibly better define the signal, but his facility did not have that capability.

We next submitted samples to ESR facility at the College of Medicine at the University of Iowa. Figure 99 shows the ESR spectra of a saturated solution of p-DAT at room temperature. A signal very similar to that observed by Dr. Kotake was observed at 3485 G but a trace of a signal at 3410 G also appears. When the p-DAT spectra were obtained at 77 °K, the spectra shifts but retains the same signal shape, see Fig 100. Consulting with the facility director, Dr. Gary Buettner, he agrees that 3 discrete signals are observed, one stronger signal centered at 3320 G, a signal with splitting at 3230 G, and a weak signal near 3420 G. He feels that each of these represent different environments. The signals are almost as strong at room temperature, and Dr. Buettner said that this was quite unusual that they are so stable. He felt the stronger signal could be associated with the aromatic with extended conjugation which is consistent with the nature of the polymer. He didn't feel that this was a nitroxide radical, but he stated that when a nitroxide is restricted from movement they may change drastically. The most interesting feature appears to be the strongly coupled signal at 3230 G, which corresponds, to a g-factor of 2.063. This could be a transition metal complexed to the polymer that entered as an impurity. If this is true, it is likely was an impurity in the 3-AT or $NaNO_2$ starting material. Similar signals are observed for p-HAHA (Fig 101) and p-Tyr (Fig 102) at room temperature. These data do confirm why our NMR signals appear so weak for the higher MW. fractions of the polymers. However the nature of this radical is still in question.

Conclusions

This project has proven a most challenging problem. The learning curve for this chemistry was quite steep for the P.I. since synthetic organic chemistry is out of his field of expertise. We are still in the process of learning ESI mass spectrometric methodology and its limitations concerning connection to CE and HPLC. Little literature, if any, discusses diazotization chemistry under our non-ideal conditions. We are now quite aware of why multitudes of products appear possible.

We seem to understand the chemistry occurring up to the point of precipitation of the initial products. Our studies of the analog systems indicate that the polymer mechanism is likely occurring through more than one mode. The diazo and/or diazoxy linkages are present to some extent. We do not have a proper understanding of the chemistry behind how an aromatic amino acid, like tyrosine, can yield a high MW polymer under these conditions. We have limited evidence that this is occurring through an ether linkage or by the substitution of the alkyl chain on the aromatic ring from the resulting deamination products as shown below.

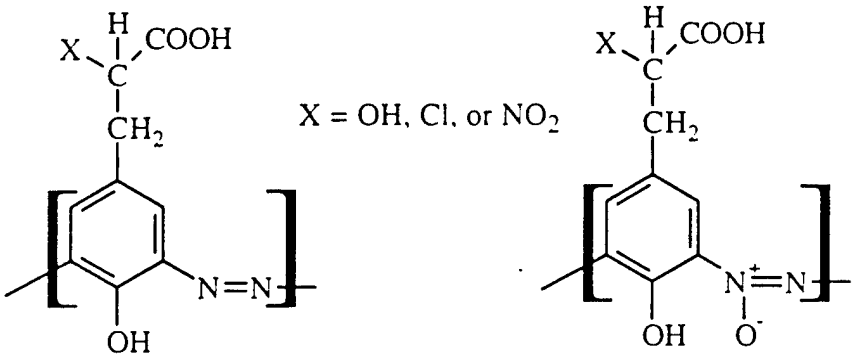

The literature predicts a diazo type bond is formed under proper conditions. If we consider that the polymer is composed of an diazo or diazoxy repeat units as shown above then the element composition indicate the following C/H, C/N and C/O ratios:

	Diazo	Azoxy	p-DAT
C/H	1.1 (X=OH)	1.1 (X=OH)	0.92
	1.3 (X=Cl)	1.3 (X=Cl)	
	1.3 ($X=NO_2$)	1.3 ($X=NO_2$)	
C/N	4.5 (X=OH)	4.5 (X=OH)	6.66

4.5 (X=Cl)	4.5 (X=Cl)
3.0 ($X=NO_2$)	3.0 ($X=NO_2$)

The fact that C/N ratio of these proposed structures is significantly different from that observed in the polymer suggests that it is not the only major component. If we consider that we have an aromatic ether linkage (A) or a substitution type linkage (B) or the polyphenyl linkage (C) then, the nitrogen is not conserved.

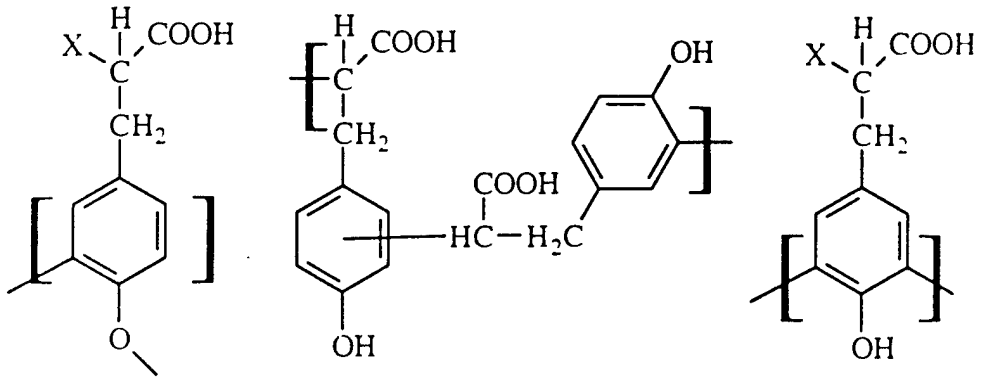

If we consider all of the possible products we observed in the analog reactions, there is an enormous combination of possible sub-units of this polymer. We unfortunately do not have a structure to assign that matches the complete data set. The extended conjugation of this molecule may only be a minor component of the total polymer composition. The fact the azo/azoxy linkage are the source of the intense pigmentation but the chemical ruggedness of the polymer can be better examined by linkages A-C. The fact that the polymerization occurs in the solid phase may suggest that the structure is continuously changing to some degree making it a "living polymer" which are among the most difficult to characterize. This would be a characteristic of the room temperature ESR signal we can observe with this material. We feel that the formation of a ^{13}C-labeled polymer and MS-MS of the initial polymerization products may be the key to understanding this system. Unfortunately these were not experiments we could perform in this funding cycle.

The issue of connection of luminol to the polymer was never addressed properly. We found the characterization of the p-DAT to be a most difficult task and that it should be

understood before addressing the attachment of luminol. We feel that luminol likely couples via a diazo bond, but experiments by Dr. Keil suggested that only it presence may be required and not chemical attachment to the p-DAT.

References

[1] Van Slyke, e. a., *J. Biol. Chem.*, 1911,*9*, 185.

[2] Van Slyke, e. a., *J. Biol. Chem.*, 1912,*12*, 275.

[3] Austin, A. T., *J. Amer. Chem. Soc.*, 1950,*45*, 149.

[4] Law, K.-Y., Tarnawskyj, I. W., Lubberts, P. W., *Dyes and Pigments*, 1993,*23*, 243-254.

[5] Mathias, L. J., Ahmed, S. U., Livant, P. D., *Polymer Bulletin*, 1985,*13*, 141-150.

[6] Goudie, R. S., Preston, P. N., *J. Chem. Soc. (C)*, 1971, 1718-1721.

[7] Banciu, M. D., Simion, A., Draghici, C., Mihaiescu, D., Oprean, I., *J. and Anal. Applied Pyrolysis*, 2000,*53*, 161-176.

Publications

The P.I. was listed as a co-author on a manuscript by Dr. John R. Wright entitled "Acoustic Wave Dosimetry on Diazotized Luminol Solution", Maddox et al., Microchemical J., **58** (1998) 209-217.

Presentations

Over the pass 2 years, the students and technicians working on this project have presented 9 oral or poster presentations at statewide and one national conference.

Interactions/Transitions

None.

New discoveries, inventions, or patent disclosures

None.

Aknowledgments

The P.I. wishes to thank the USAF-AFOSR for funding of this project. The P.I. is very grateful of the efforts put forth by the undergraduate students working on this project. These include Jason Gray, LeAnn Logan, Wayne Mixon, John Conley, Robin Bynum, and Keri Campbell. The project could not have accomplished what it did work the efforts of the dedicated technicians, now Dr. Chris Hansen and Dr. Victor Asirvatham. We have had many analysis performed off-campus that where critical to determining our current knowledge of the system at no or much reduced cost. These include: Dr. Feng Qui for the 600 MHz NMR work at OSU; Dr. Gary Buckley for the DSC at Cameron Univ.; Kenny Roberts for the surface enhanced raman at ISU; Dr. Queta Cortez for the solution raman at Monsanto; Dr. Lloyd Sumner for the MS-MS and MALDI-TOF-MS at the Samuel Roberts Noble Foundation; Dr. Mark Filipkowski for the ESR at UA. Dr Yashige Kotake for the ESR at Oklahoma Medical Research Foundation; Dr. Garry Buettner for the ESR at UI; and Dr. Robert White at the OU for thermal degradation GC-MS studies. The P.I. is greatly appreciative of the countless discussion over this project at SOSU.

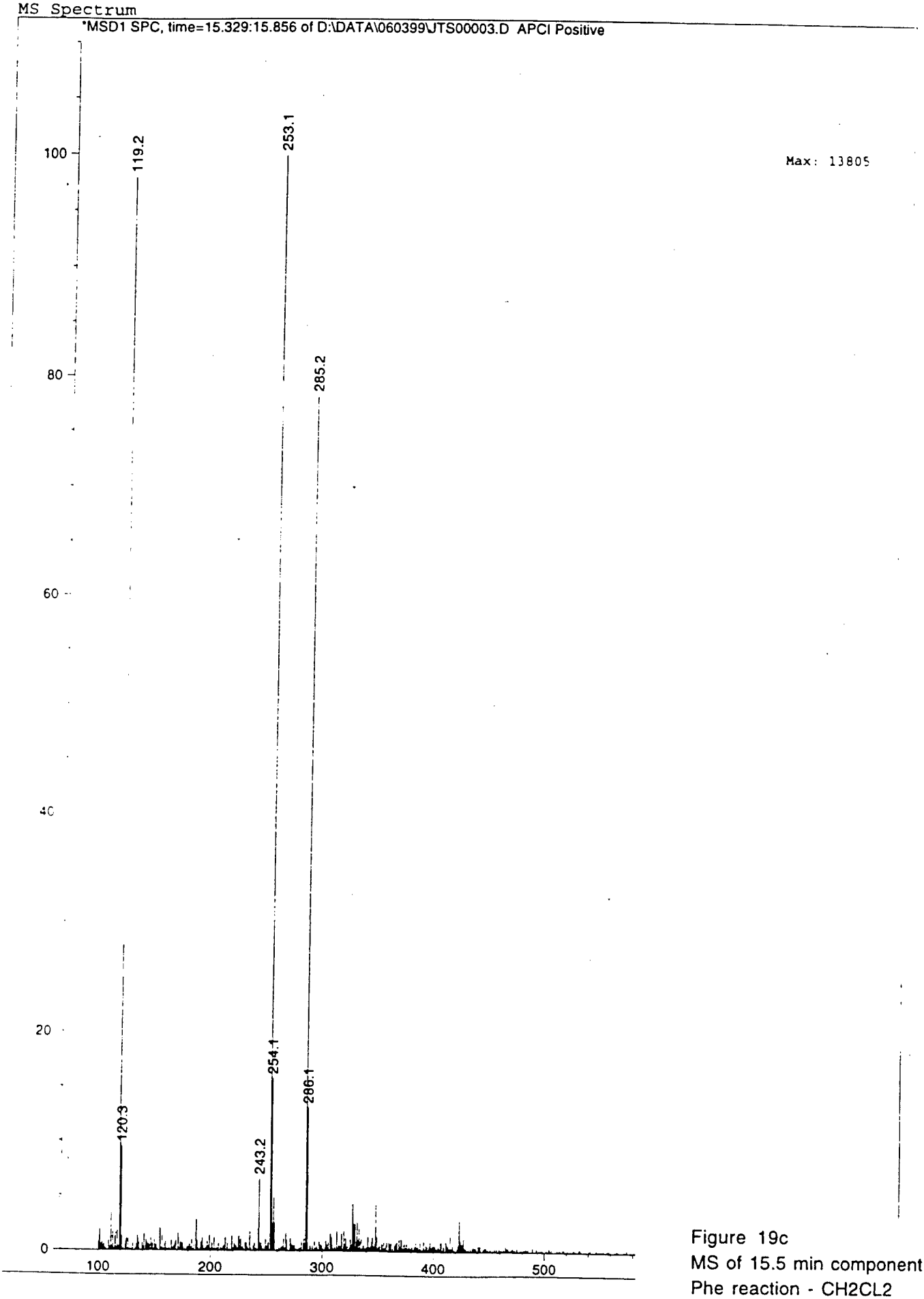

sstrument 1 7/3/00 1:16:34 PM

Figure 19c
MS of 15.5 min component
Phe reaction - CH2CL2
(+)-APCI

SOUTHEASTERN OKLAHOMA STATE

filename=07019801
dir=/home/nmruser/data/SMITH_RESEARCH/07019801
com=alanine pure
date=7/1/98
time=10:46:02
ac=53
ppfn=1PULSEH
# acq's (x 4)=64
spect freq=200.723600MHz
spect freq=200.723600MHz
pulse width =26.50u
spectrum width=2.870kHz
acq time=2854.100m
acq length=8192
pulse delay=8.000s
receiver gain=11
temperature=-274C
# dummy pulses=0
receiver delay=15.00u
spin rate=30Hz
acq delay=35.00u
dim2 length=1
channel=1
dwell=348.40u
predelay=100.0m
acq completed=0
y_scale=10076.156250
tph01=65.040802
tph11=-181.000000
rmp=200.723352
rmv=4.610000
current_size=8192

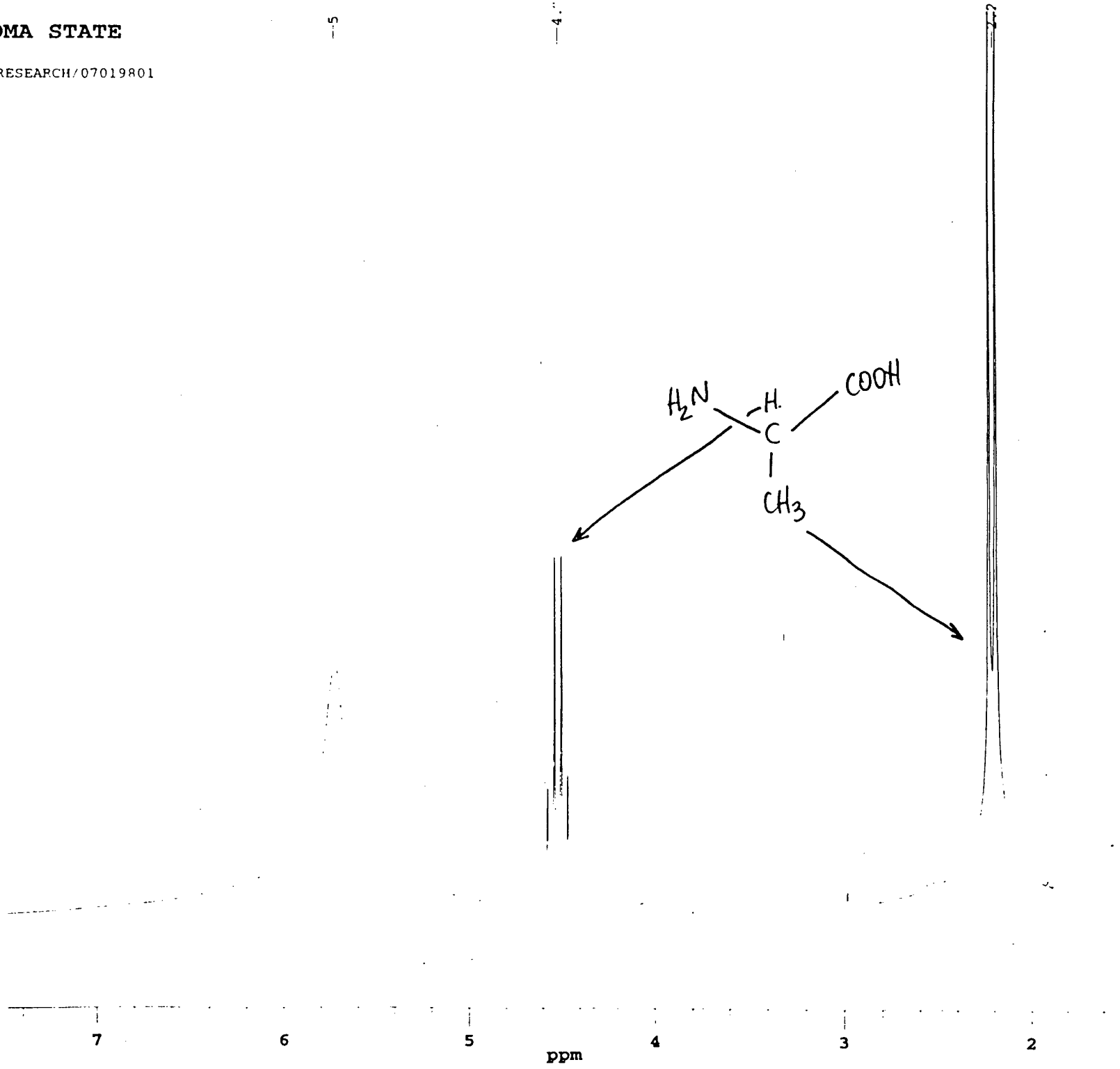

Figure 2
1H NMR of Alanine in D2O

SOUTHEASTERN OKLAHOMA STATE

filename=06309801
dir=/home/nmruser/data/SMITH_RESEARCH/06309801
com=alanine rxn
date=6/30/98
time=17:10:31
ac=64
ppfn=1PULSEH
# acq's (x 4)=64
spect freq=200.723600MHz
spect freq=200.723600MHz
pulse width =26.50u
spectrum width=2.870kHz
acq time=2854.100m
acq length=8192
pulse delay=8.000s
receiver gain=11
temperature=-274C
# dummy pulses=0
receiver delay=15.00u
spin rate=30Hz
acq delay=35.00u
dim2 length=1
channel=1
dwell=348.40u
predelay=100.0m
acq completed=64
y_scale=10076.156250
tph01=42.892490
tph11=-150.000000
rmp=200.723352
rmv=4.610000
current_size=8192

in MeOH-d4

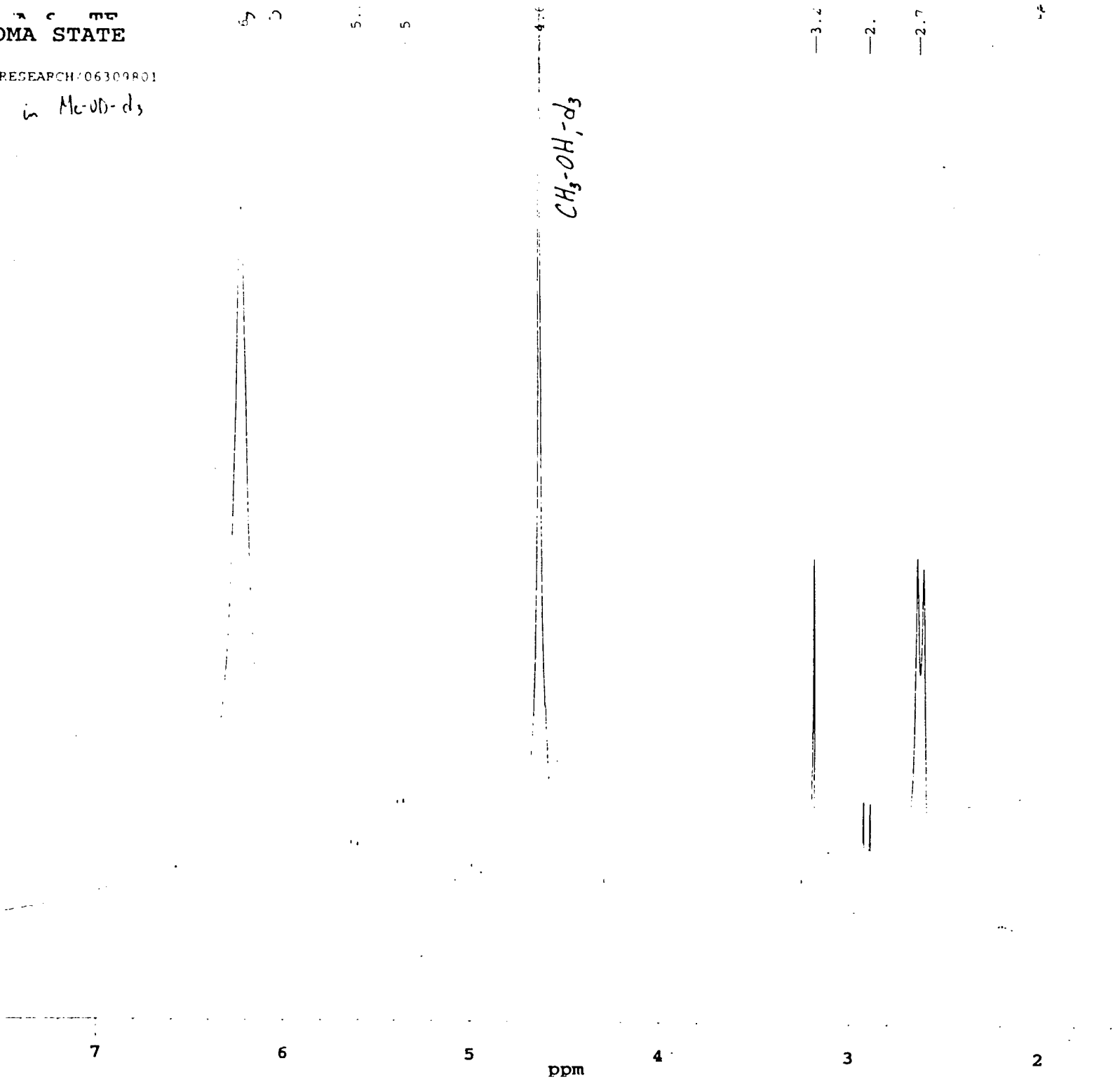

Figure 3
1H NMR of Alanine reaction produc
in MeOH-d4

SOUTHEASTERN OKLAHOMA STATE

filename=07029801
dir=/home/nmruser/data/SMITH_RESEARCH.07029801
com=13C of alanine rxn
date=7/1/98
time=16:27:20
ac=11896
ppfn=WALTZGATE
# acq's (x 4)=200000
spect freq=50.476981MHz
spect freq=200.723200MHz
pulse width =25.00u
spectrum width=14.993kHz
acq time=1092.800m
acq length=16384
pulse delay=8.000s
receiver gain=11
temperature=-274C
# dummy pulses=0
receiver delay=15.00u
spin rate=-1Hz
acq delay=35.00u
# of rows=1
channel=1
dwell=66.70u
predelay=100.0m
acq completed=3
lb1=1.500000
y_scale=82730.578125
tph01=-2.590260
tph11=180.000000
rmp=50.474170
rmv=49.000000
current_size=16384

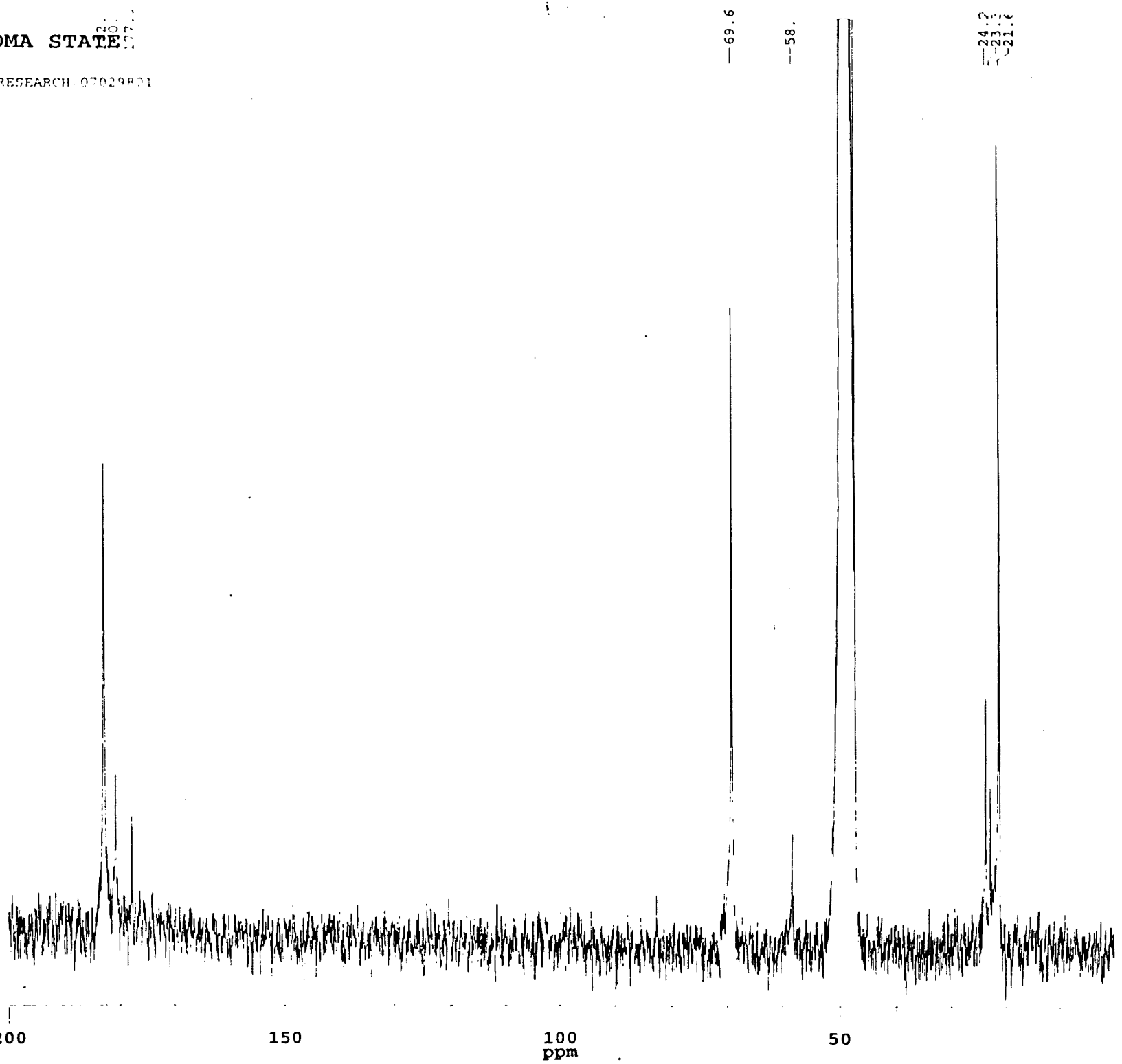

Figure 5
13C NMR of Alanine reaction product in MeOH-d4

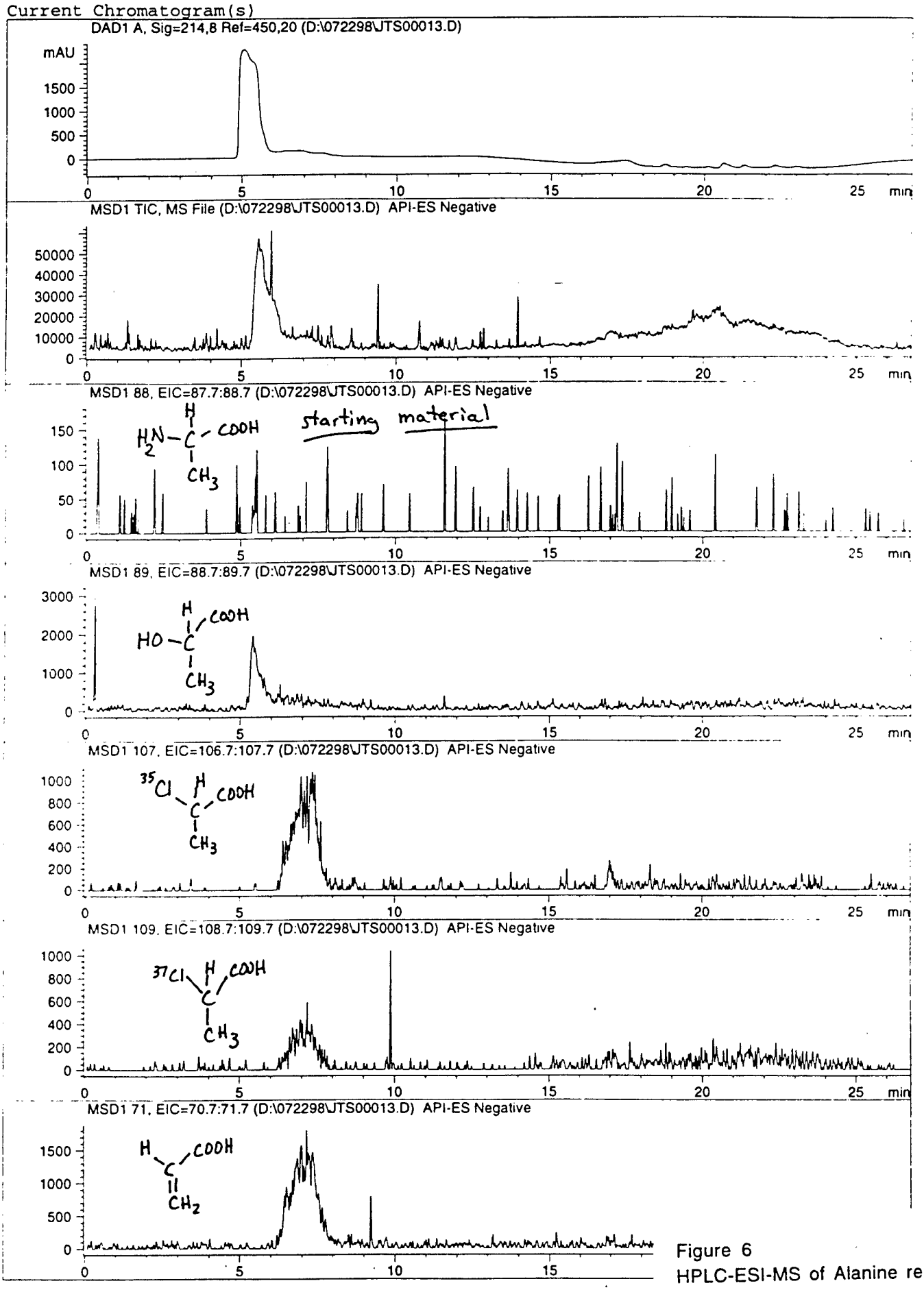

Figure 6
HPLC-ESI-MS of Alanine reactio

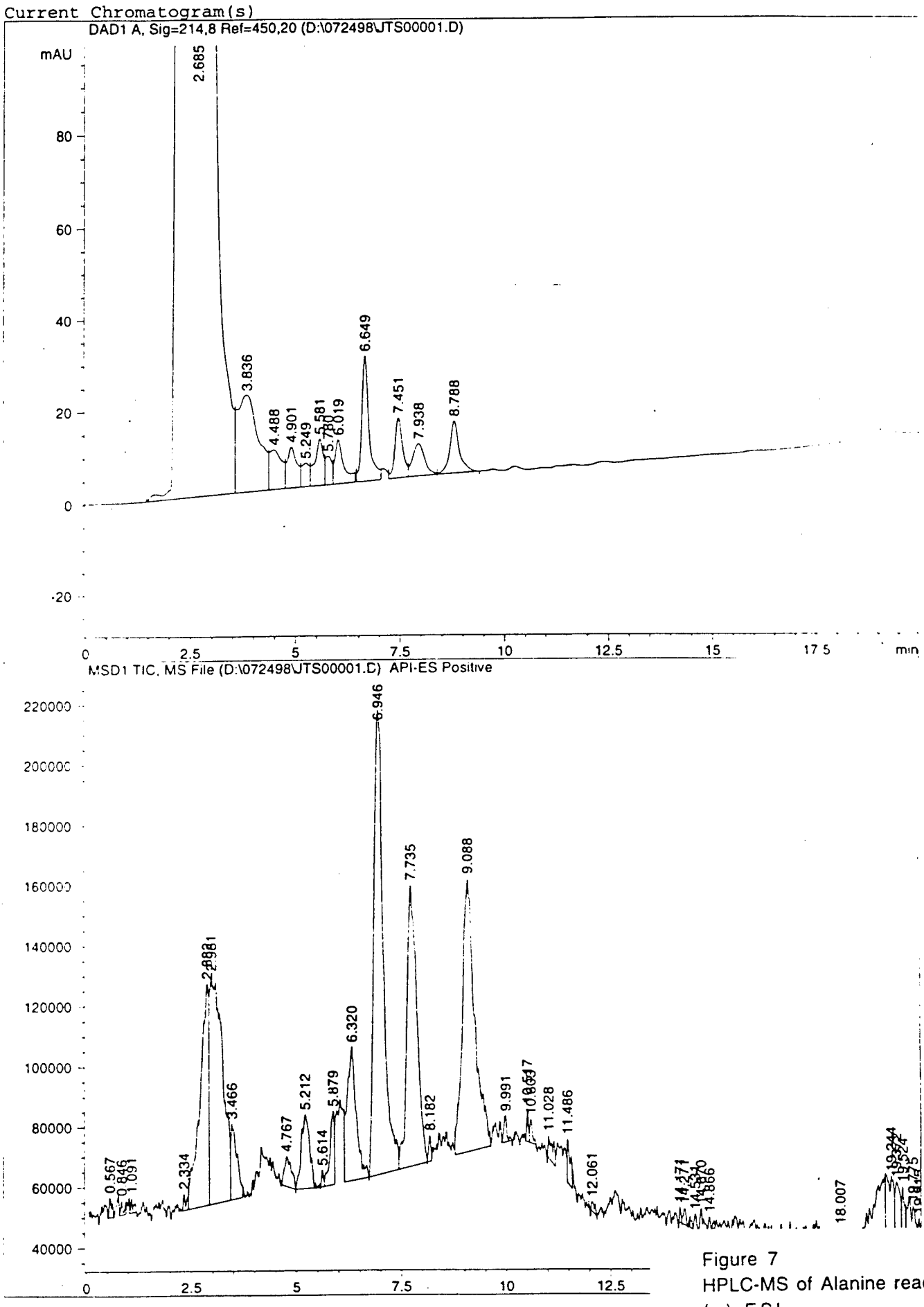

Figure 7
HPLC-MS of Alanine reaction
(+)-ESI

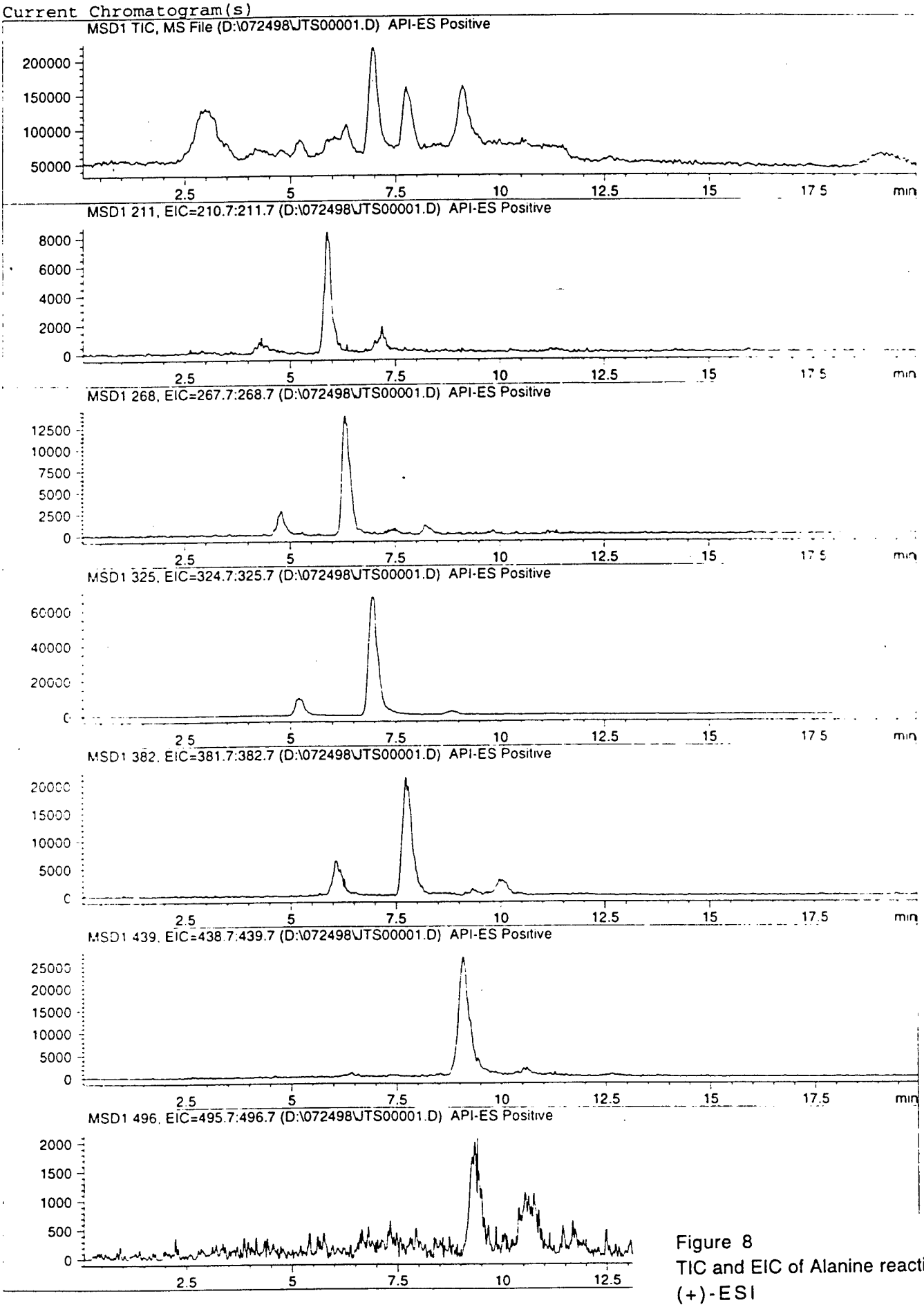

Figure 8
TIC and EIC of Alanine reaction
(+)-ESI

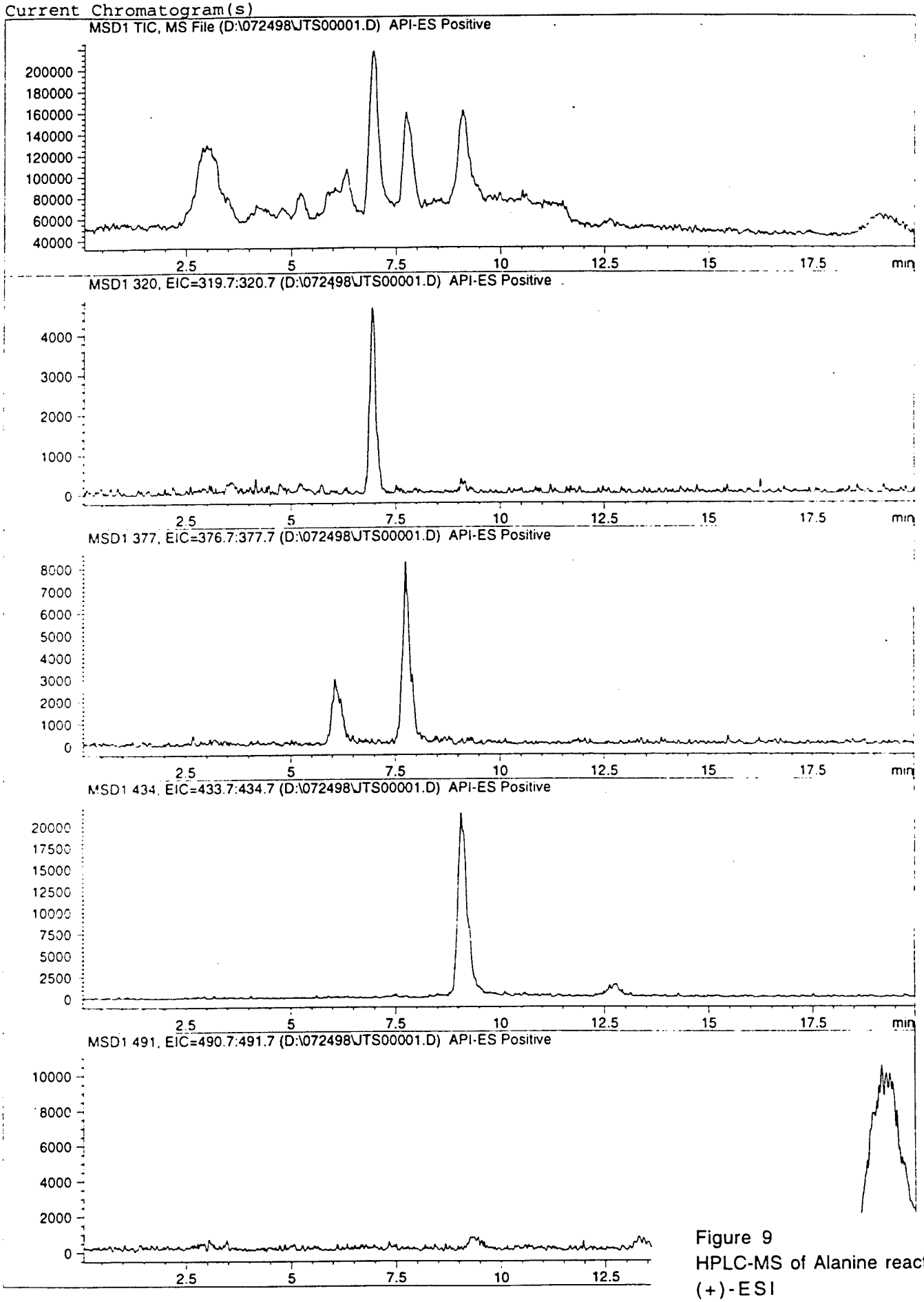

Figure 9
HPLC-MS of Alanine reaction
(+)-ESI

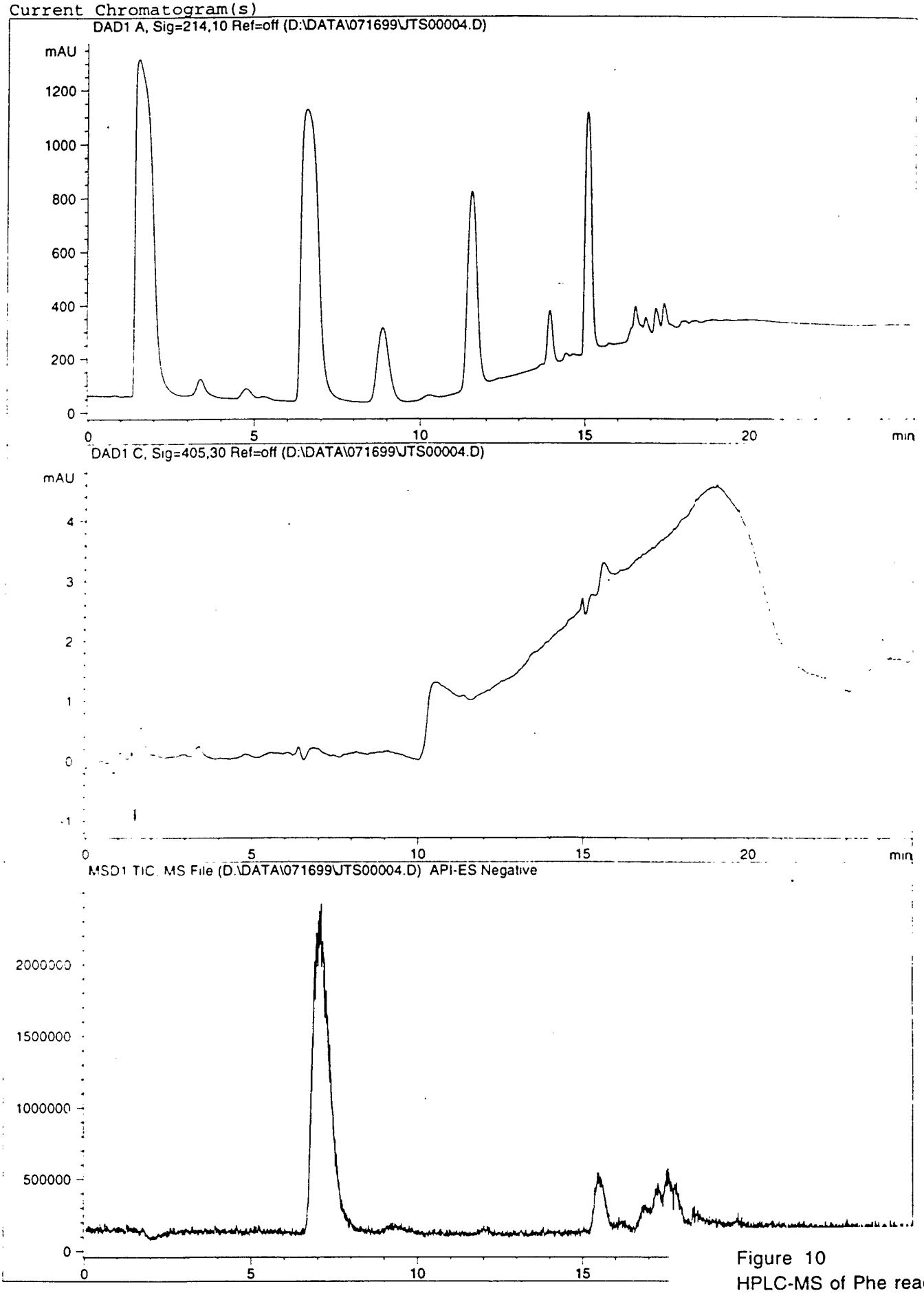

Figure 10
HPLC-MS of Phe reaction
(-)-ESI

strument 1 7/3/00 11:02:35 AM

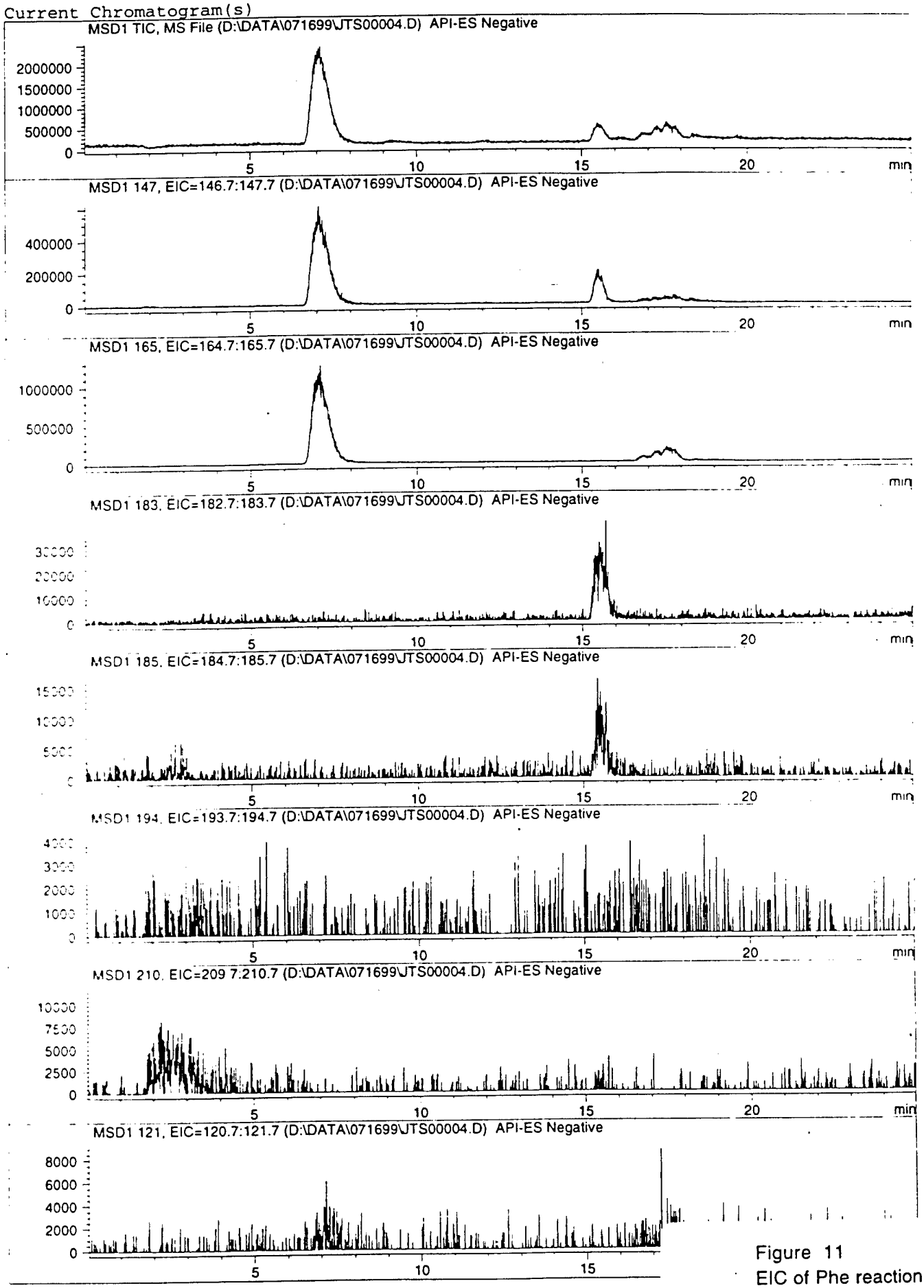

Figure 11
EIC of Phe reaction
(-)-ESI

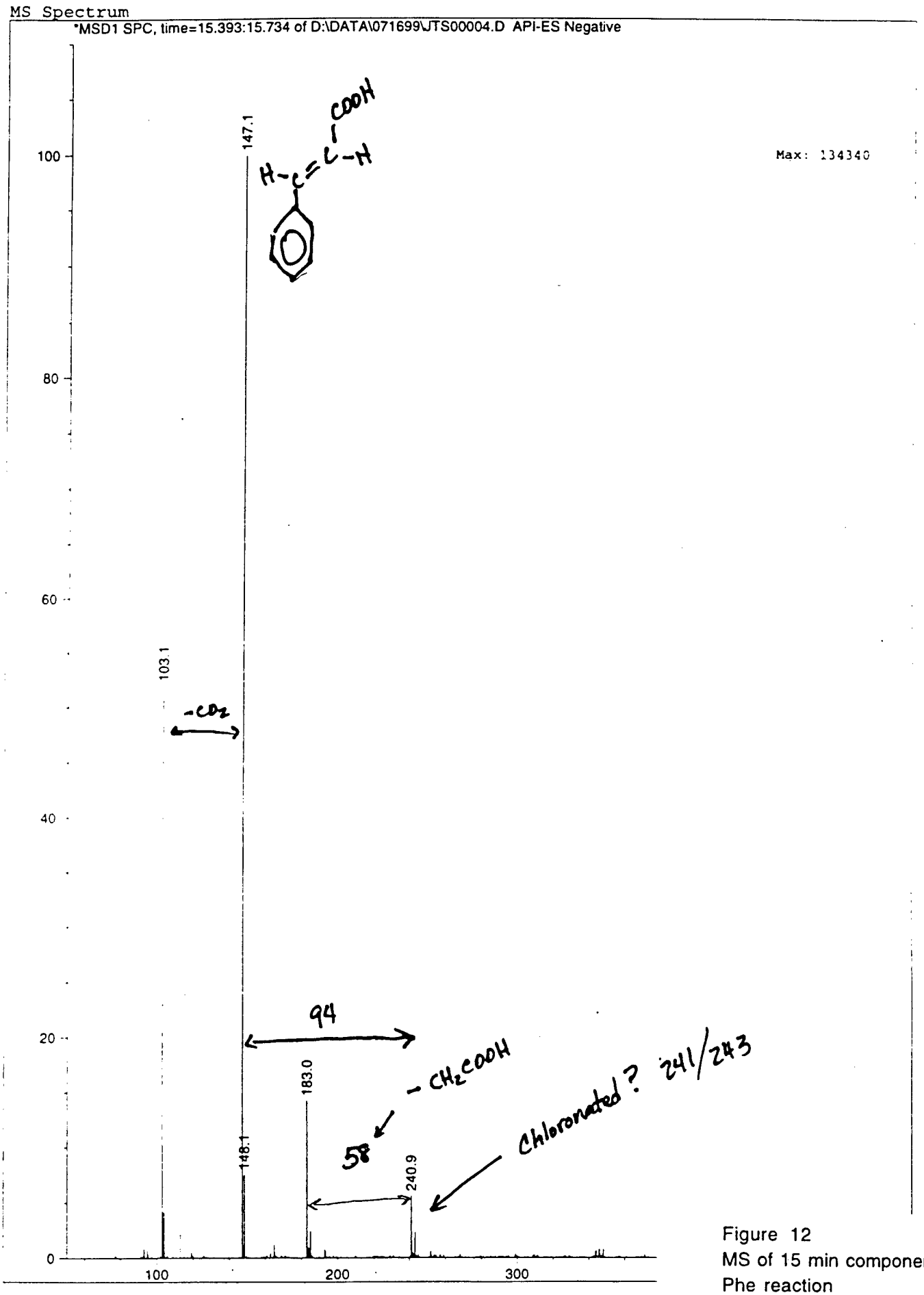

Figure 12
MS of 15 min component
Phe reaction
(-)-ESI

strument 1 7/3/00 11:23:56 AM

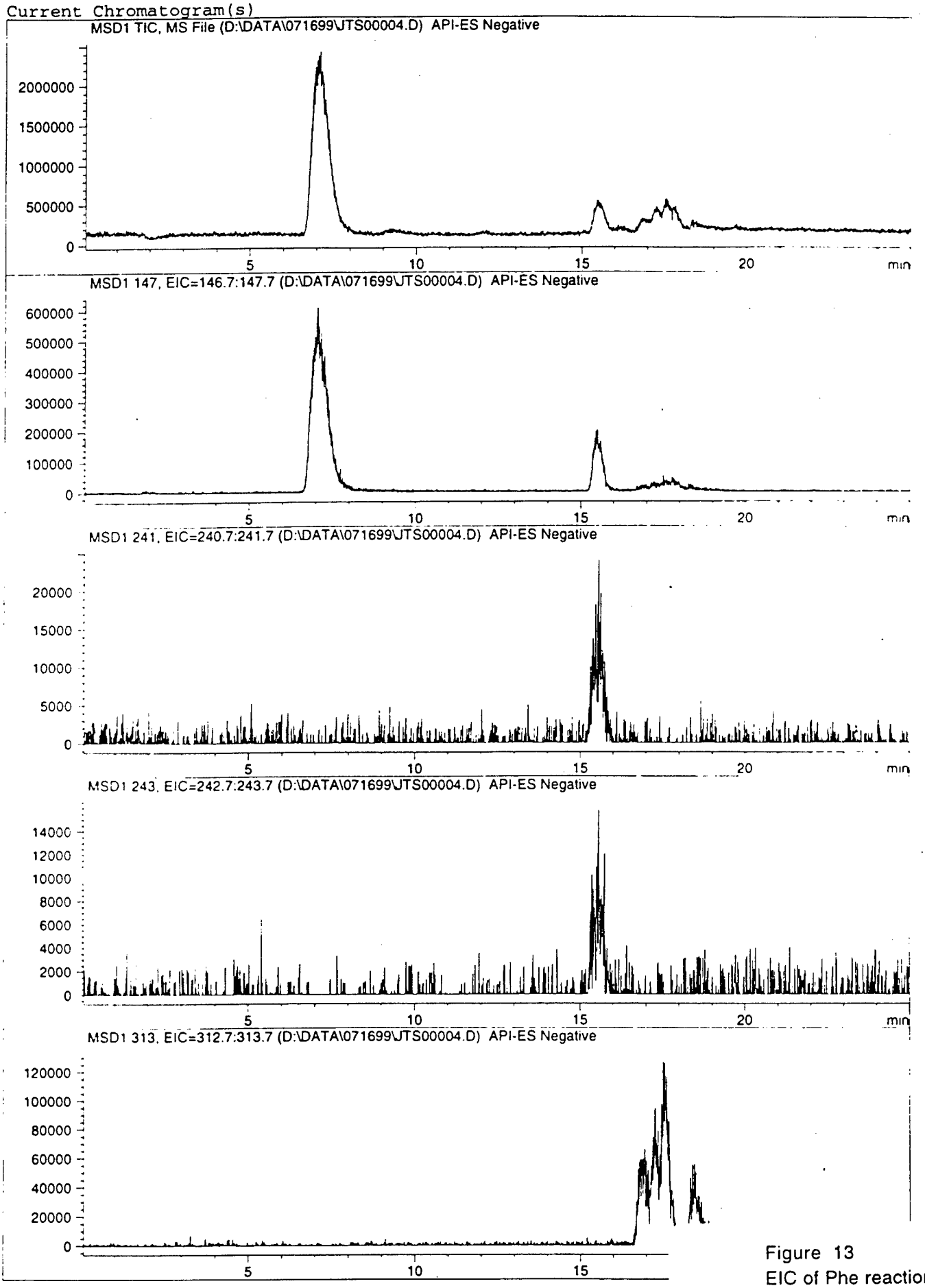

Figure 13
EIC of Phe reaction
(-)-ESI

MS Spectrum

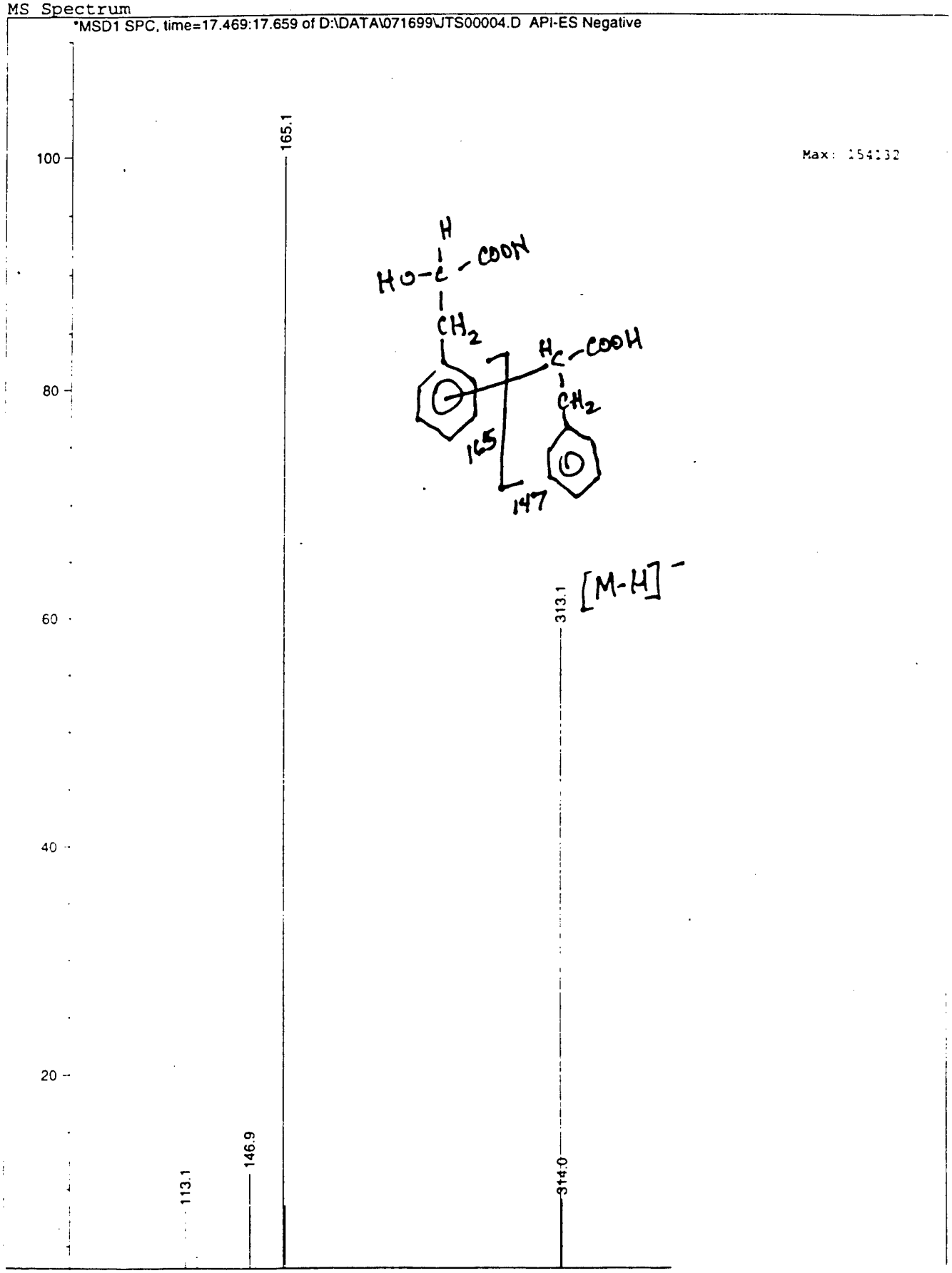

Figure 14
MS of 17.5 min component
Phe reaction
(-)-ESI

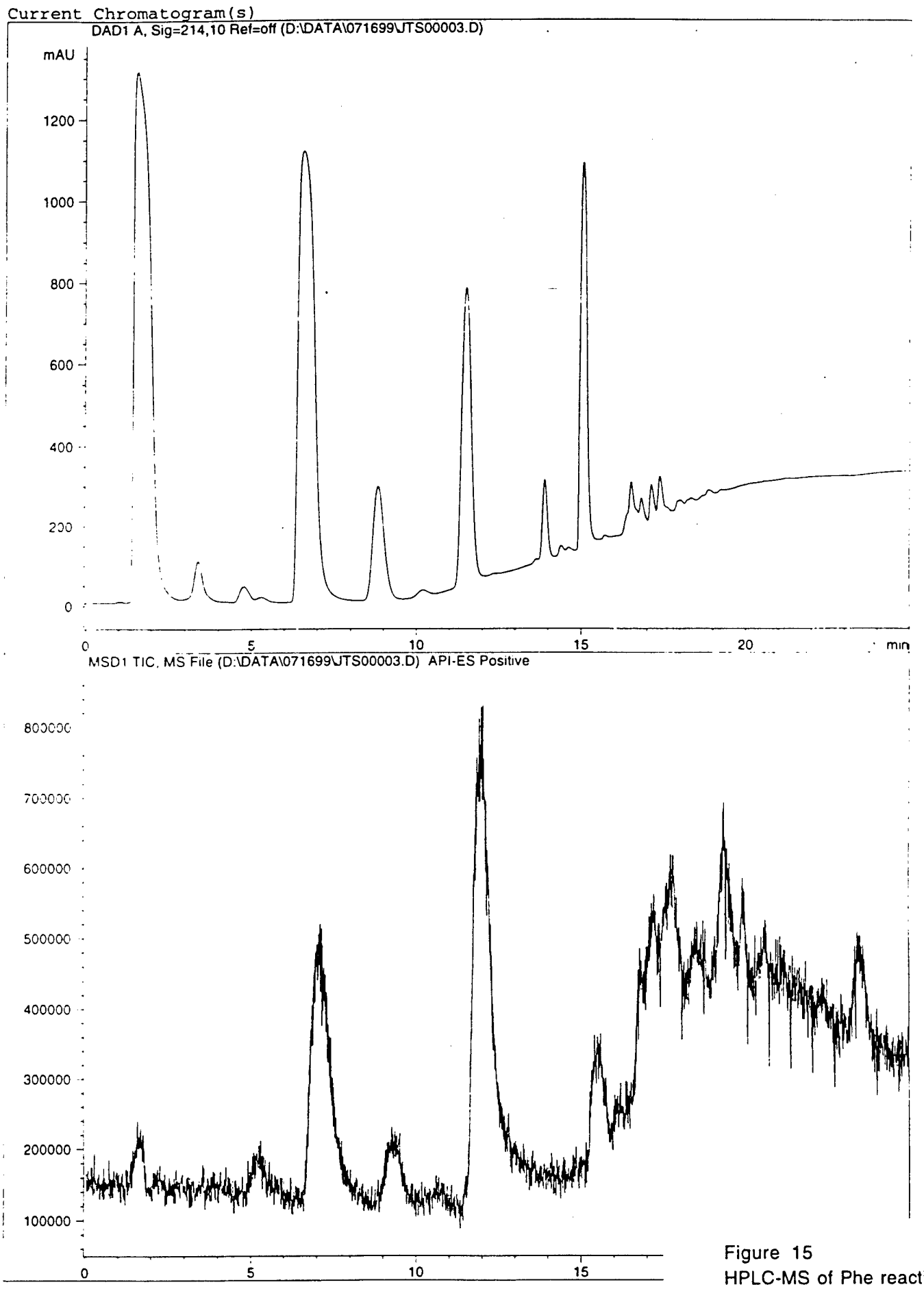

Figure 15
HPLC-MS of Phe reaction
(+)-ESI

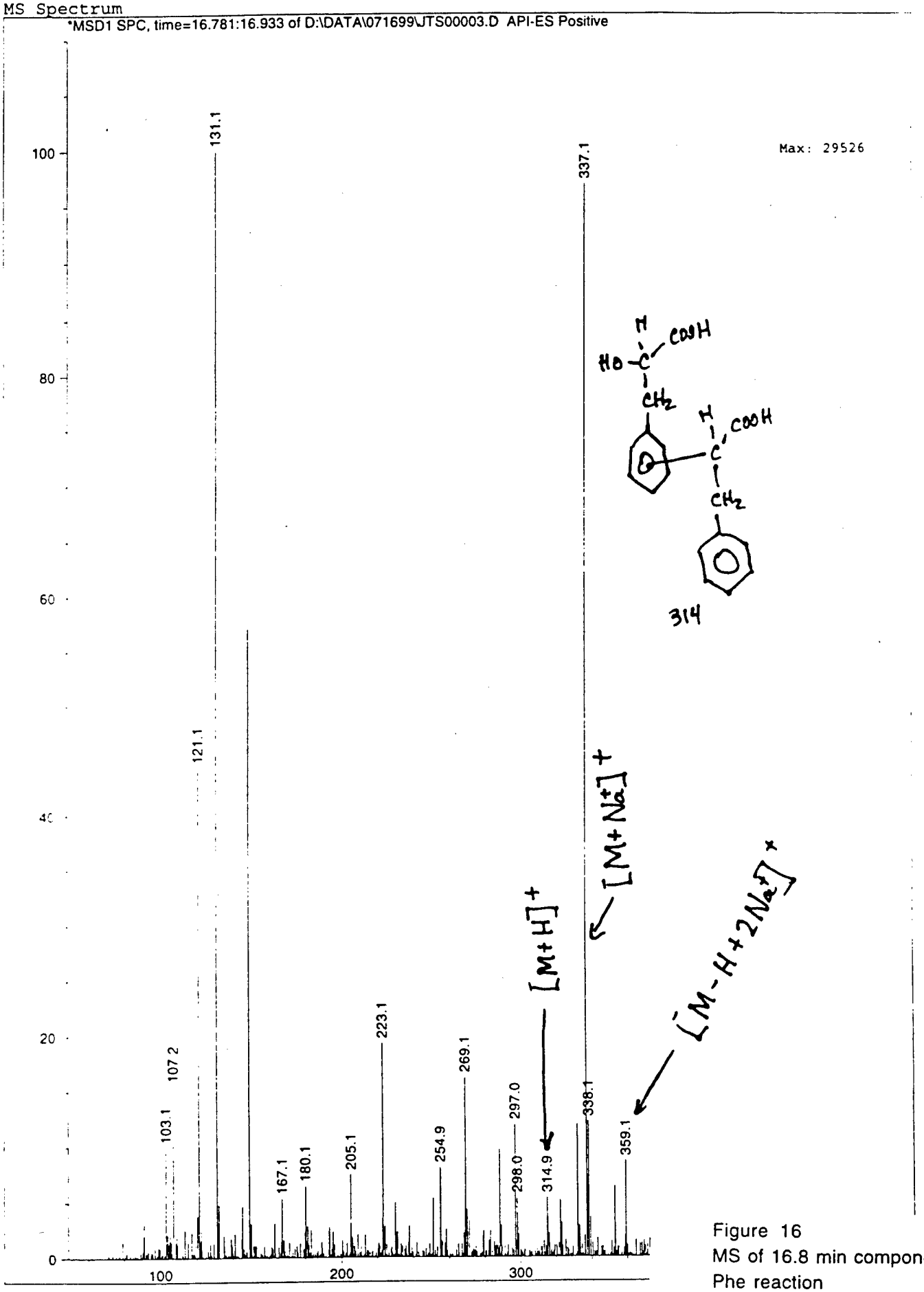

Figure 16
MS of 16.8 min component
Phe reaction
(+)-ESI

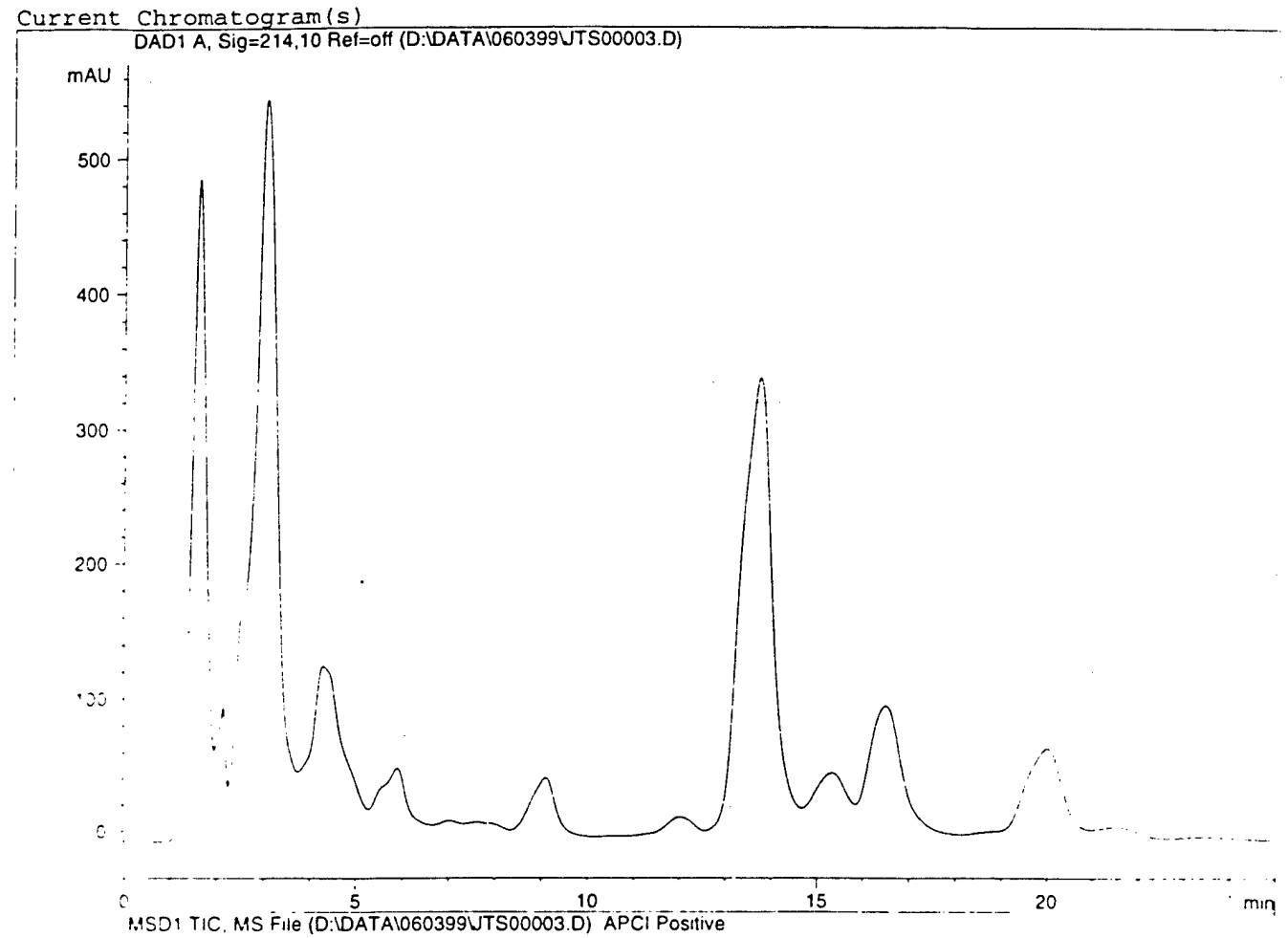

Figure 17
HPLC-MS of Phe reaction
CH2Cl2 extract
(+)-APCI

strument 1 7/3/00 1:16:14 PM

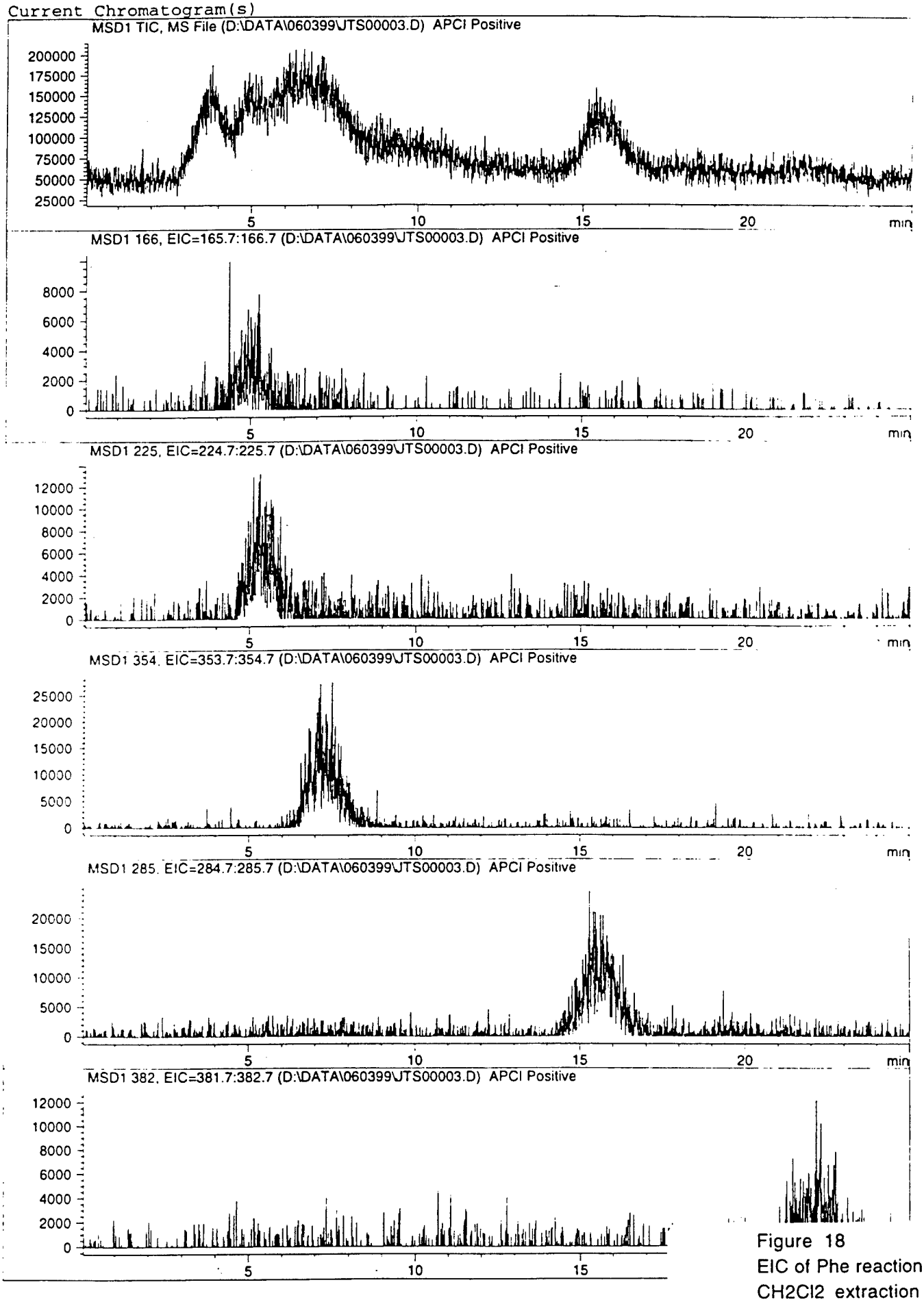

Figure 18
EIC of Phe reaction
CH2Cl2 extraction
(+)-APCI

strument 1 7/3/00 1:22:36 PM

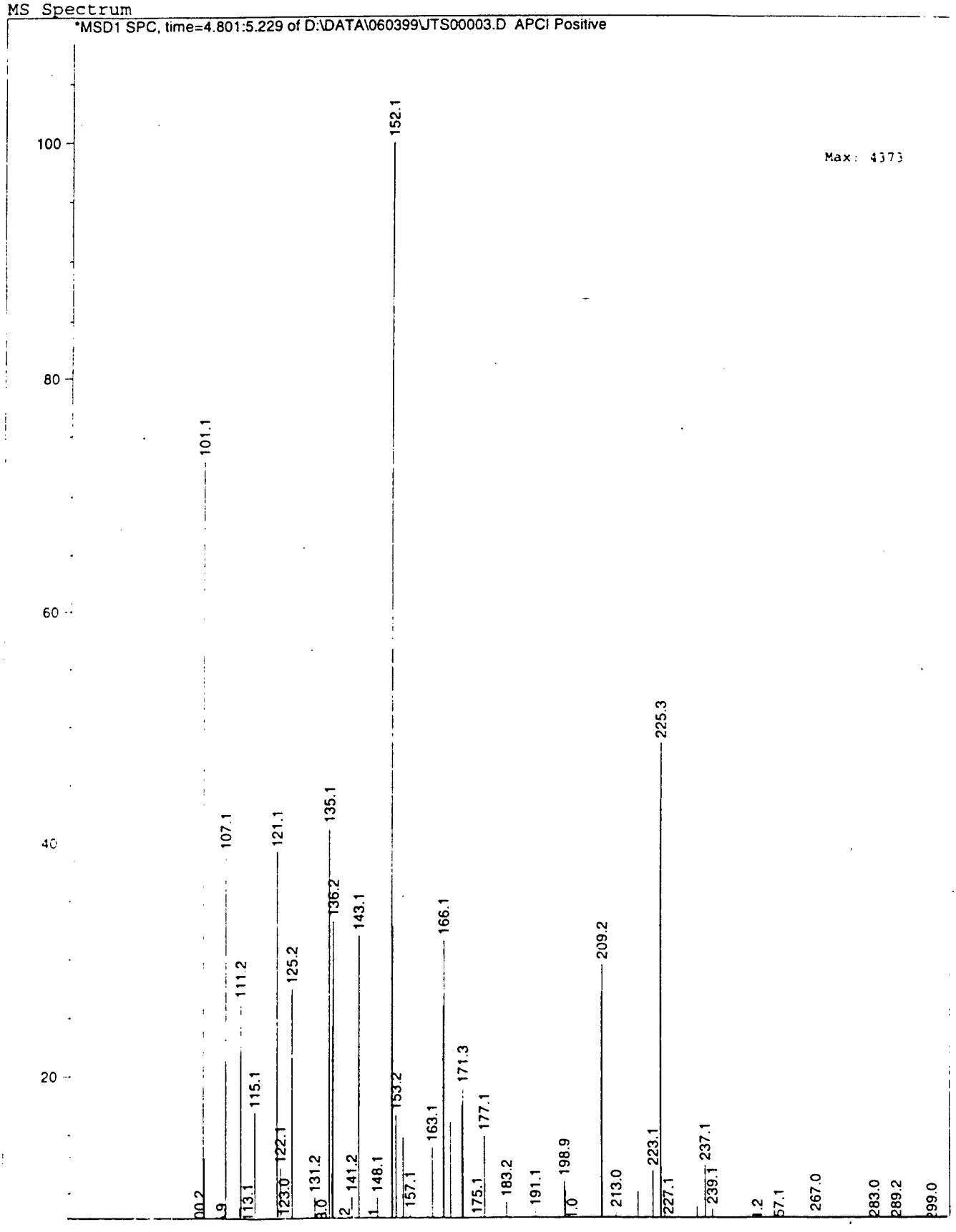

Figure 19a
MS of 5.0 min component
Phe reaction - CH2CL2
(+)-APCI

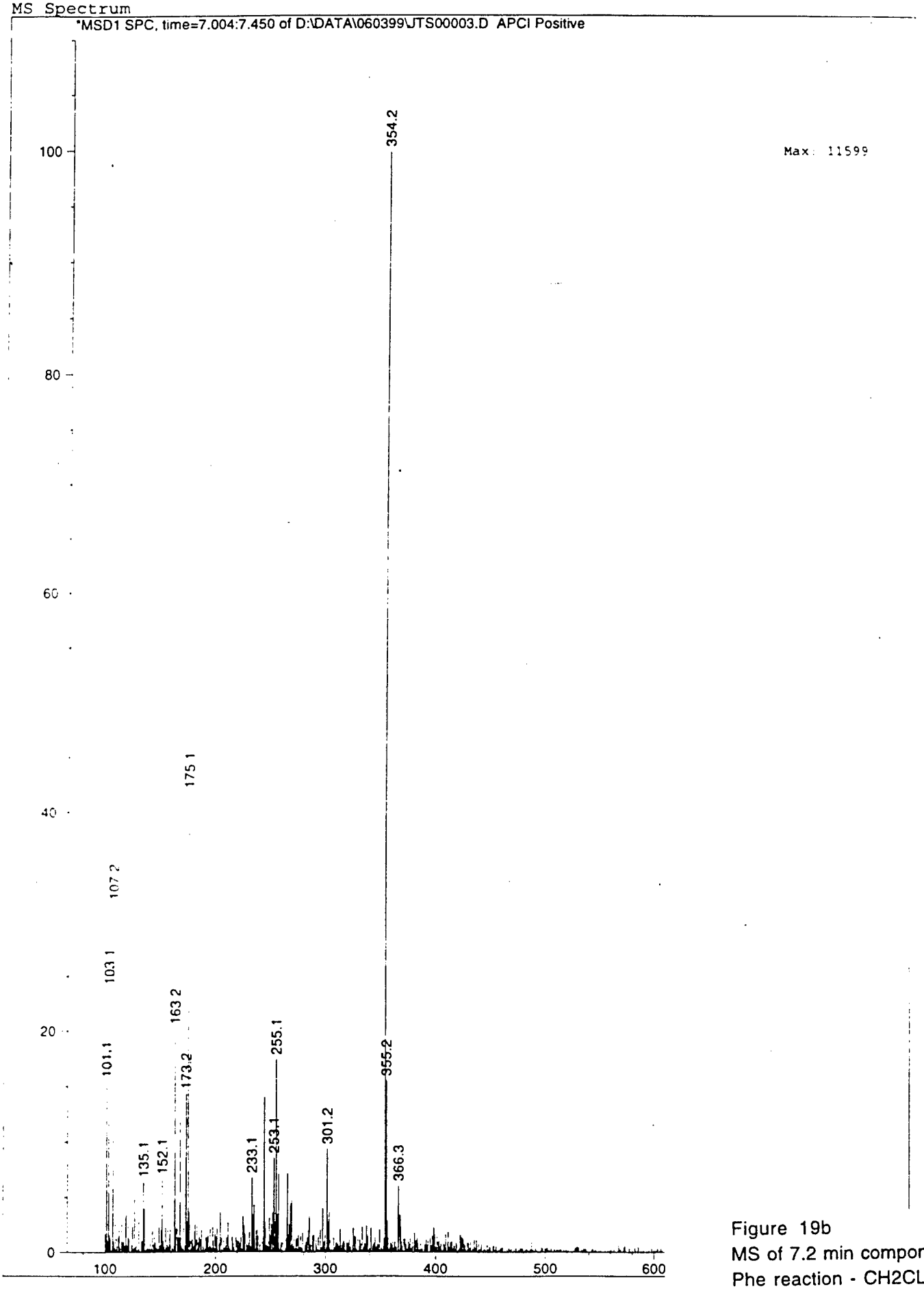

Figure 19b
MS of 7.2 min component
Phe reaction - CH2CL2
(+)-APCI

.strument 1 7/3/00 1:16:56 PM

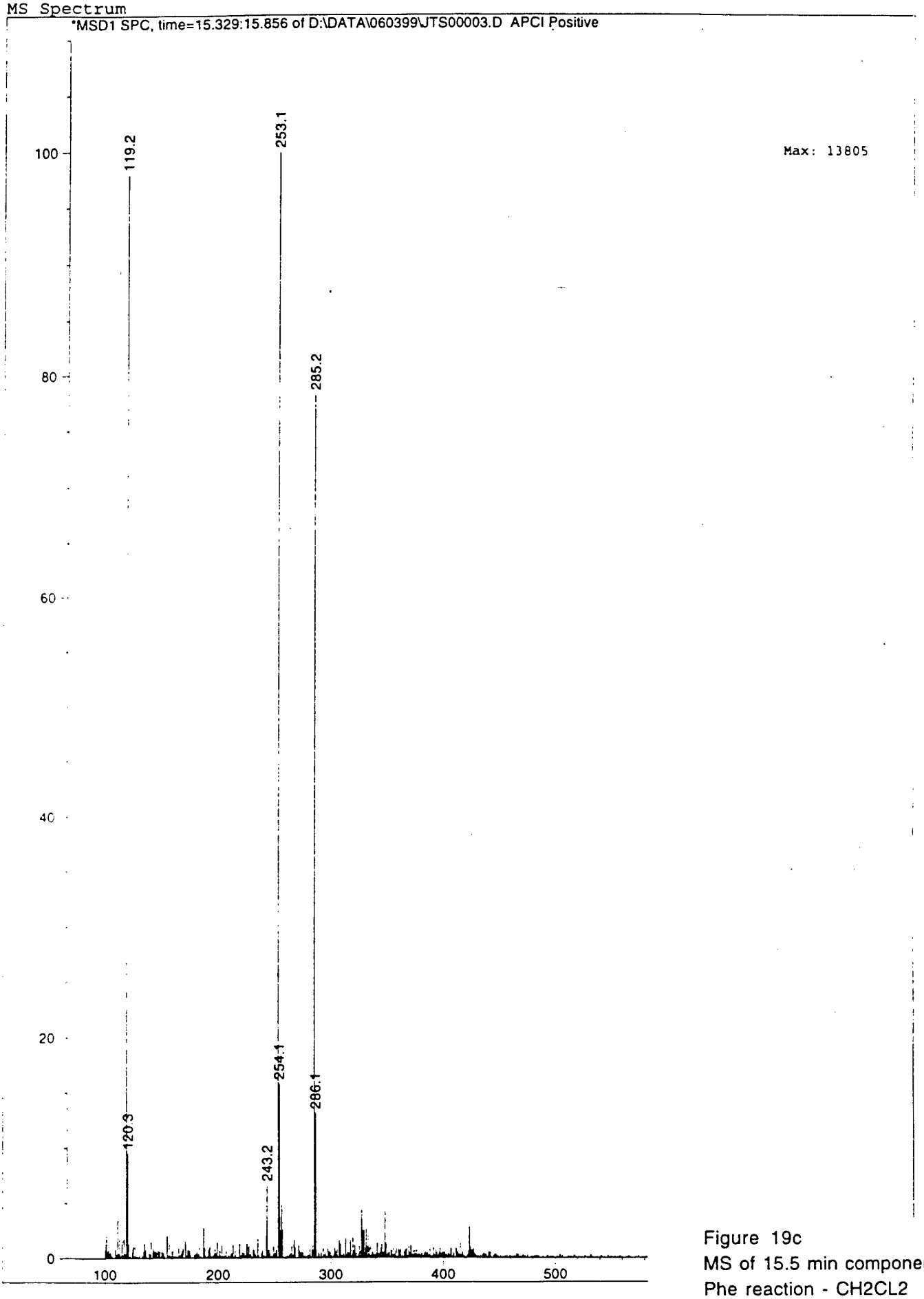

strument 1 7/3/00 1:16:34 PM

Figure 19c
MS of 15.5 min component
Phe reaction - CH2CL2
(+)-APCI

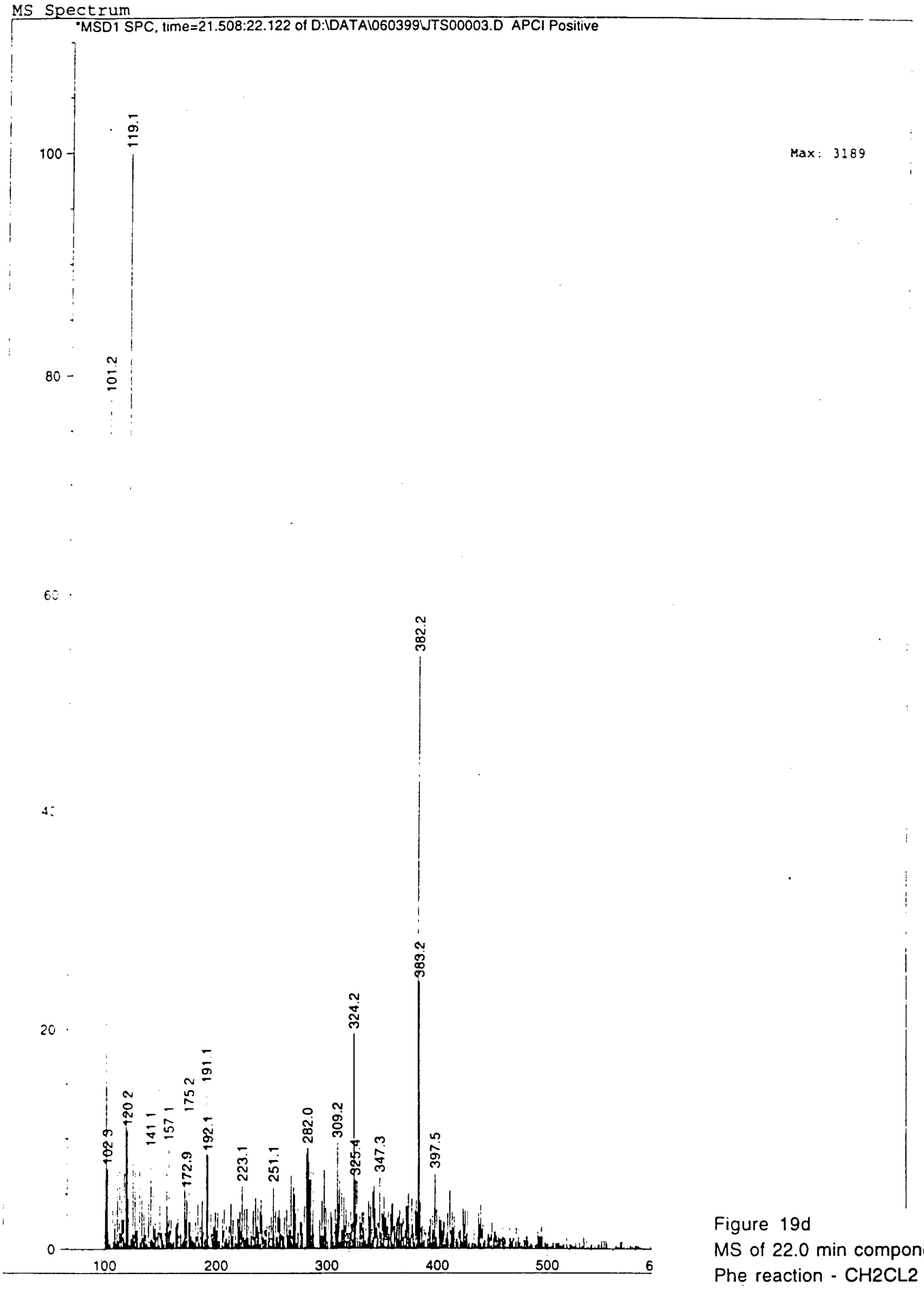

Figure 19d
MS of 22.0 min component
Phe reaction - CH2CL2
(+)-APCI

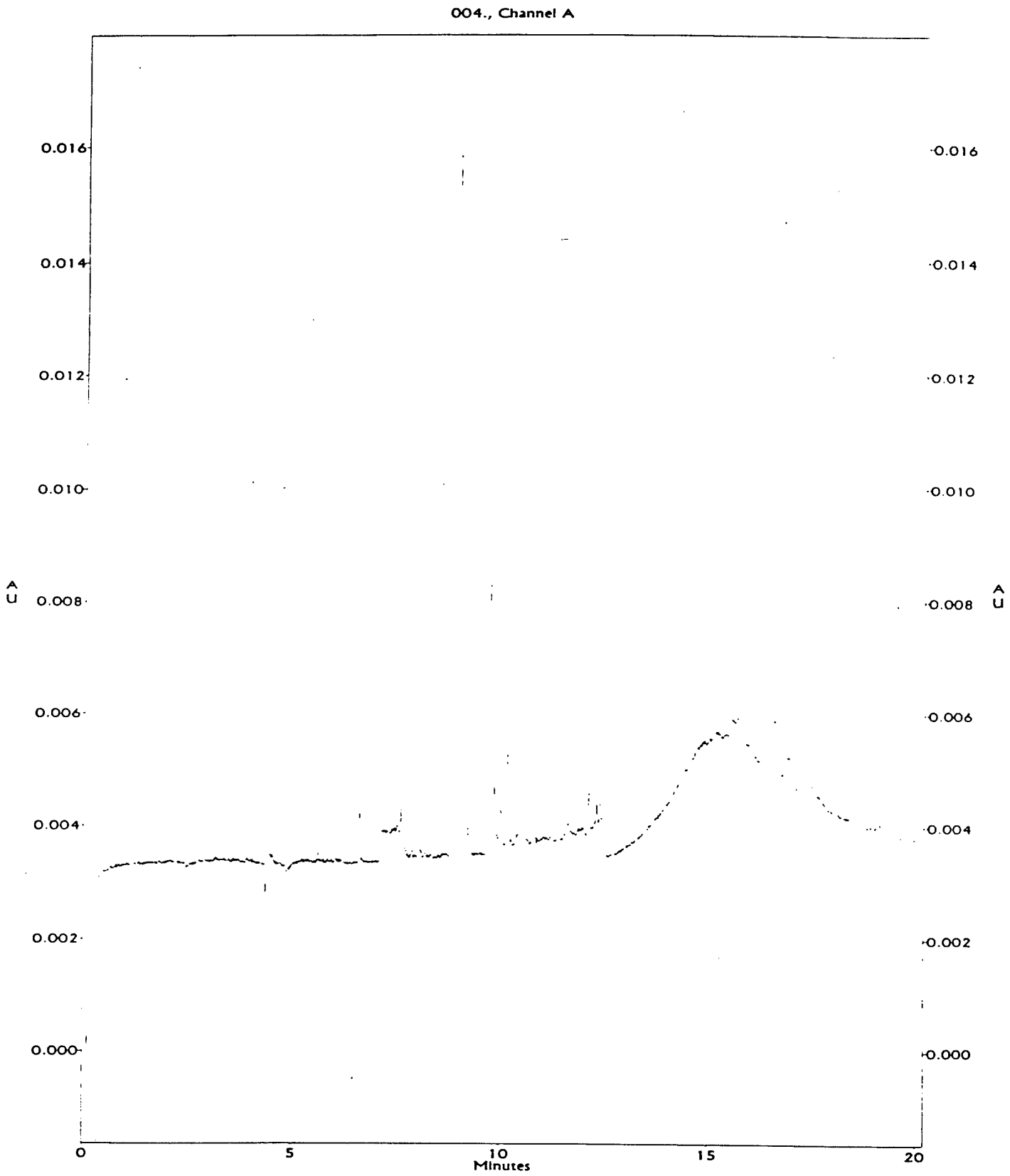

Figure 20
CE of Tyr reaction products
214 nm

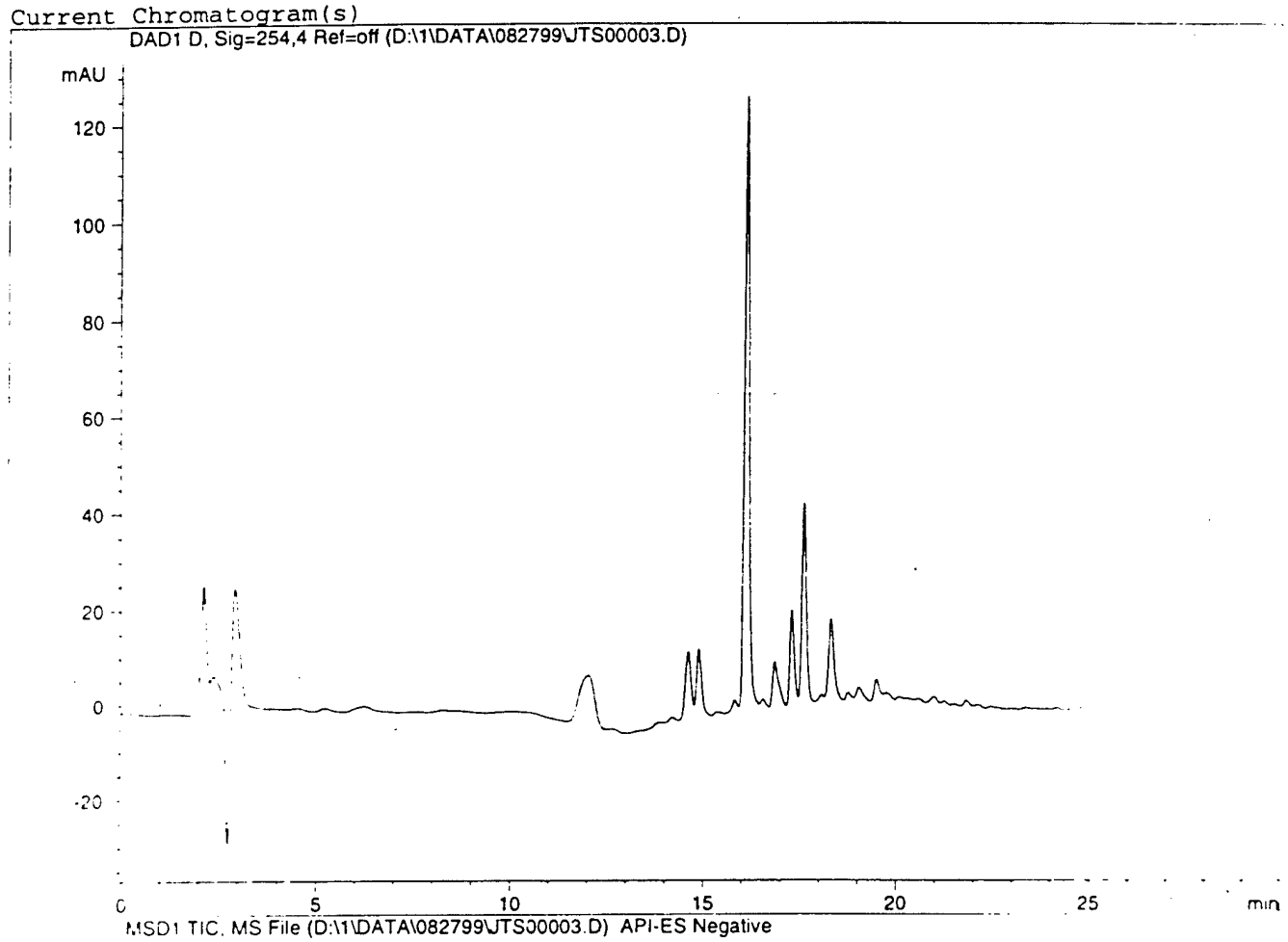

Figure 22
HPLC-MS of Tyr reaction
(-)-ESI

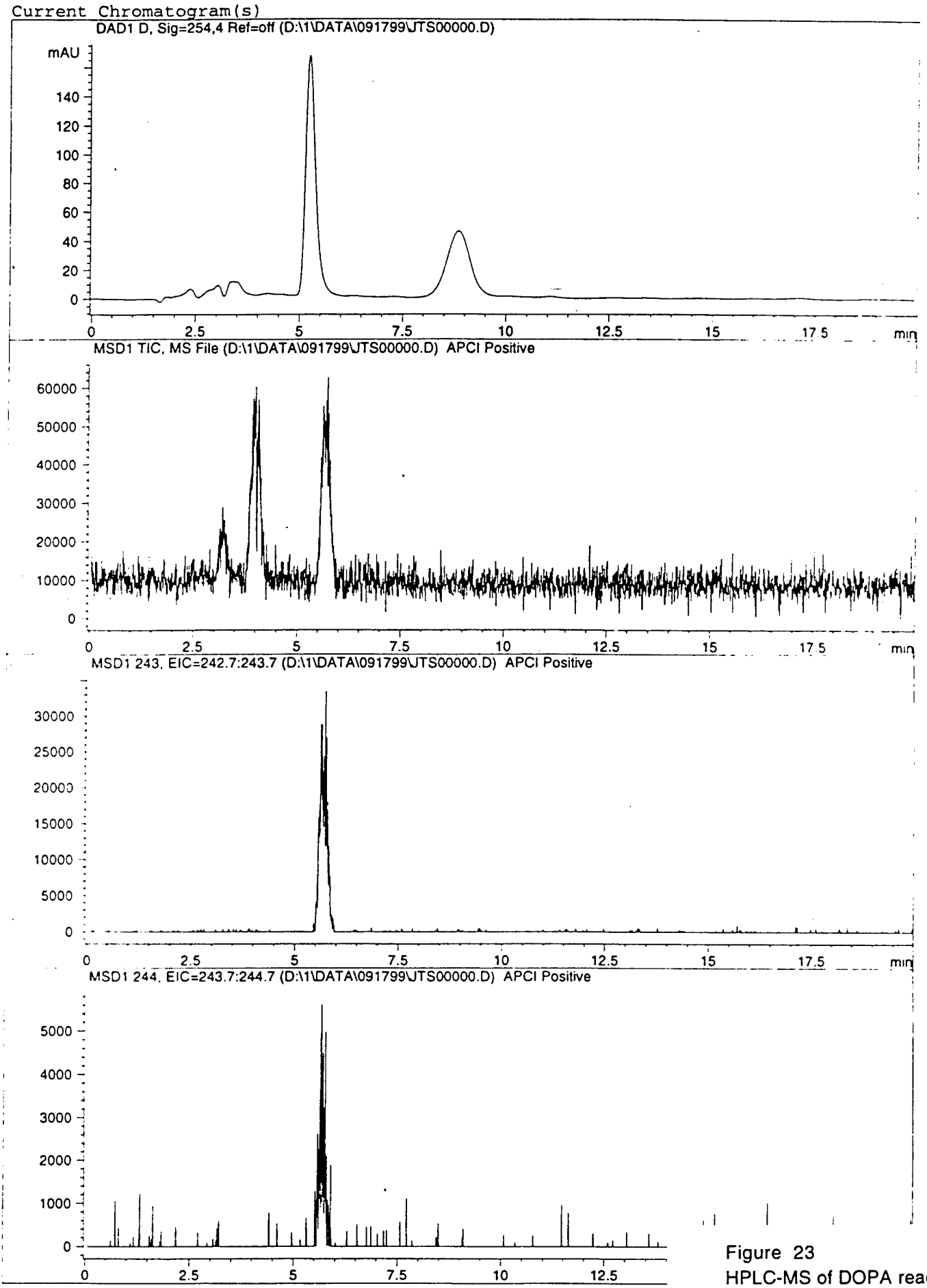

Figure 23
HPLC-MS of DOPA reaction
(+)-APCI

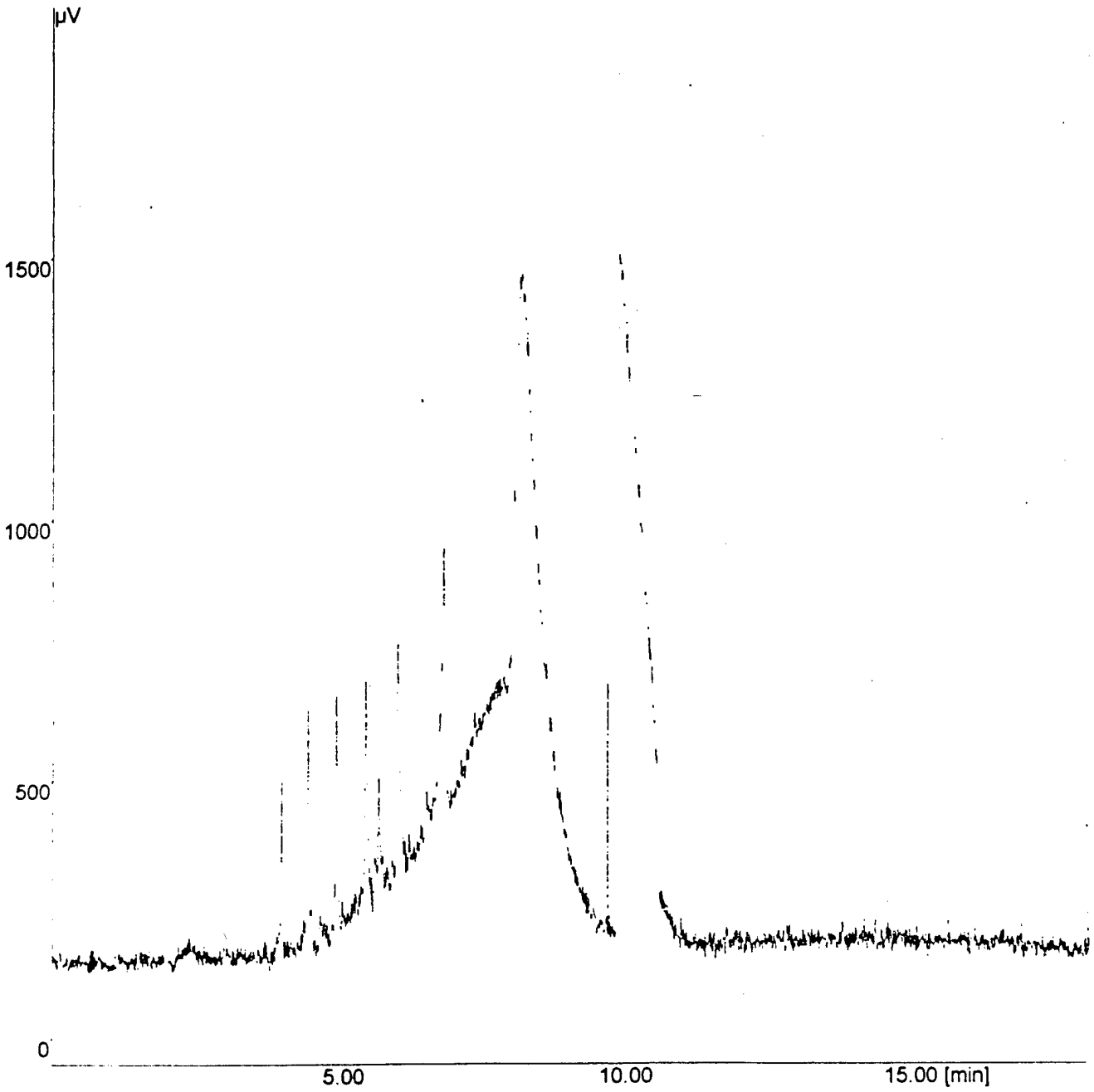

File name : 08059001.CH1 User : ETH Curr. Date : 3-Jul-00 16:41:52

Acqu. Date : 5-Aug-99 10:03:06

Info :
HAHA rxn Aqueous freeze dried in run buffer
run Buffer 25 mM NH4OH
214 wavelength
(+) polarity 15 kilovolts; Current 5 microamps

Vial # = 1 Rack # = 1

Control Method :

Peak Detection Not Available

-Jul-00 16:41:52,ETH,Page 1

Figure 24
CE of HAHA reaction
214 nm

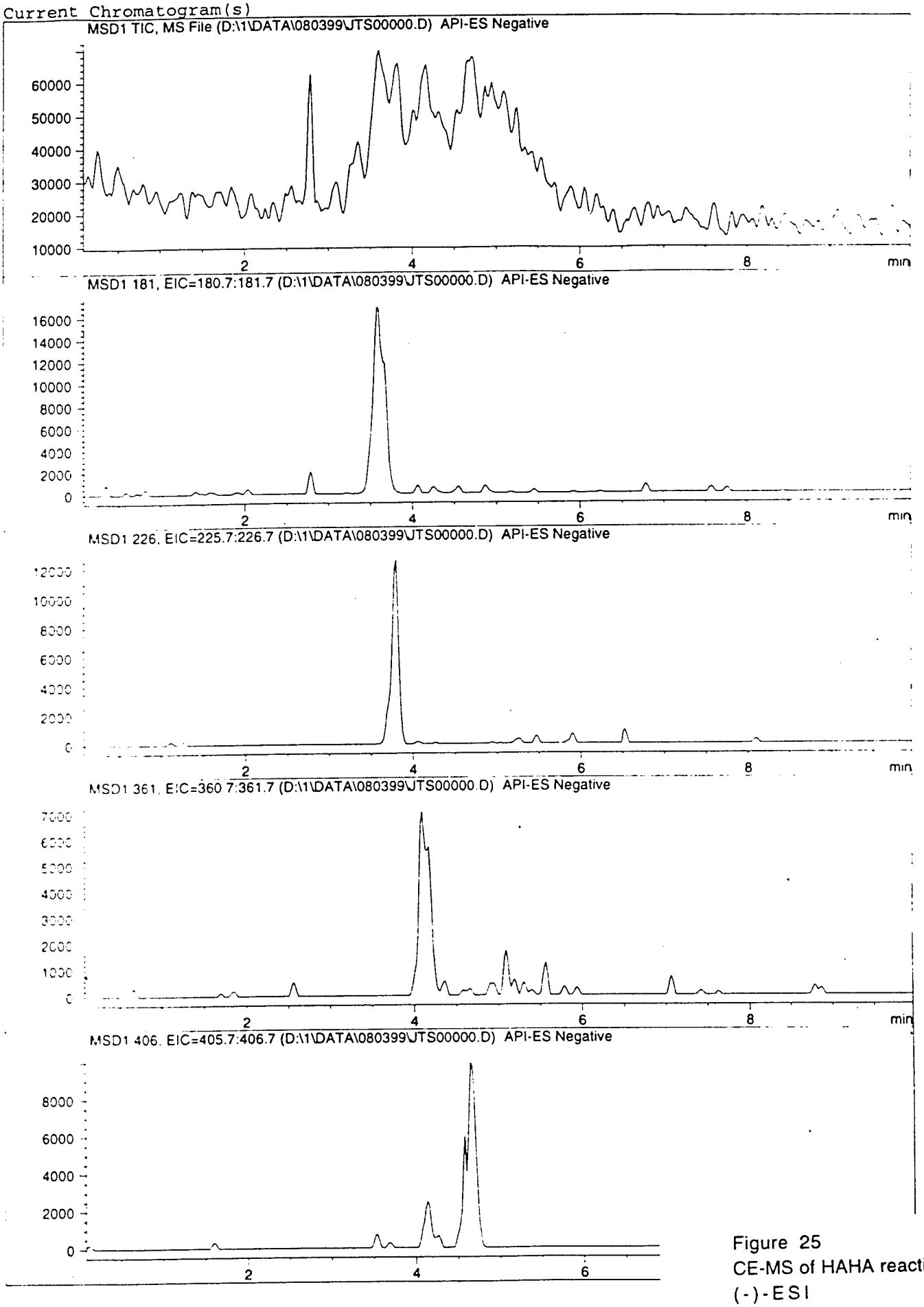

Figure 25
CE-MS of HAHA reaction
(-)-ESI

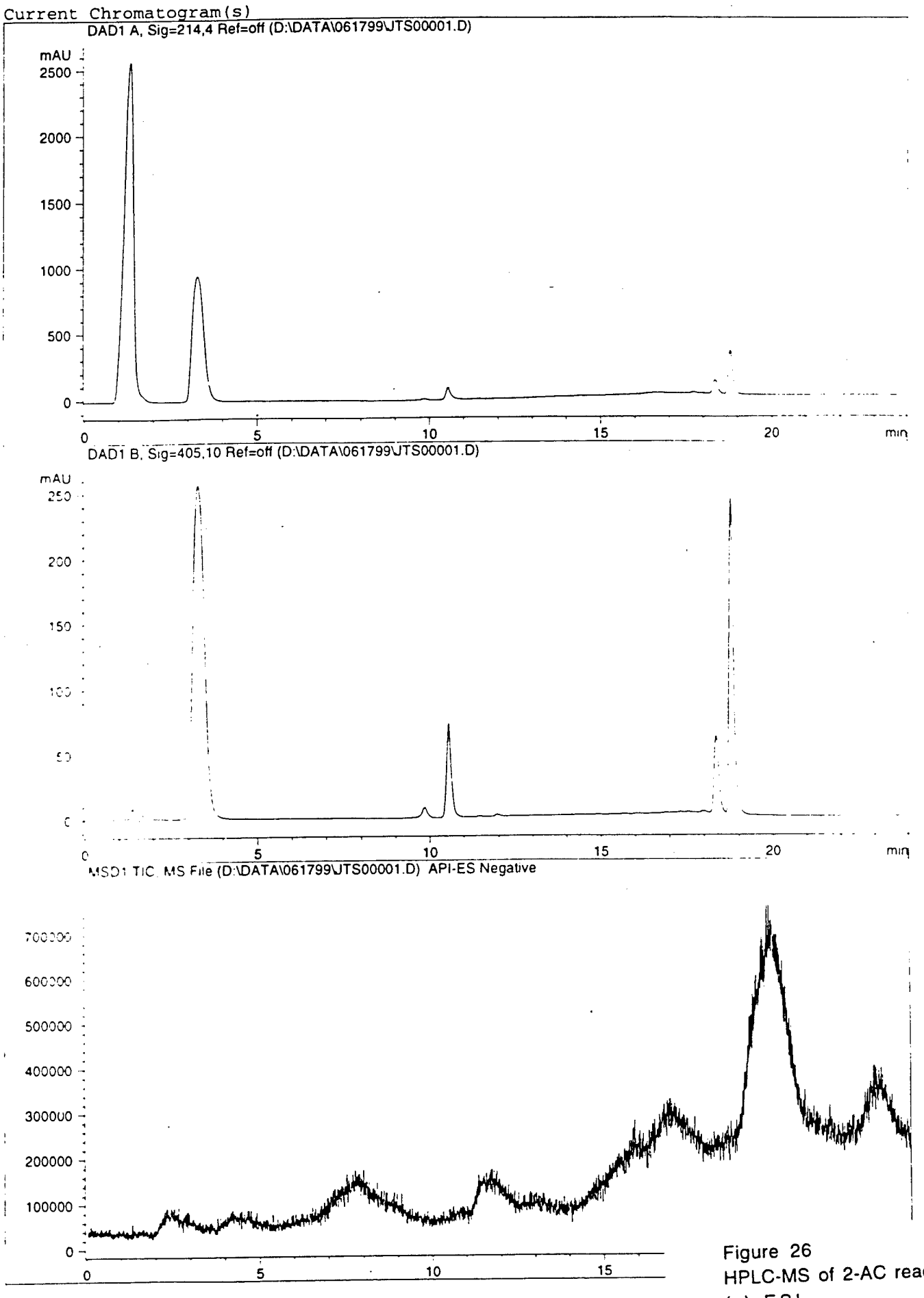

Figure 26
HPLC-MS of 2-AC reaction
(-)-ESI

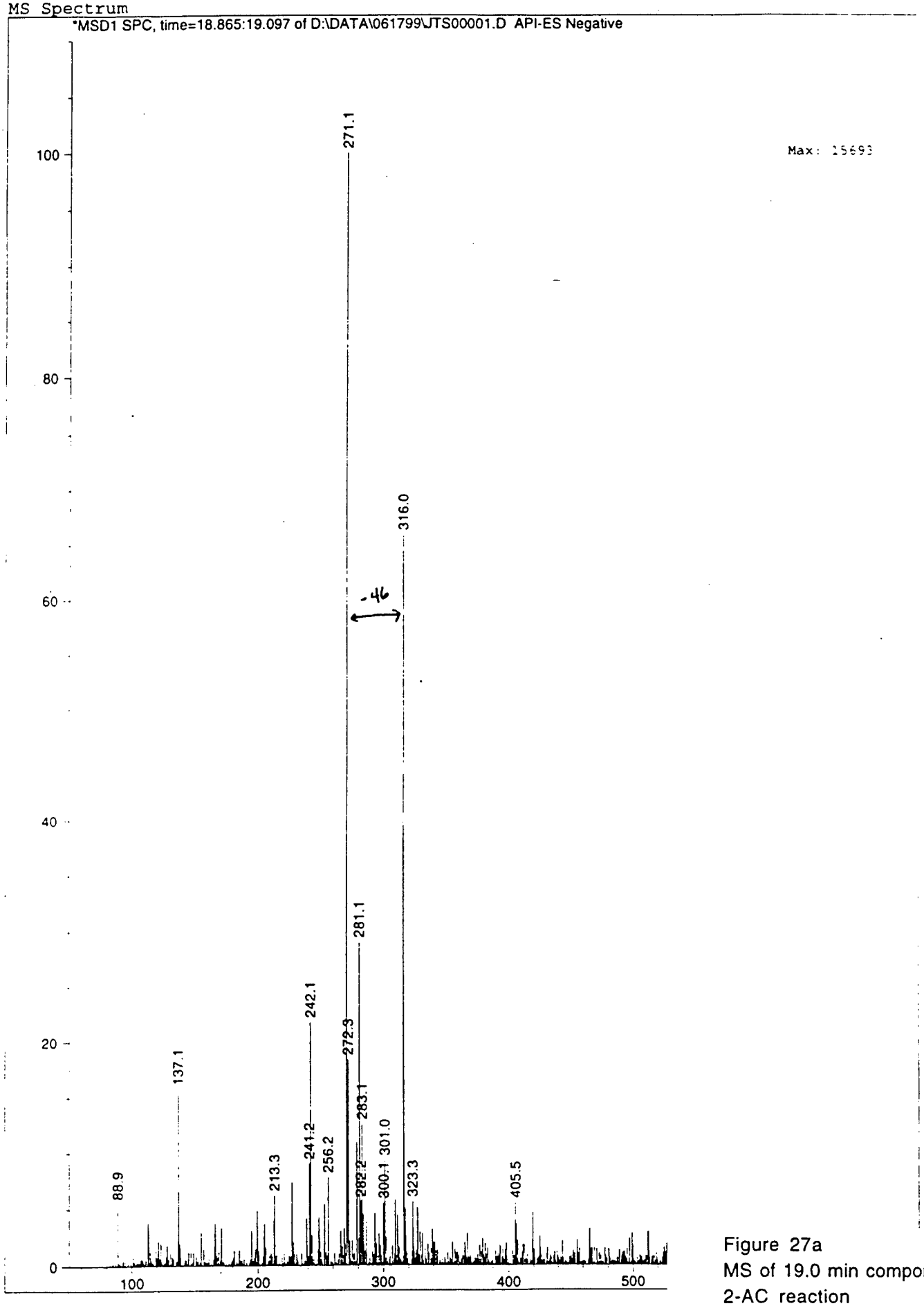

Figure 27a
MS of 19.0 min component
2-AC reaction
(-)-ESI

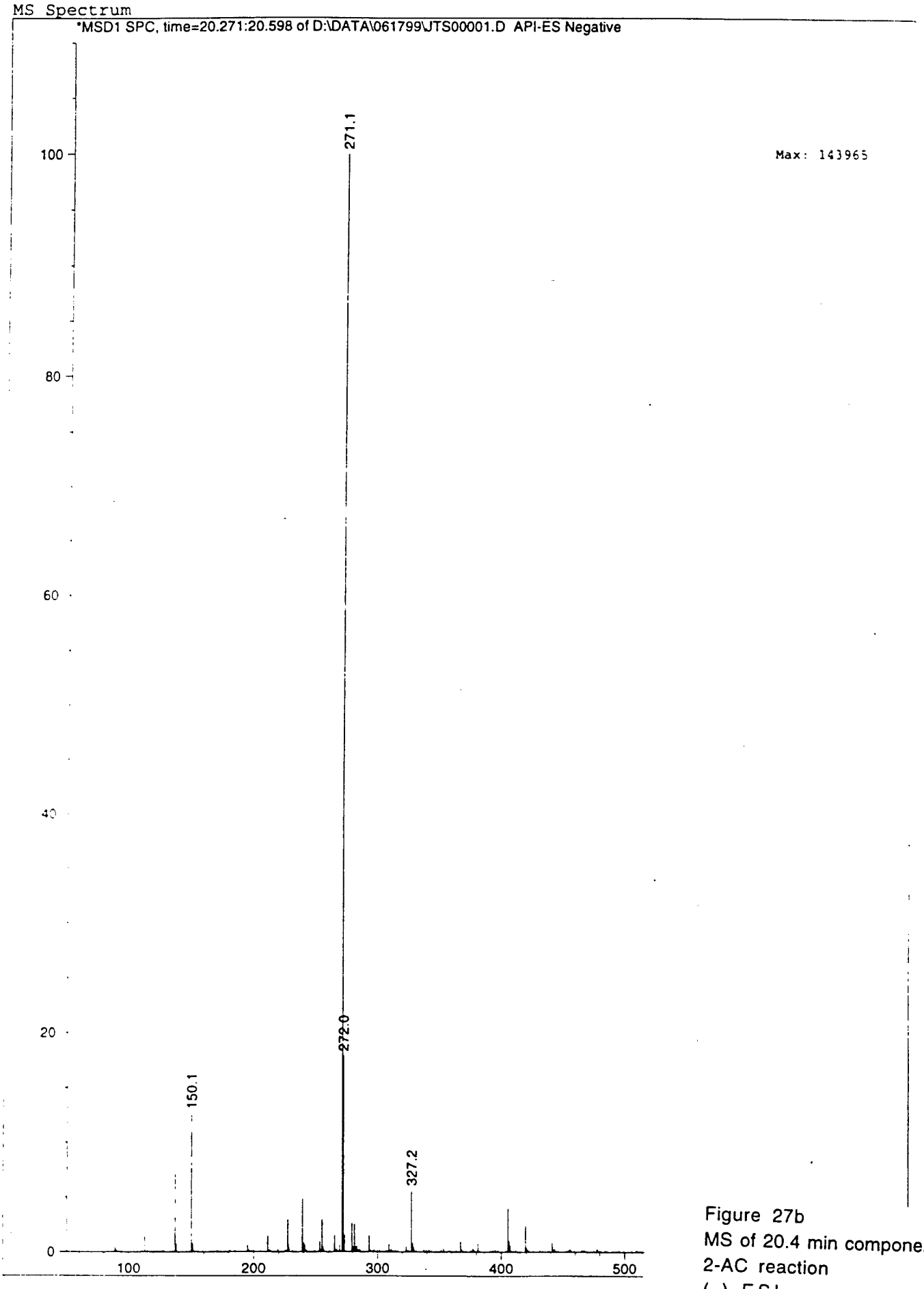

Figure 27b
MS of 20.4 min component
2-AC reaction
(-)-ESI

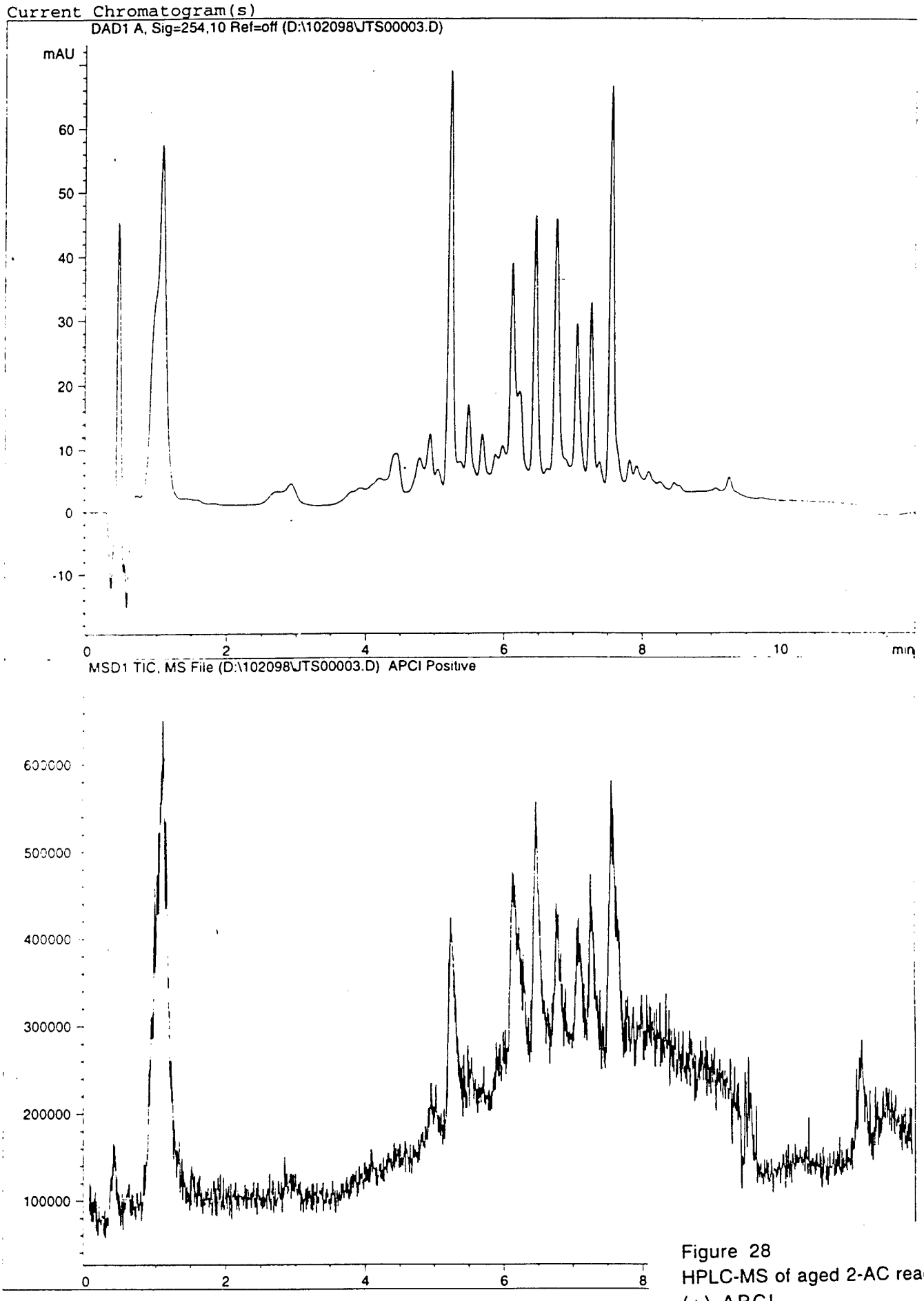

Figure 28
HPLC-MS of aged 2-AC reaction
(+)-APCI

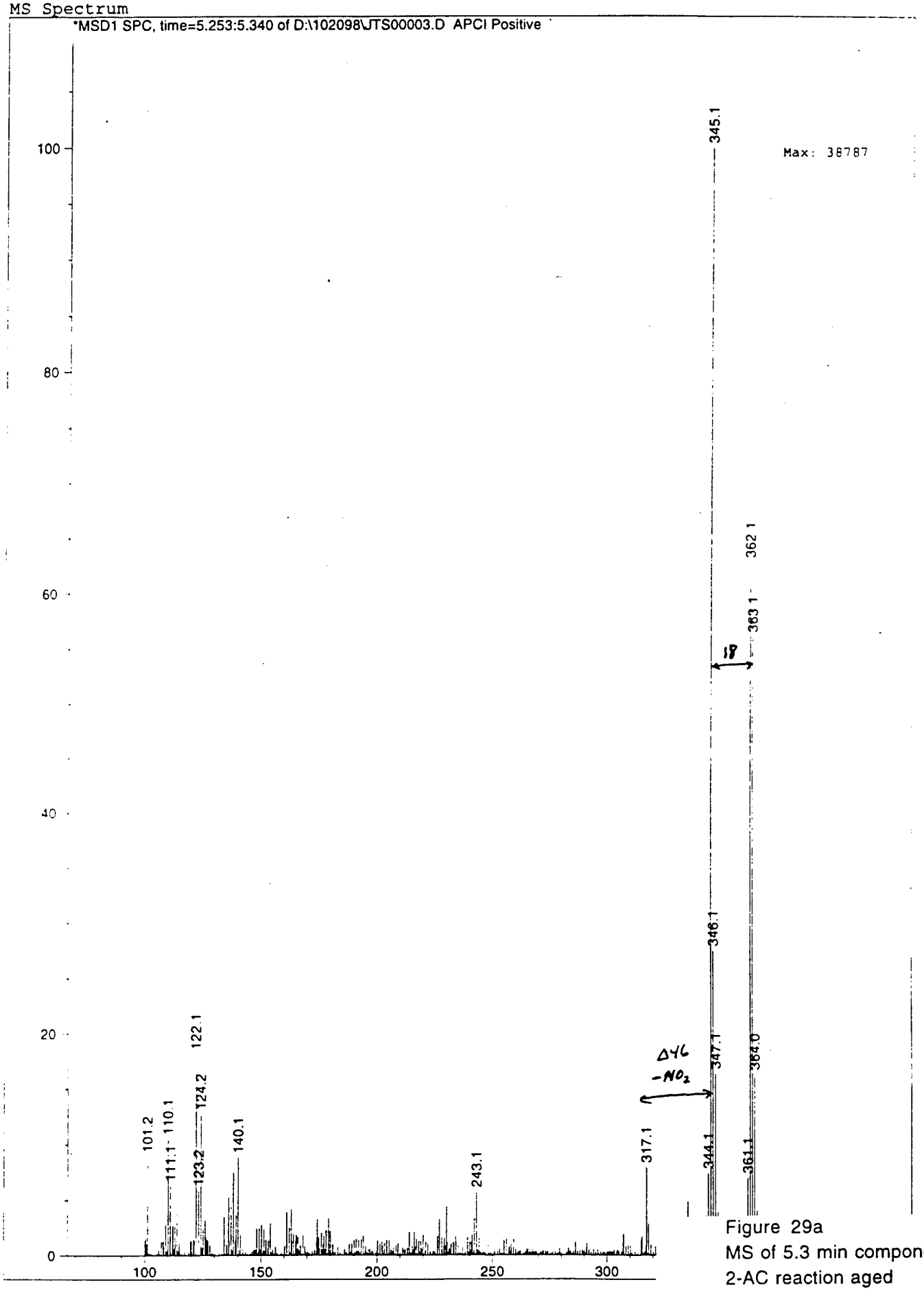

Figure 29a
MS of 5.3 min component
2-AC reaction aged
(+)-APCI

MS Spectrum

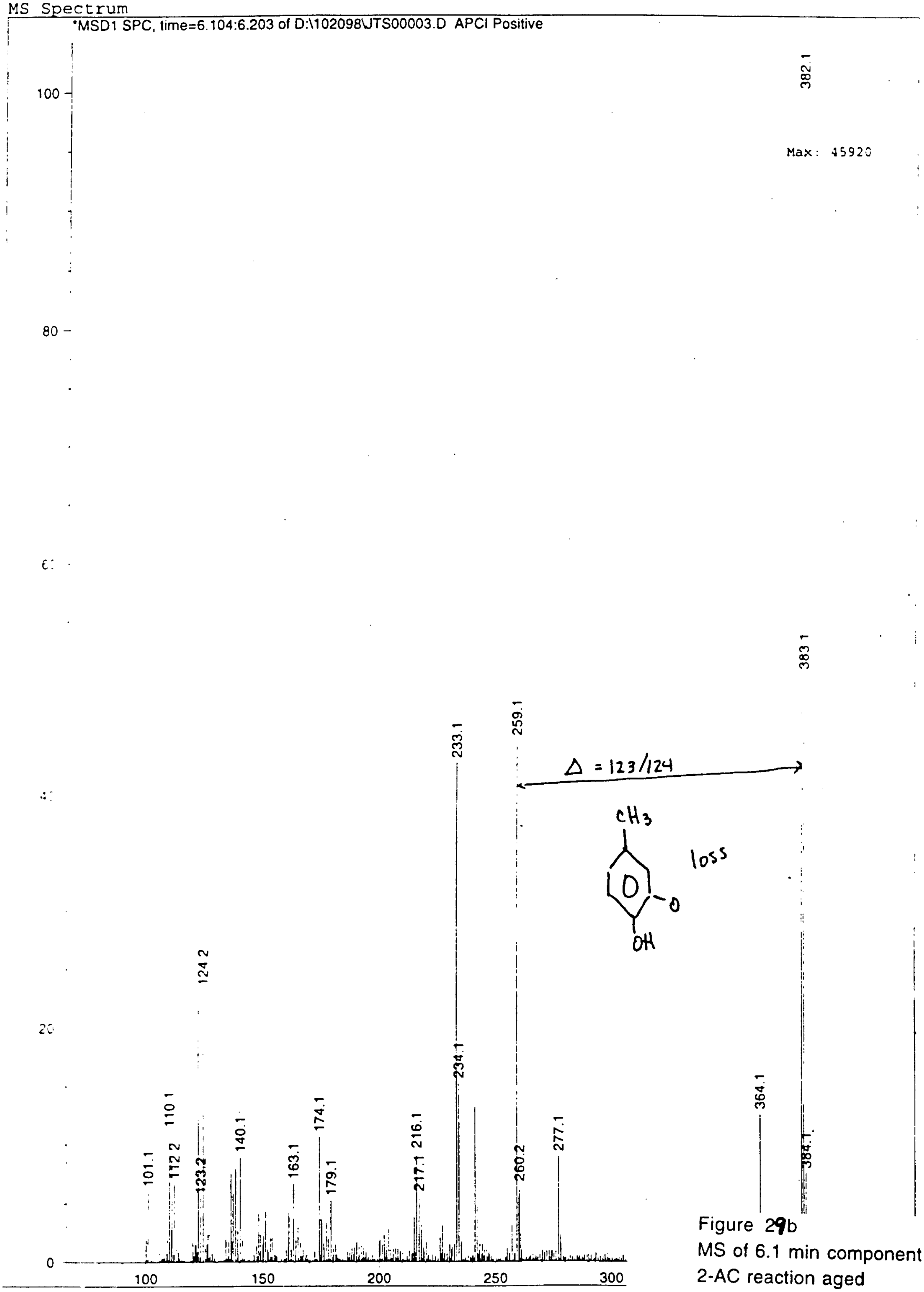

Figure 29b
MS of 6.1 min component
2-AC reaction aged
(+)-APCI

Instrument 1 7/5/00 5:22:25 PM

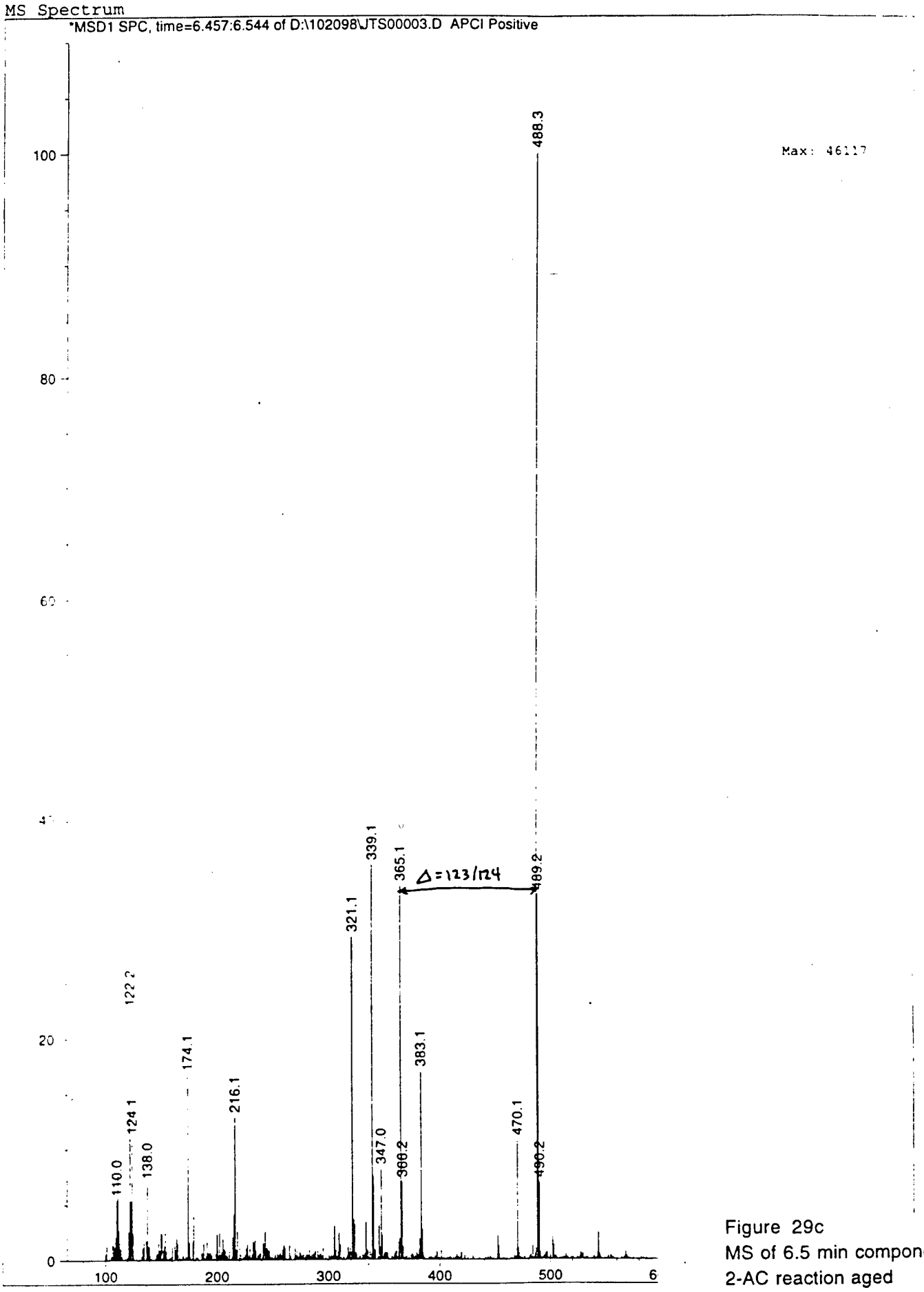

Figure 29c
MS of 6.5 min component
2-AC reaction aged
(+)-APCI

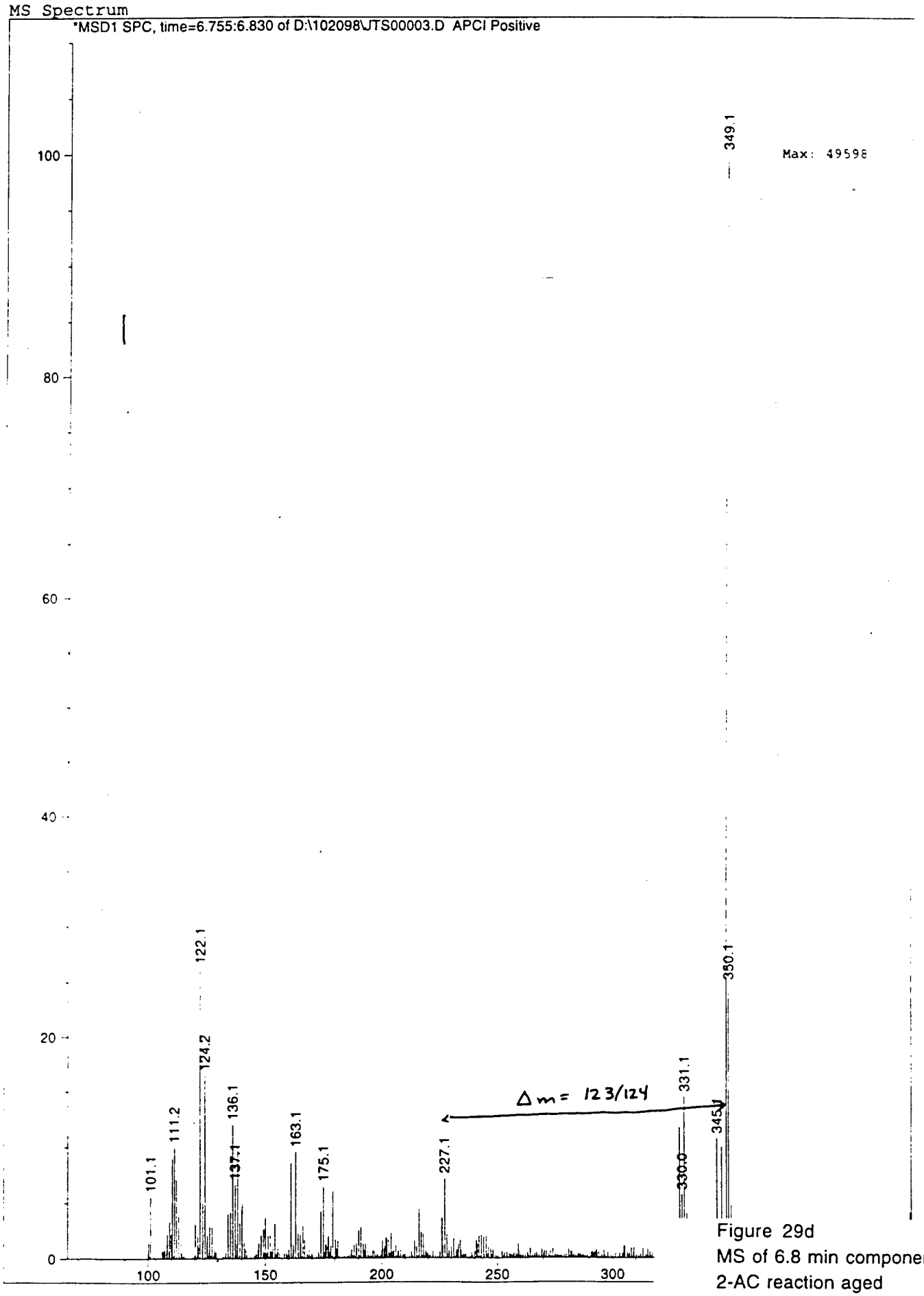

Figure 29d
MS of 6.8 min component
2-AC reaction aged
(+)-APCI

MS Spectrum

*MSD1 SPC, time=7.053:7.152 of D:\102098\JTS00003.D APCI Positive

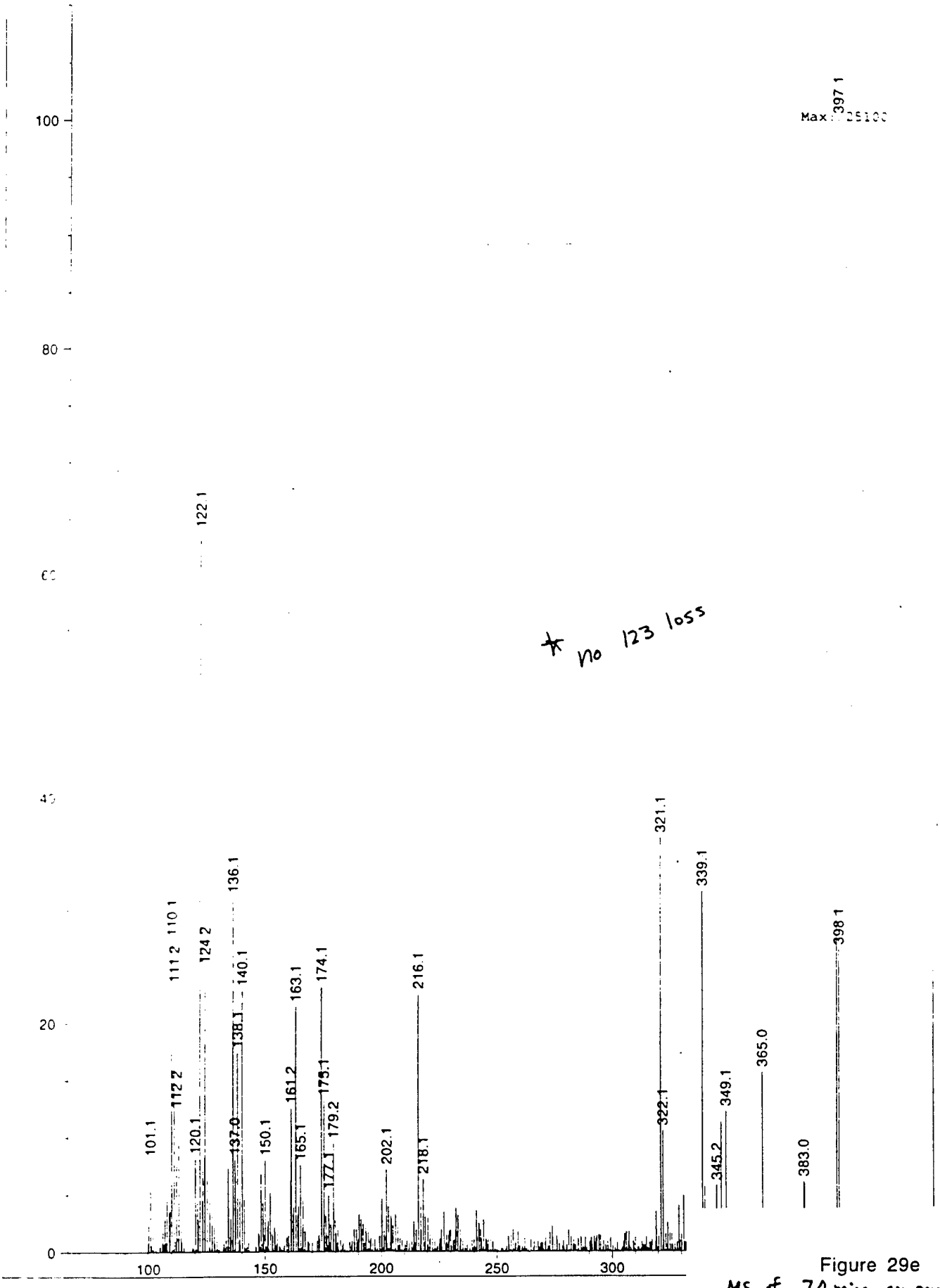

* no 123 loss

Figure 29e
MS of 7.0 min component
2-AC reaction aged

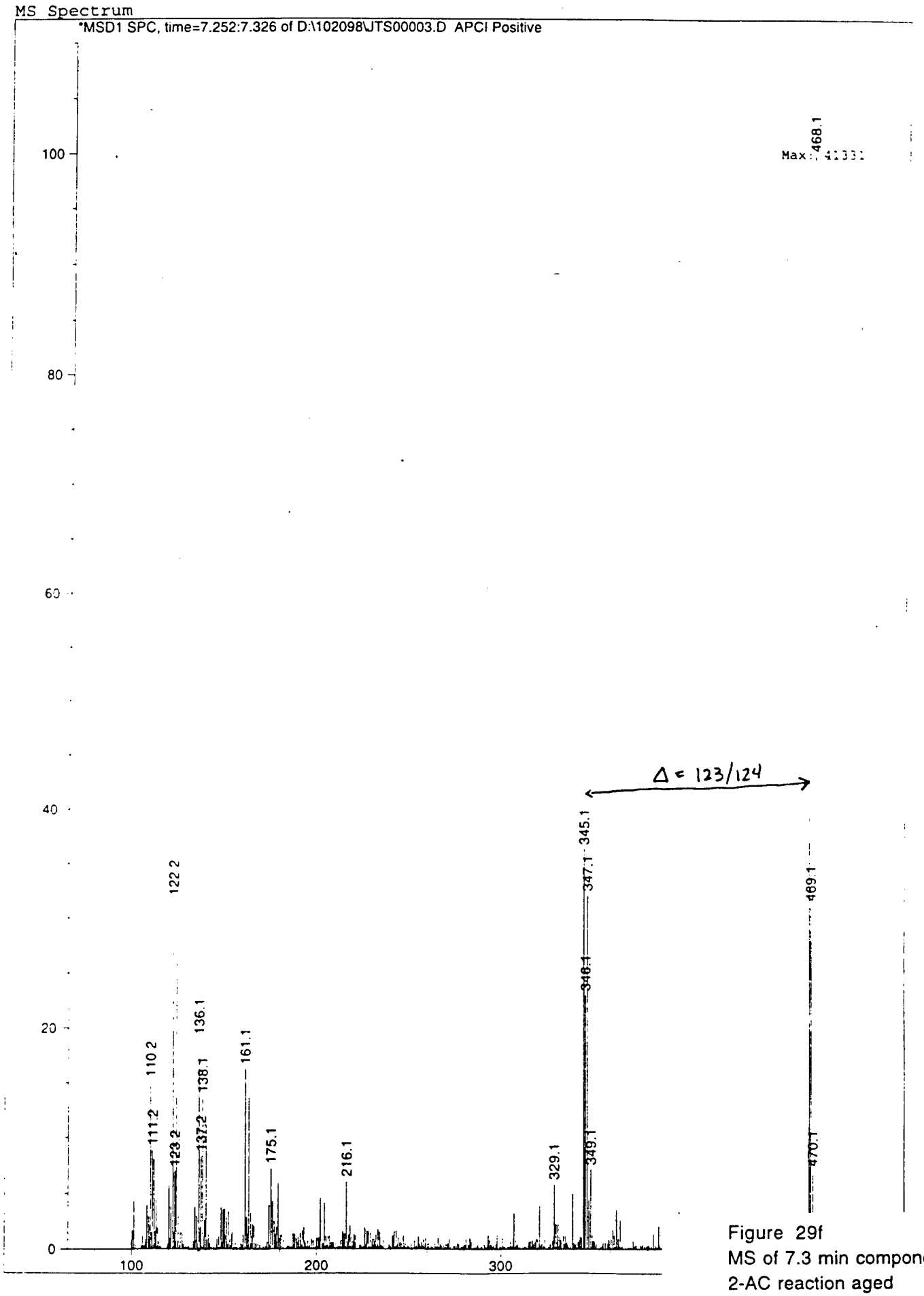

Figure 29f
MS of 7.3 min component
2-AC reaction aged
(+)-APCI

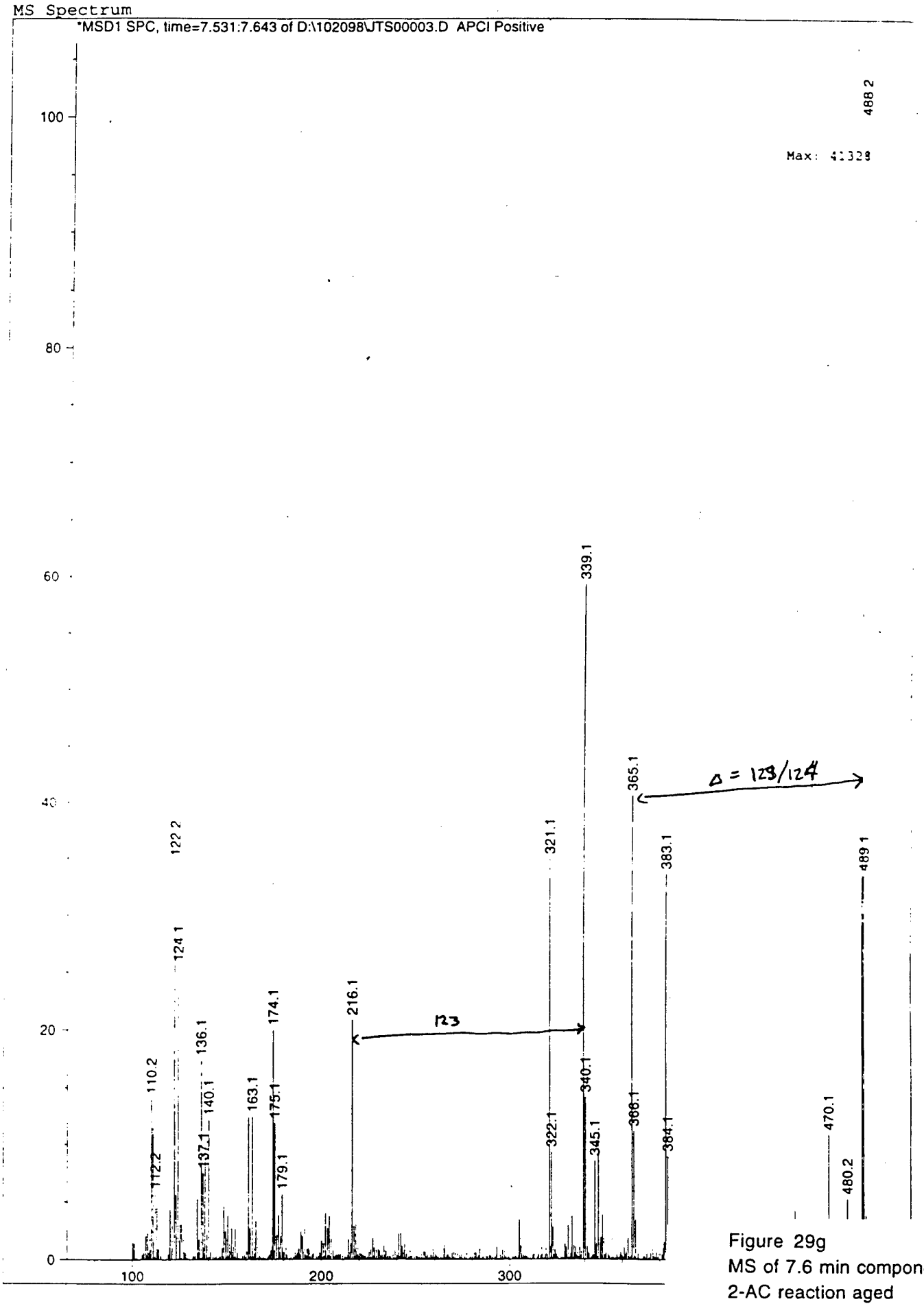

Figure 29g
MS of 7.6 min component
2-AC reaction aged
(+)-APCI

SOUTHEASTERN OKLAHOMA STATE

filename=VSA071_1_H3
dir=/home/nmruser/data/SMITH_RESEARCH/VSA071_1_H3
com=pure 3-AT in D2O
date=12/24/99
time=14:05:31
ac=148
ppfn=1PULSEH
# acq's (x 4)=512
spect freq=200.723600MHz
spect freq=200.723100MHz
pulse width =26.50u
spectrum width=2.870kHz
acq time=2854.100m
acq length=8192
pulse delay=8.000s
receiver gain=11
temperature=-274C
# dummy pulses=0
receiver delay=15.00u
spin rate=30Hz
acq delay=35.00u
dim2 length=1
channel=1
dwell=348.40u
predelay=500.0m
acq completed=148
y_scale=5779.074219
tph01=-86.966530
tph11=-173.000000
rmp=200.722427
rmv=1.240000
current_size=8192

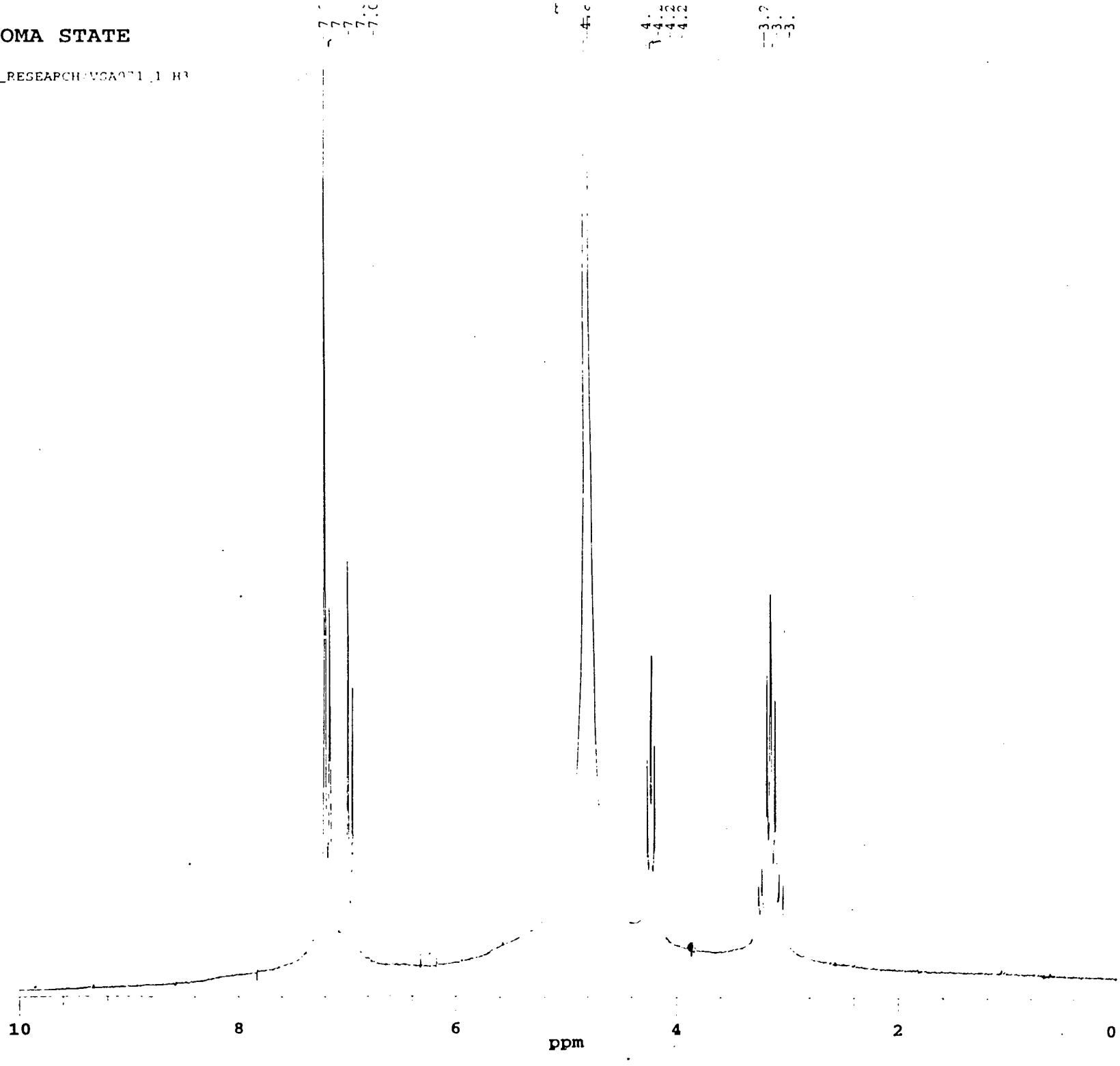

Figure 30
1H NMR of 3-AT
in D2O

SOUTHEASTERN OKLAHOMA STATE

filename=VSA071_1_C3
dir=/home/nmruser/data/SMITH_RESEARCH/VSA071_1_C3
com=pure 3-AT in D2O
date=12/24/99
time=14:36:22
ac=10183
ppfn=WALTZGAT2
# acq's (x 4)=1000000
spect freq=50.476981MHz
spect freq=200.723100MHz
pulse width =24.00u
spectrum width=14.993kHz
acq time=546.410m
acq length=8192
pulse delay=8.000s
receiver gain=11
temperature=-274C
# dummy pulses=0
receiver delay=15.00u
spin rate=-1Hz
acq delay=35.00u
# of rows=1
channel=1
dwell=66.70u
predelay=100.0m
acq completed=10183
lb1=8.000000
y_scale=27970.720703
tph01=-135.768753
tph11=180.000000
rmp=50.477969
rmv=127.970000
current_size=8192

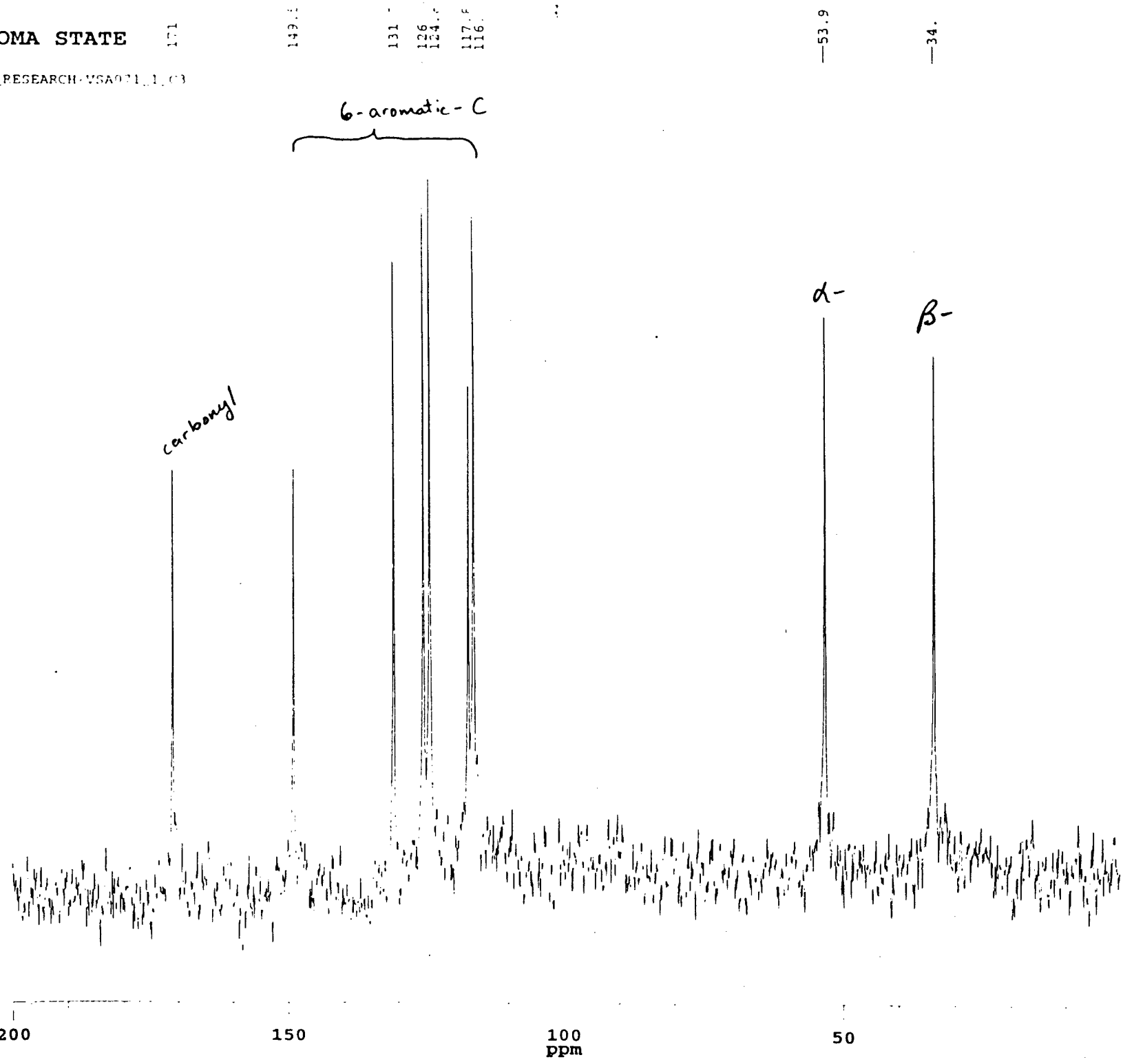

Figure 31
13C NMR of 3-AT
in D2O

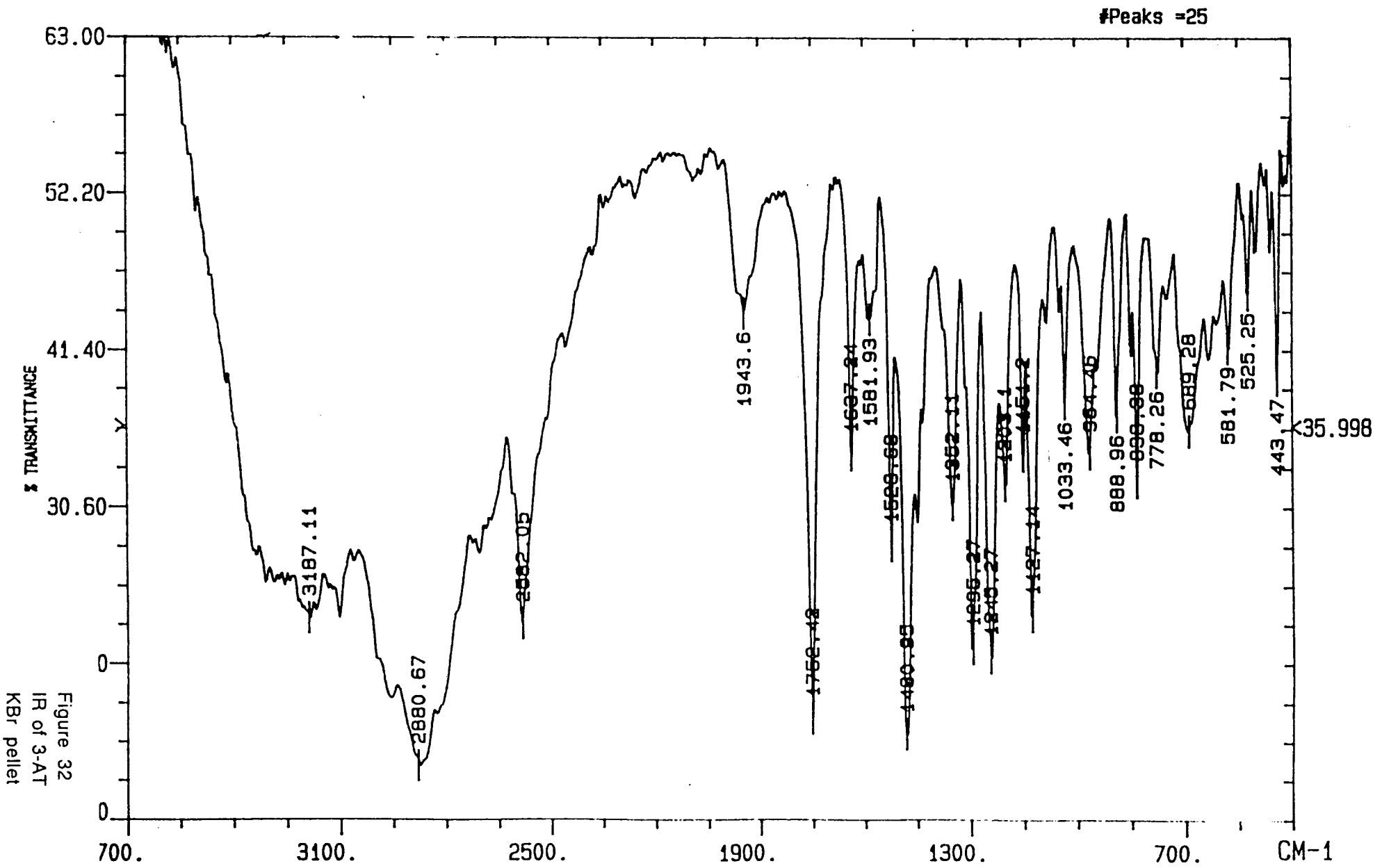

Figure 32
IR of 3-AT
KBr pellet

SOUTHEASTERN OKLAHOMA STATE

filename=VSA071_1_H2
dir=/home/nmruser/data/SMITH_RESEARCH/VSA071_1_H2
com=3-AT+1 eq. NaNO2 rxn yellow pdt. in D2O
date=12/23/99
time=09:52:48
ac=172
ppfn=1PULSEH
# acq's (x 4)=512
spect freq=200.723600MHz
spect freq=200.723100MHz
pulse width =26.50u
spectrum width=2.870kHz
acq time=2854.100m
acq length=8192
pulse delay=8.000s
receiver gain=11
temperature=-274C
# dummy pulses=0
receiver delay=15.00u
spin rate=30Hz
acq delay=35.00u
dim2 length=1
channel=1
dwell=348.40u
predelay=500.0m
acq completed=172
y_scale=6992.680176
tph01=-86.966530
tph11=-173.000000
rmp=200.722427
rmv=1.240000
current_size=8192

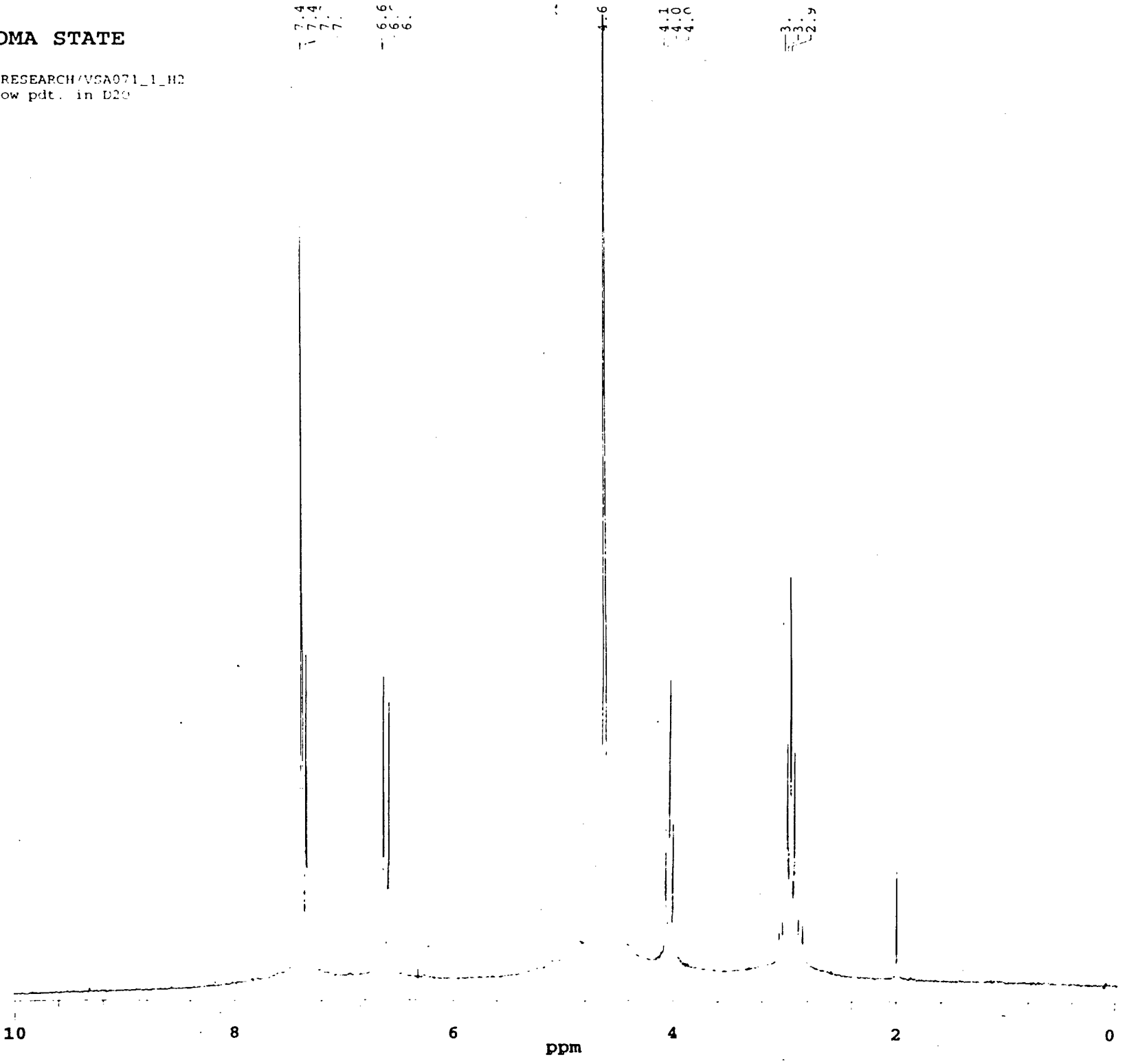

Figure 33
1H NMR of 3-AT reaction
with 1 equiv NO2
in D2O

SOUTHEASTERN OKLAHOMA STATE

filename=VSA071_1_C2
dir=/home/nmruser/data/SMITH_RESEARCH/VSA071_1_C2
com=3-AT+1 eq. NaNO2 rxn pdt. in D2O
date=12/23/99
time=10:47:09
ac=10119
ppfn=WALTZGAT2
# acq's (x 4)=1000000
spect freq=50.476981MHz
spect freq=200.723100MHz
pulse width =24.00u
spectrum width=14.993kHz
acq time=546.410m
acq length=8192
pulse delay=8.000s
receiver gain=11
temperature=-274C
# dummy pulses=0
receiver delay=15.00u
spin rate=-1Hz
acq delay=35.00u
# of rows=1
channel=1
dwell=66.70u
predelay=100.0m
acq completed=10119
lb1=8.000000
y_scale=22719.294922
tph01=-135.768753
tph11=180.000000
rmp=50.477969
rmv=127.970000
current_size=8192

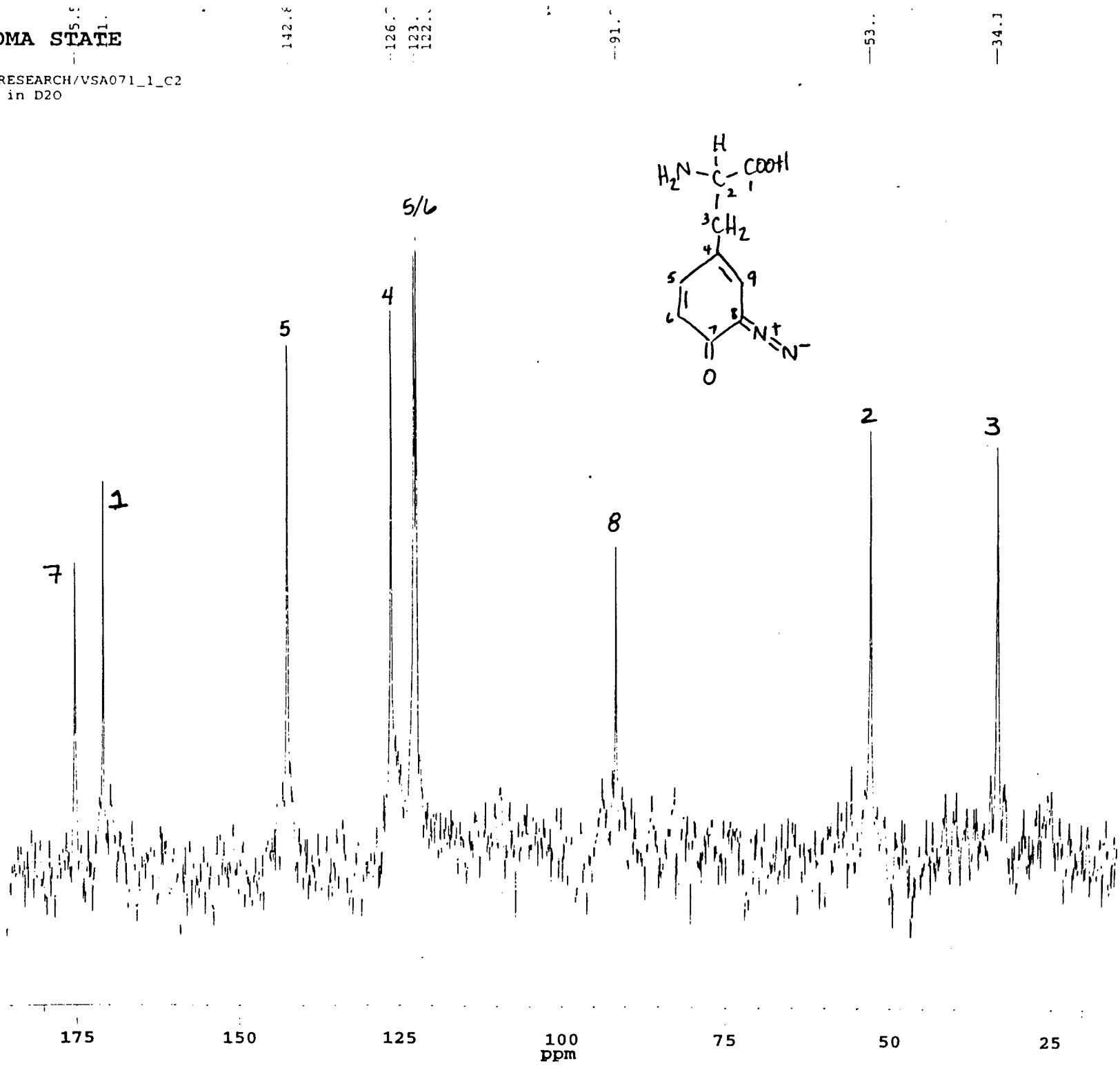

Figure 34
13C NMR of 3-AT reaction with 1 equiv NO2 in D2O

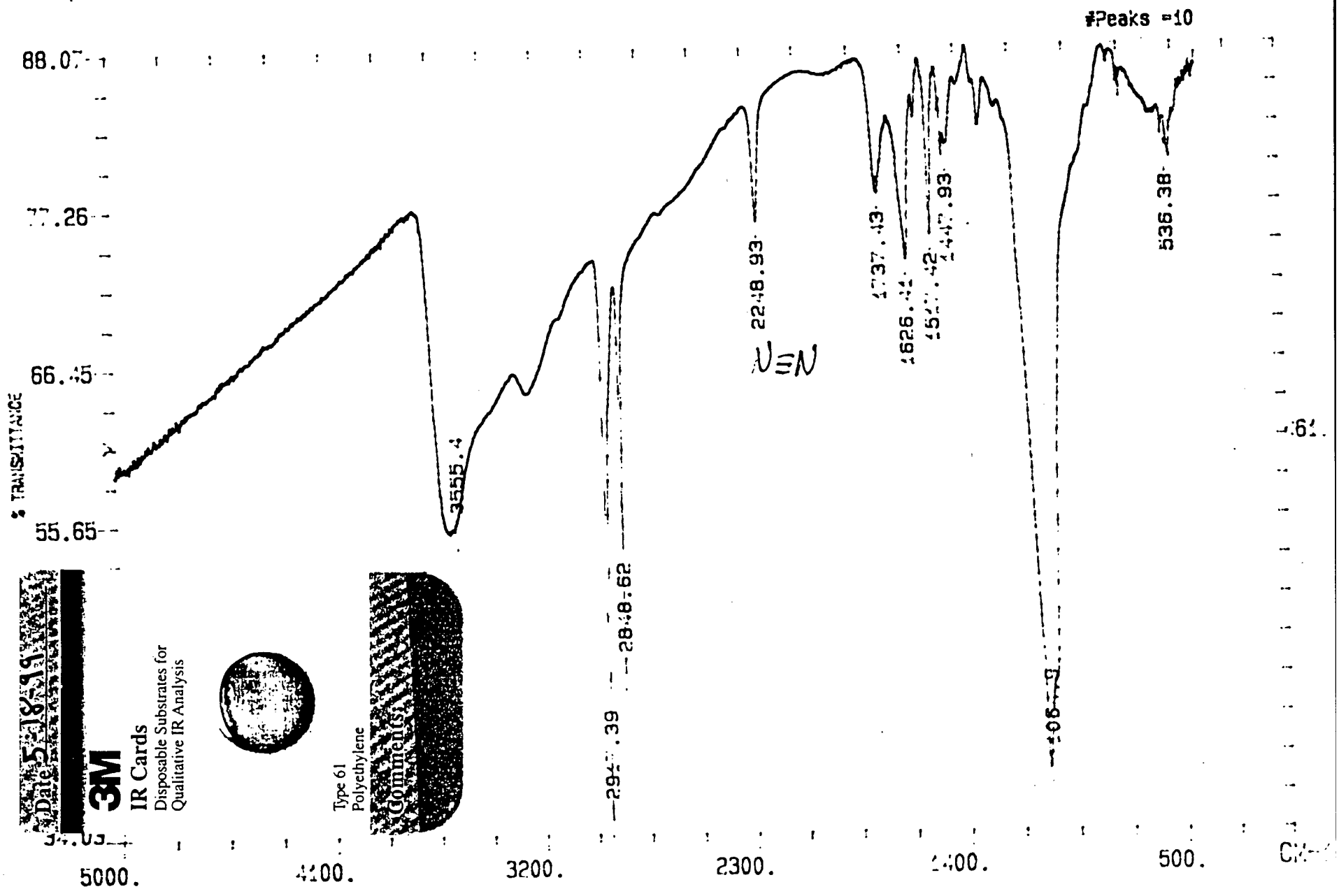

Figure 35
IR of 3-AT reaction with 1 equiv NO2

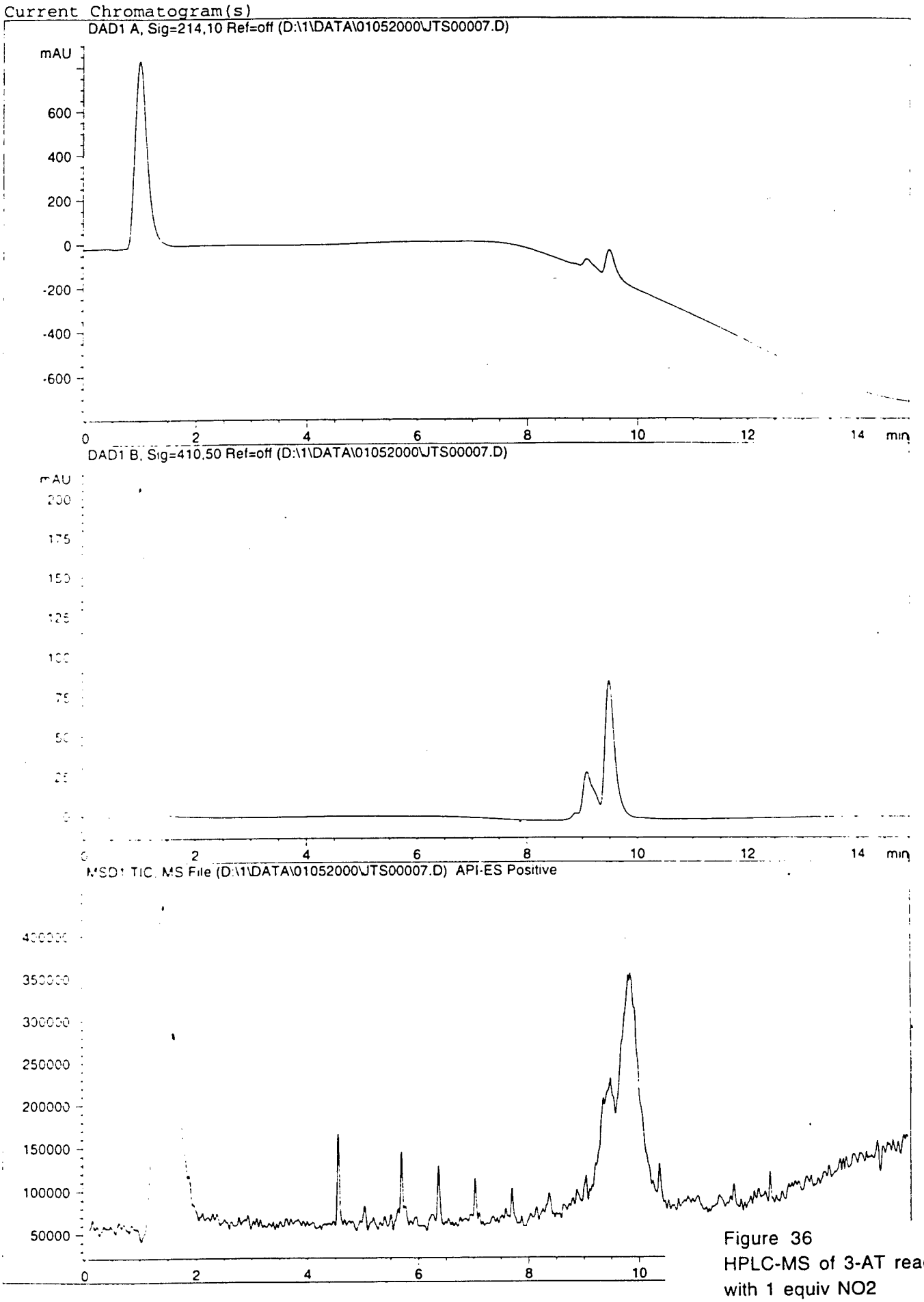

Figure 36
HPLC-MS of 3-AT reaction with 1 equiv NO2
(+)-ESI

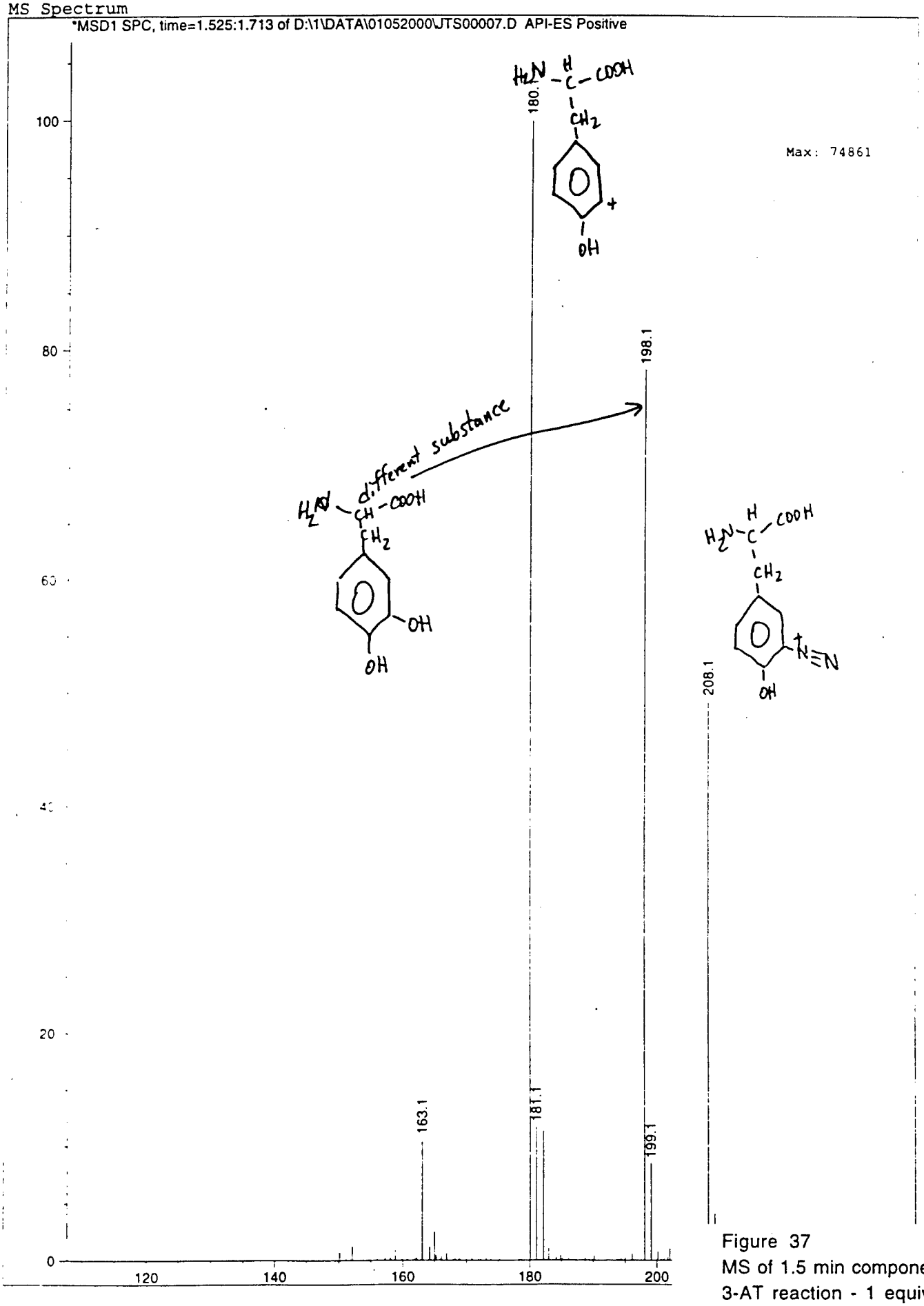

Figure 37
MS of 1.5 min component
3-AT reaction - 1 equiv NO2
(+)-ESI

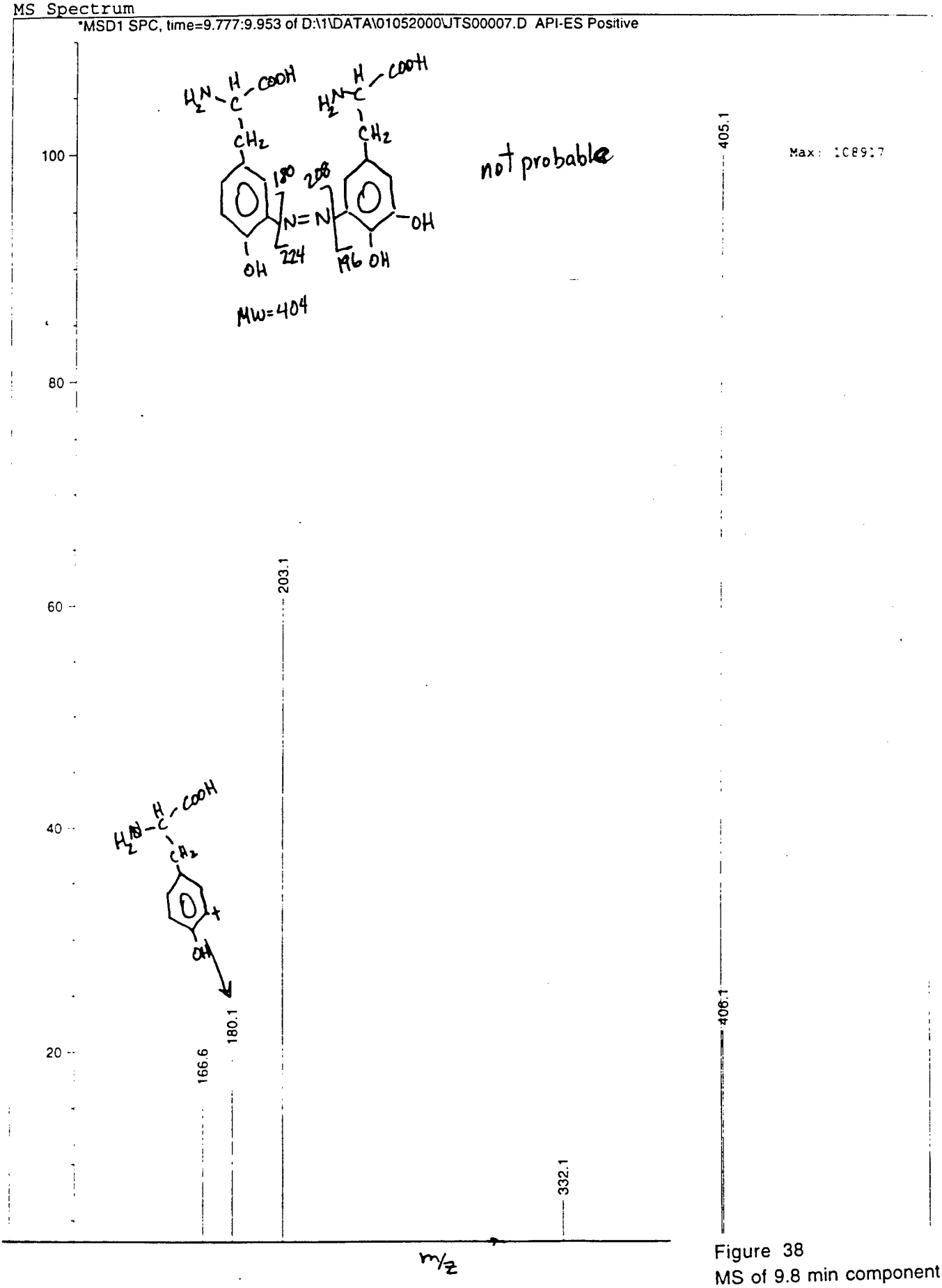

Figure 38
MS of 9.8 min component
3-AT reaction - 1 equiv NO2
(+)-ESI

Display Report

Analysis Info:

File: D:\DATA\16FEB00\TIM20005.D
Printed: Wed Feb 16 15:21:46 2000
Date acquired: Wed Feb 16 15:07:46 2000
Instrument: EsquireLC_00098
Operator : Administrator
Task :
Method :
Sample : tim2
Description: Tim MS/MS 405.1 amp 1.0 skim 25 Cap Exit 80 Trap 35 Neb20 Dry gas6 Temp 300

Acquisition Parameter:

Source : ESI
Polarity : Positive
Mode : Std/Normal
CapExit : 80.0 Volt
Skim 1 : 25.0 Volt
Scan Range: 50.00 - 1500.00 m/z
Trap Drive: 35
Accum.time: 200000 µs
Summation : 10 Spectra
MS/MS : 405.1 u

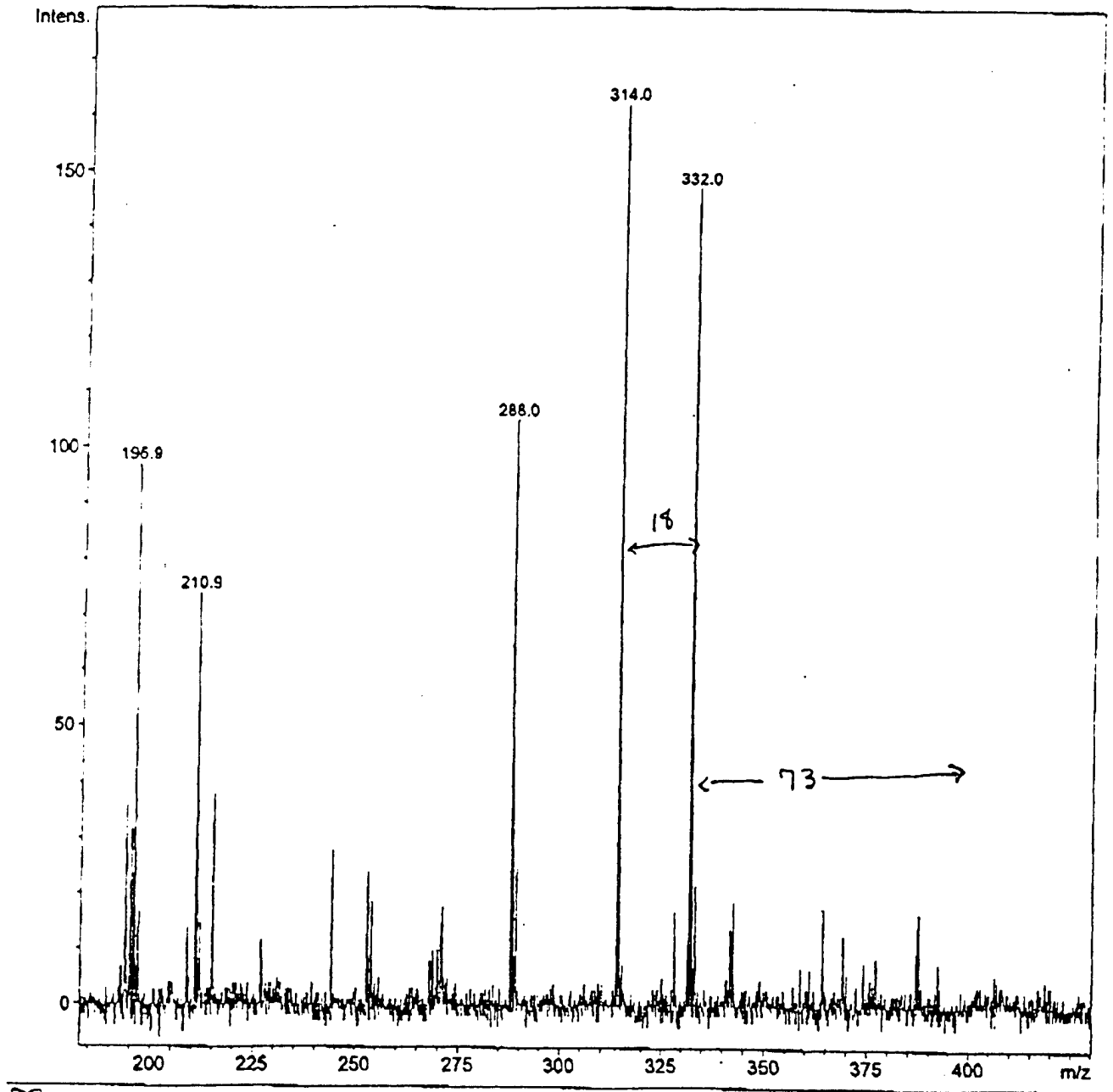

Bruker DataAnalysis Esquire-LC 1.6m, © Bruker Daltonik GmbH
Licensed to ESQUIRE, Nobel

Figure 39
MS-MS of 405 m/z component from 3-AT reaction - 1 equiv NO2
(+)-ESI

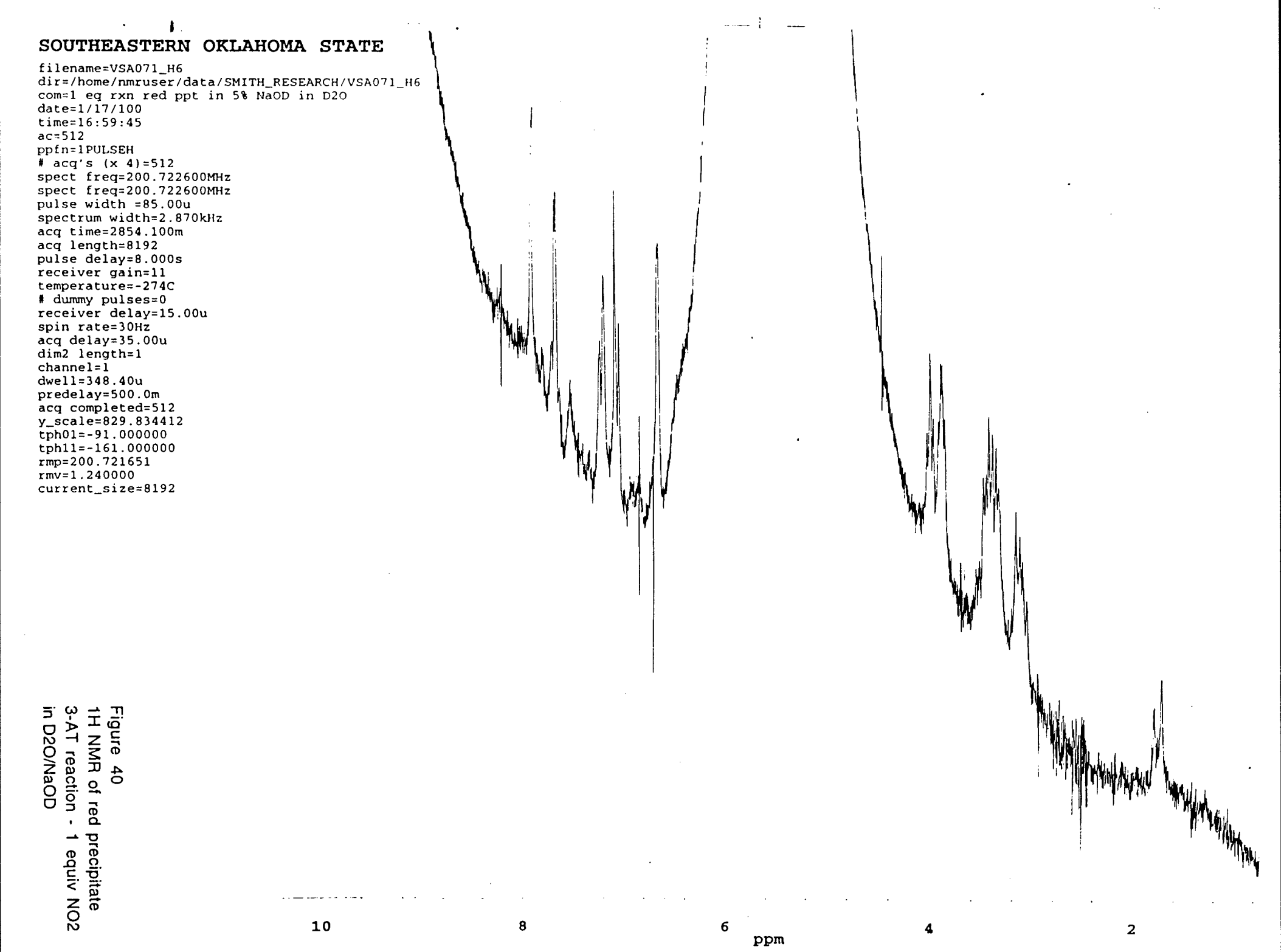

Figure 40
1H NMR of red precipitate
3-AT reaction - 1 equiv NO2
in D2O/NaOD

SOUTHEASTERN OKLAHOMA STATE

filename=2H3ATNO2.R89
dir=/home/nmruser/data/SMITH_RESEARCH/2H3ATNO2.R89
com=#2 rxn 3AT + NO2 2/9/98
date=2/9/98
time=12:17:59
ac=64
ppfn=1PULSEH
# acq's (x 4)=64
spect freq=200.723600MHz
spect freq=200.723600MHz
pulse width =26.50u
spectrum width=2.870kHz
acq time=2854.100m
acq length=8192
pulse delay=8.000s
receiver gain=11
temperature=-274C
# dummy pulses=0
receiver delay=15.00u
spin rate=30Hz
acq delay=35.00u
dim2 length=1
channel=1
dwell=348.40u
predelay=100.0m
acq completed=64
y_scale=106050480.000000
tph01=-122.405830
tph11=-193.000000
rmp=200.723359
rmv=4.610000
current_size=8192

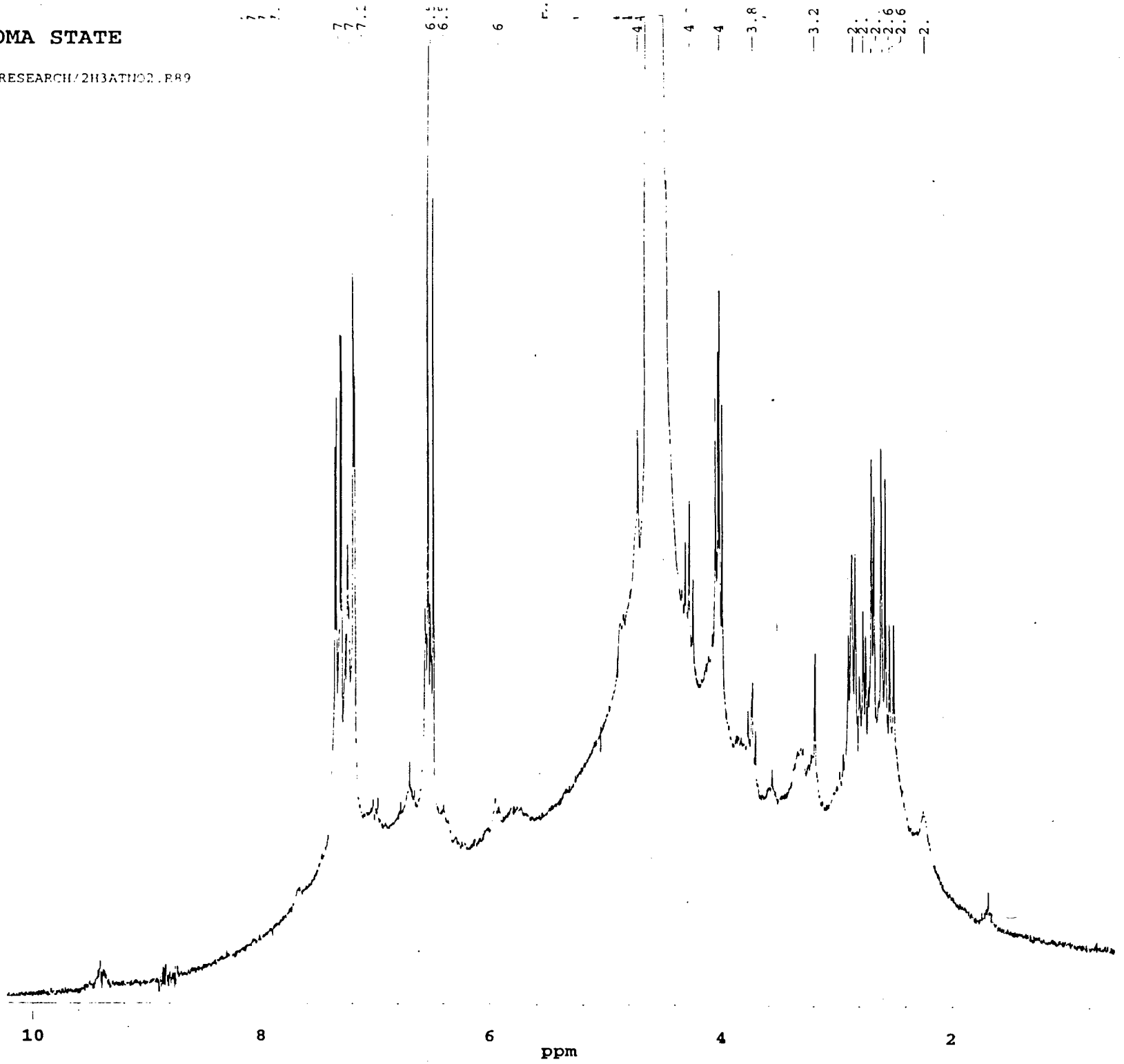

Figure 41
1H NMR of 3-AT reaction
5.5 equiv NO2
in D2O

SOUTHEASTERN OKLAHOMA STATE

filename=06229801.T86
dir=/home/nmruser/data/DIR_JTS/06229801.T86
com=C13 of rxn of 3AT and NO2. 2/6/98 #1
date=6/22/98
time=17:29:33
ac=8111
ppfn=WALTZGATE
# acq's (x 4)=64000
spect freq=50.476981MHz
spect freq=200.723400MHz
pulse width =14.25u
spectrum width=14.993kHz
acq time=1092.800m
acq length=16384
pulse delay=8.000s
receiver gain=11
temperature=-274C
# dummy pulses=0
receiver delay=15.00u
spin rate=-1Hz
acq delay=35.00u
# of rows=1
channel=1
dwell=66.70u
predelay=100.0m
acq completed=0
lb1=0.500000
y_scale=128826.484375
tph01=89.049355
tph11=152.000000
rmp=50.473689
rmv=43.500000
current_size=16384

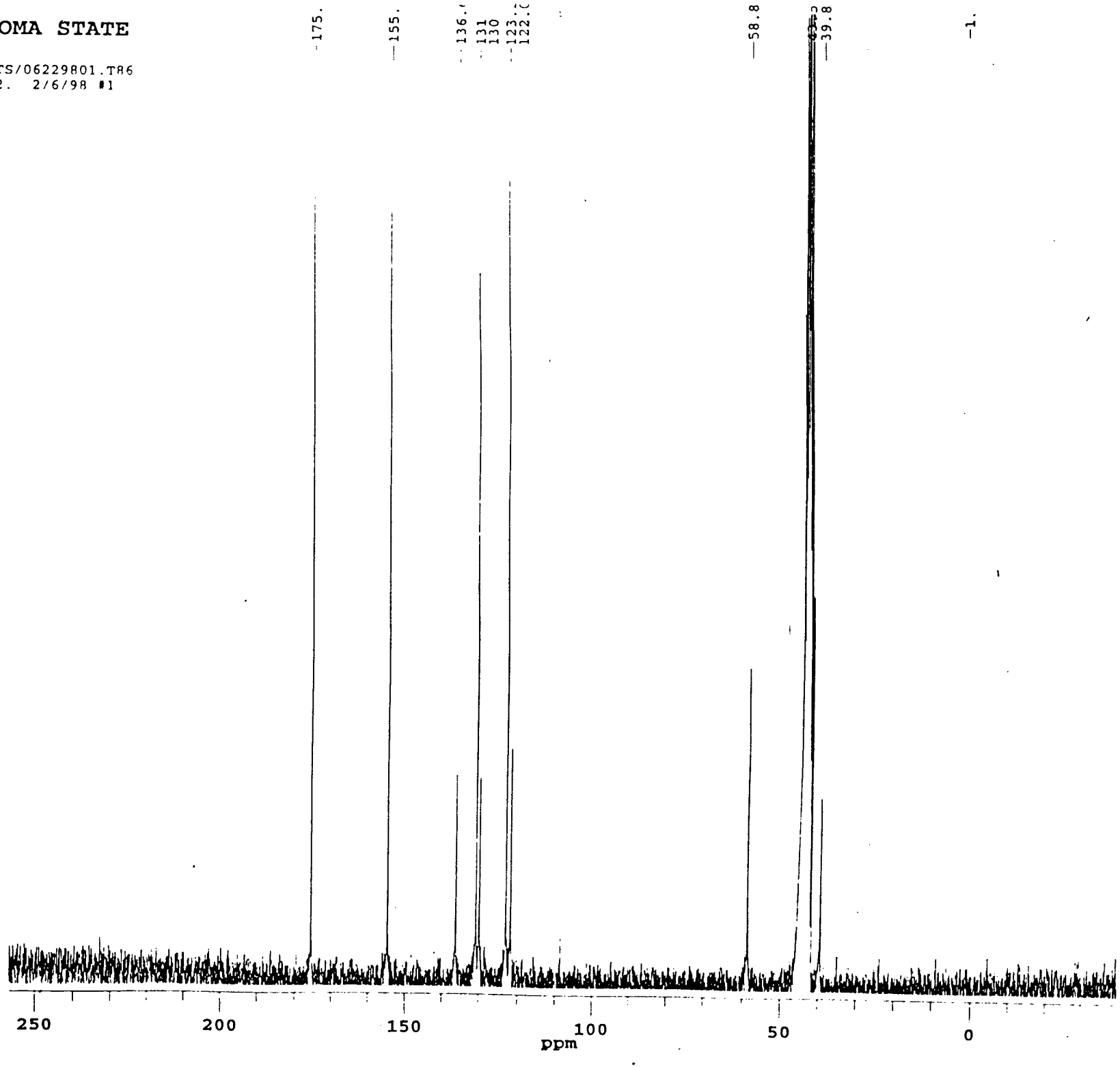

Figure 42b
13C NMR of 3-AT
in D2O/DMSO

SOUTHEASTERN OKLAHOMA STATE

filename=06199801
dir=/home/nmruser/data/DIR_JTS/06199801
com=rxn:3AT+NO2, 10mm
date=6/19/98
time=14:35:45
ac=64
ppfn=1PULSEH
# acq's (x 4)=64
spect freq=200.723400MHz
spect freq=200.723400MHz
pulse width =26.50u
spectrum width=2.870kHz
acq time=2854.100m
acq length=8192
pulse delay=8.000s
receiver gain=11
temperature=-274C
# dummy pulses=0
receiver delay=15.00u
spin rate=30Hz
acq delay=35.00u
dim2 length=1
channel=1
dwell=348.40u
predelay=100.0m
acq completed=64
y_scale=1226.152344
tph01=32.000000
tph11=-157.000000
rmp=200.723564
rmv=4.610000
current_size=8192

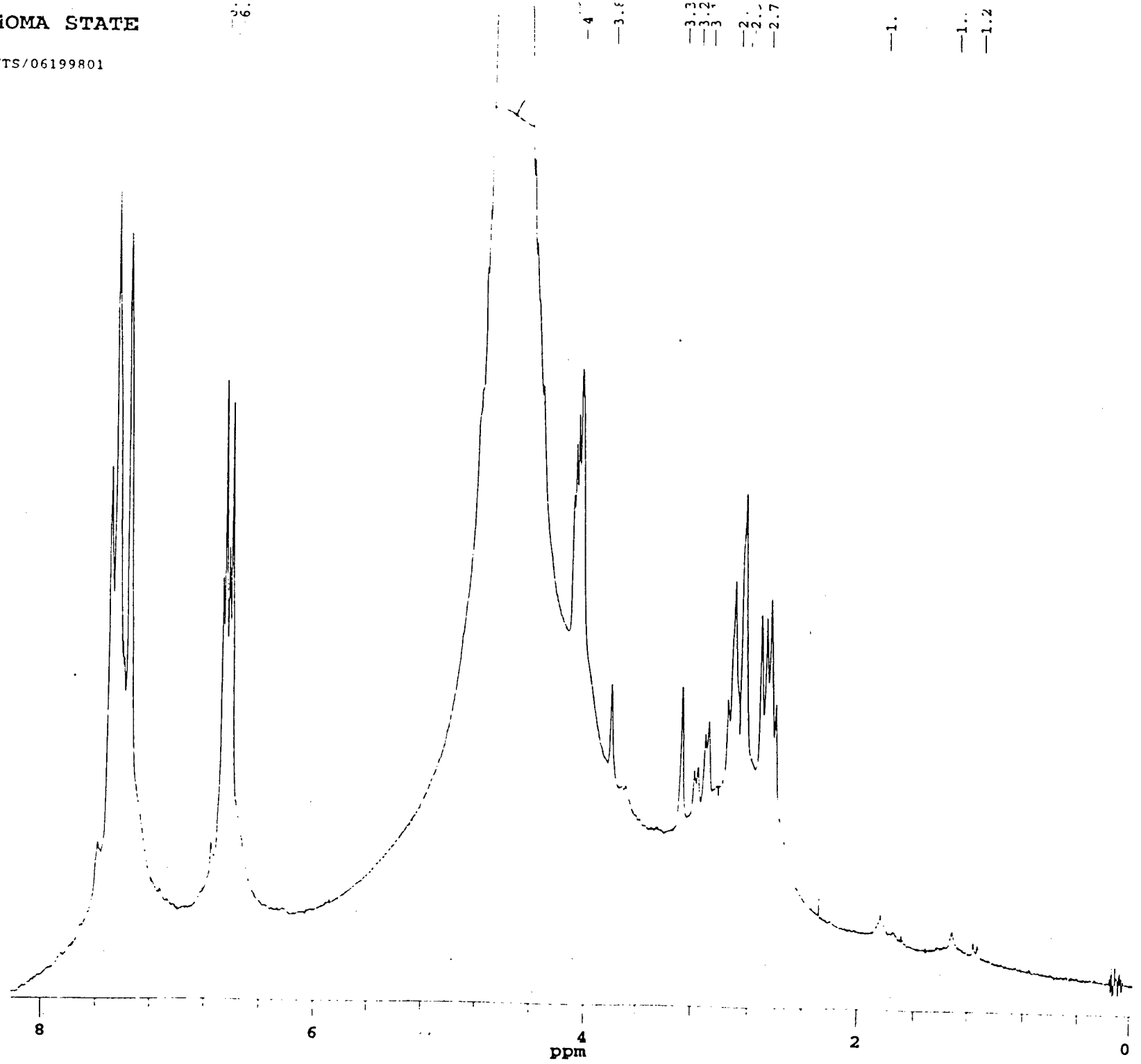

Figure 43
1H NMR of 3-AT reaction
5.5 equiv NO2
in D2O/DMSO

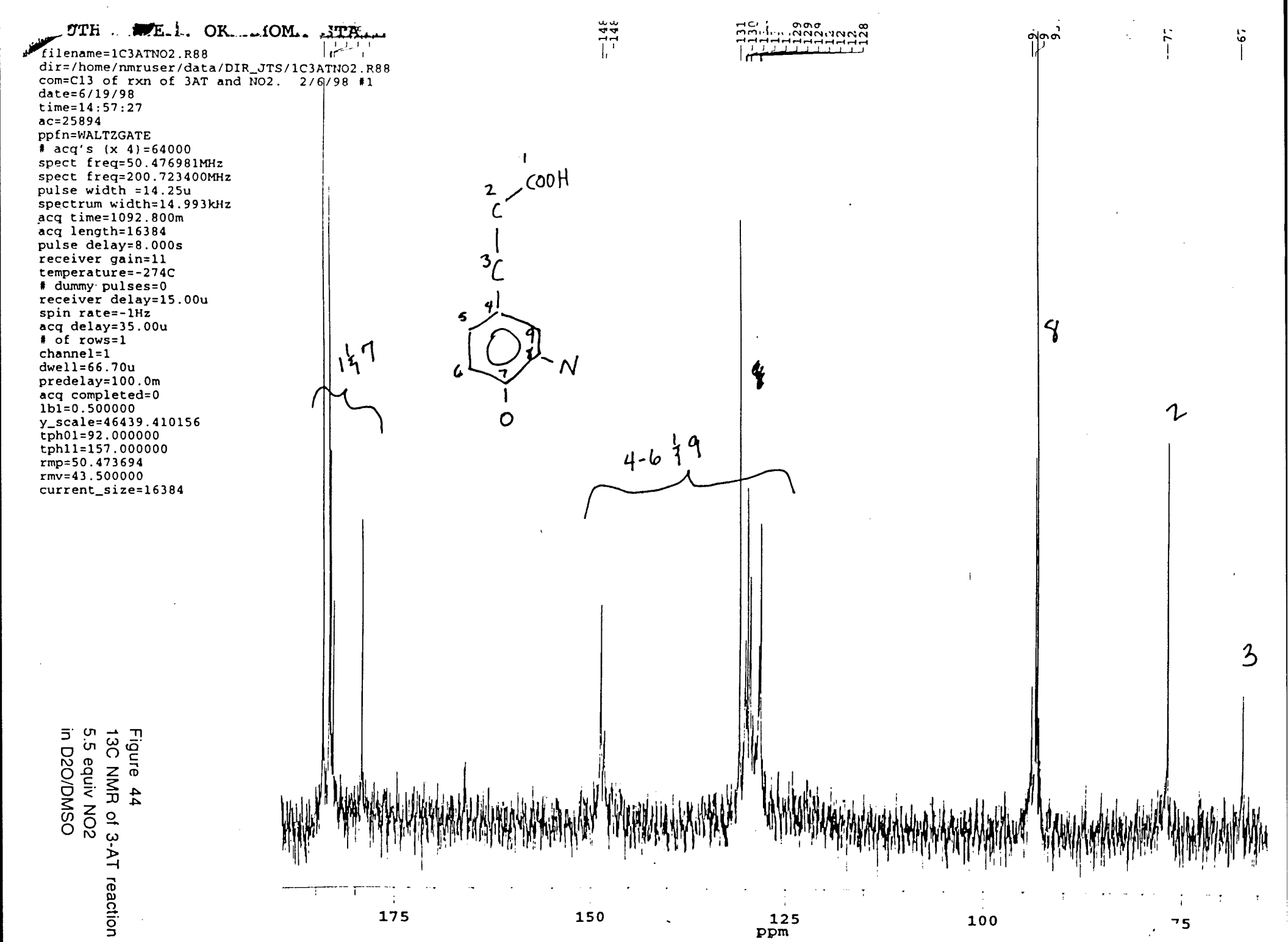

Figure 44
13C NMR of 3-AT reaction
5.5 equiv NO2
in D2O/DMSO

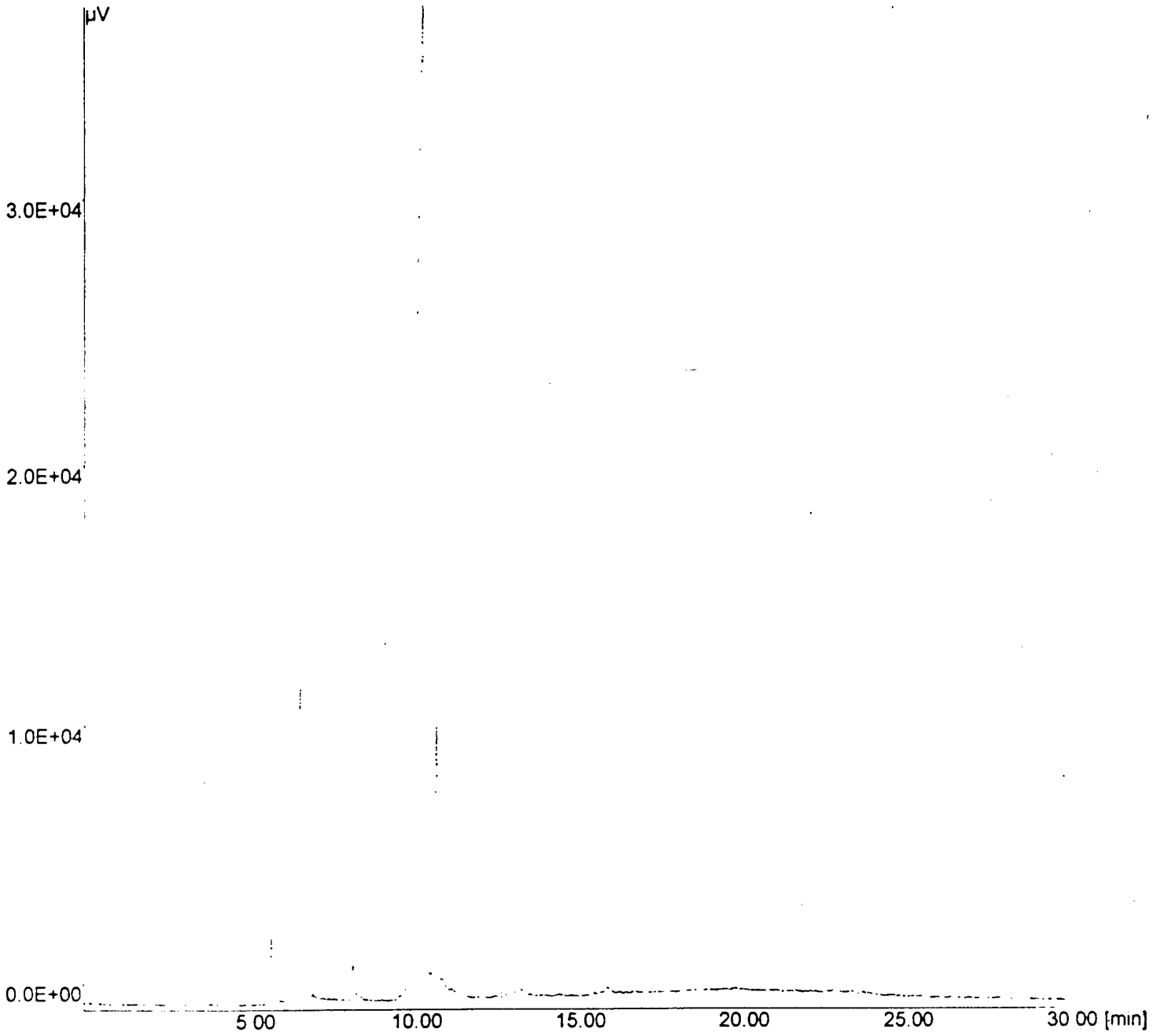

File name : 07299004.CH1 User : ETH Curr. Date : 6-Jul-00 16:02:02

Acqu. Date : 29-Jul-99 14:01:48

Info :
3-AT rxn no Acetone
run Buffer 50 mM NH4Acetate
214 wave
(+) polarity 15 kilovolts

Vial # = 1 Rack # = 1

Control Method :

Peak Detection Not Available

-Jul-00 16:02:02,ETH,Page 1

Figure 45
CE of 3-AT reaction
5.5 equiv NO2
214 nm

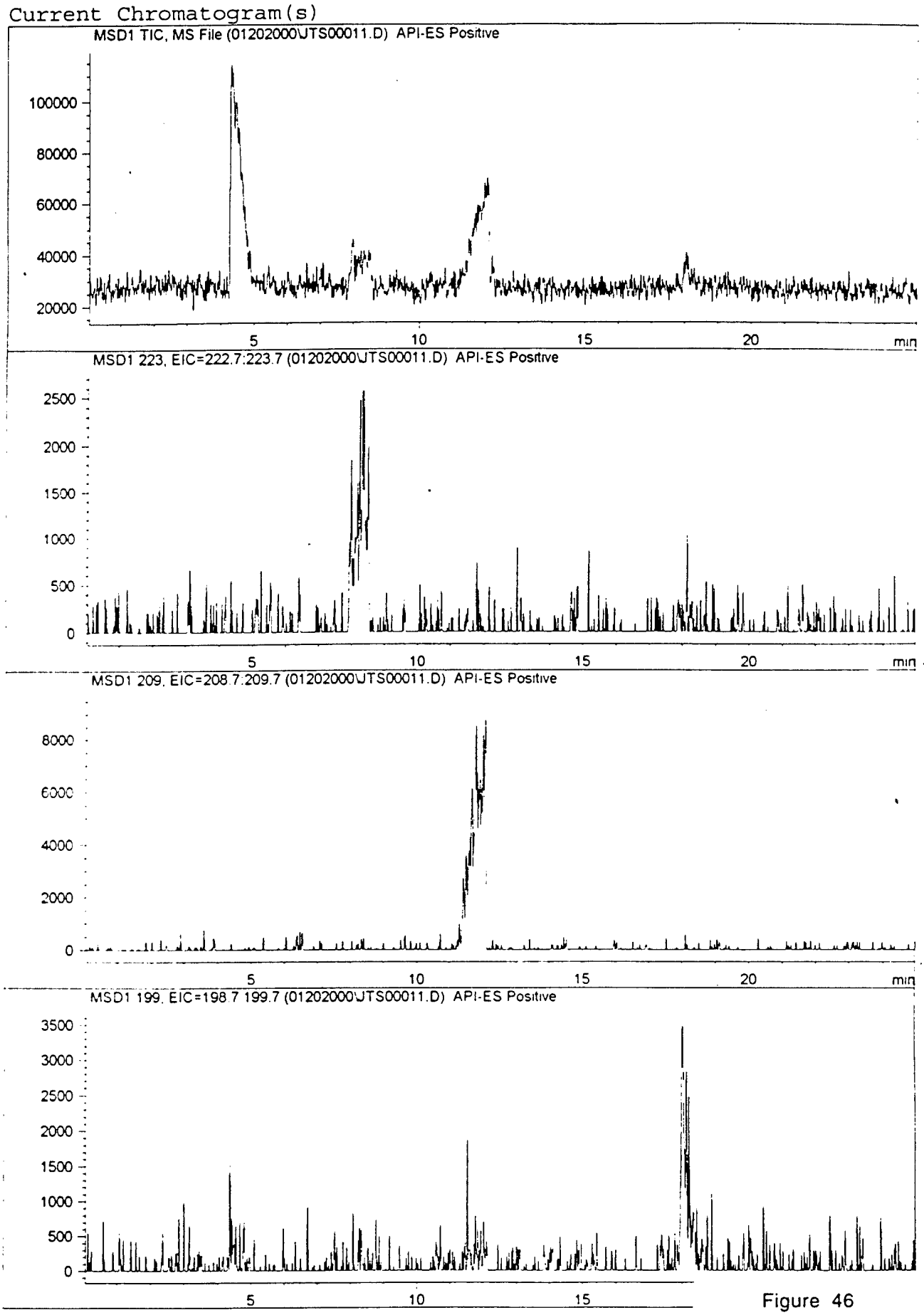

Figure 46
CE-MS of 3-AT reaction
5.5 equiv NO2

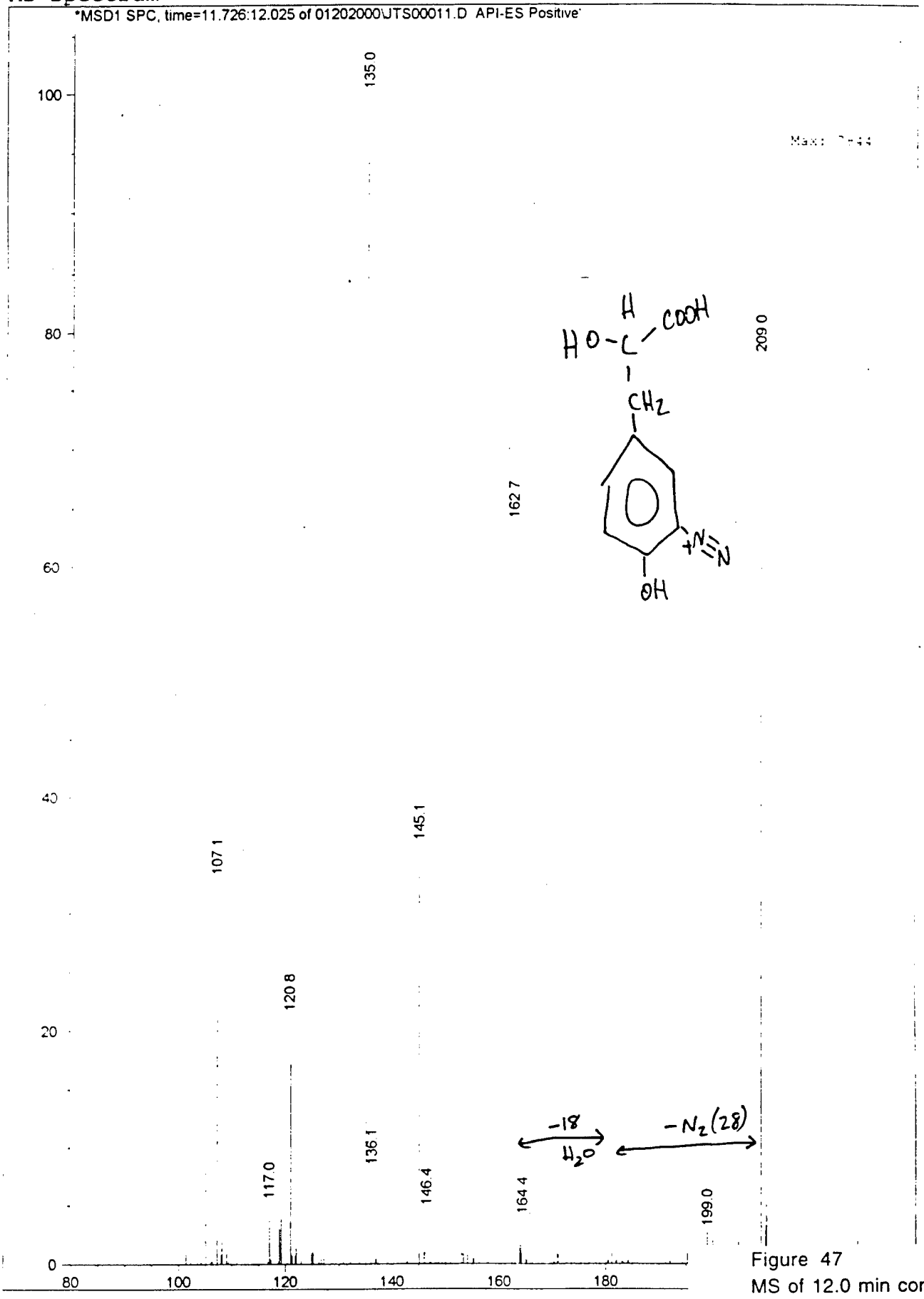

Figure 47
MS of 12.0 min component
3-AT reaction
CE-MS (+)-ESI

MS Spectrum

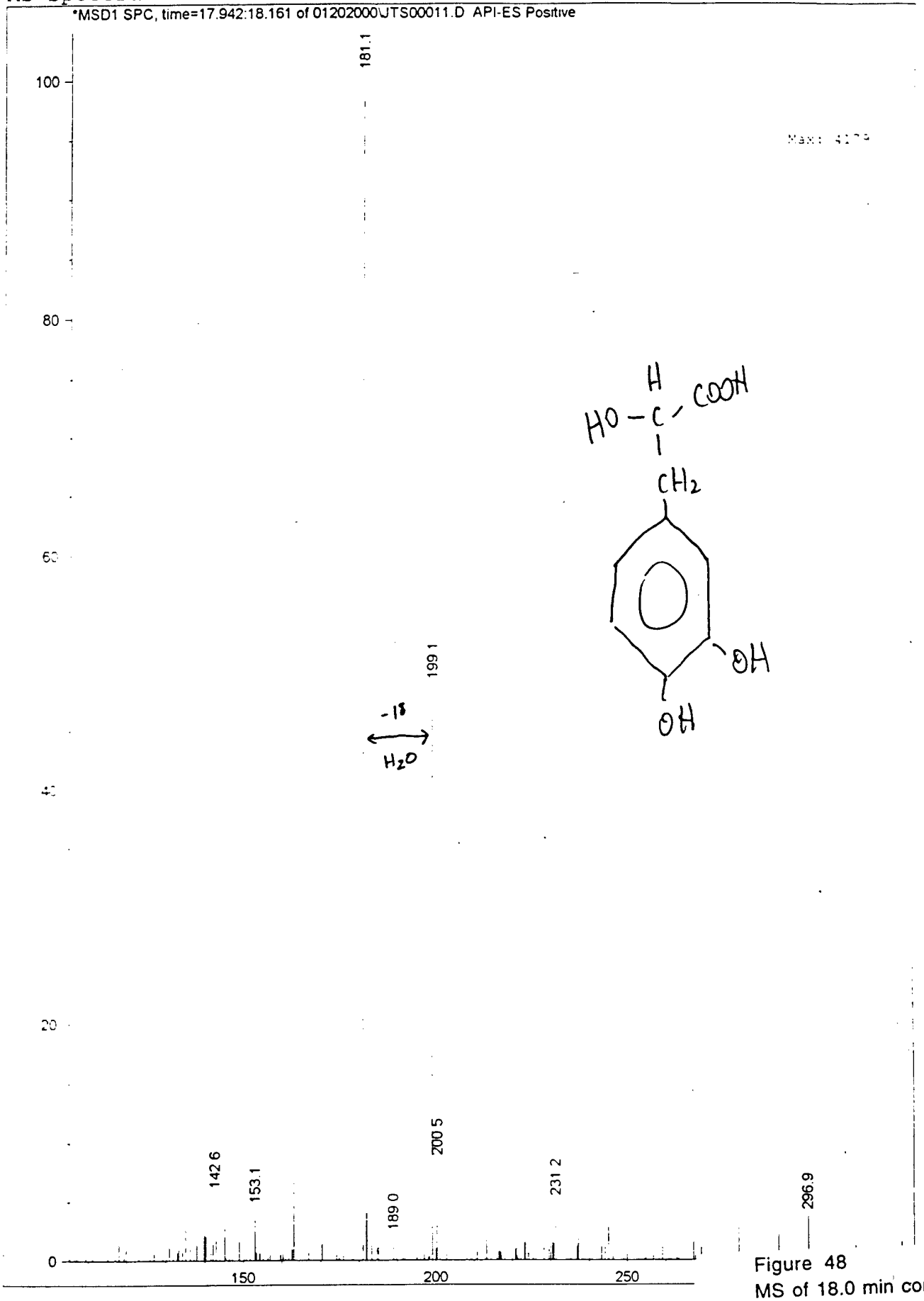

Figure 48
MS of 18.0 min component
3-AT reaction
CE-MS (+)-ESI

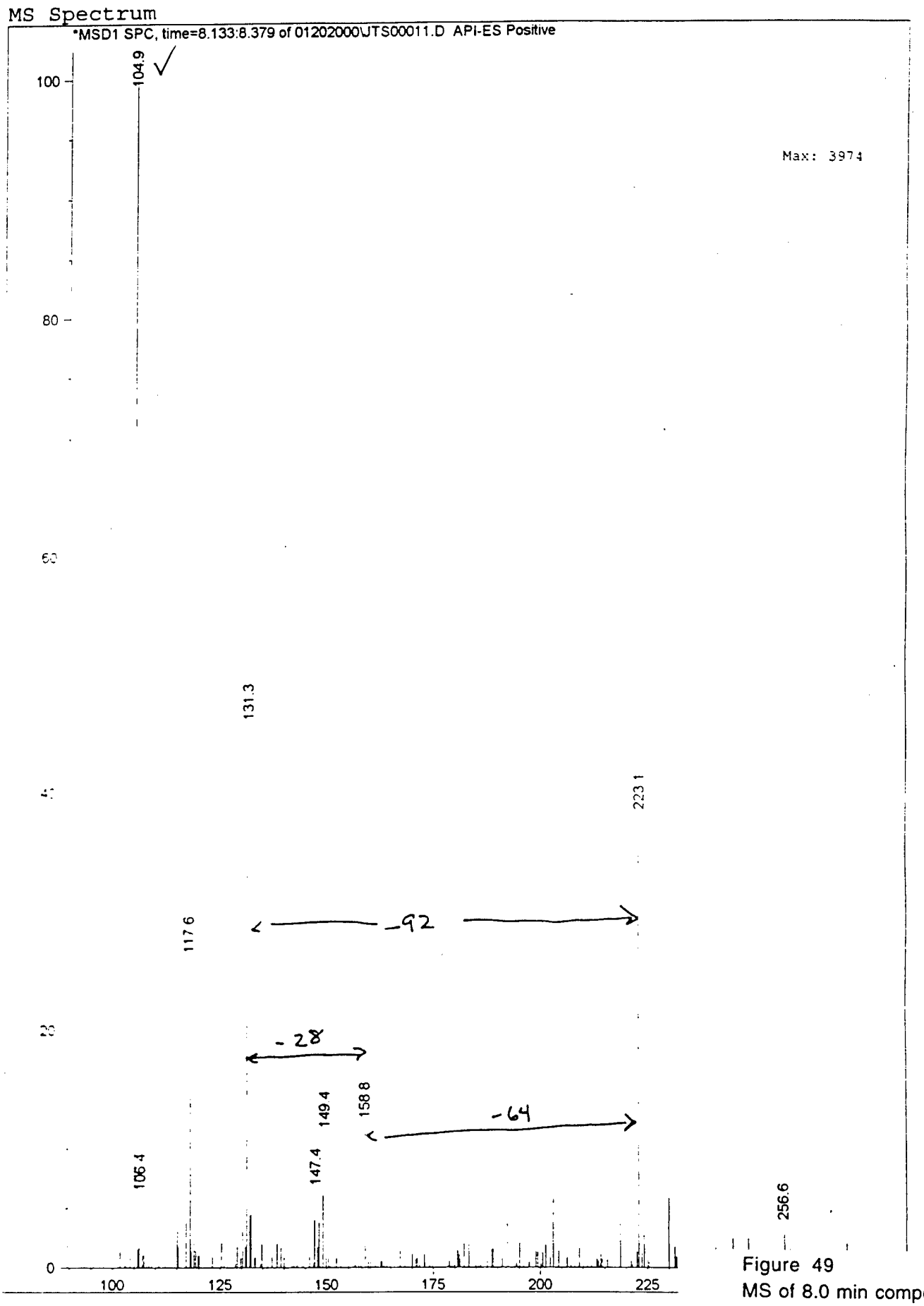

Figure 49
MS of 8.0 min component
3-AT reaction
CE-MS (+)-ESI

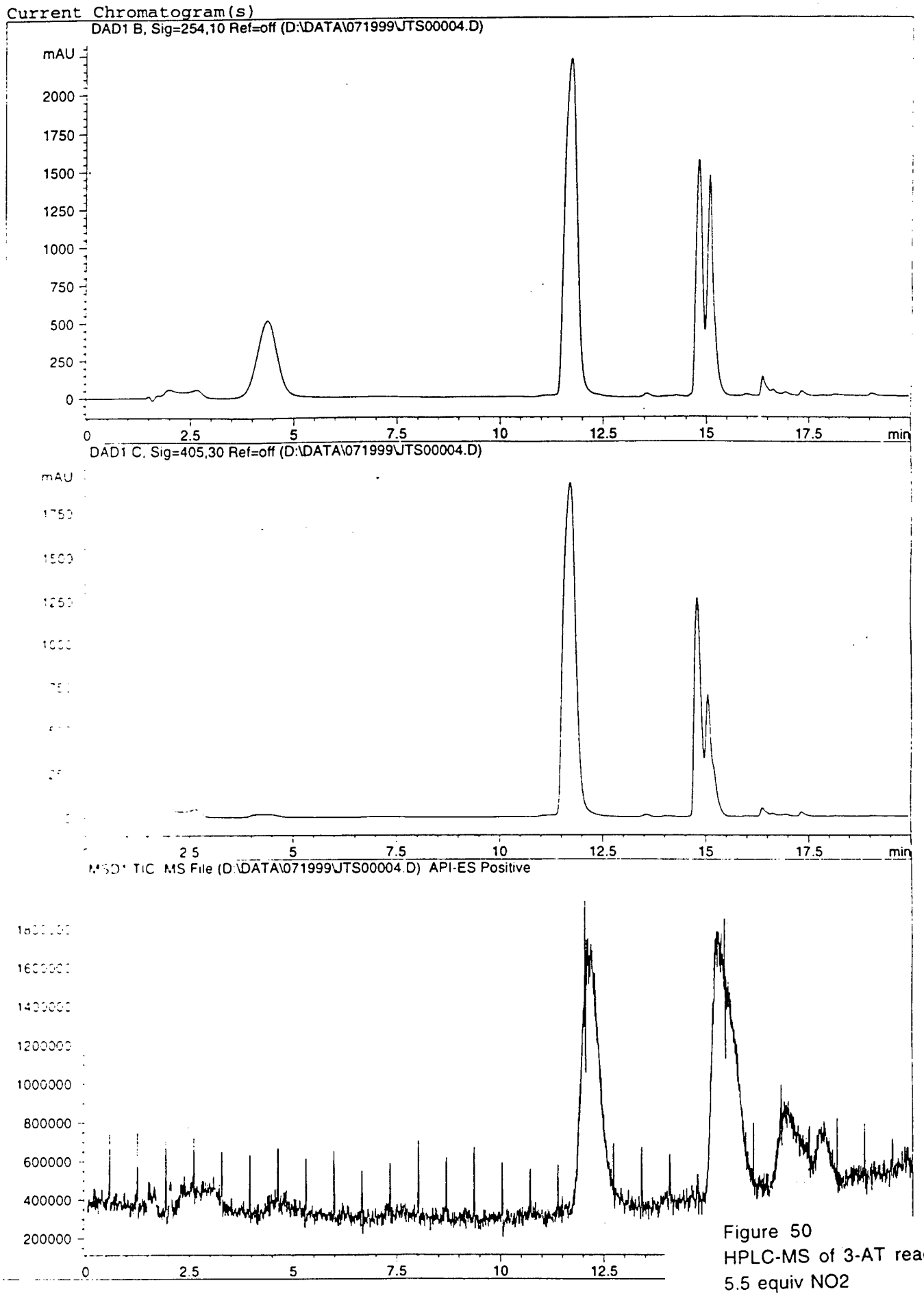

Figure 50
HPLC-MS of 3-AT reaction
5.5 equiv NO2
(+)-ESI

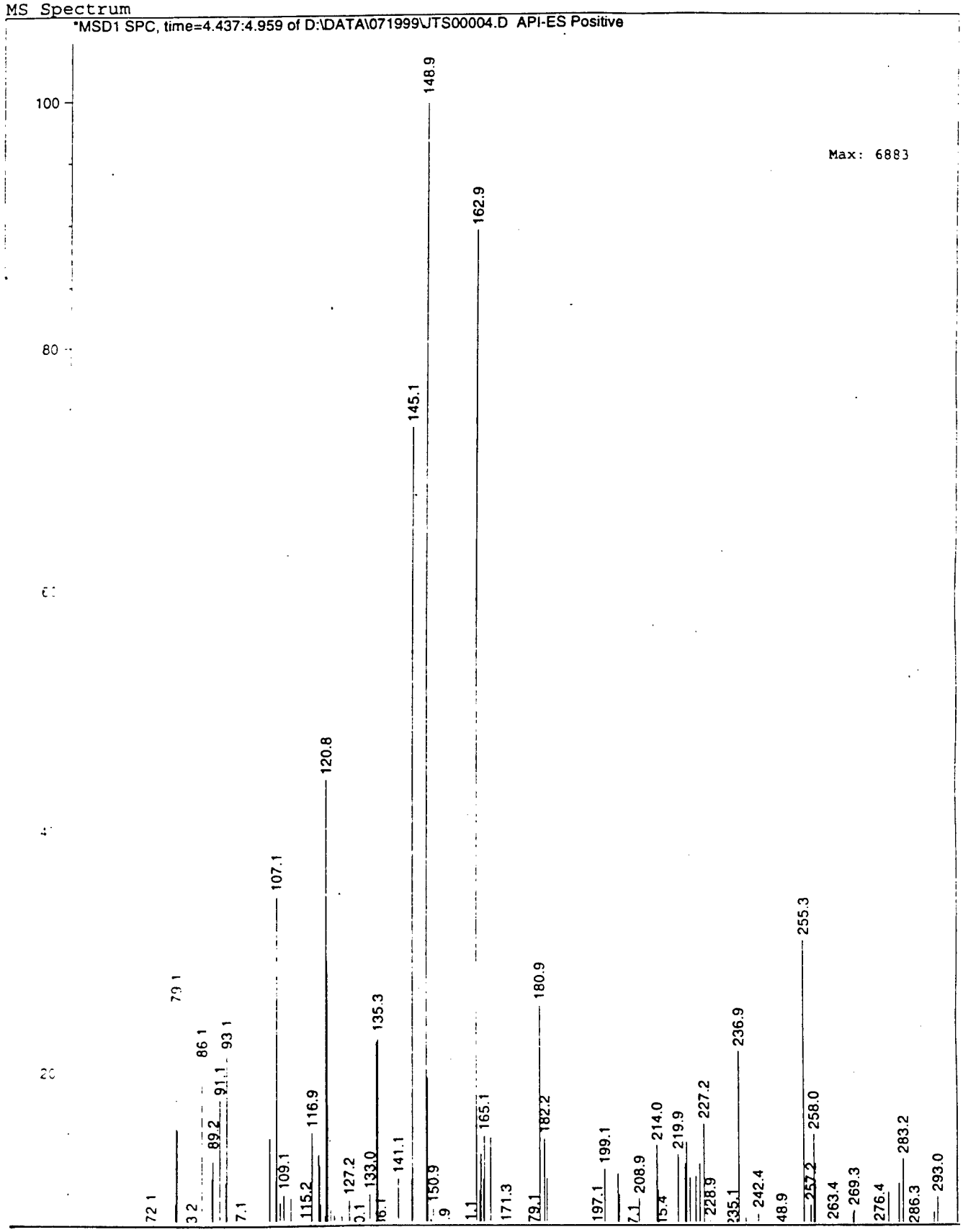

Figure 51
MS of 4.6 min component
3-AT reaction - 5.5 equiv NO2
(+)-ESI

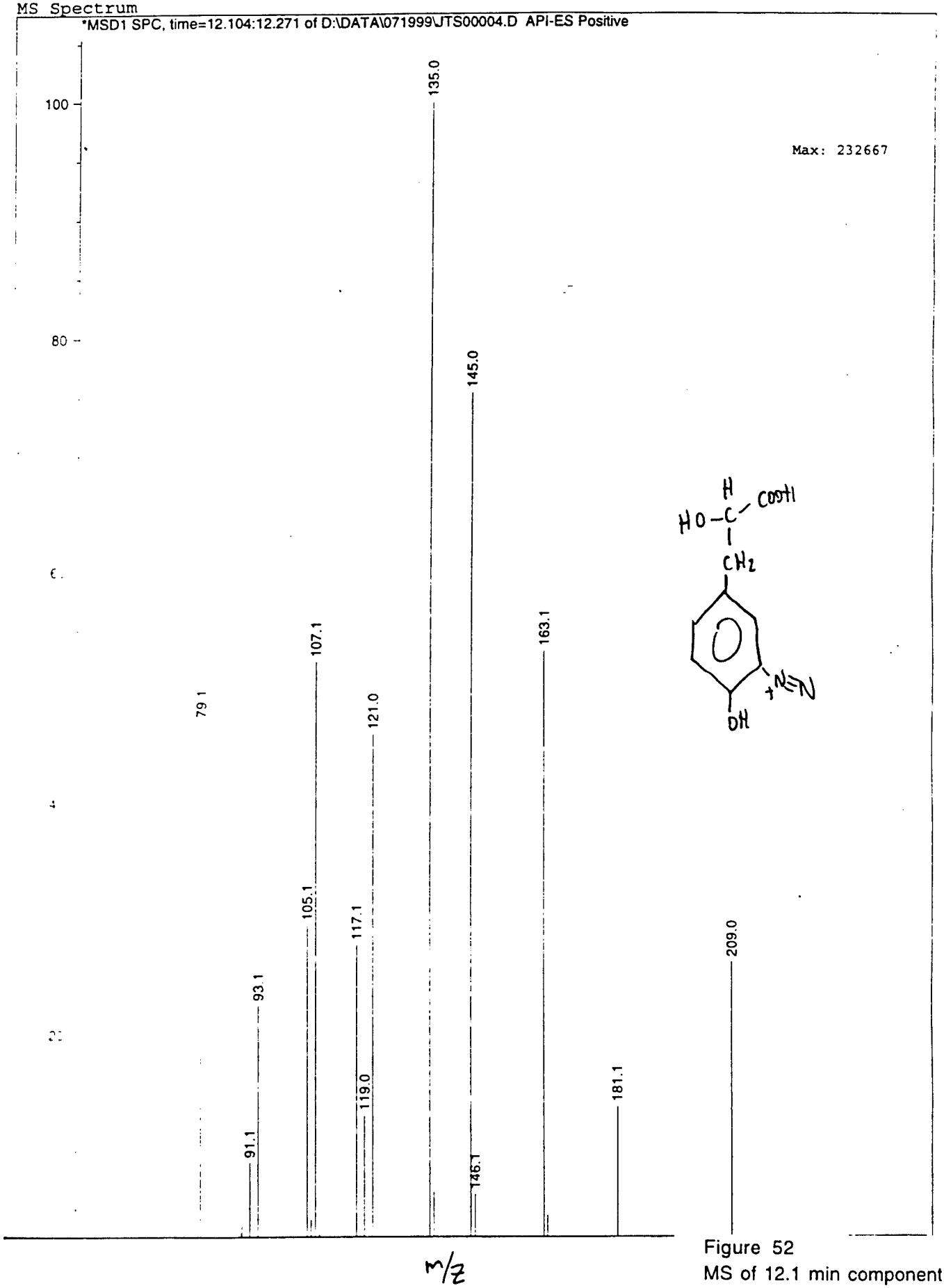

Figure 52
MS of 12.1 min component
3-AT reaction - 5.5 equiv NO2
(+)-ESI

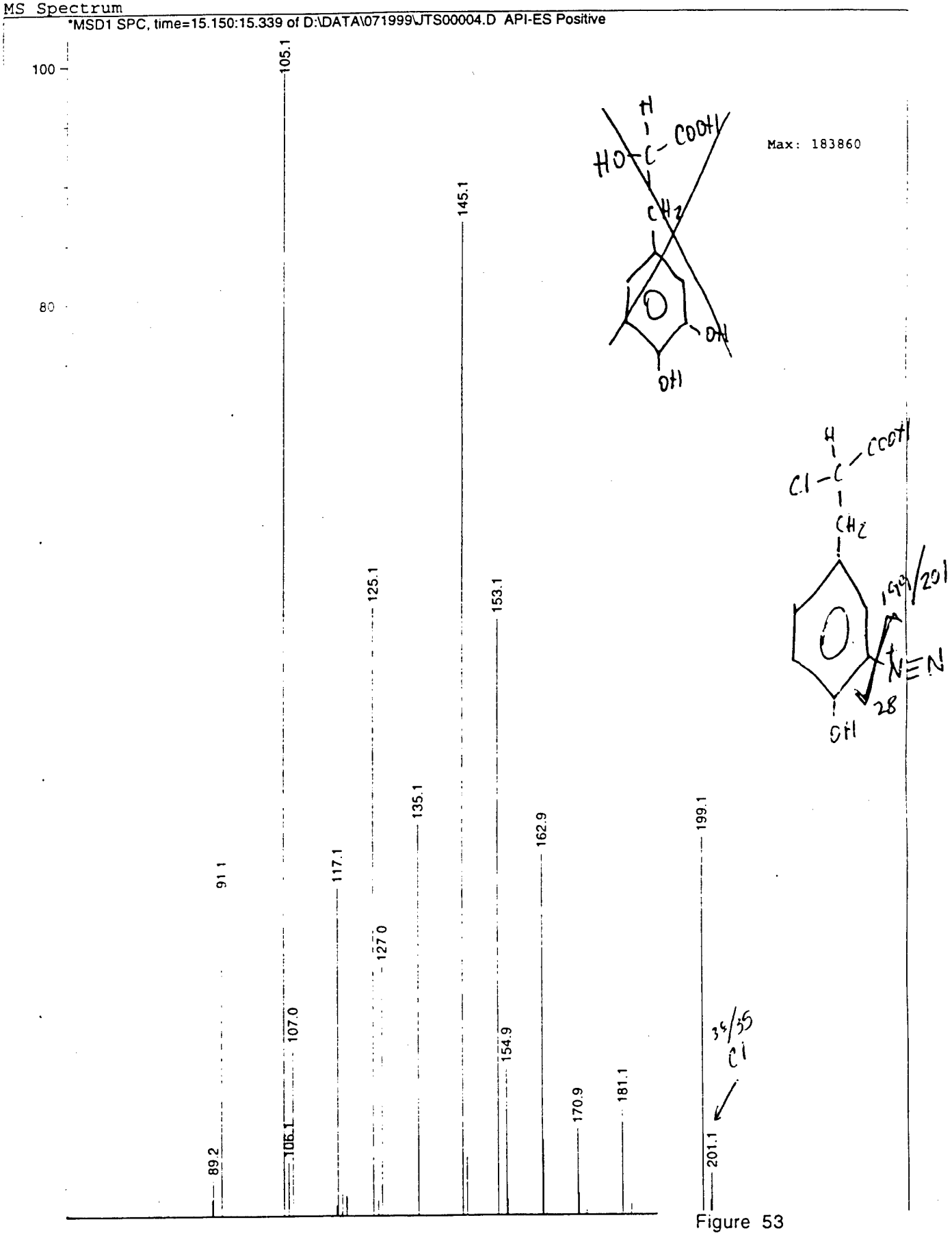

Figure 53
MS of 15.2 min component
3-AT reaction - 5.5 equiv NO2
(+)-ESI

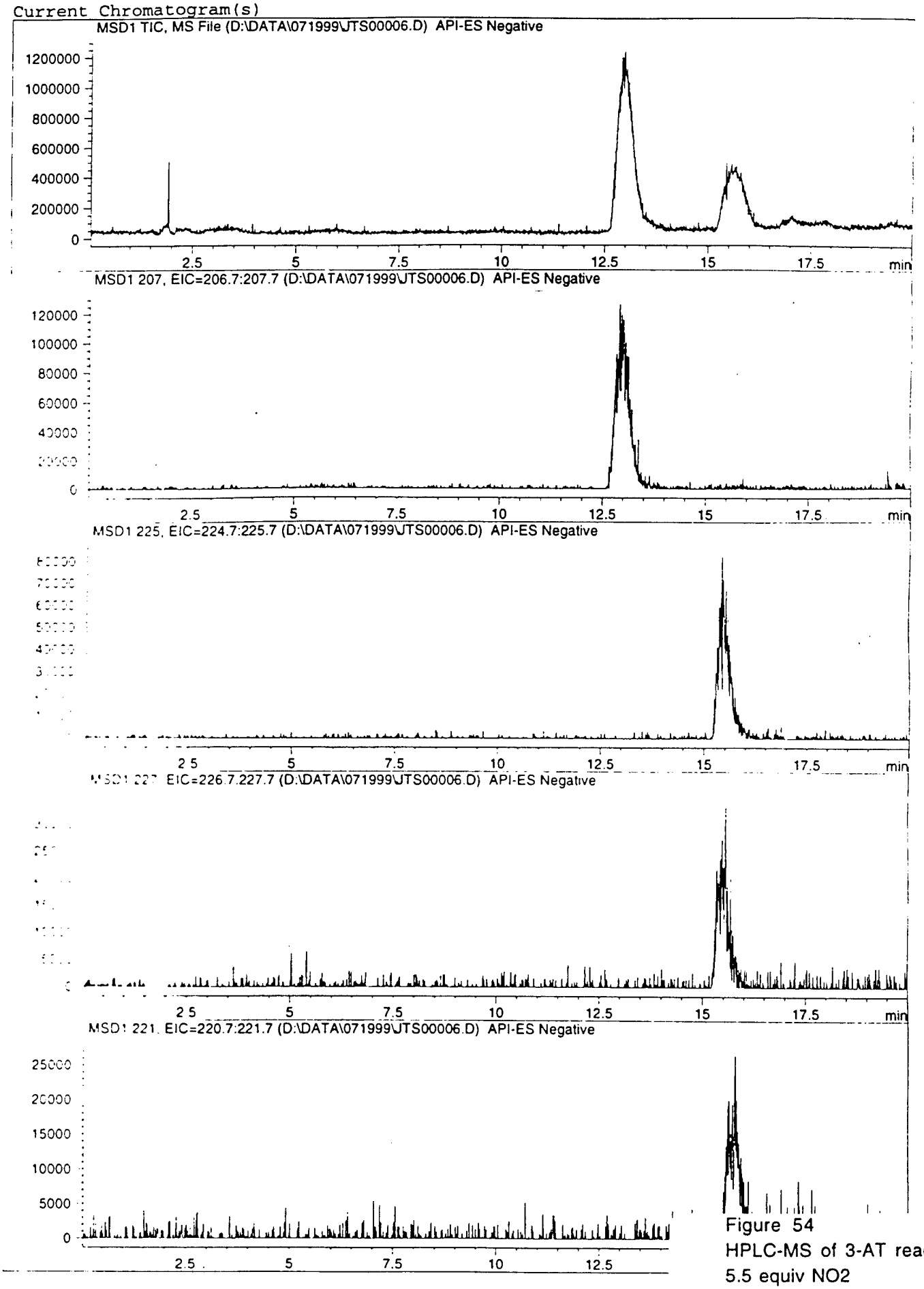

Figure 54
HPLC-MS of 3-AT reaction
5.5 equiv NO2
(-)-ESI

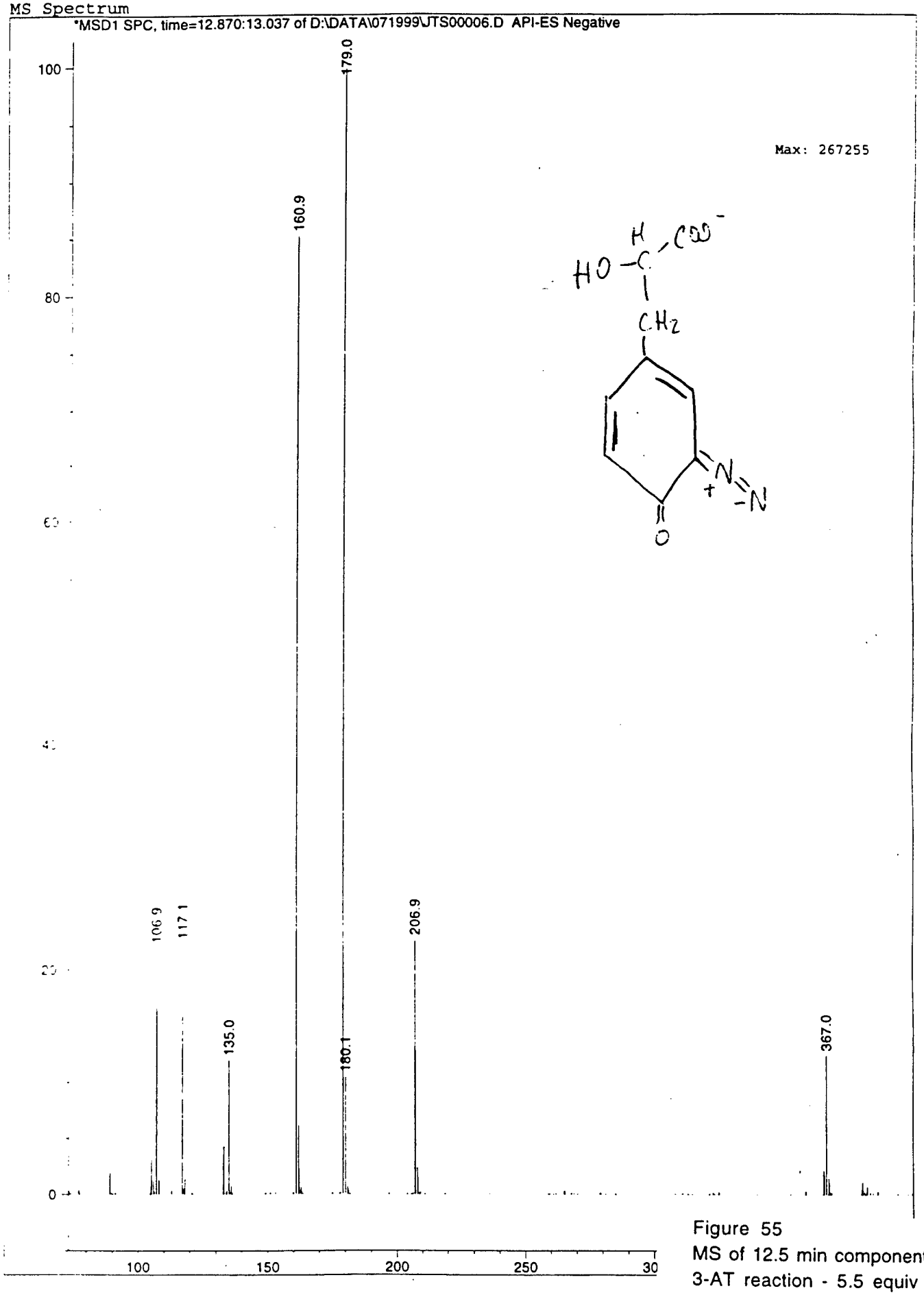

Figure 55
MS of 12.5 min component
3-AT reaction - 5.5 equiv NO2
(-)-ESI

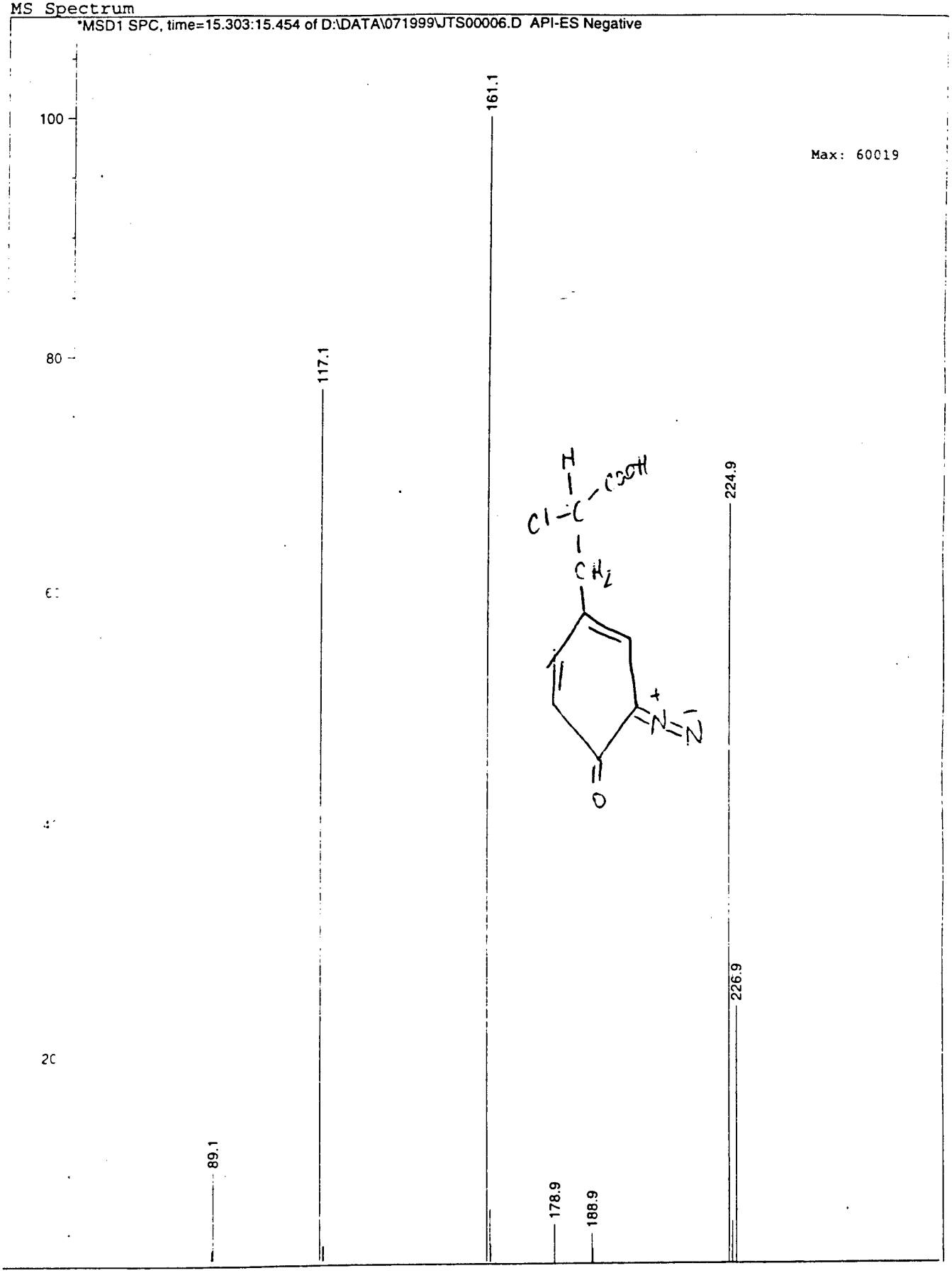

Figure 56
MS of 15.3 min component
3-AT reaction - 5.5 equiv NO2
(-)-ESI

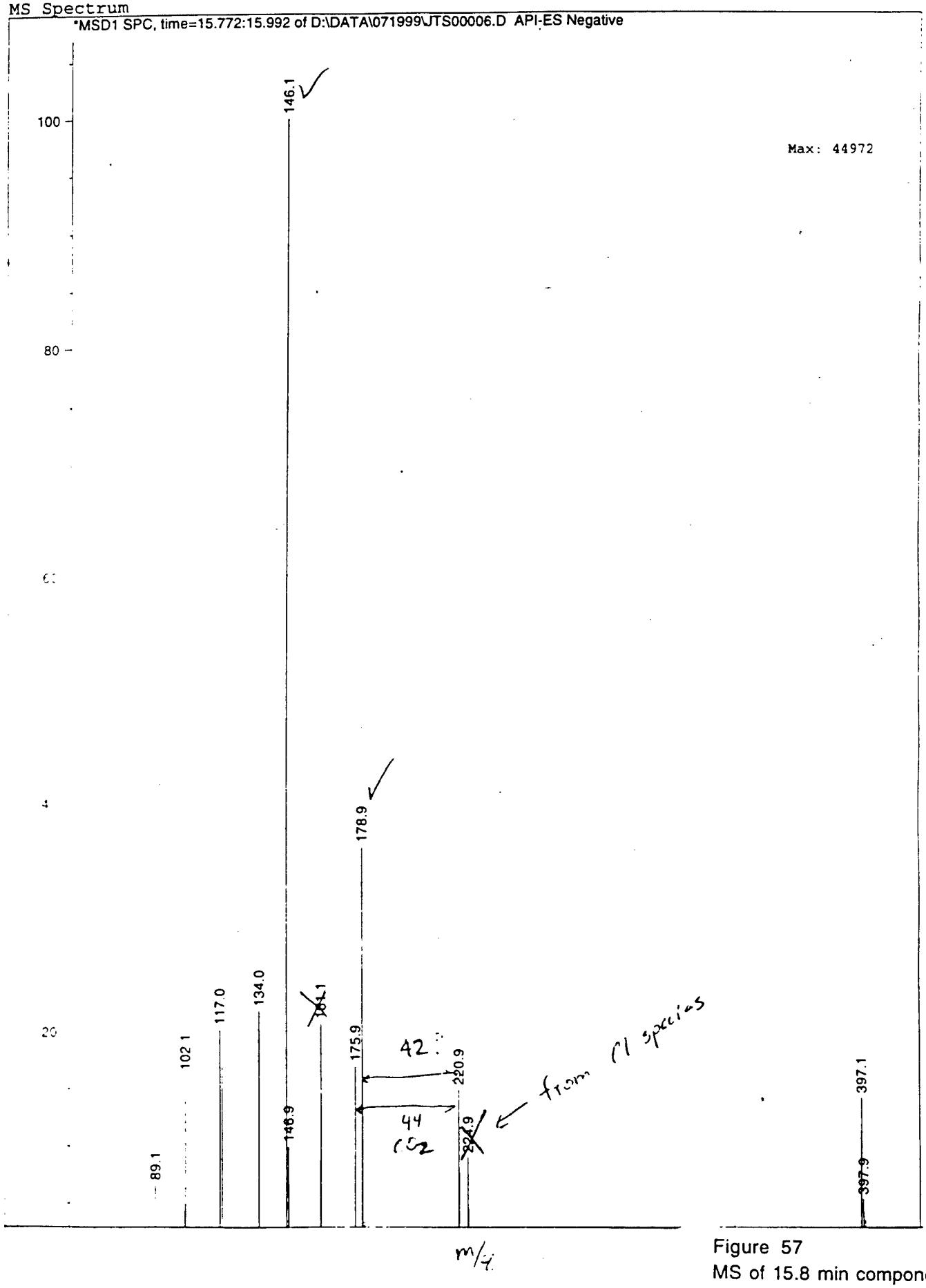

Figure 57
MS of 15.8 min component
3-AT reaction - 5.5 equiv NO2
(-)-ESI

Overlaid Sample Spectra

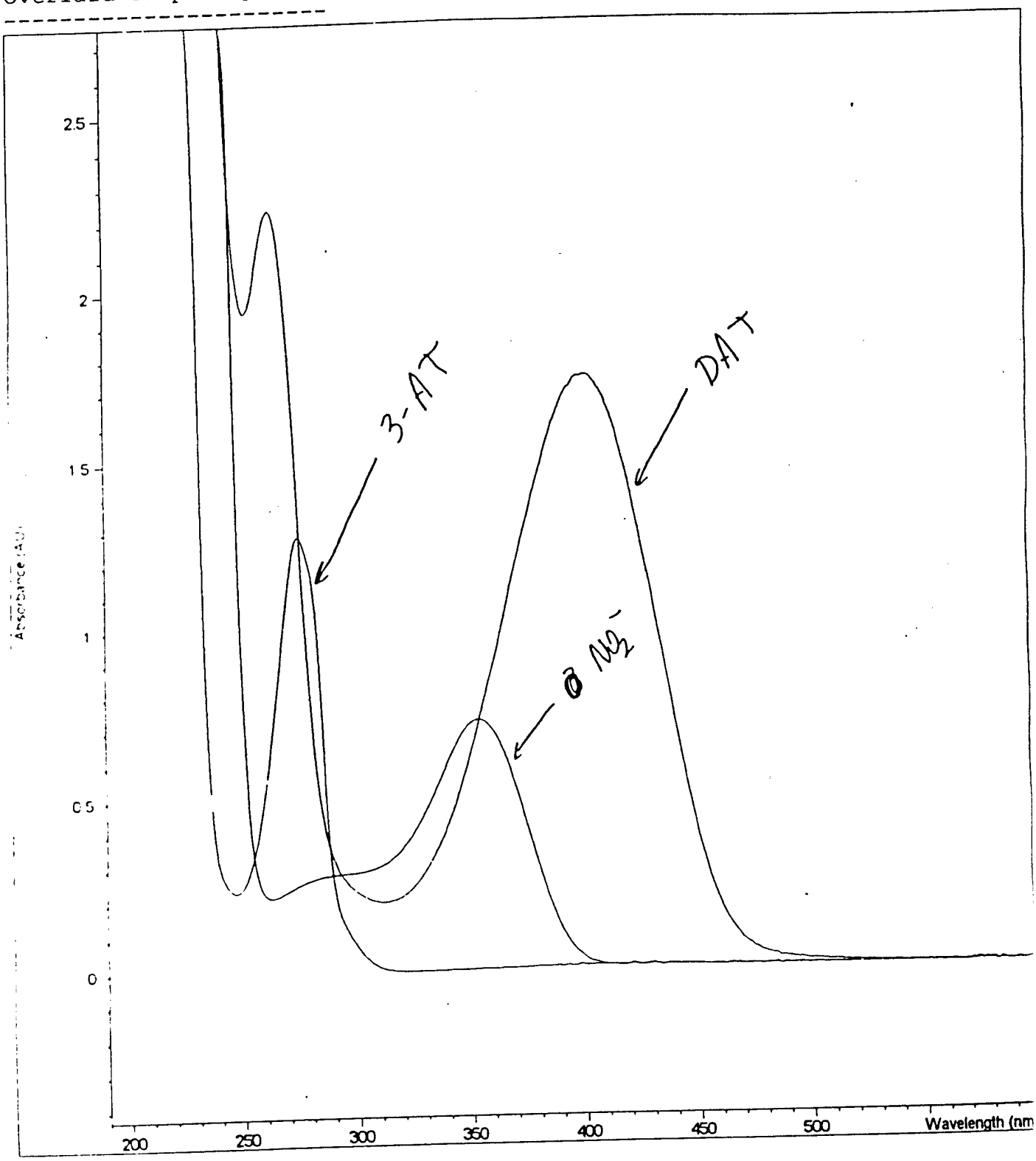

*** End ***

Figure 58
UV/Vis specta of
3-AT, NaNO2, and 3-AT reactior

Fixed Wavelength Report Date 02/05/98 Time 11:54:29 Page 1 of 1

Method file : <untitled>
Information : Default Method
Data File : C:\HPCHEM\1\DATA\JTSSPE~1\LAL\2-5-98\#1.SD
Created : 2/5/98 11:52:00

Overlaid Spectra:

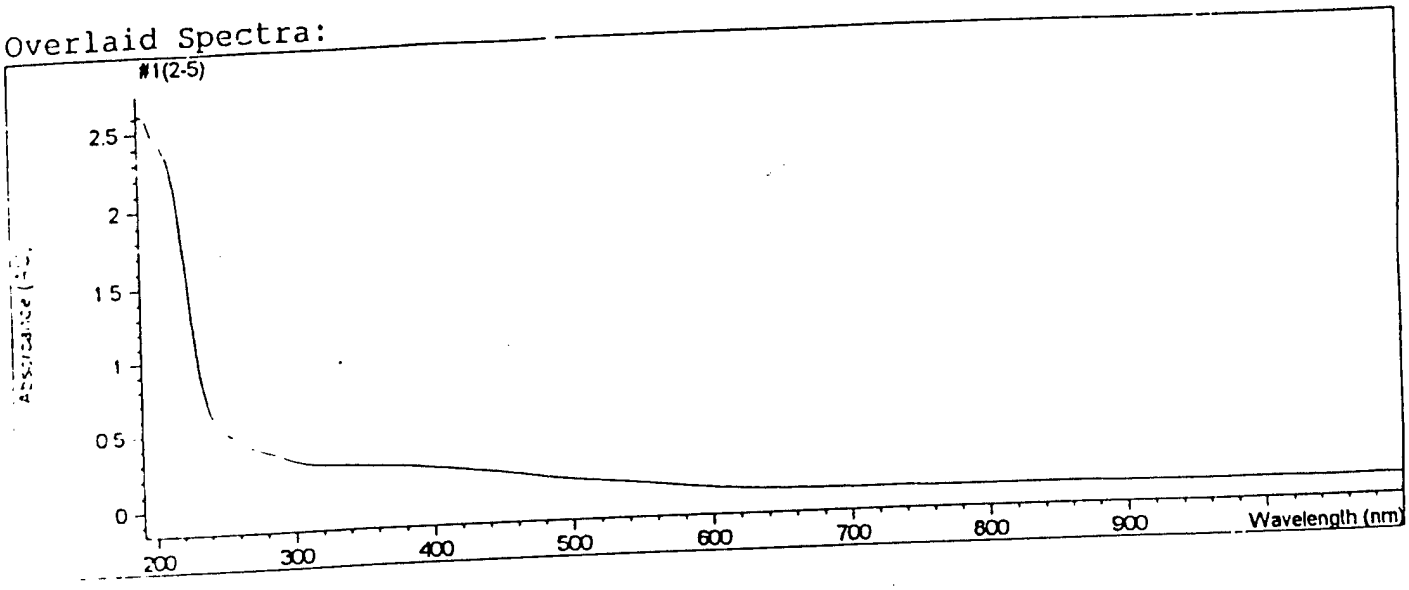

#	Name	Abs<480nm>
1	#1(2-5) Solid	0.13682

Report generated by : lea ann Signature: .....

*** End Fixed Wavelength Report ***

Figure 59
UV/Vis of crude p-DAT in H2O

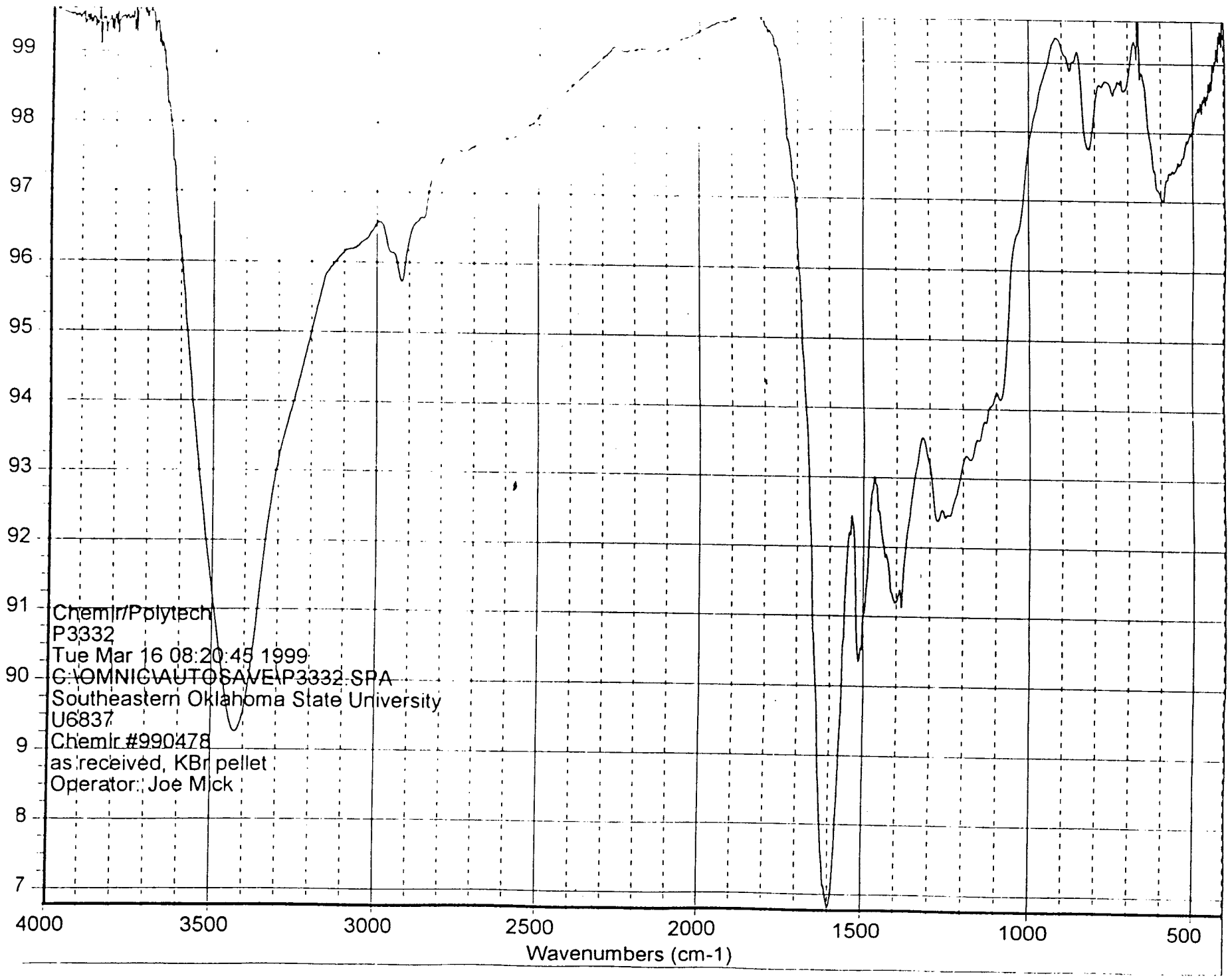

Figure 60
IR of dialyzed p-DAT
KBr pellet

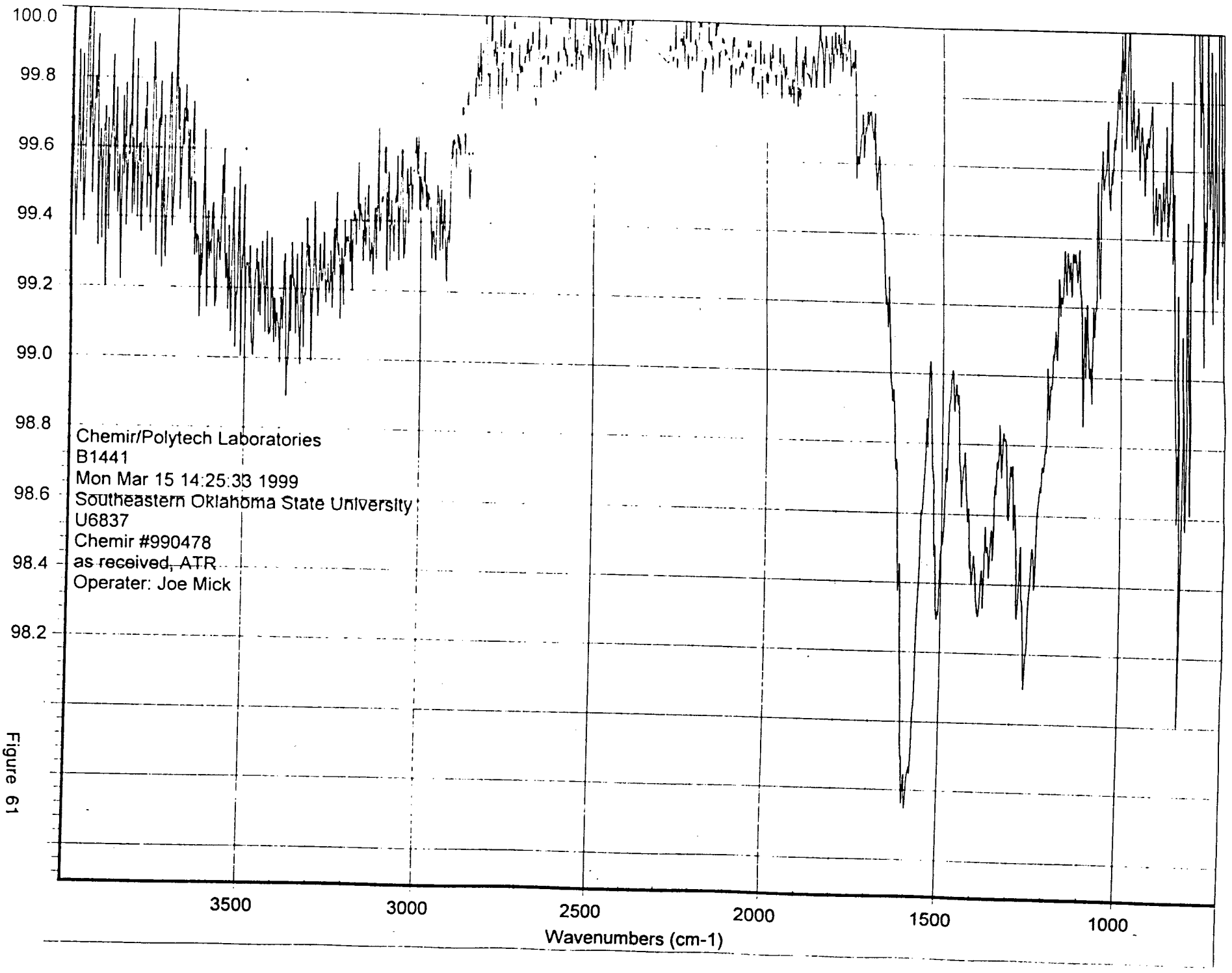

Figure 61
Reflectance IR spectra
dialyzed p-DAT

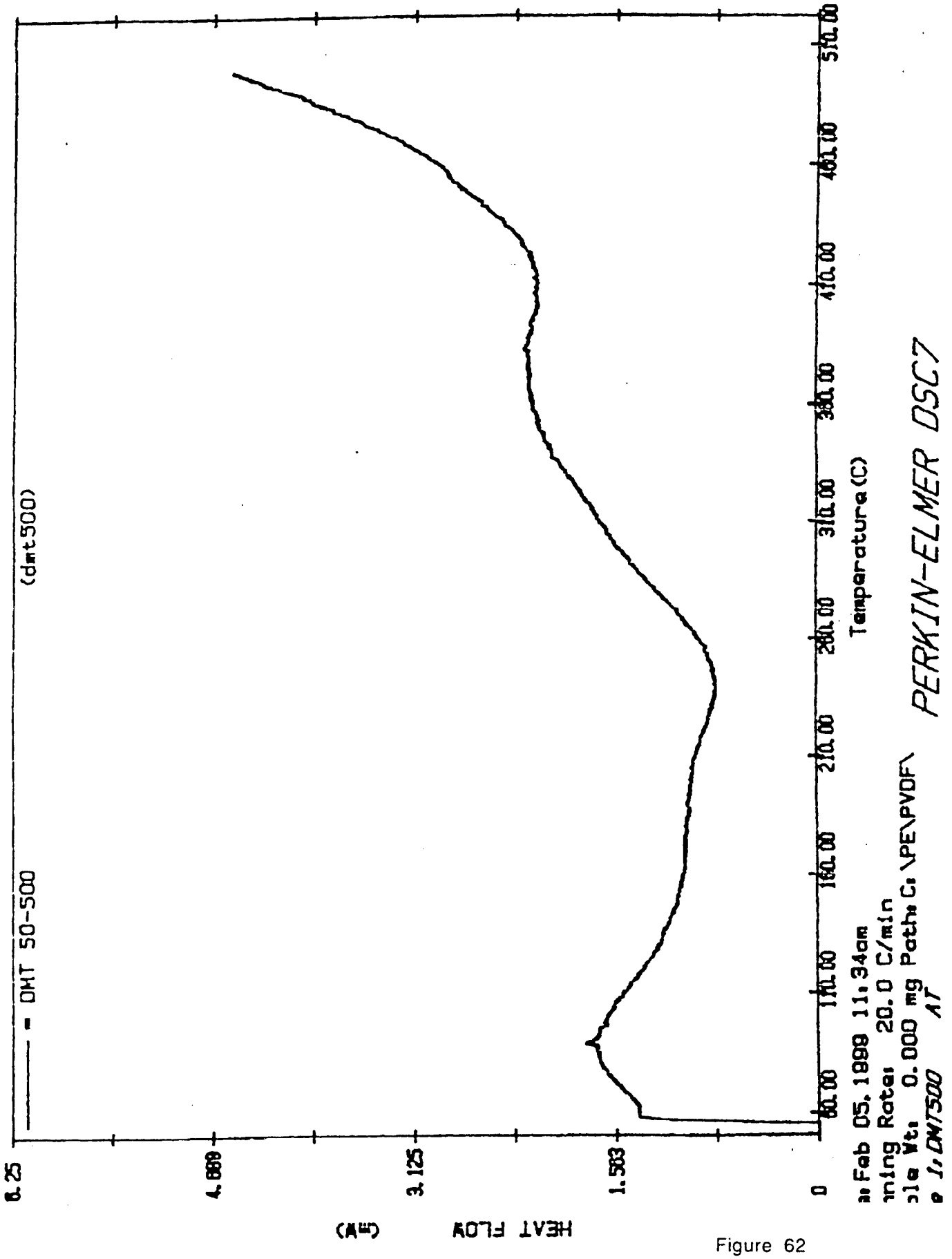

Figure 62
DSC of dialyzed p-DAT

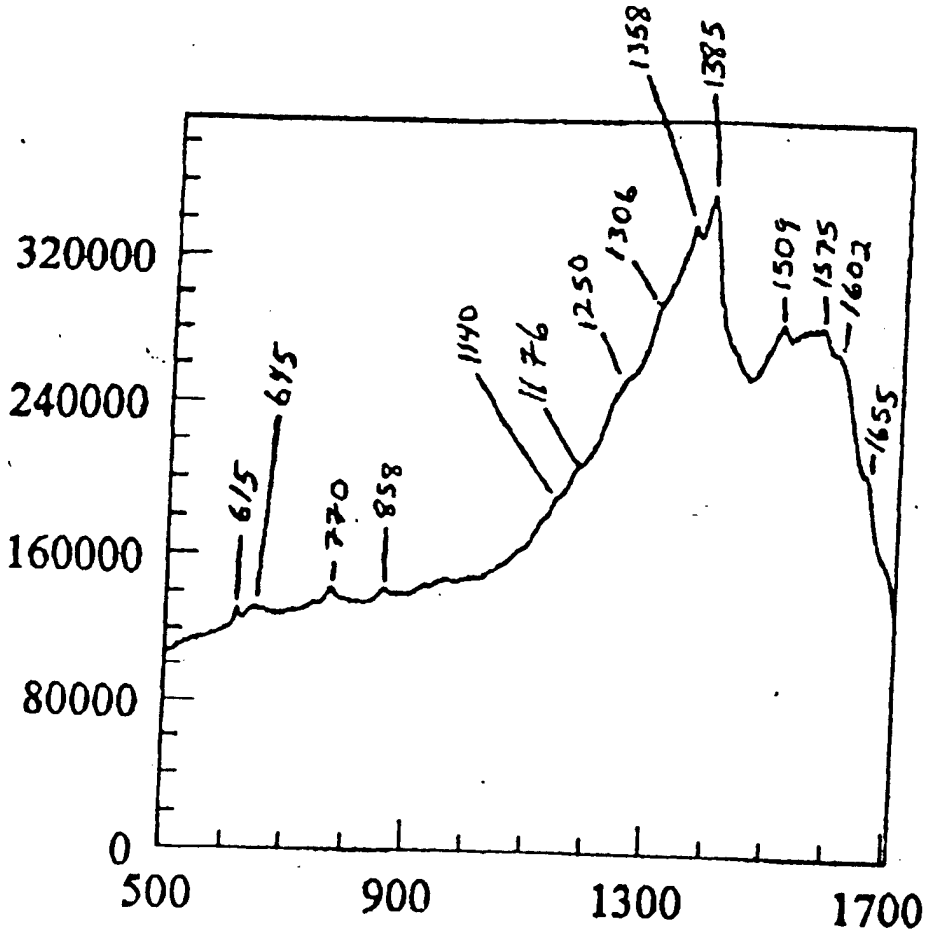

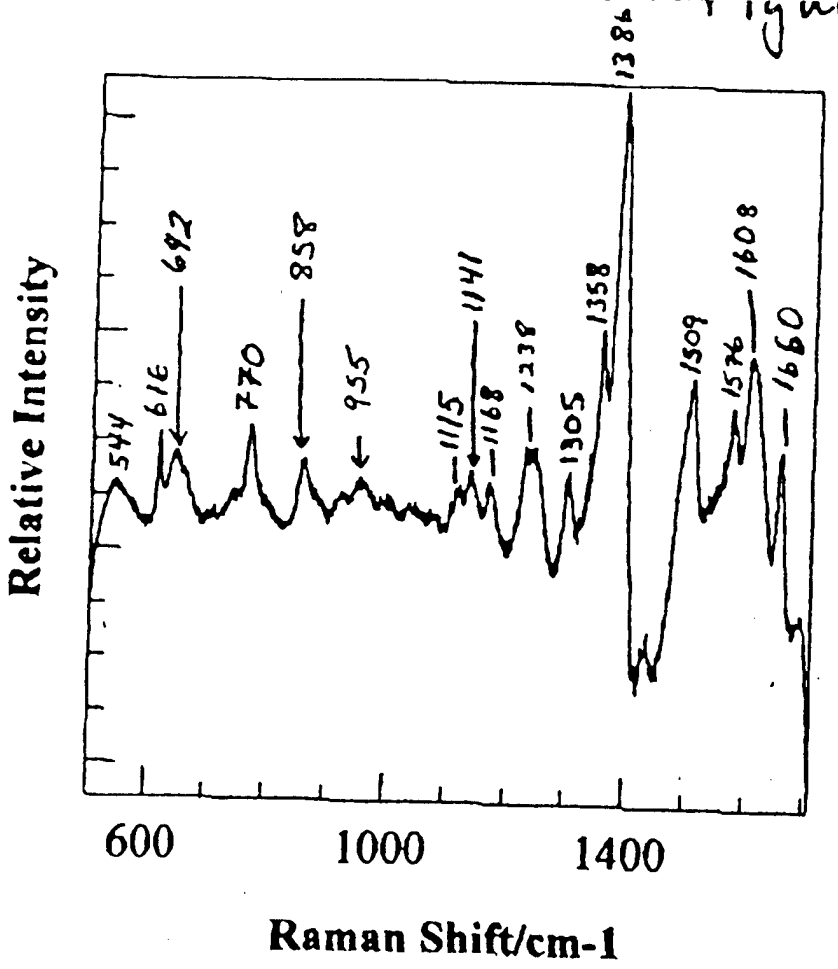

Figure 63
Surface Enhanced Raman
of dialyzed p-DAT

TO: Dr. Tim Smith

STANDARD PROTON PARAMETERS

expl preset

SAMPLE		SATURATION	
date	Apr 23 98	stpul	n
solvent	D2O	satpwr	0
file	exp	satfrq	719.0
ACQUISITION		satdly	1.500
sfrq	598.758	satmode	yyn
tn	H1	composit	n
at	1.892	DEC & VT	
np	30772	dn	H1
sw	8988.6	dof	-719.0
fb	6860	dm	nnn
bs	32	dmm	c
tpwr	50	dmf	200
pw	8.5	temp	27.0
dl	0	PROCESSING	
tof	0	lb	10.00
nt	128	wtfile	
ct	128	proc	ft
alock	n	fn	not used
gain	a	math	r
FLAGS			
il	n	werr	
in	n	wexp	
dp	y	wbs	
hs	nn	wnt	wft
		DISPLAY	
		sp	-937.4
		wp	8988.6
		vs	2.97089e+06
		sc	0
		wc	200
		hzmm	60.00
		is	33.57
		rfl	3781.5
		rfp	7844.1
		th	7
		ins	1.000
		al	ph

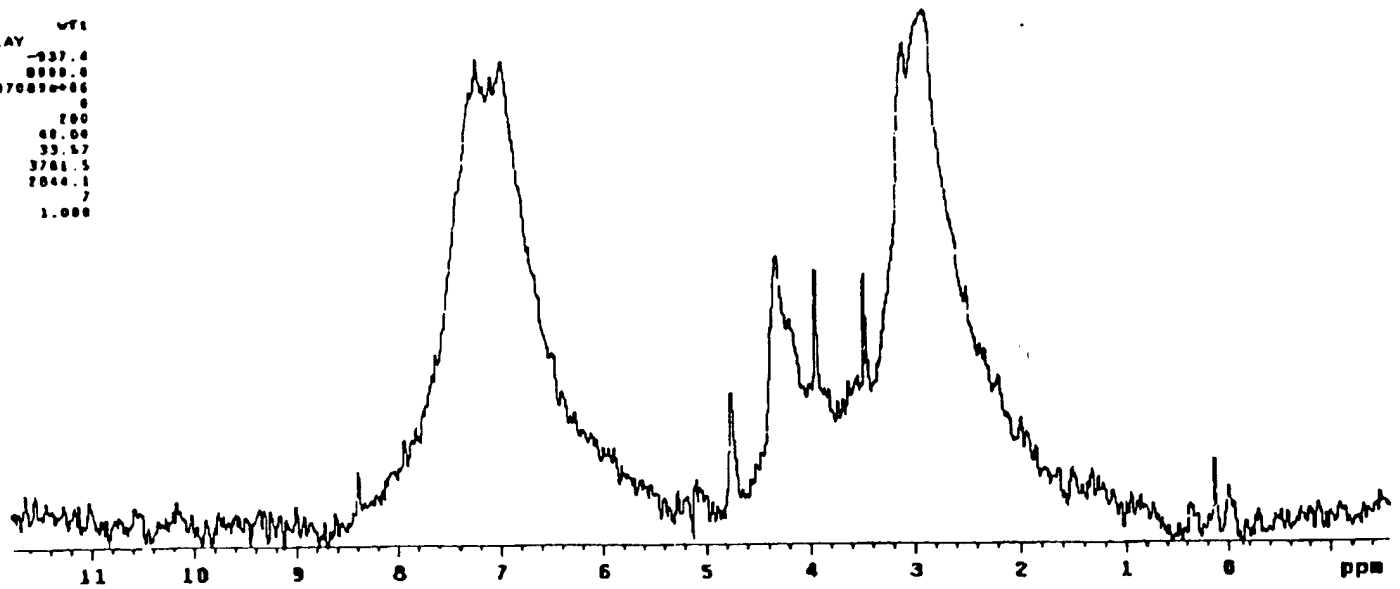

Figure 64
1H NMR of p-DAT (MWCO 10k)
in D2O
600 MHz NMR

TO: Dr. Tim Smith

^{13}C Spectrum

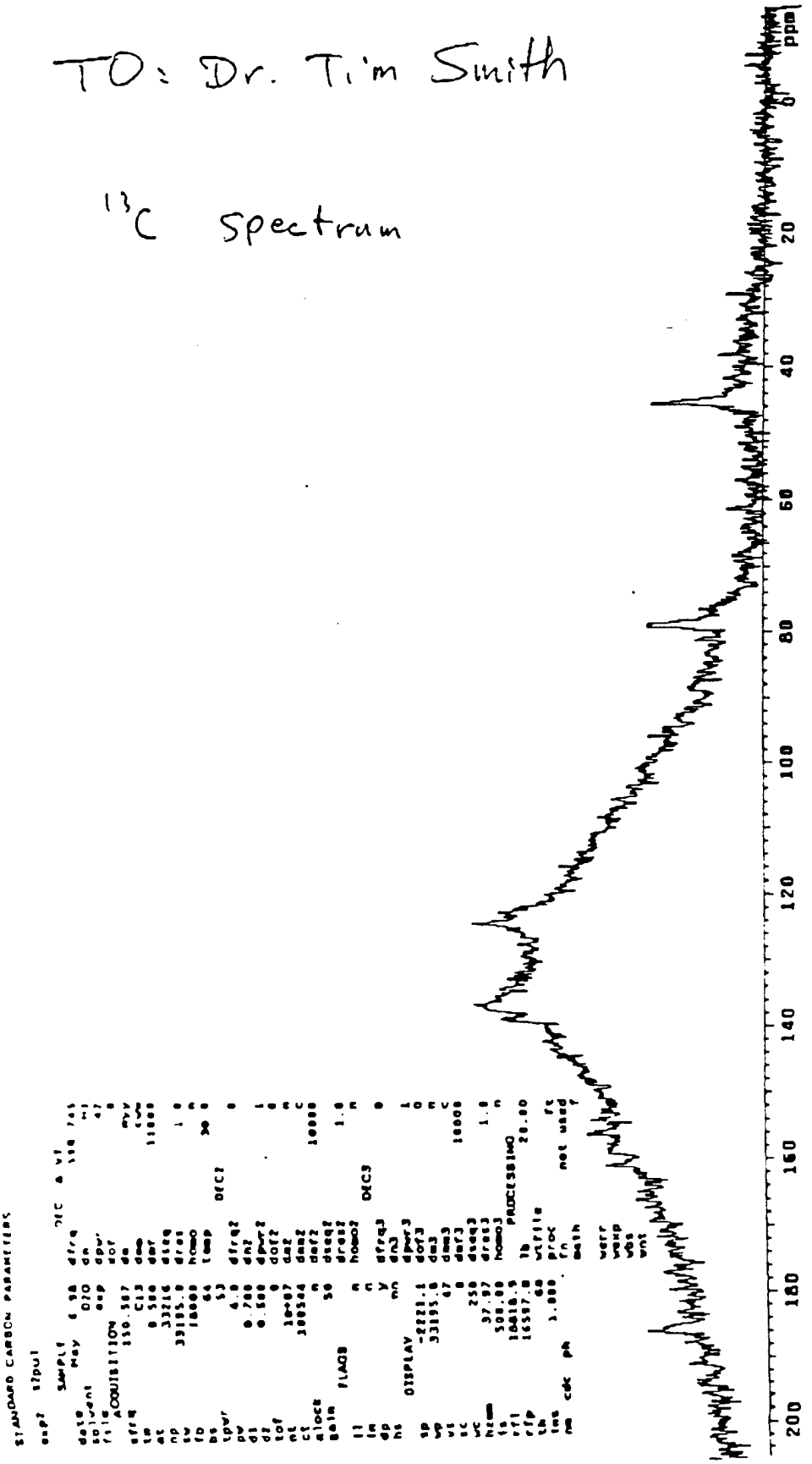

Figure 65
13C NMR of p-DAT (MWCO 10k)
in D2O
600 MHz NMR

STANDARD PROTON PARAMETERS

expl presat

SAMPLE			
date	Nov 6 1998		
solvent	D2O		
file	exp		
ACQUISITION			
sfrq	598.726		
tn	H1		
at	1.892		
np	30272		
sw	8000.0		
fb	4000		
bs	32		
tpwr	54		
pw	5.3		
d1	0		
tof	0		
nt	32		
ct	32		
alock	n		
gain	50		
FLAGS			
il	n		
in	n		
dp	y		
hs	nn		
		SAT PARM	
		sspul	
		satpwr	
		satfrq	
		satdly	
		satmode	
		composit	
		DEC & .2	
		dn	H1
		dof	-215.1
		dm	nnn
		dmm	c
		dmf	200
		dpwr	30
		temp	30.0
		PROCESSING	
		lb	2.00
		wtfile	
		proc	ft
		fn	not used
		math	f
		werr	
		wexp	
		wbs	
		wnt	wft
		DISPLAY	
		sp	-1006.4
		wp	8000.0
		vs	112
		sc	0
		wc	200
		hzmm	0.63
		is	33.57
		rfl	1006.4
		rfp	0
		th	7
		ins	1.000
		nm cdc ph	

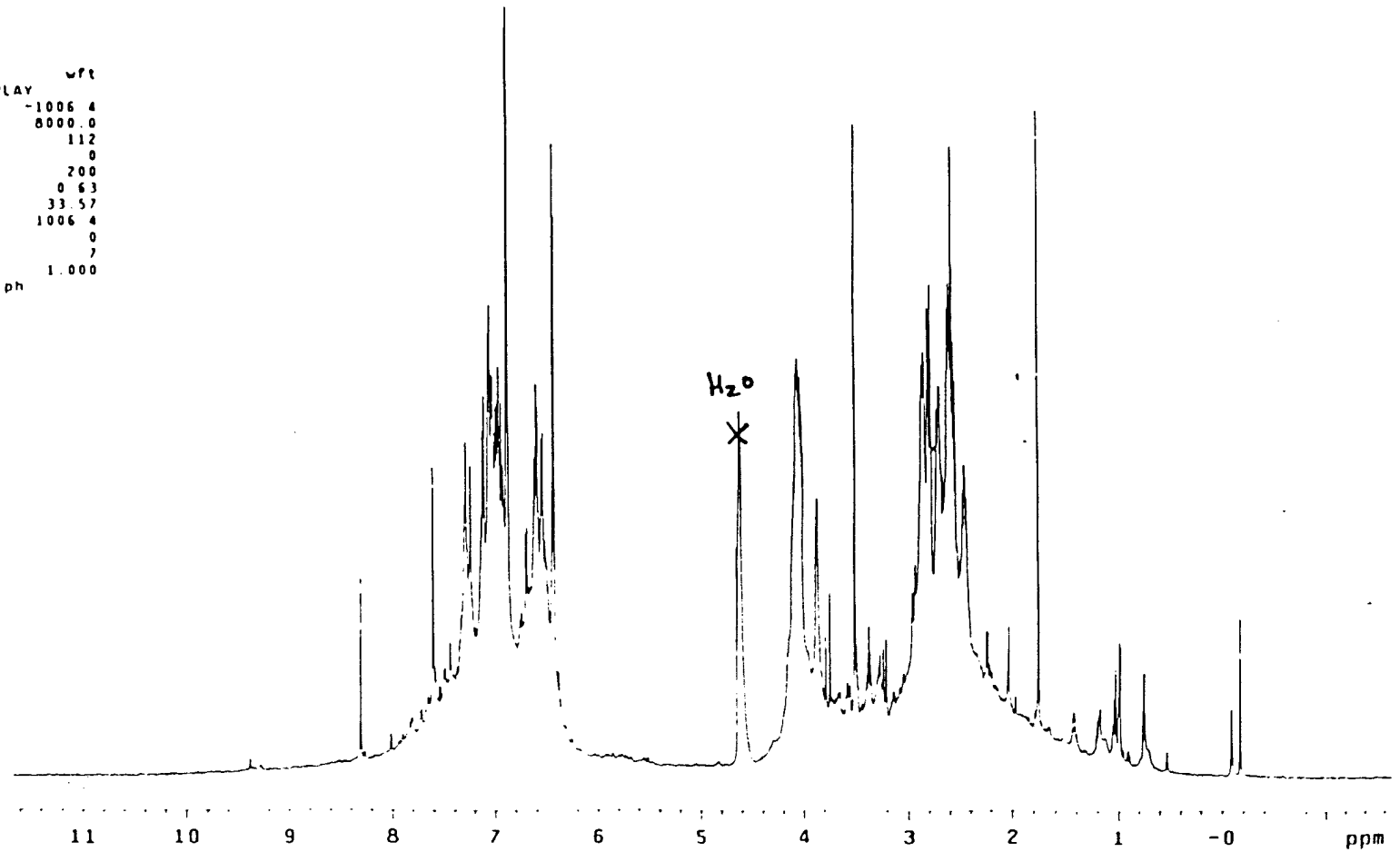

Figure 66
1H NMR of p-DAT<2k
in D2O/NaOD
600 MHz NMR

pDAT < 2000

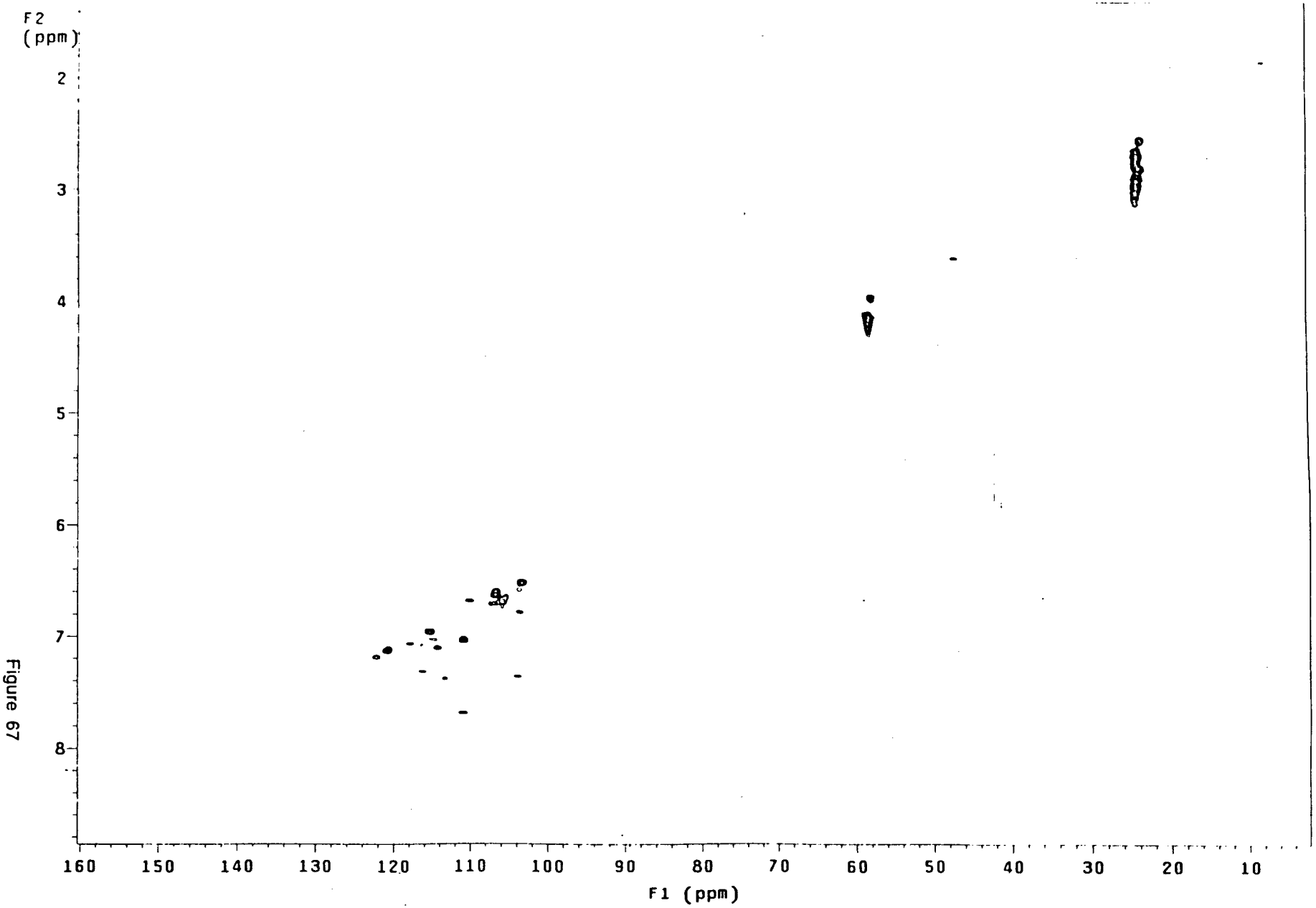

Figure 67
1H-13C HETCOR NMR of p-DAT<2k
in D2O/NaOD
600 MHz NMR

STANDARD PROTON PARAMETERS

expl presat

SAMPLE			SATURATION	
date	Nov 6 1998		sspul	n
solvent	D2O		satpwr	2
file	exp		satfrq	-216.6
ACQUISITION			satdly	1.500
sfrq	598.726		satmode	ynn
tn	H1		composit	n
at	1.892	DEC & vf		
np	30272	dn		H1
sw	8000.0	dof		-216.6
fb	4000	dm		nnn
bs	32	dmm		c
ss	2	dmf		200
tpwr	54	dpwr		30
pw	5.3	temp		30.0
d1	0	PROCESSING		
tof	0	lb		2.00
nt	32	wtfile		
ct	32	proc		ft
alock	n	fn		not used
gain	50	math		f
FLAGS				
il	n	werr		
in	n	wexp		
dp	y	wbs		
hs	nn	wnt		wft
		DISPLAY		
		sp		-1006.4
		wp		8000.0
		vs		163
		sc		0
		wc		200
		hzmm		40.00
		is		33.57
		rfl		1006.4
		rfp		0
		th		7
		ins		1.000
		nm cdc ph		

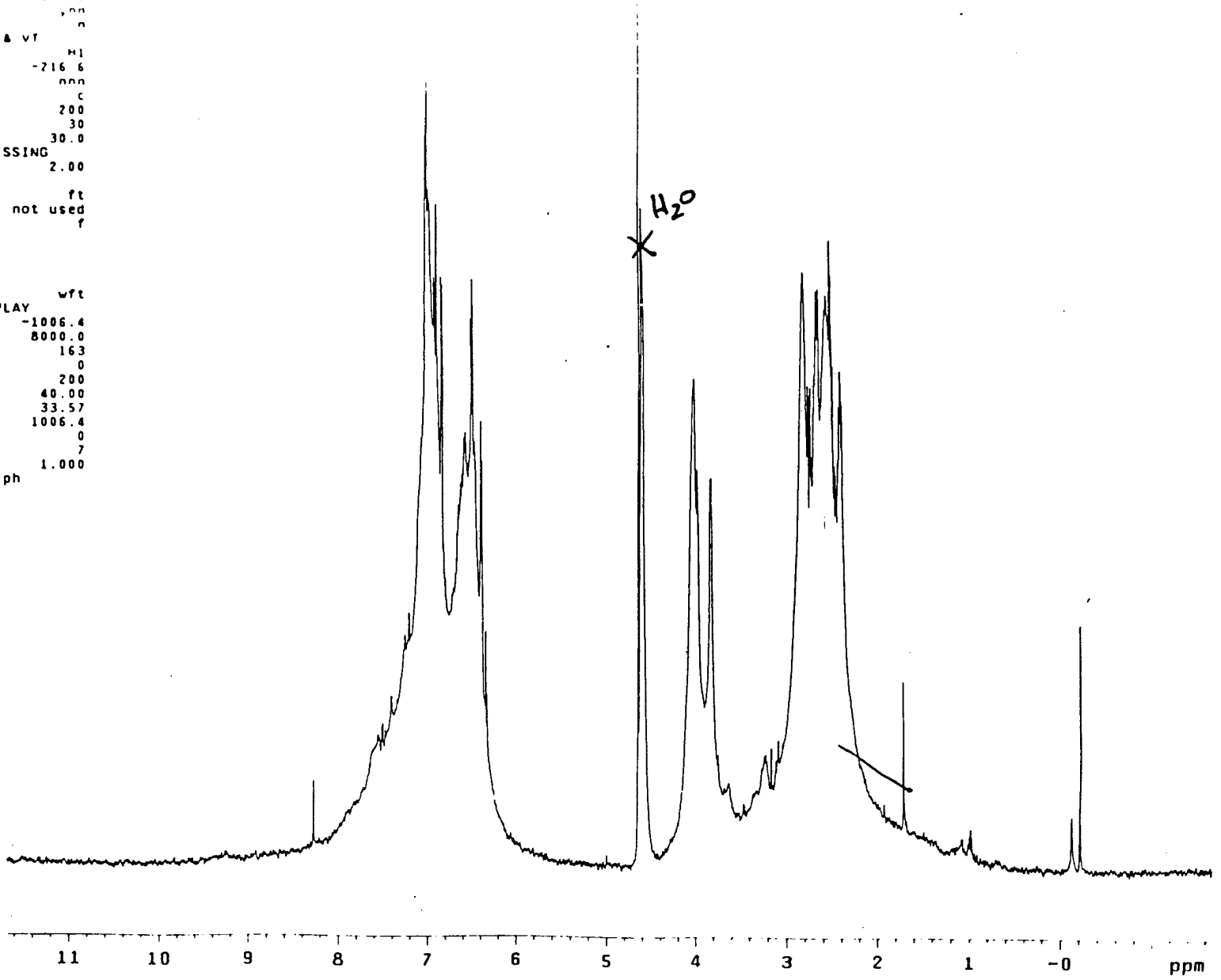

Figure 68
1H NMR of p-DAT>2k
in D2O/NaOD
600 MHz NMR

TO: Dr. Tim Smith.

greater than 2000

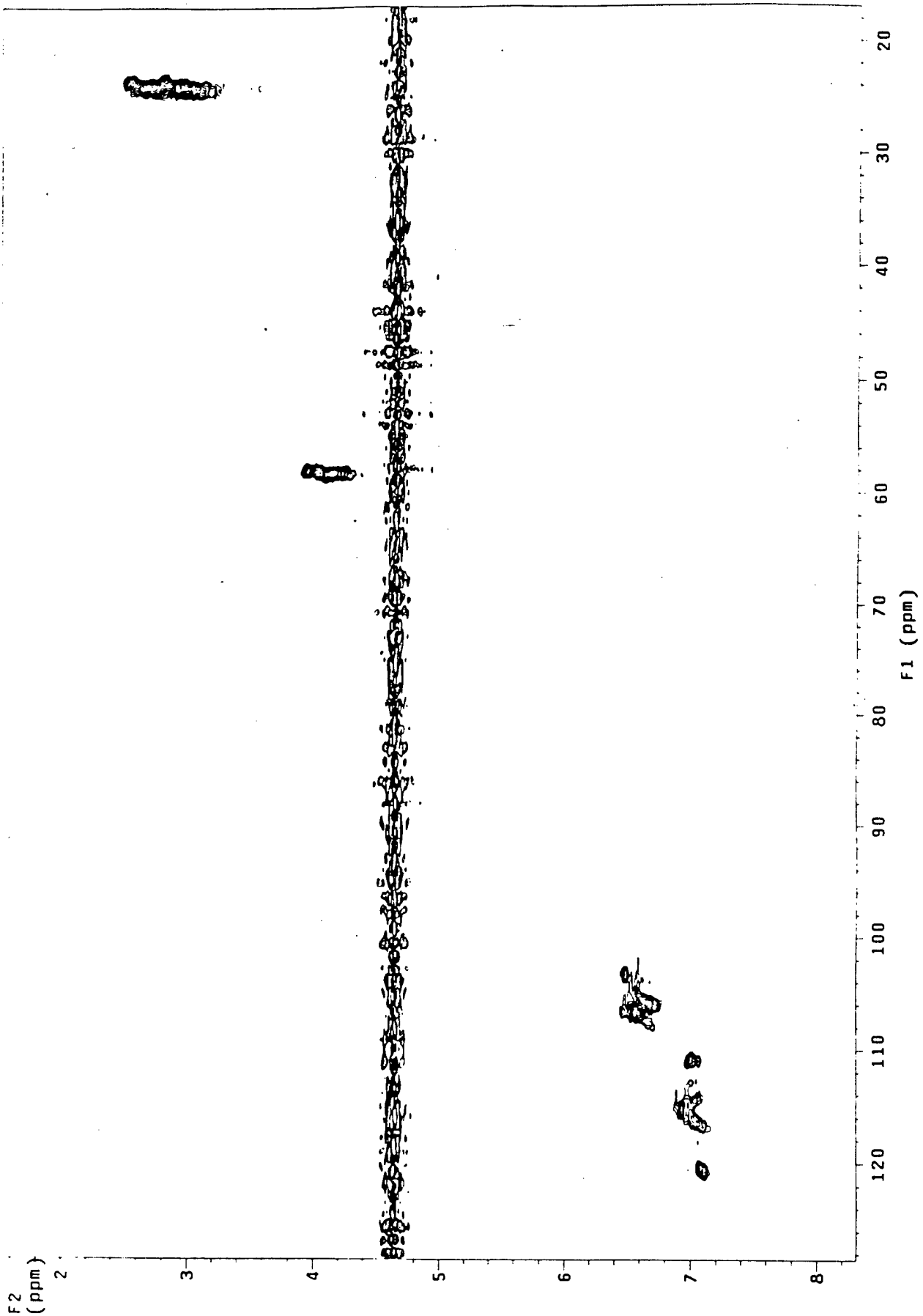

Figure 69
1H-13C HETCOR NMR of p-DAT>2k
in D2O/NaOD
600 MHz NMR

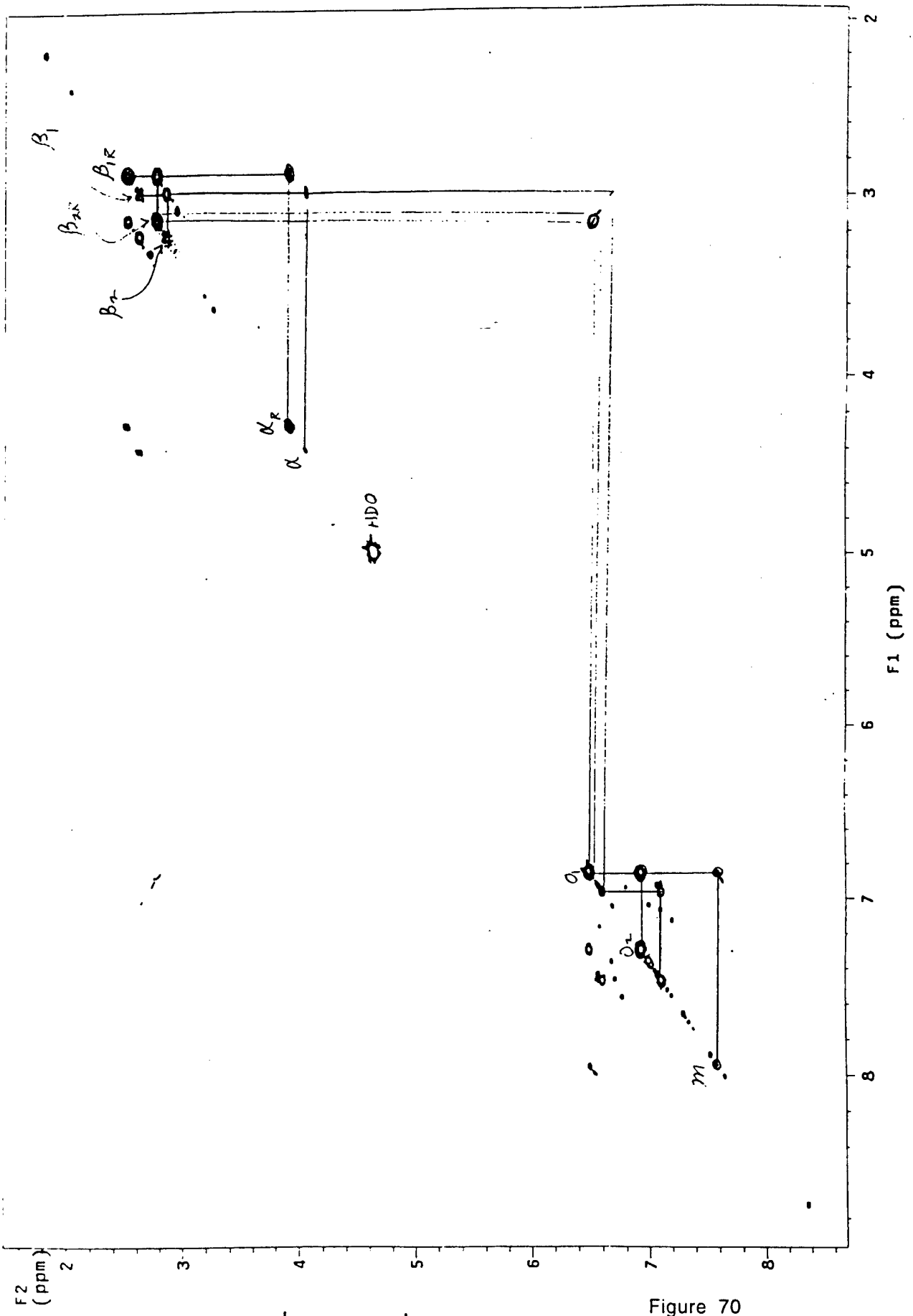

Figure 70
1H-1H COSY NMR of p-DAT>2k
in D2O/NaOD
600 MHz NMR

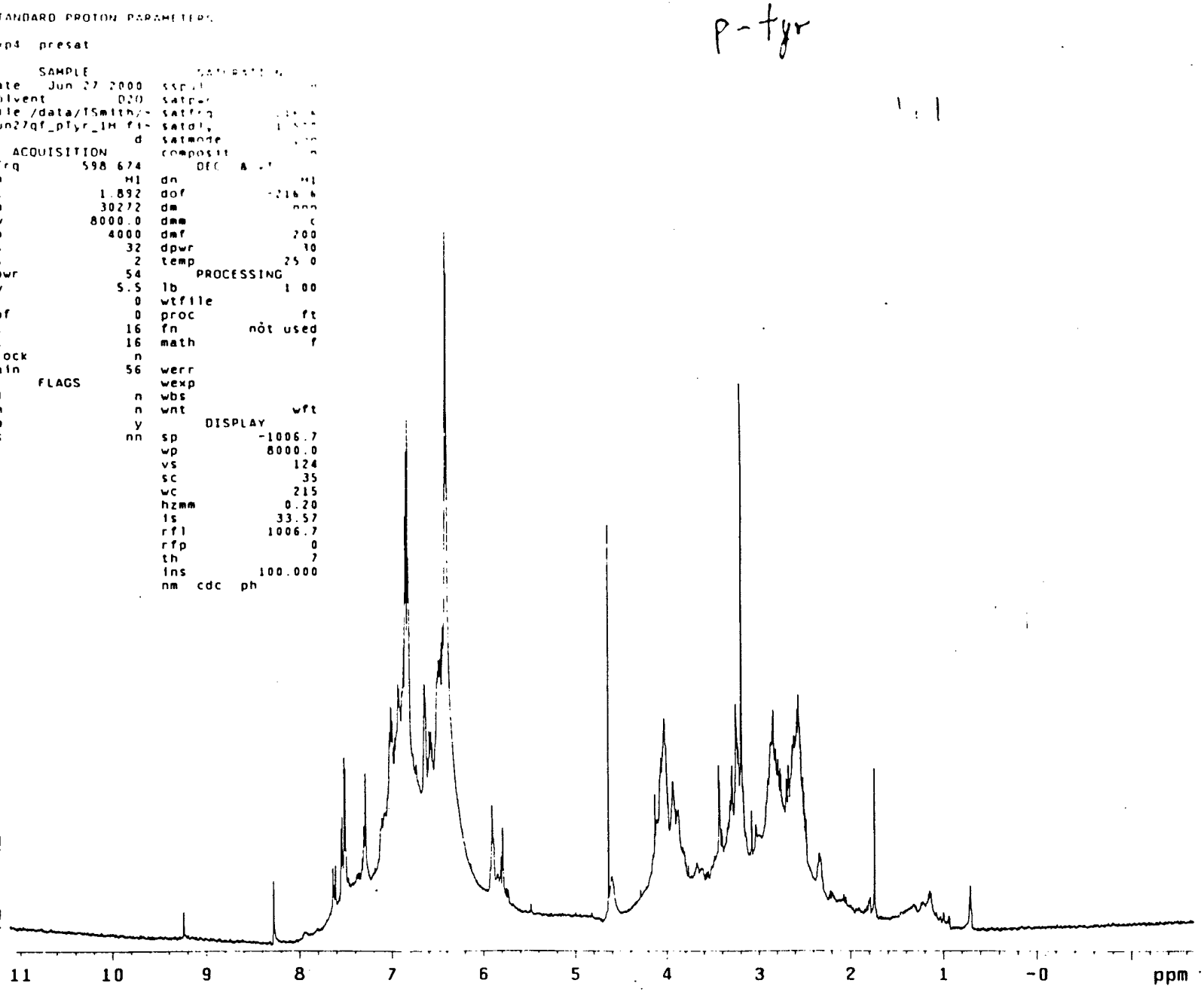

Figure 71
1H NMR of p-Tyr>2k
in D2O/NaOD
600 MHz NMR

TO: Tim Smith
this is referenced on both Dimensions.

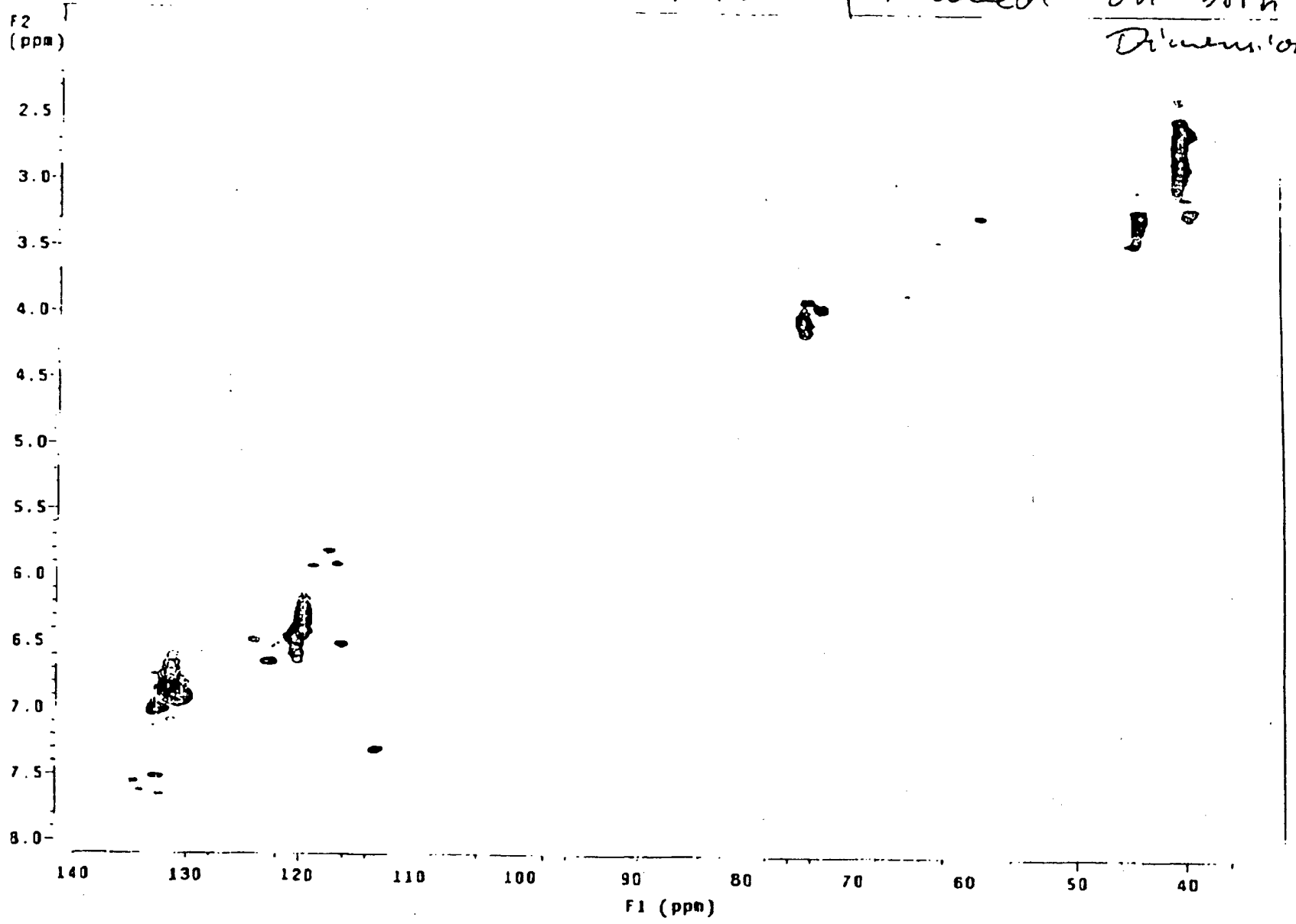

Figure 72
1H -13C HETCOR NMR of p-Tyr>2t
in D2O/NaOD
600 MHz NMR

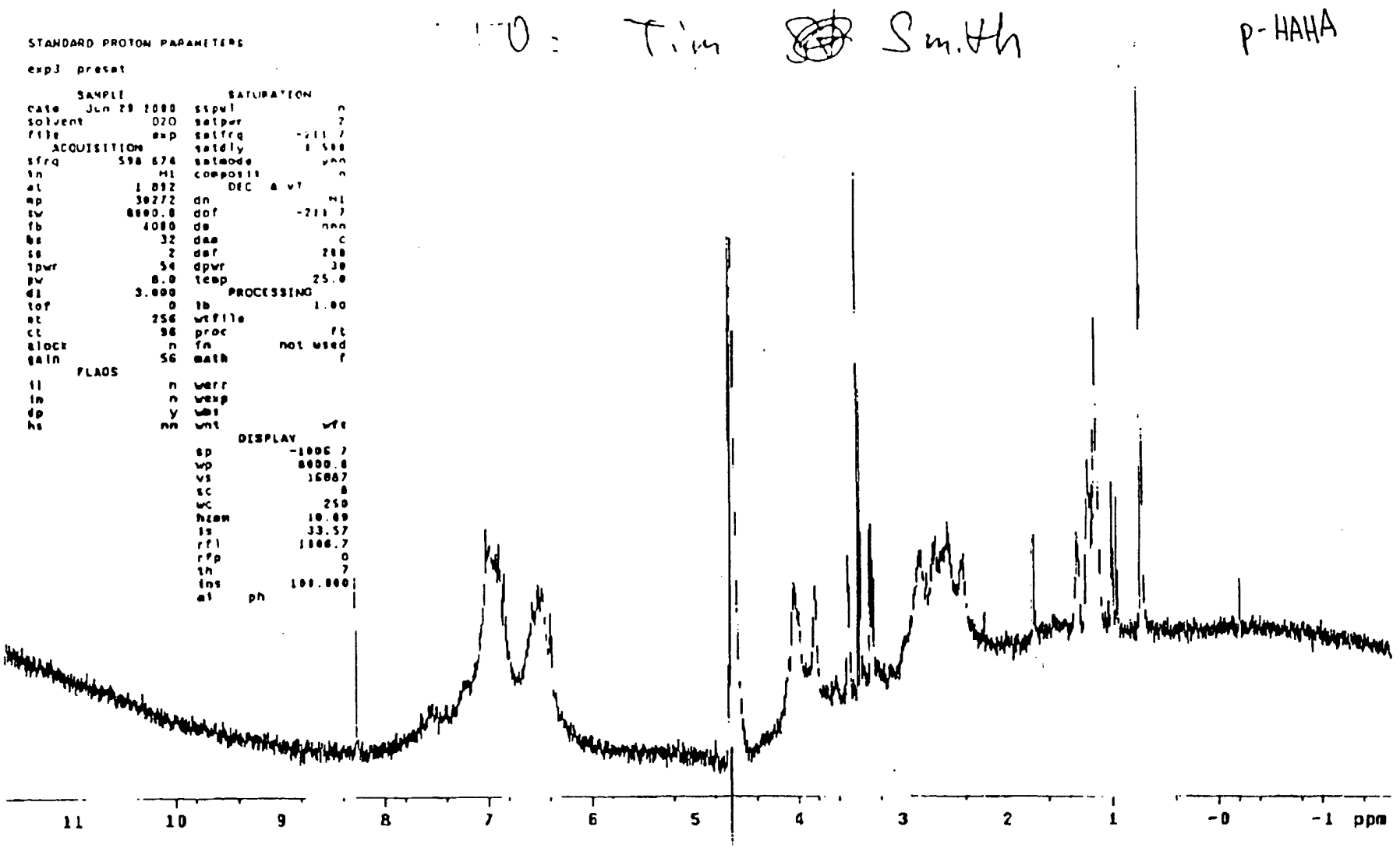

Figure 73
1H NMR of p-HAHA>2k
in D2O/NaOD
600 MHz NMR

The components identified in the pyrolysis GC/MS are summarized below. The assignment of 2-methylbenzoxazole is considered tentative because of small discrepancies in relative intensities between the observed and the reference spectra.

PYROLYSIS AT 450°C PROBABLE CHEMICAL IDENTITY
Carbon dioxide
Phenol
Benzoxazole
4-Methylphenol
2-Methylbenzoxazole (tentative)
4-Ethylphenol
4-Isocyanatobenzonitrile

PYROLYSIS AT 550°C PROBABLE CHEMICAL IDENTITY
Carbon dioxide
Phenol
Benzoxazole
2-Methylphenol
4-Methylphenol
2-Methylbenzoxazole (tentative)
2,4-Dimethylphenol
4-Ethylphenol
2,5-Dimethylbenzoxazole

PYROLYSIS AT 650°C PROBABLE CHEMICAL IDENTITY
Carbon dioxide
Phenol
Benzoxazole
2-Methylphenol
4-Methylphenol
3-Methyl benzenamine
2-Methylbenzoxazole (tentative)
2,4-Dimethylphenol
4-Ethylphenol
2,5-Dimethylbenzoxazole

Figure 74
Product of Pyrolysis
GC-MS

File : C:\HPCHEM\1\DATA\HP04502.D
Operator : JOSEPH MICF
Acquired : 8 Mar 9[illegible] 8:03 am using AcqMethod HP04499
Instrument : 5972 - In
Sample Name : CHEMIR #990478 PYROLYSIS 550 °C
Misc Info : SOUTHEASTERN OKLAHOMA STATE UNIVERSITY
Vial Number : 1

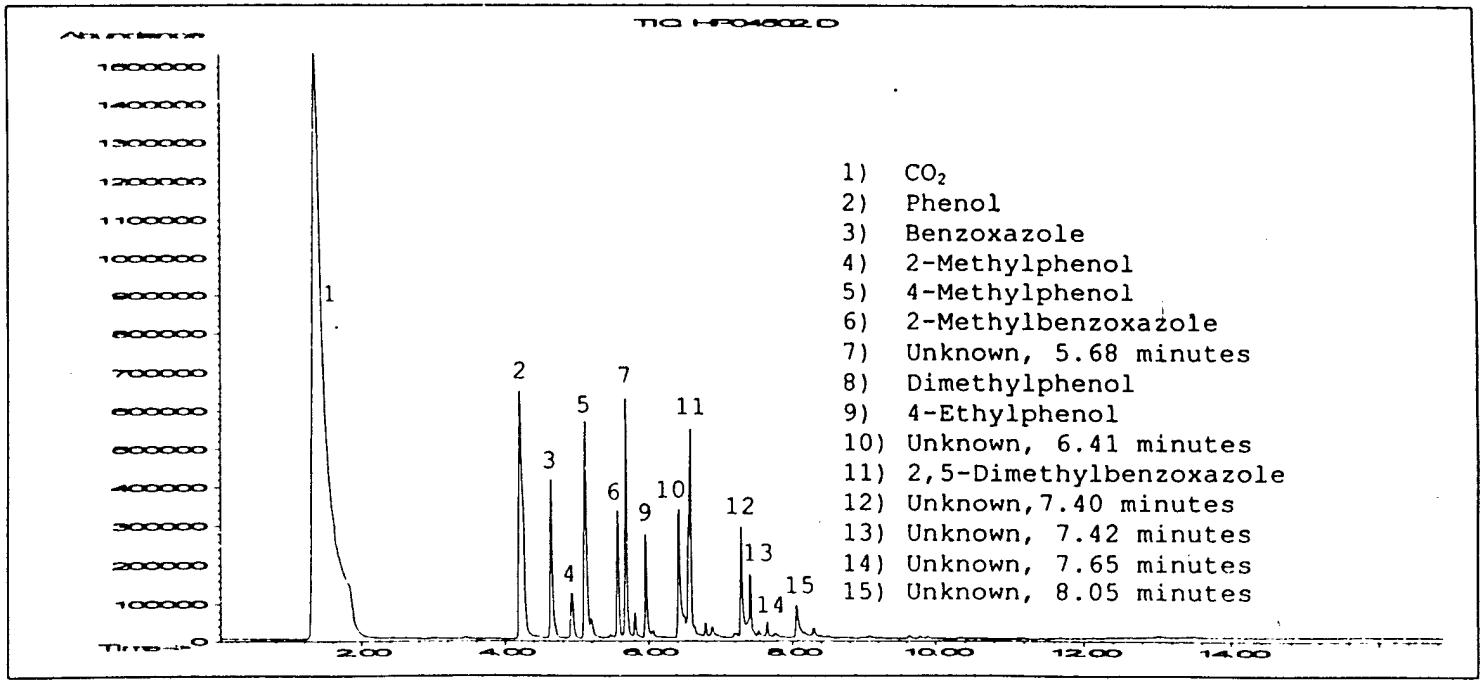

Figure 75
Pyrolysis GC-MS of p-DAT
550 C

Fig 12

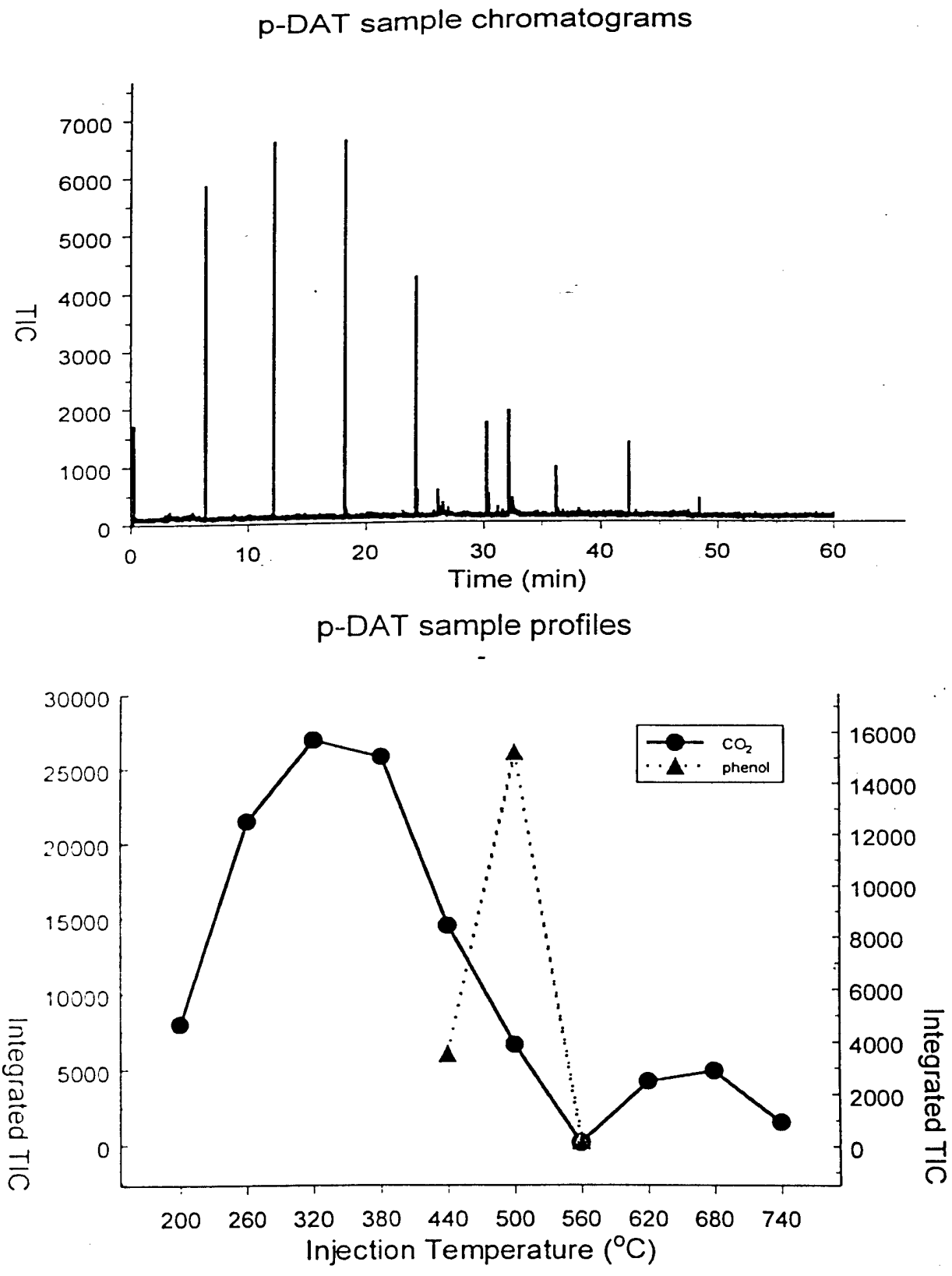

Figure 76
Thermal decomposition GC-MS
p-DAT

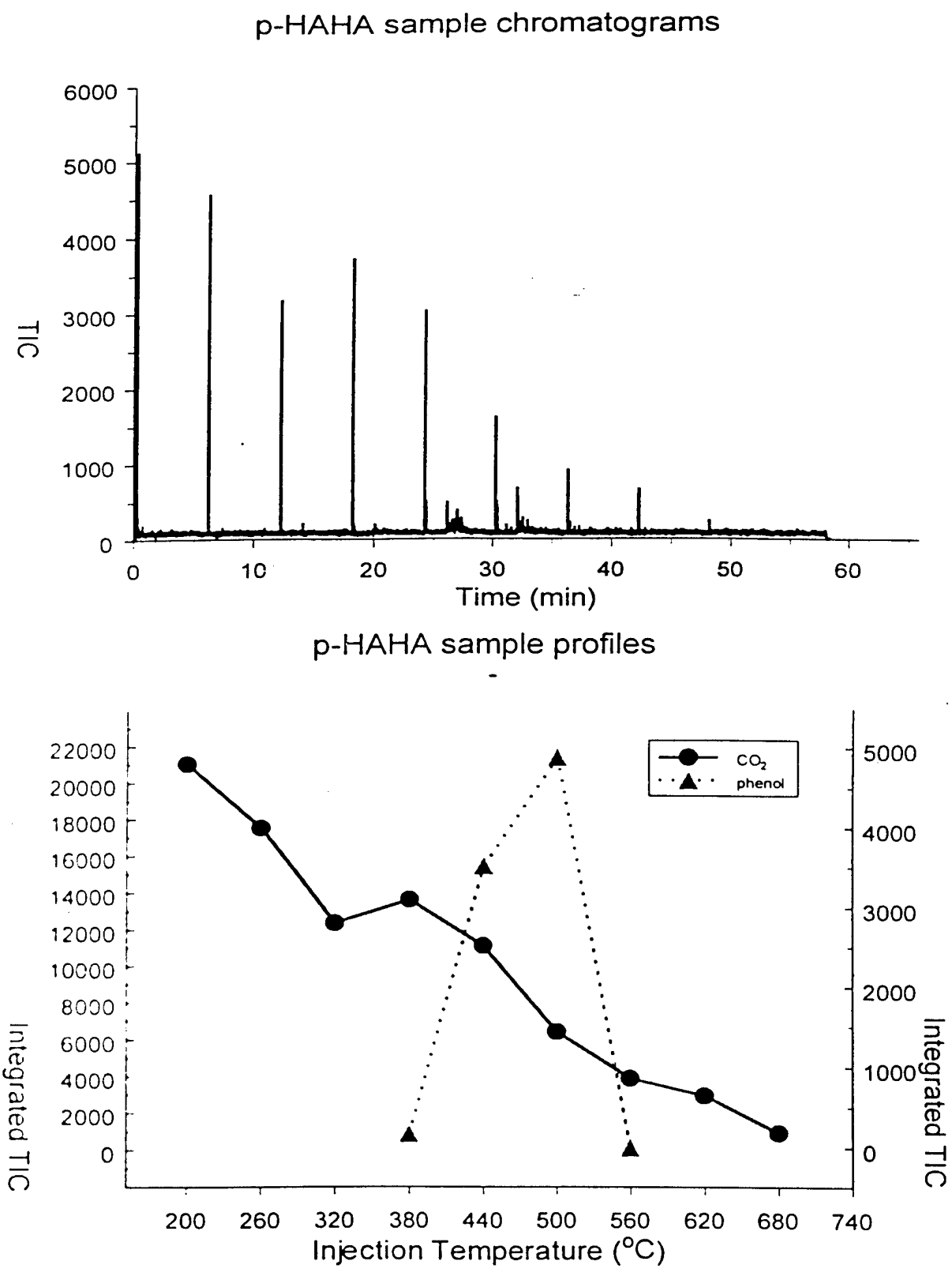

Figure 77
Thermal decomposition GC-MS
p-Tyr

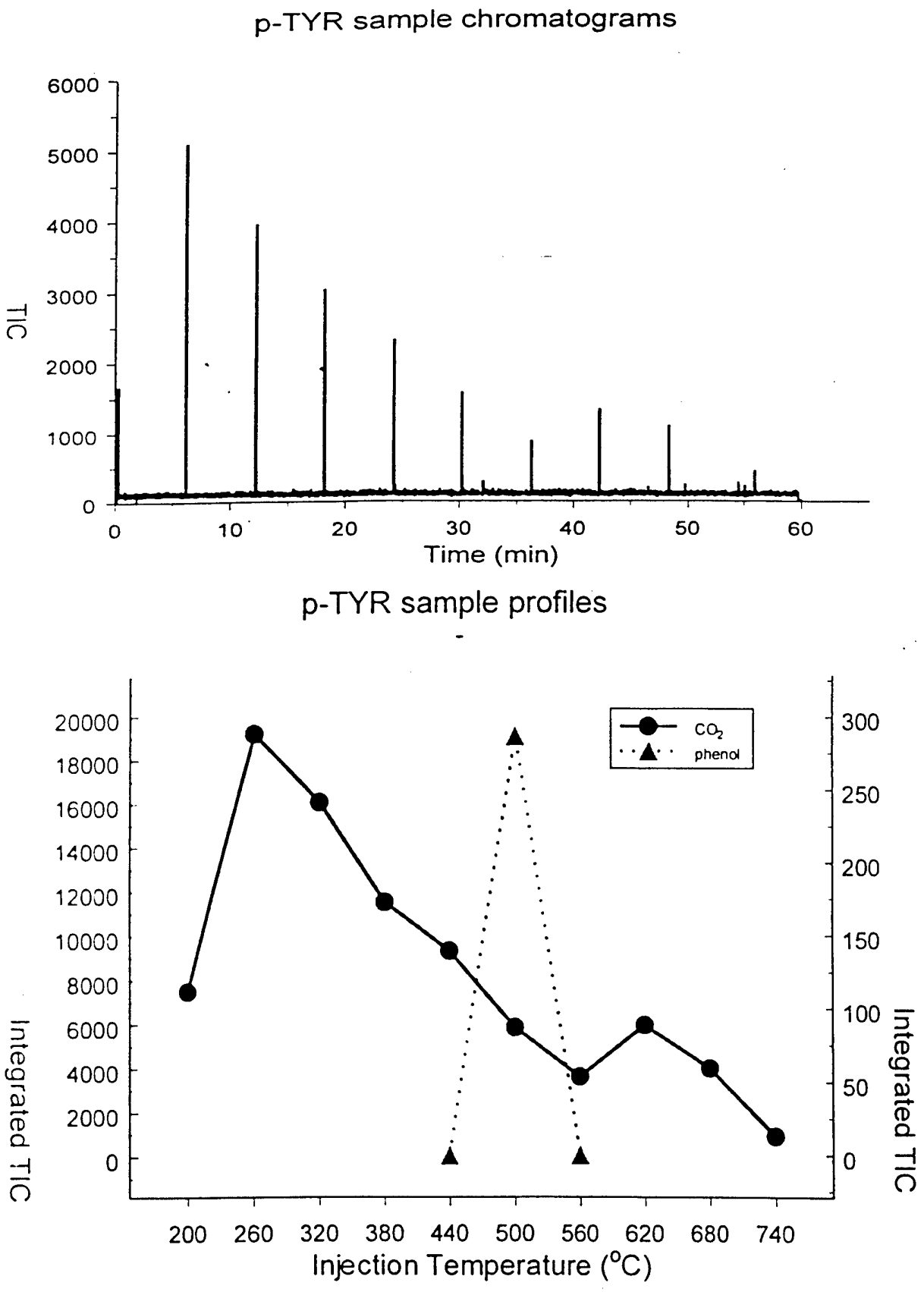

Figure 78
Thermal decomposition GC-MS
p-Tyr

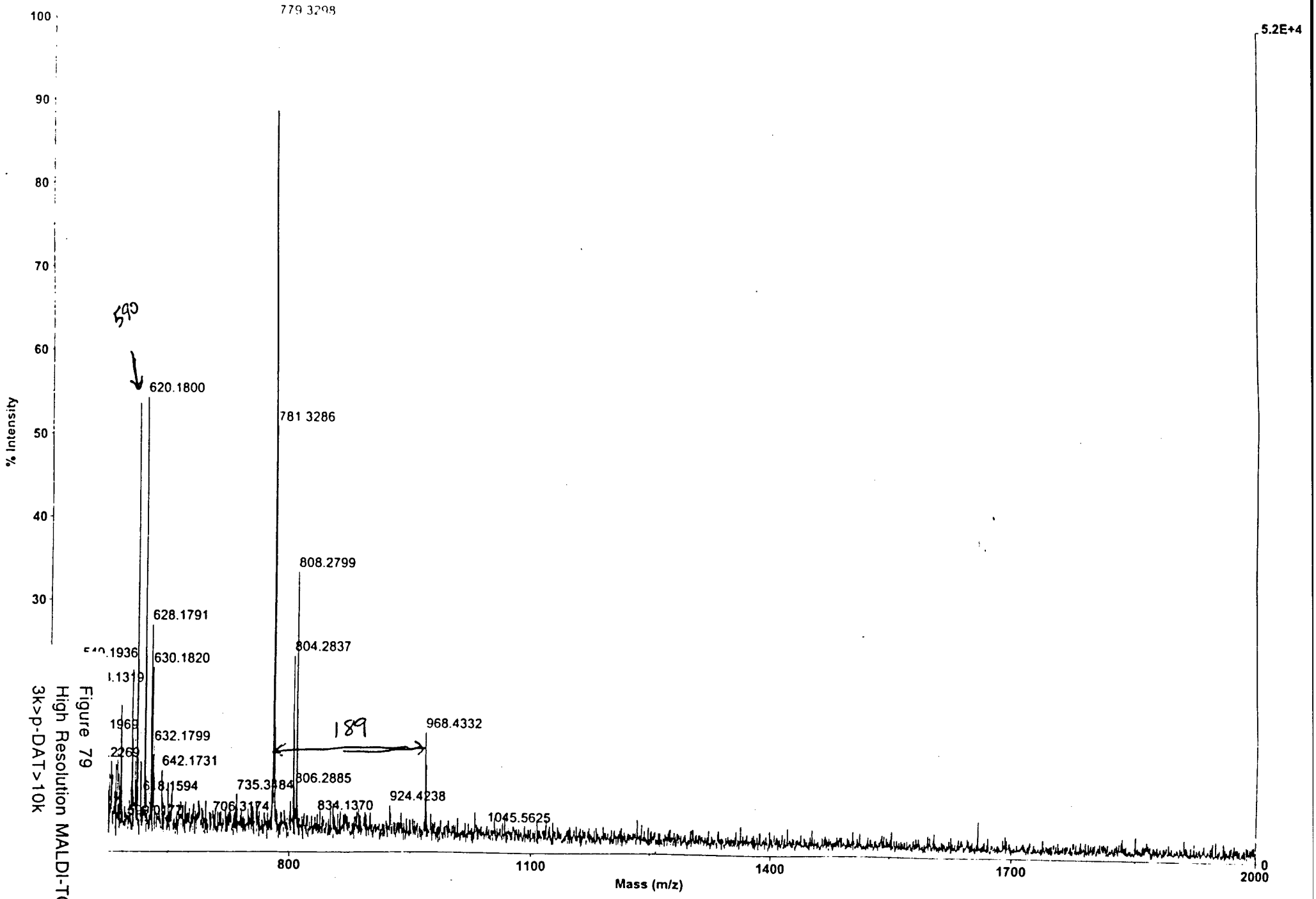

Figure 79
High Resolution MALDI-TOF-MS
3k>p-DAT>10k

)MALDI/DE/RTOF in HCCA
ıt
ecember 22, 1999

Desalt @ 3k<MW<10k

Date: Tue, Jul 14, 1998 11:15 AM
Data: JCG001

Sampling Int: 0.1 Seconds

Data:

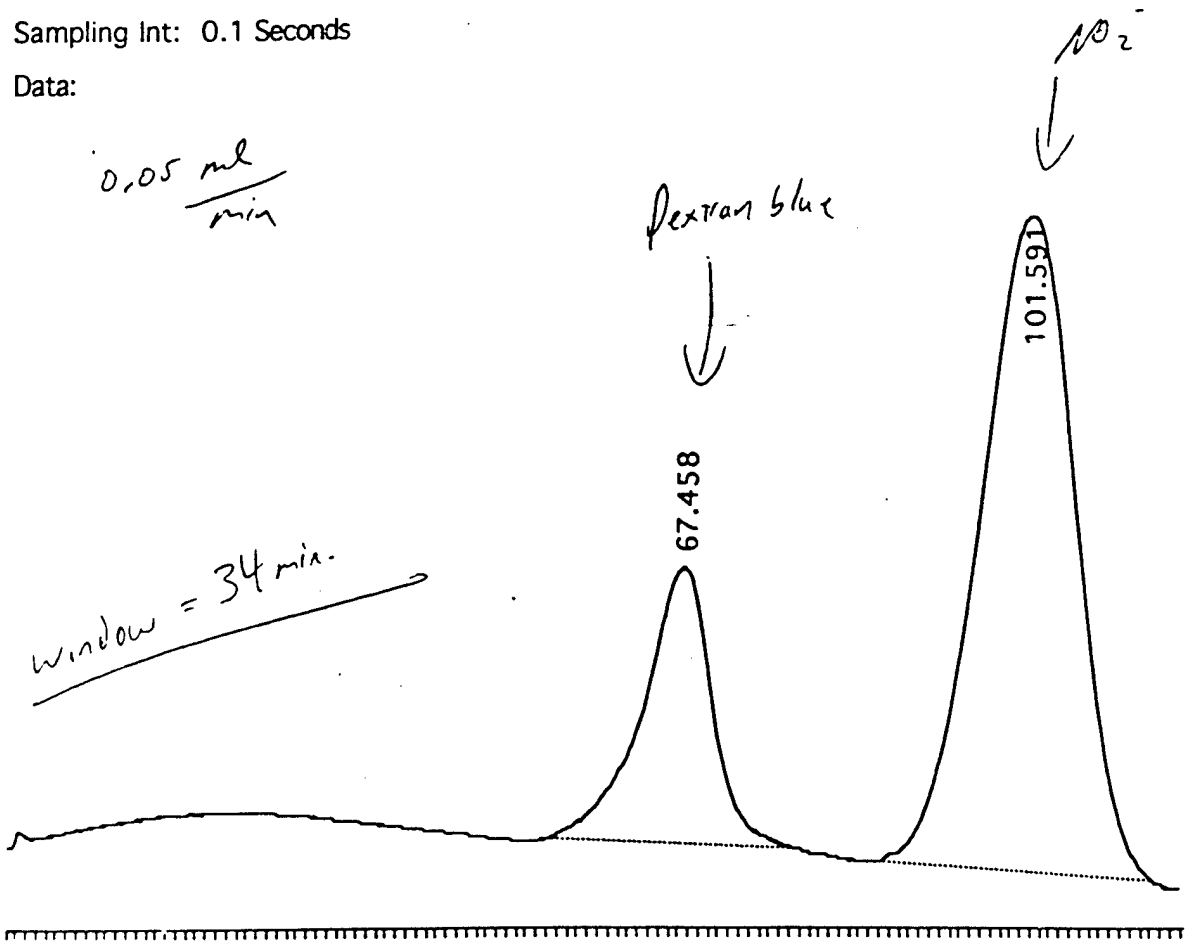

Analysis: Channel A

Peak No.	Time	Type	Height(μV)	Area(μV-sec)	Area%
1	67.458	*N	16560	7607706	23.024
2	101.591	*N	39050	25434410	76.975
Total Area				33042116	99.999

Figure 80
GPC of MW markers
Toyopearl HW-55s

Date: Tue, Jul 14, 1998 1:50 PM
Data: JCG002

Sampling Int: 0.1 Seconds

Data: Crude p-DAT

0.05 ml/min

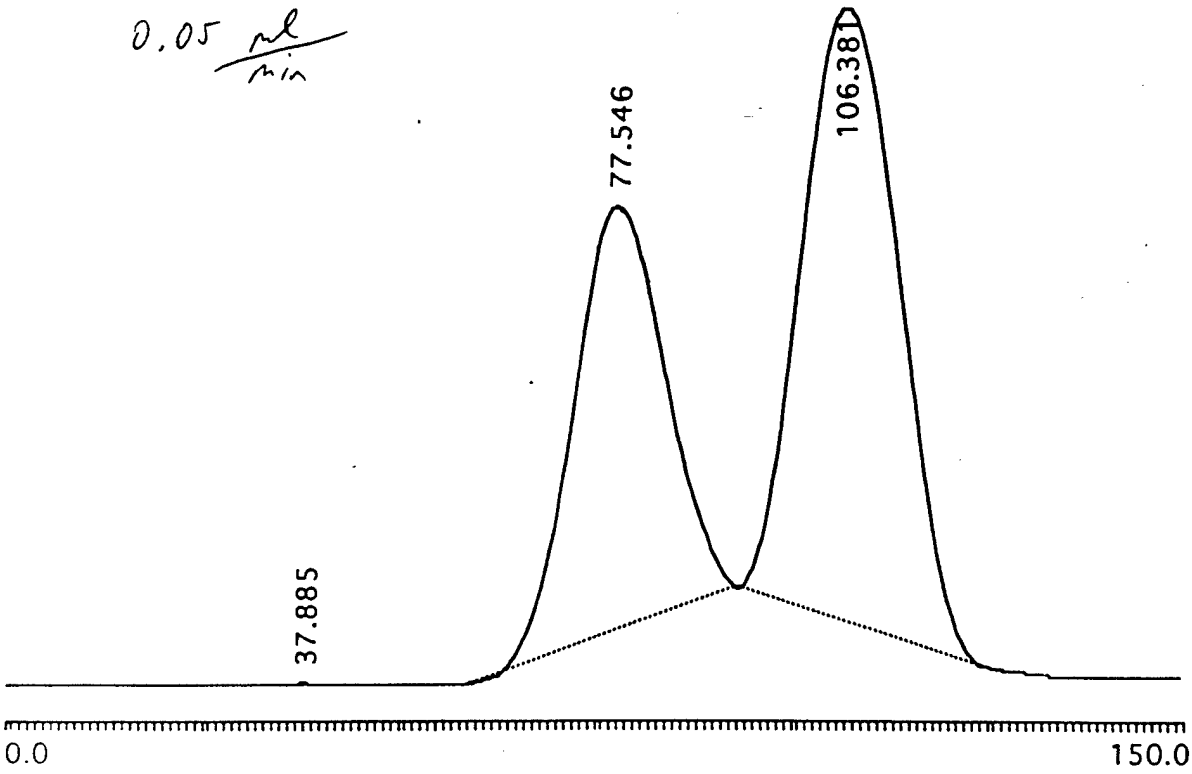

Analysis: Channel A

Peak No.	Time	Type	Height(μV)	Area(μV-sec)	Area%
1	37.885	N	262	10921	0.004
	42.378	N	169	3033	0.001
	47.161	N	62	269	0.000
	49.616	N	41	174	0.000
	50.410	N	45	217	0.000
	50.985	N	41	560	0.000
	54.466	N	57	266	0.000
2	77.546	*N	113111	89403140	39.907
3	106.381	*N	161283	134606204	60.085
Total Area				224024784	99.997

Figure 81
GPC of crude p-DAT
Toyopearl HW-55s

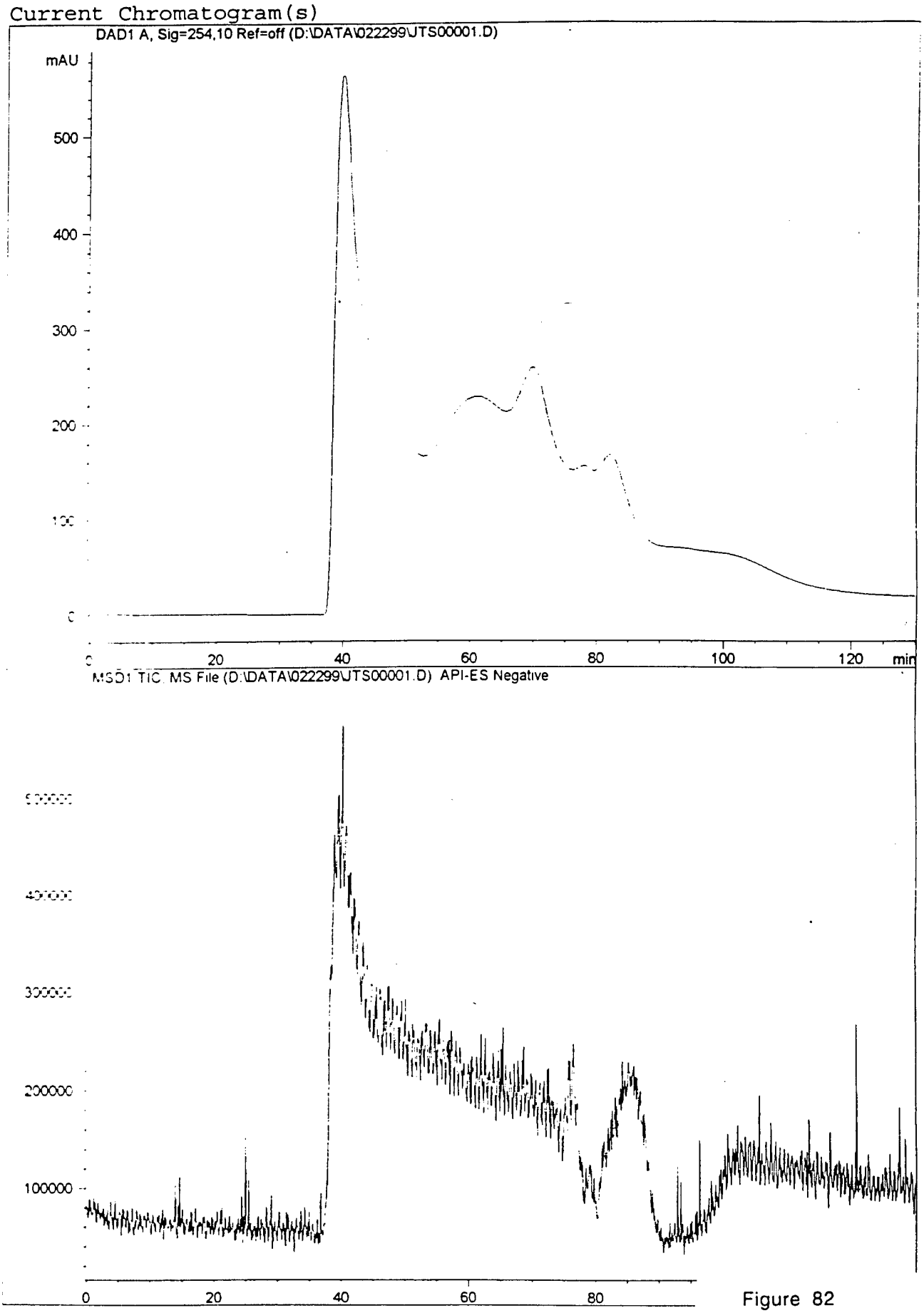

Figure 82
GPC-MS of 3-AT reaction aged Sphadex G15-120

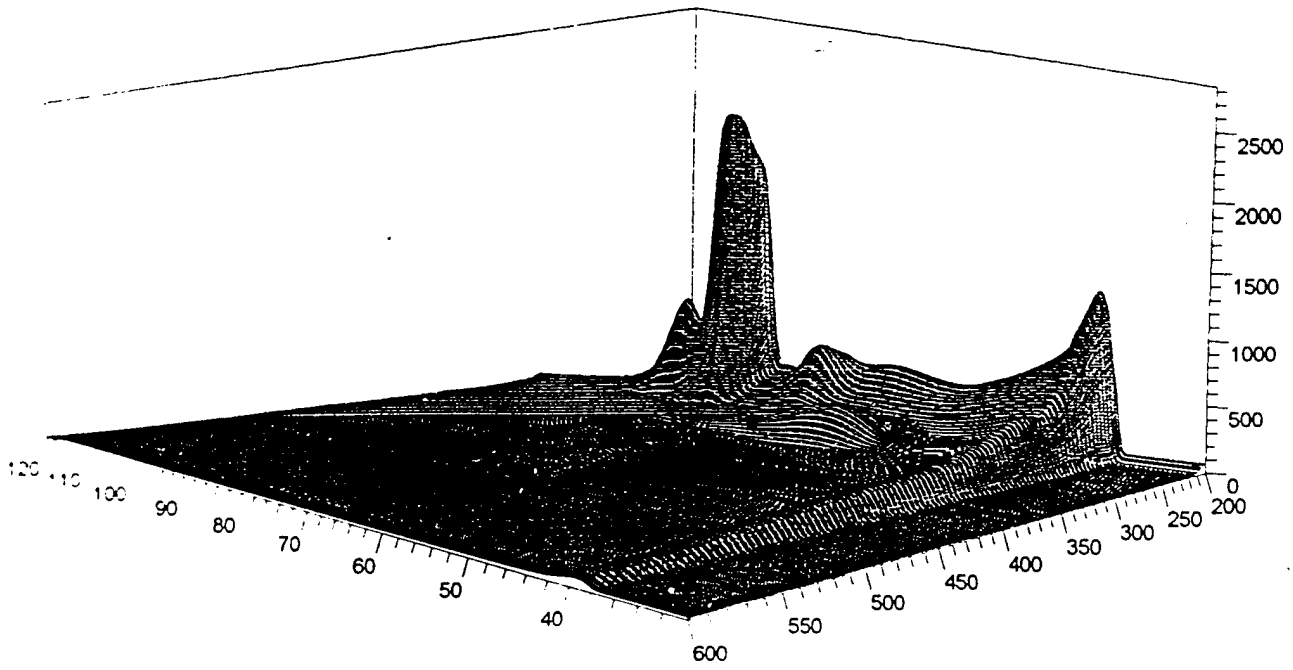

Datafile: D:\DATA\022299\JTS00001.D Sample name: react JC 2/18/99
Tilt: 2.5 °, Swivel: 133.0 °
Ranges: 30.0 to 120.0 min, 200.0 to 600.0 nm, -2.8 to 2829.3 mAU

Figure 83
GPC of 3-AT reaction aged
Sphadex G15-120
3-D plot

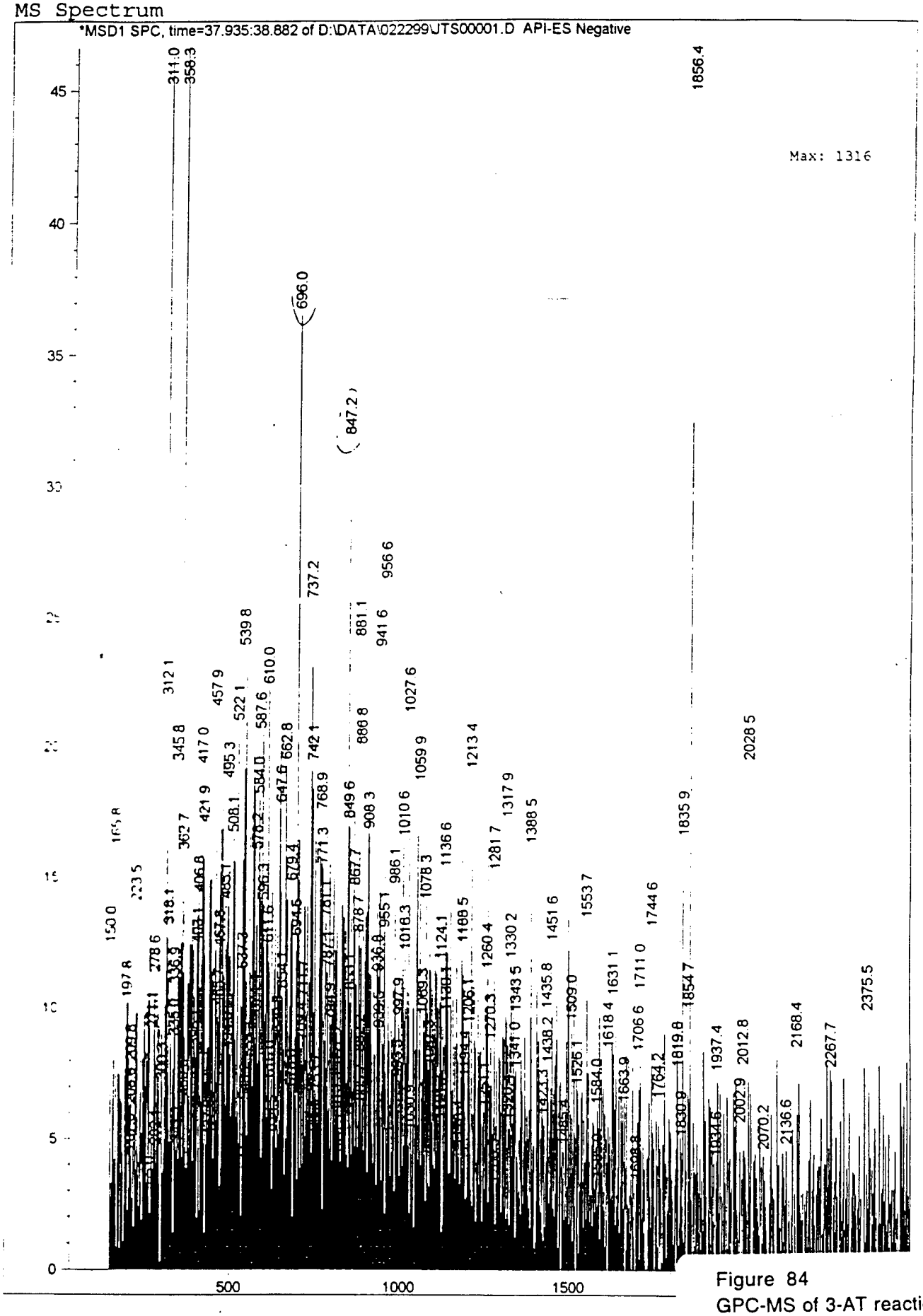

Figure 84
GPC-MS of 3-AT reaction aged
MS of 38 min fraction

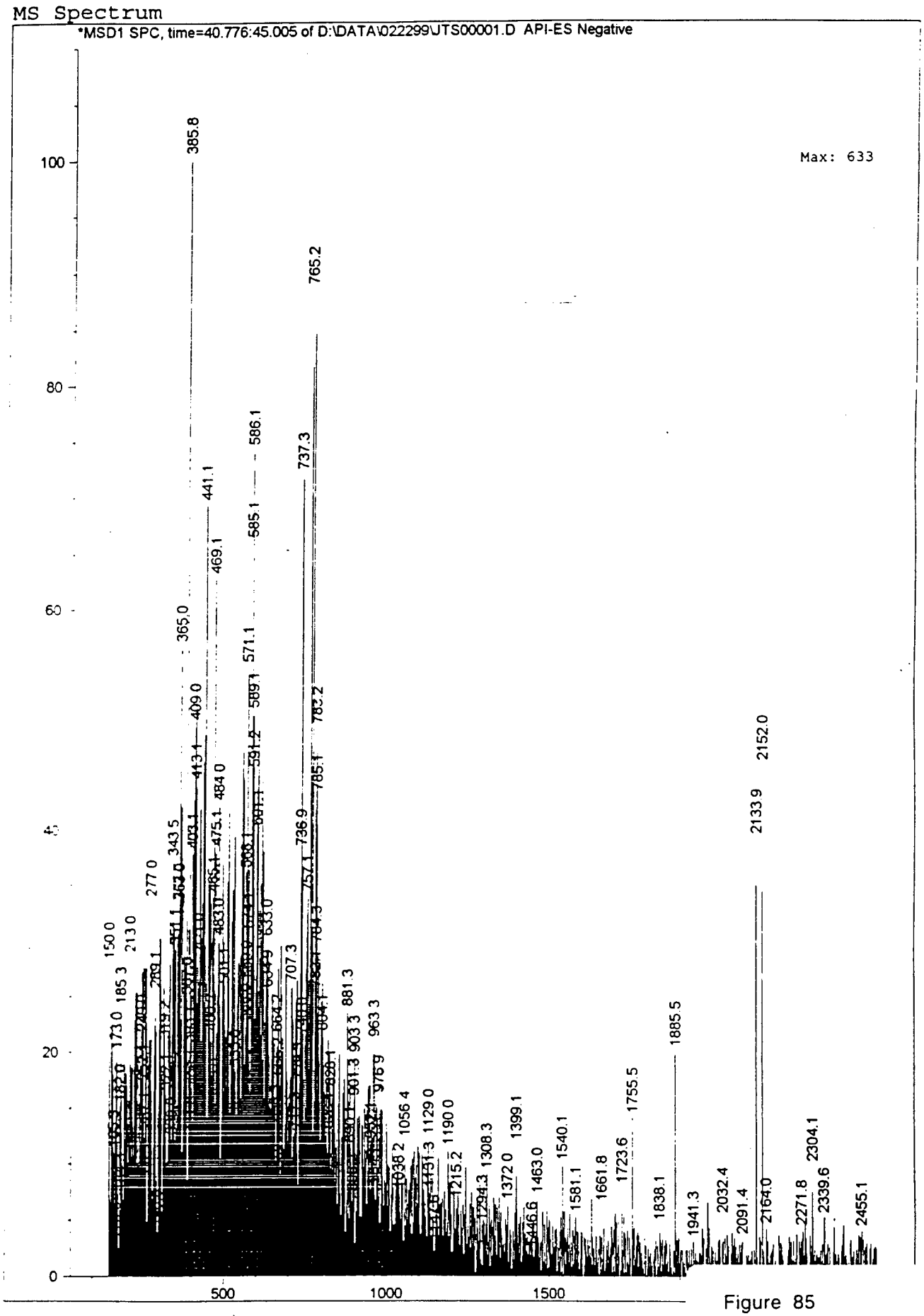

Figure 85
GPC-MS of 3-AT reaction aged
MS of 40-45 min fraction

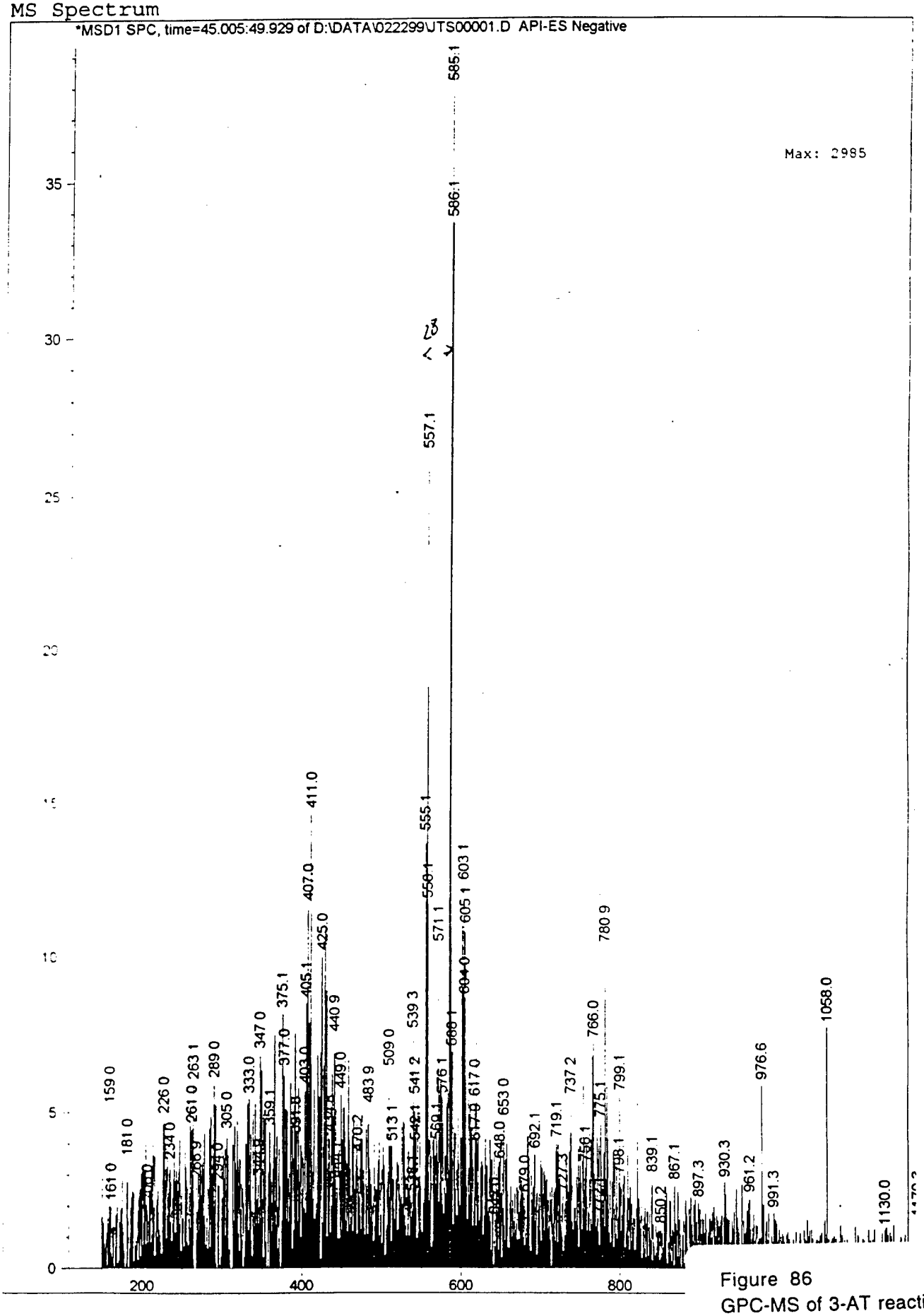

Figure 86
GPC-MS of 3-AT reaction aged
MS of 45-50 min fraction

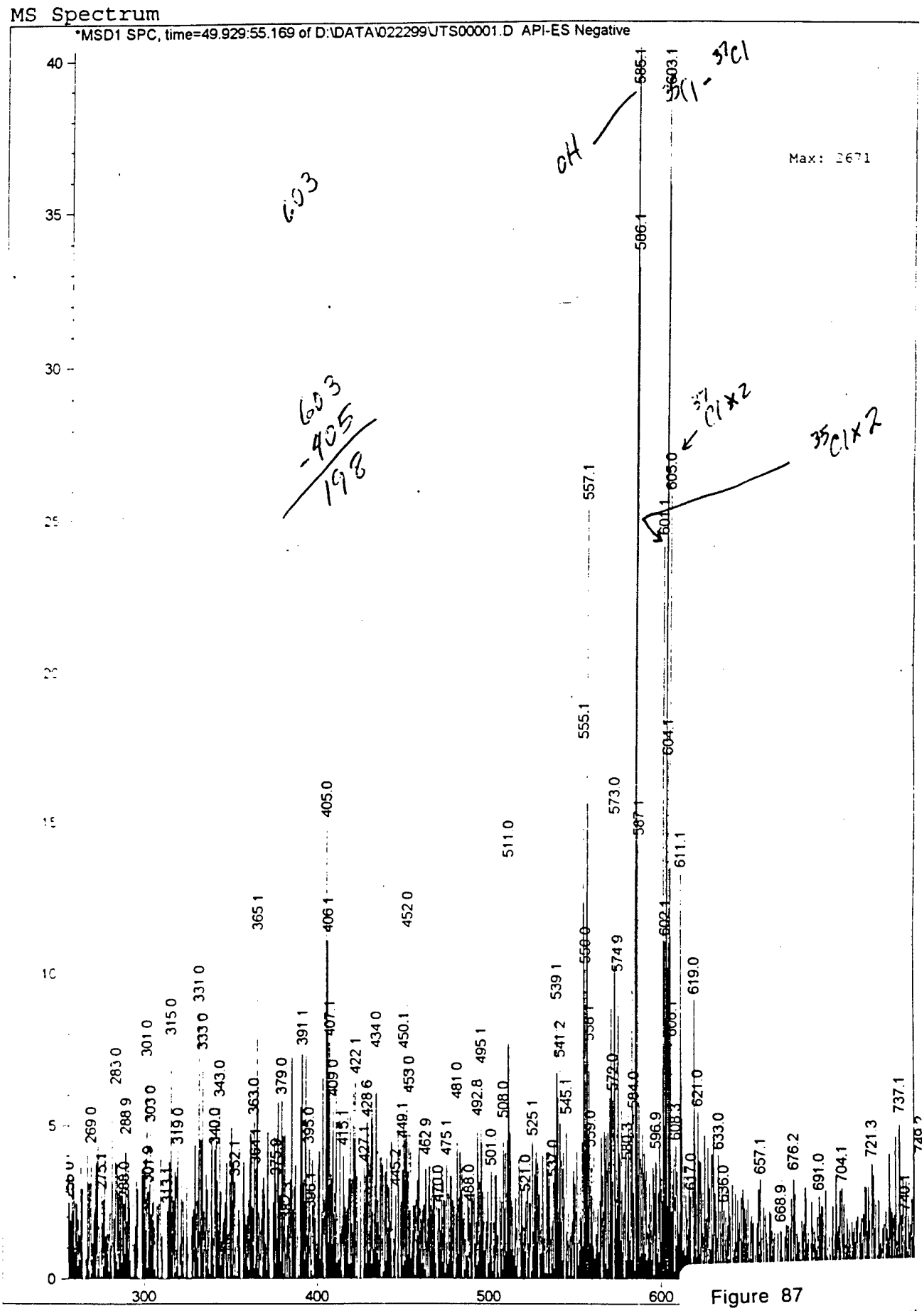

Figure 87
GPC-MS of 3-AT reaction aged
MS of 50-55 min fraction

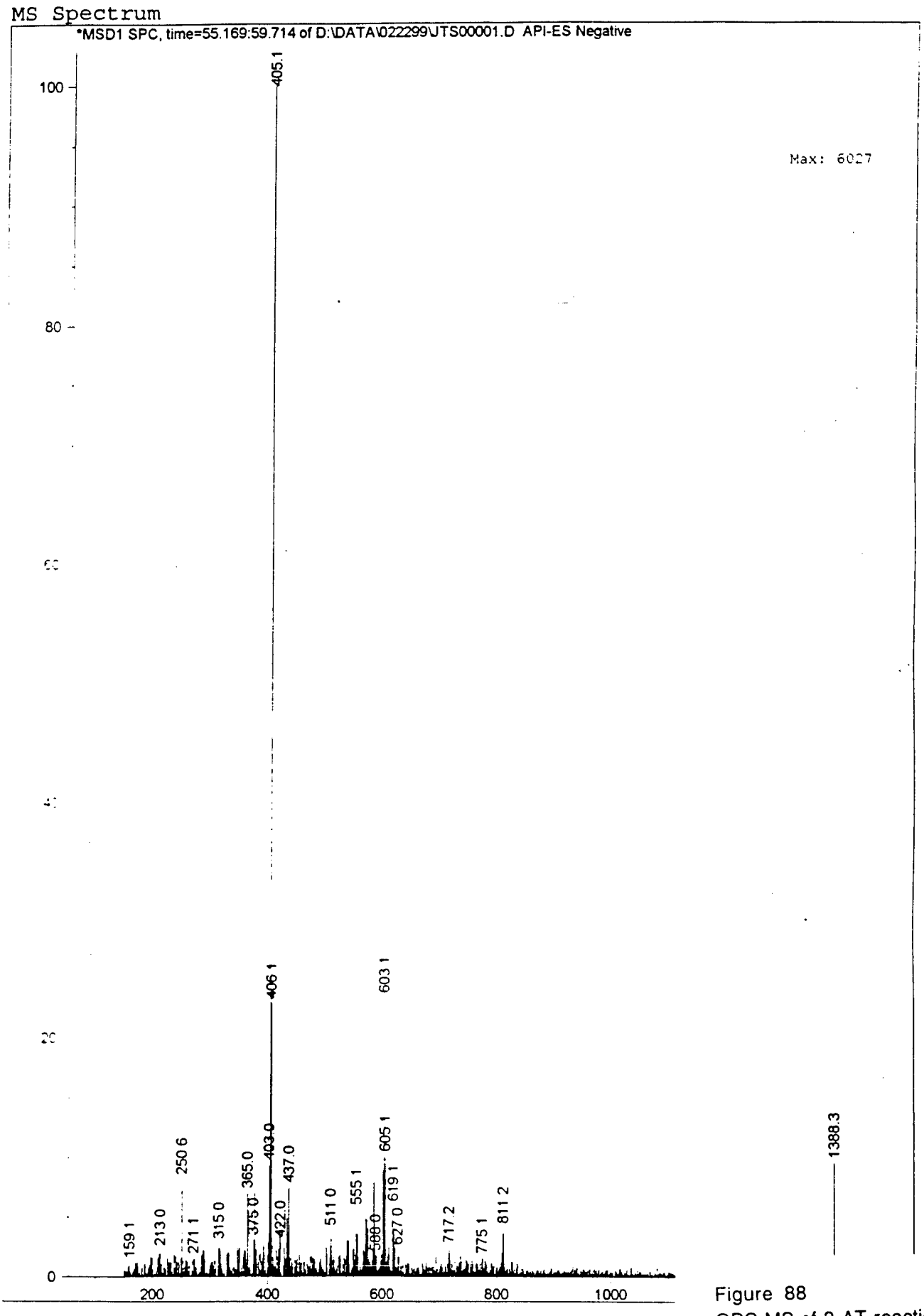

Figure 88
GPC-MS of 3-AT reaction aged
MS of 55-60 min fraction

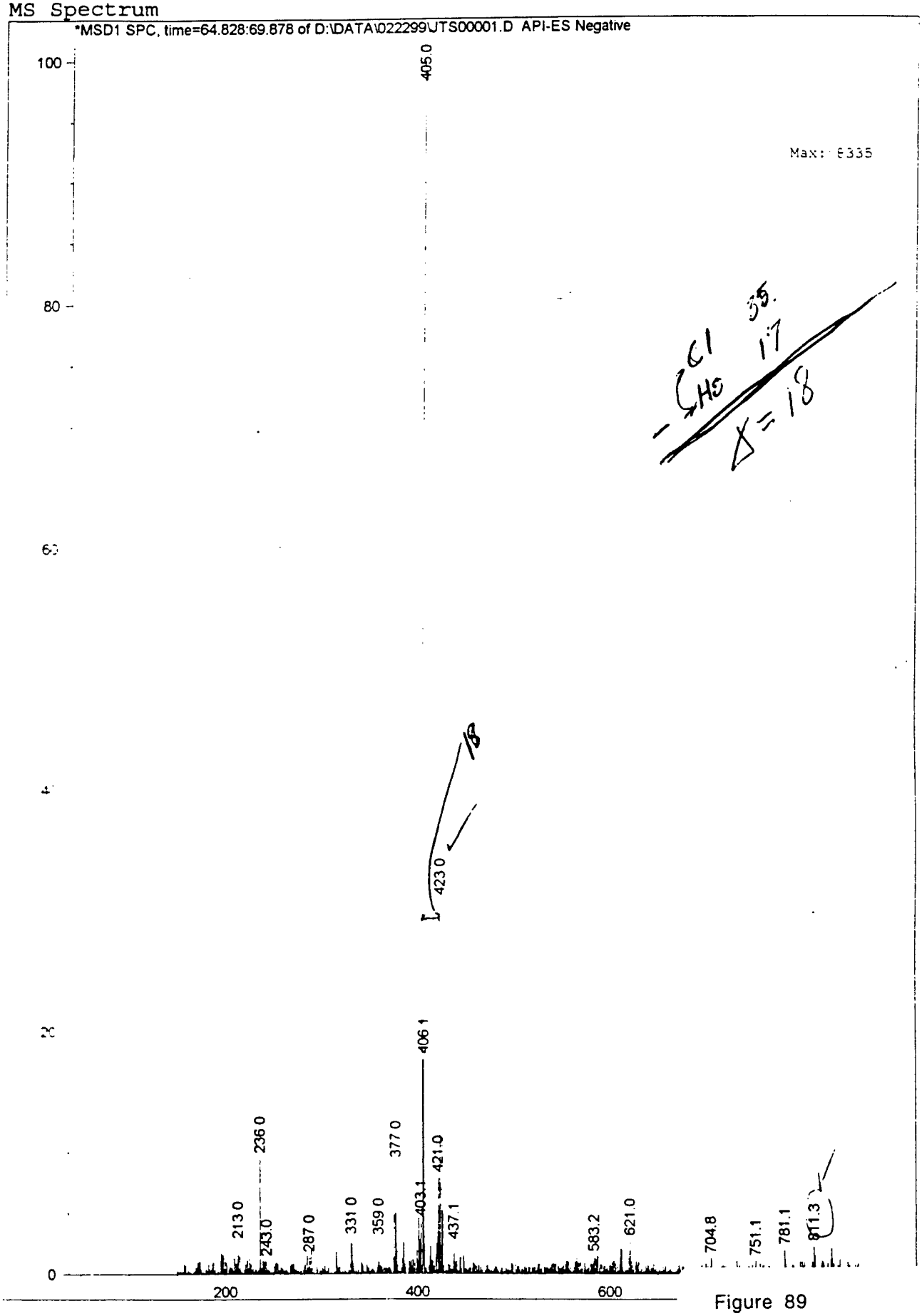

Figure 89
GPC-MS of 3-AT reaction aged
MS of 65-70 min fraction

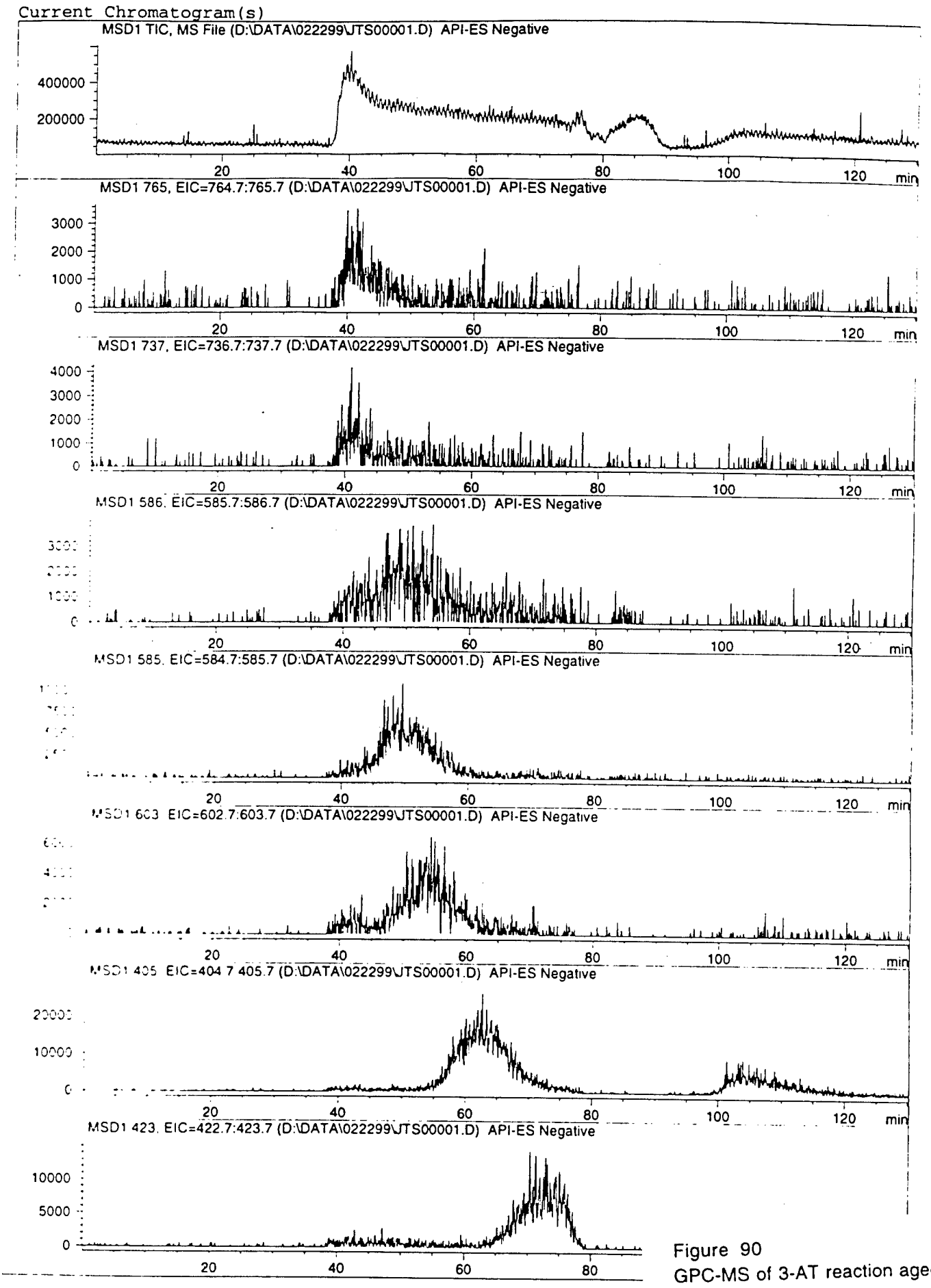

Figure 90
GPC-MS of 3-AT reaction aged
EIC

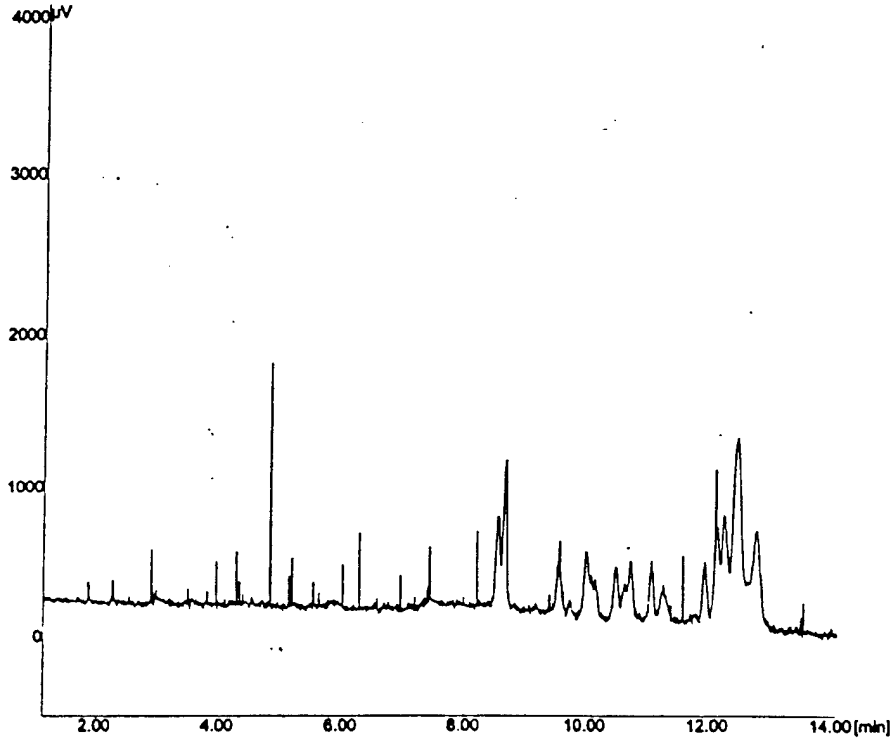

File name : 01289014.CH1 User : RNB Curr. Date : 8-Jun-99 17:01:18

Acqu. Date : 28-Jan-99 15:22:56

Info :
50/60 cm x 50 um,
+20 kV, 214 nm
Buffer: 10mM Na2HPO4, pH=7.99M
Sample: Fraction 10 w/ 50uL of Buffer

Vial # = 1 Rack # = 1

Control Method :

Peak Detection Not Available

Fraction 10 obtained from 3-AT rxn. (1-6-99). Ran through Sephadex G 15-120 HPLC column in 1 M NH_4OAc. Speed Vac overnight Then ran on CE in 10m M Na_2HPO_4 buffer. Column 50/40 x 50um @ 214nm, +20KV

Figure 91
CE of dried GPC fraction #10
214 nm

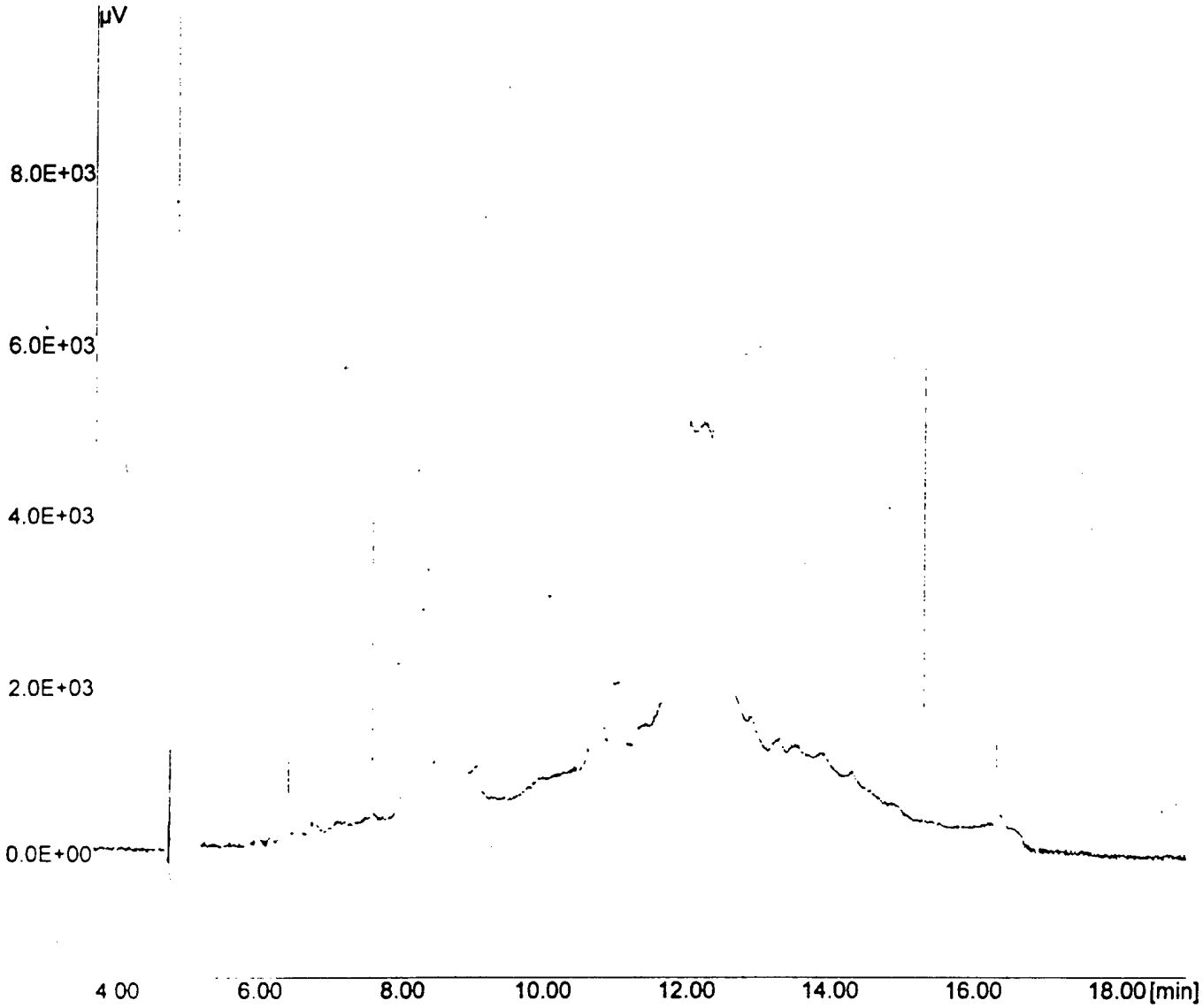

File name : 12029004.CH1 User : JOHNCON Curr. Date : 9-Jul-00 23:26:4

Acqu. Date : 2-Dec-99 15:07:40

Info :
neutralized SnCl2 Digest w/ 2 drops NH4OH added JDC#2 pg37
Run Buffer: 25mM Borate pH adjusted to 9 w/ NaOH/100mM SDS
214 wavelength
(+) polarity 15 kilovolts; Current 21 microamps

Vial # = 1 Rack # = 1

Control Method :

Peak Detection Not Available

Figure 92
CE of SnCl2 digest of p-DAT
214 nm

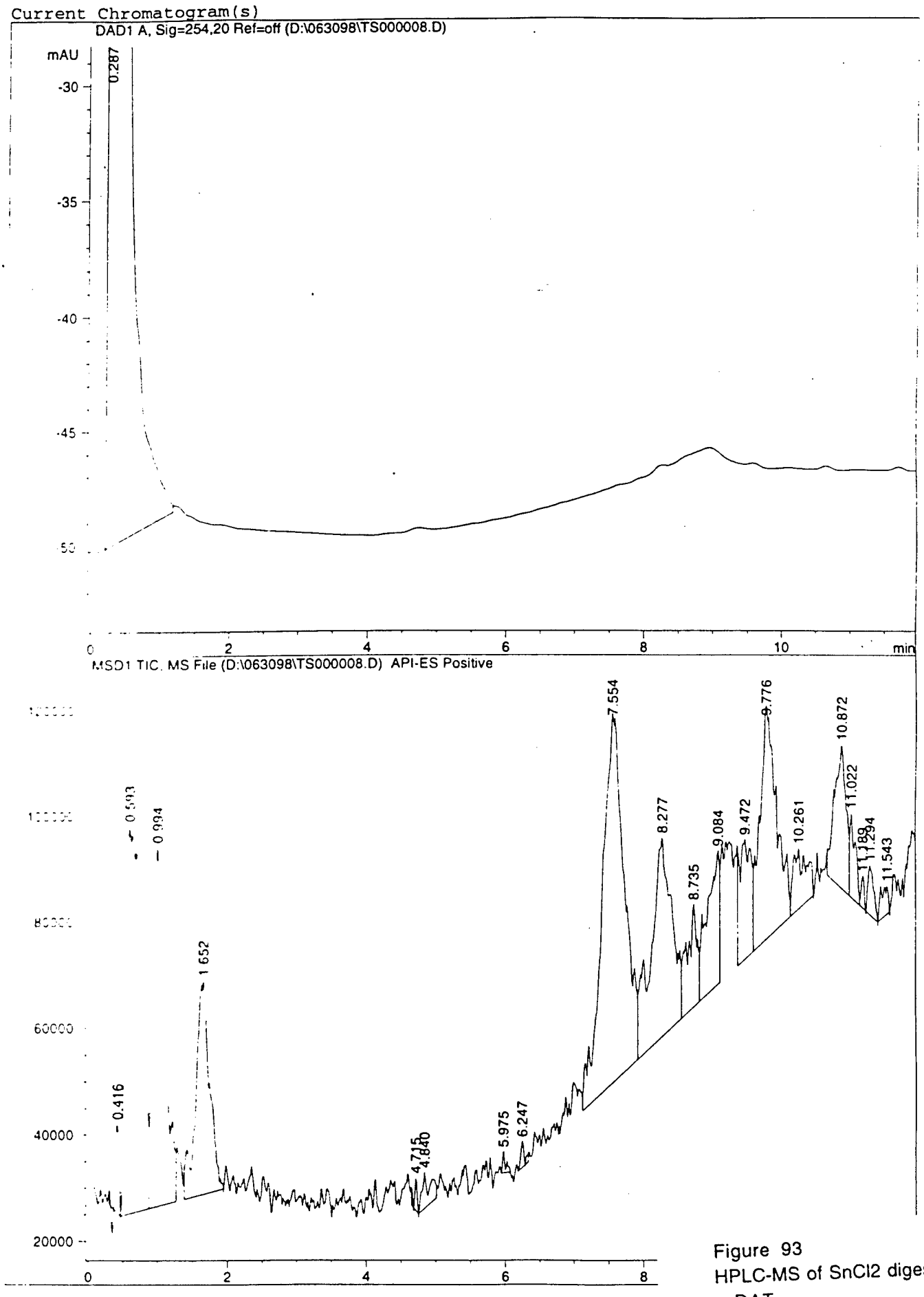

Figure 93
HPLC-MS of SnCl2 digest
p-DAT

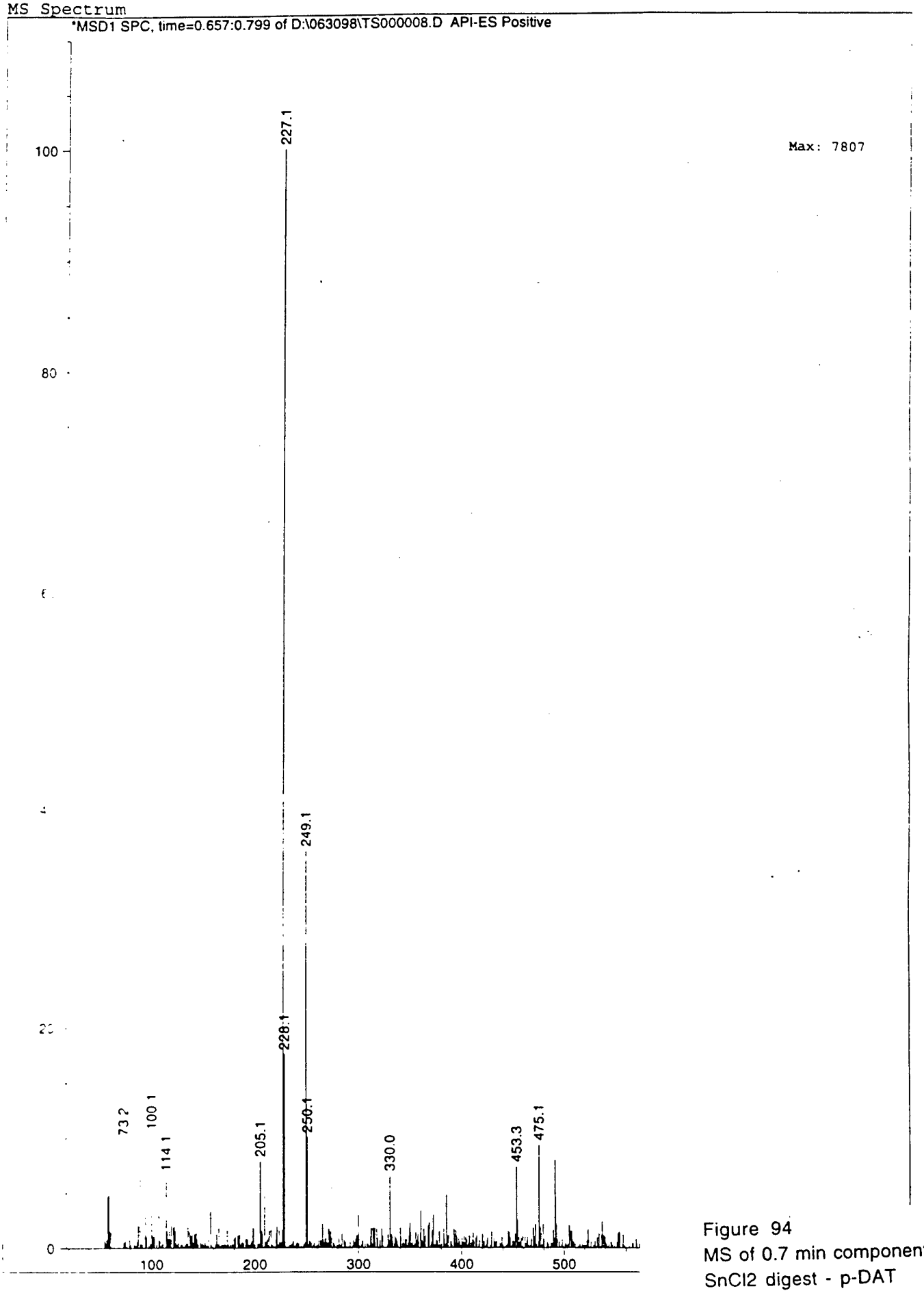

Figure 94
MS of 0.7 min component
SnCl2 digest - p-DAT
(+)-ESI

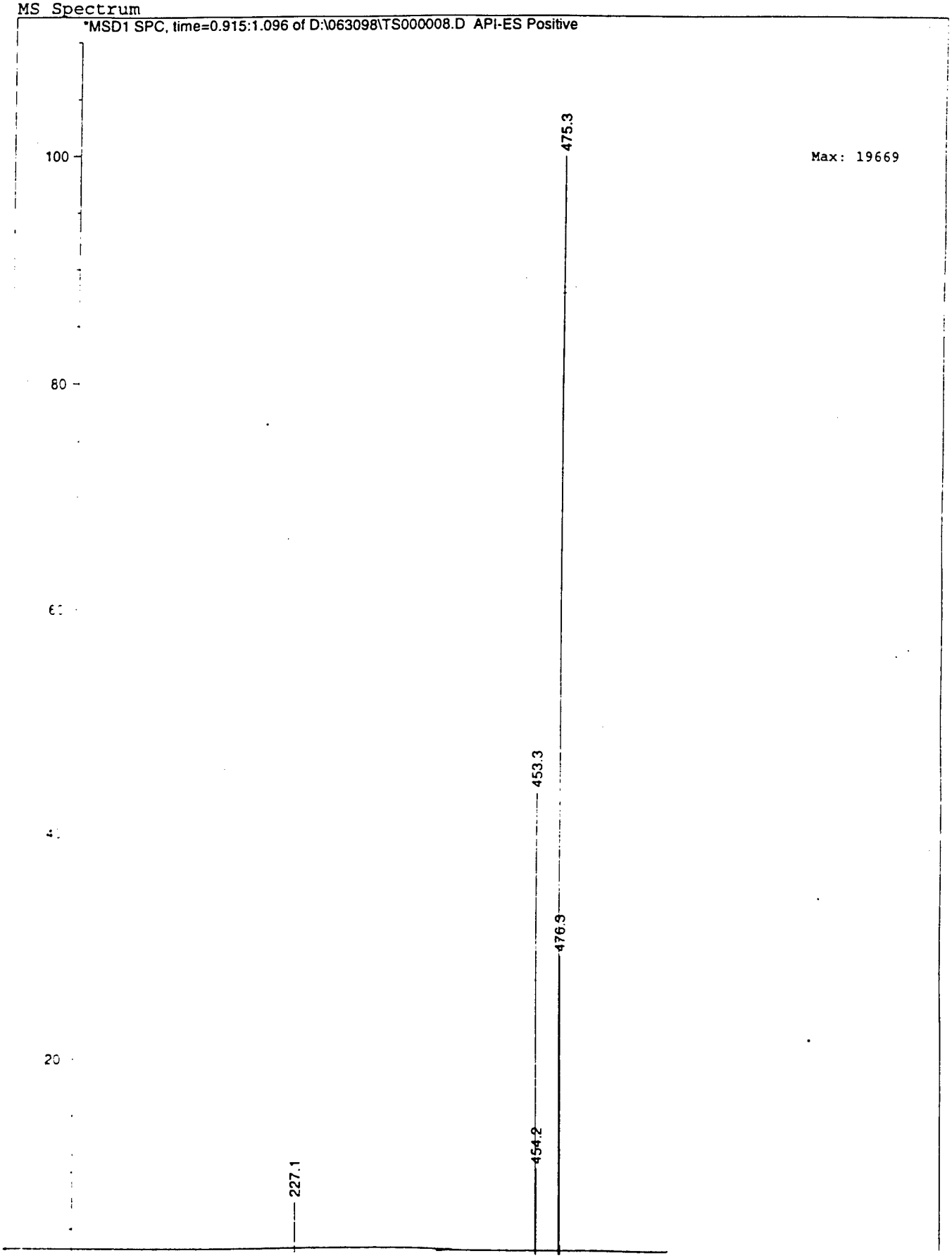

Figure 95
MS of 1.0 min component
SnCl2 digest - p-DAT
(+)-ESI

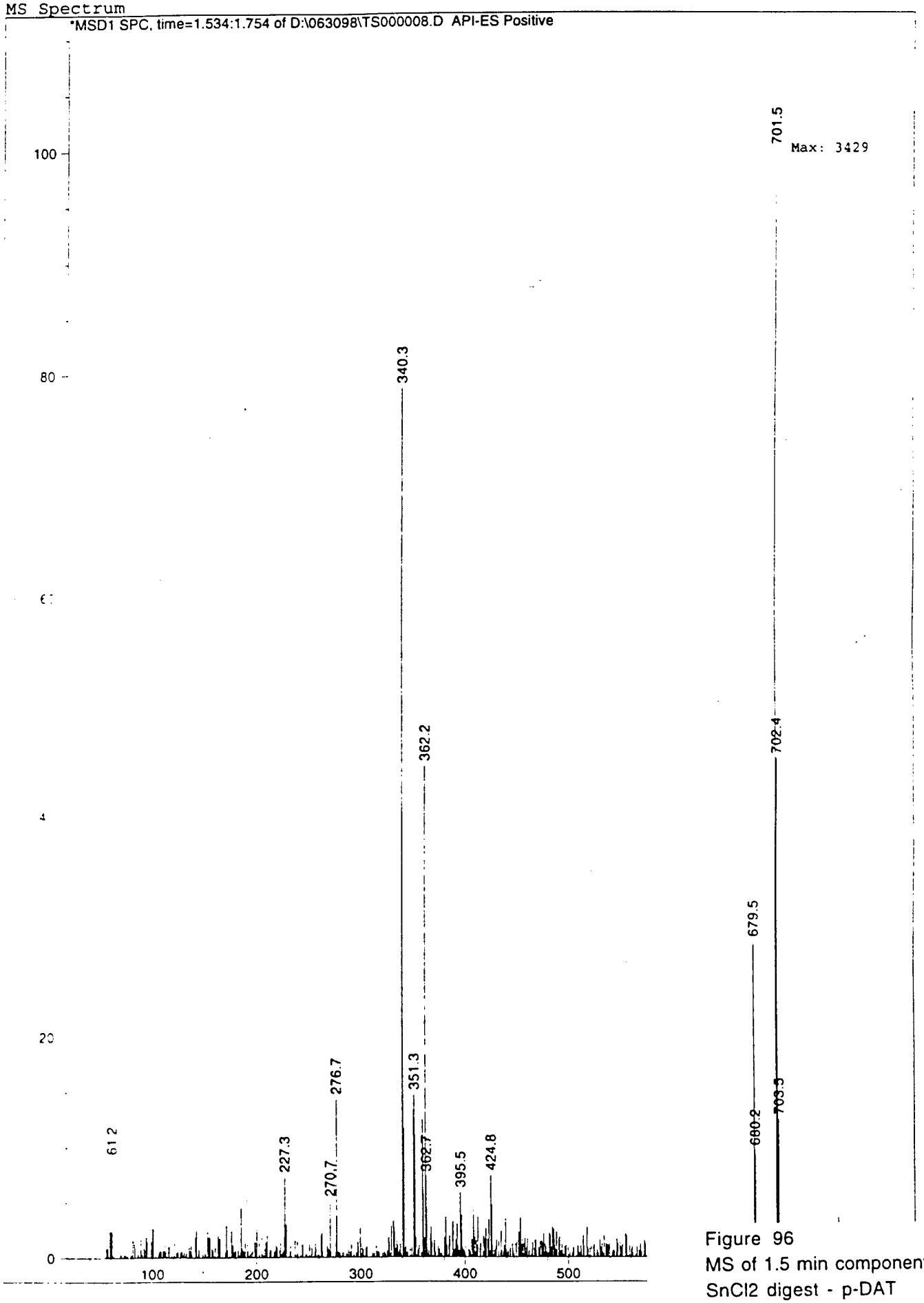

Figure 96
MS of 1.5 min component
SnCl2 digest - p-DAT
(+)-ESI

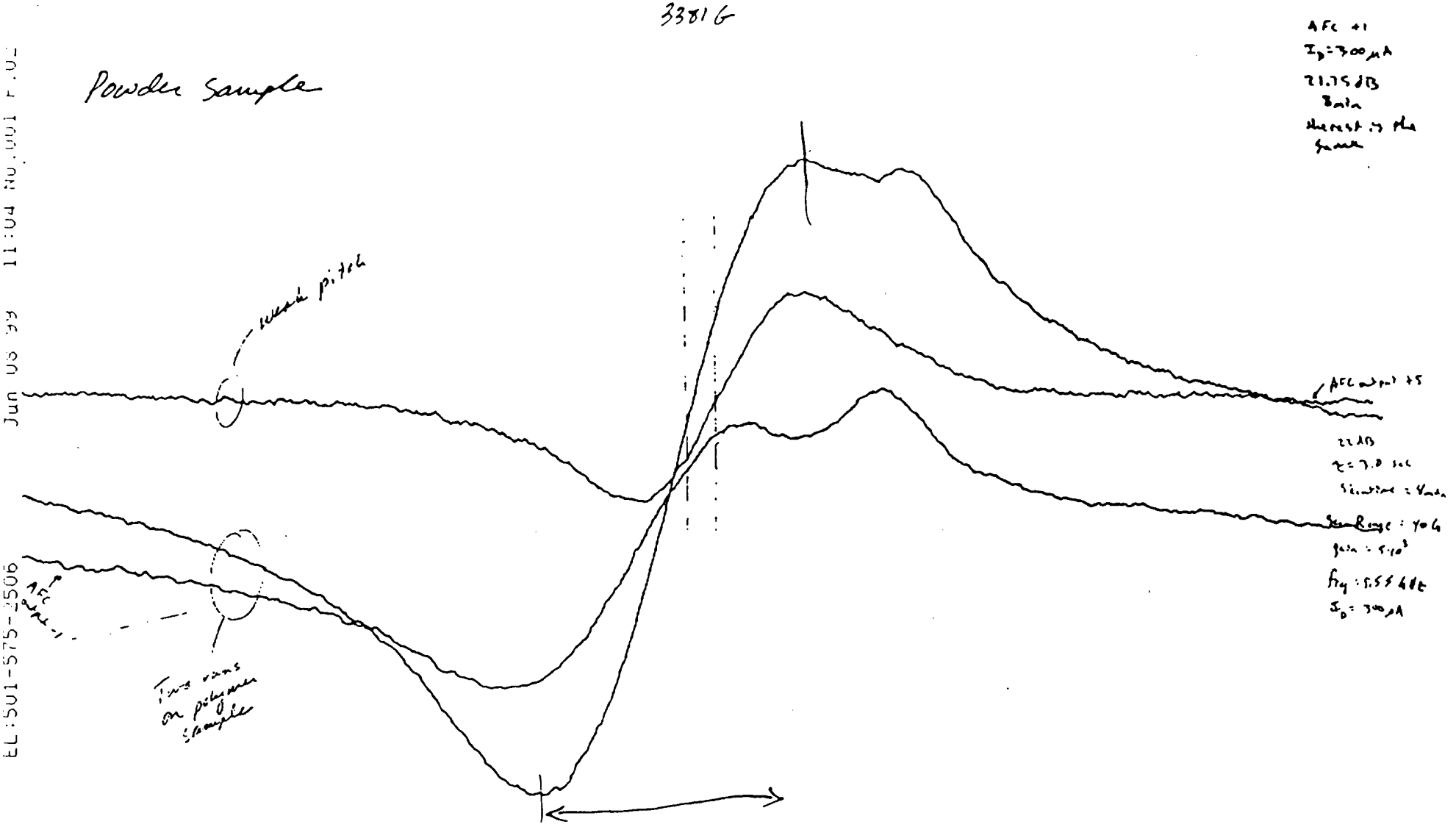

Figure 97
ESR of solid p-DAT
RT

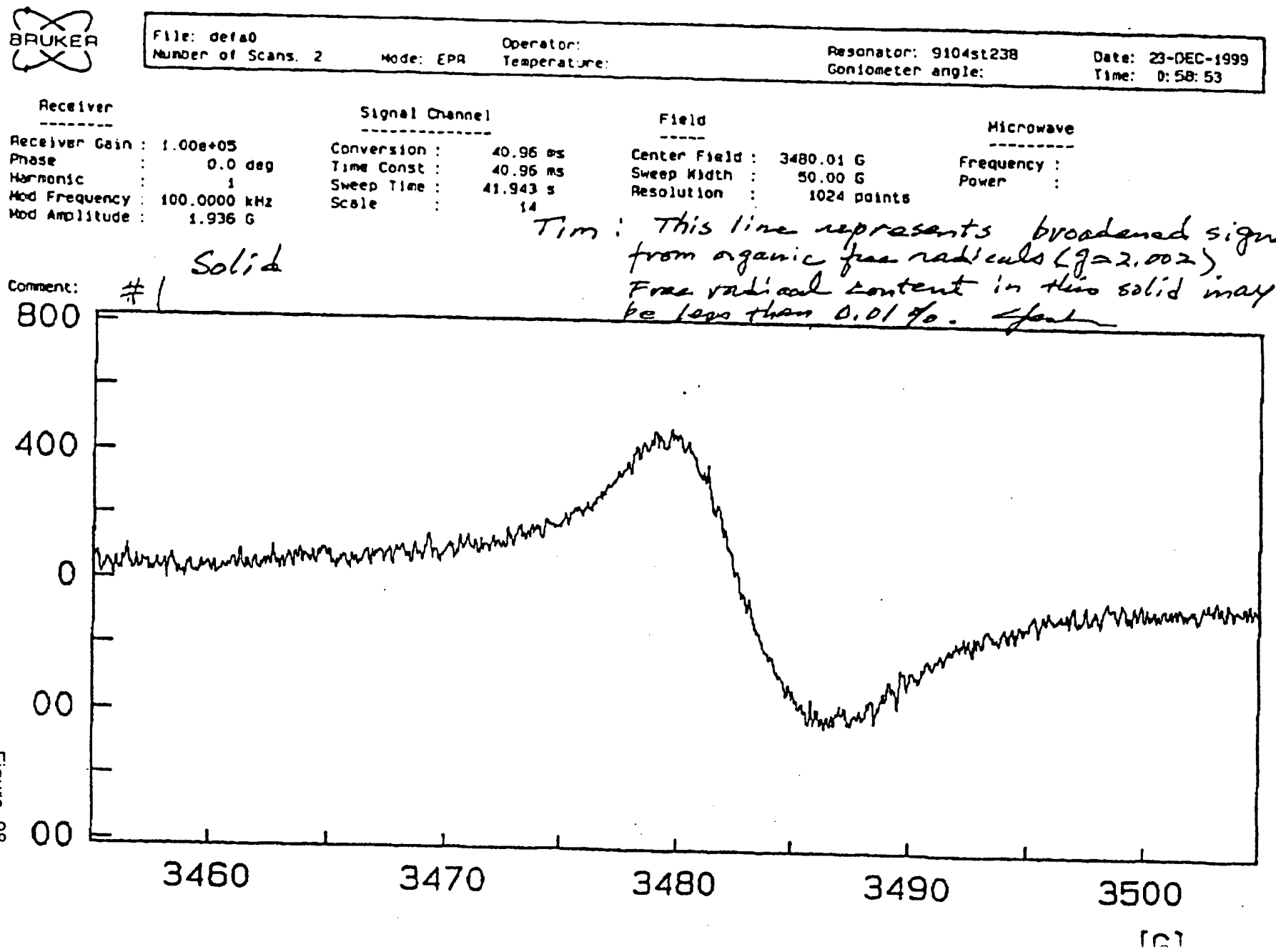

Figure 98
ESR of solid p-DAT
RT

WIN-EPR Acquisition

Date: 03/23/2000 Time: 14:00

FileName: C:\WINDOWS\epr data\oklahoma\032200\Spectrum4.par
Comment: p.dat, RT

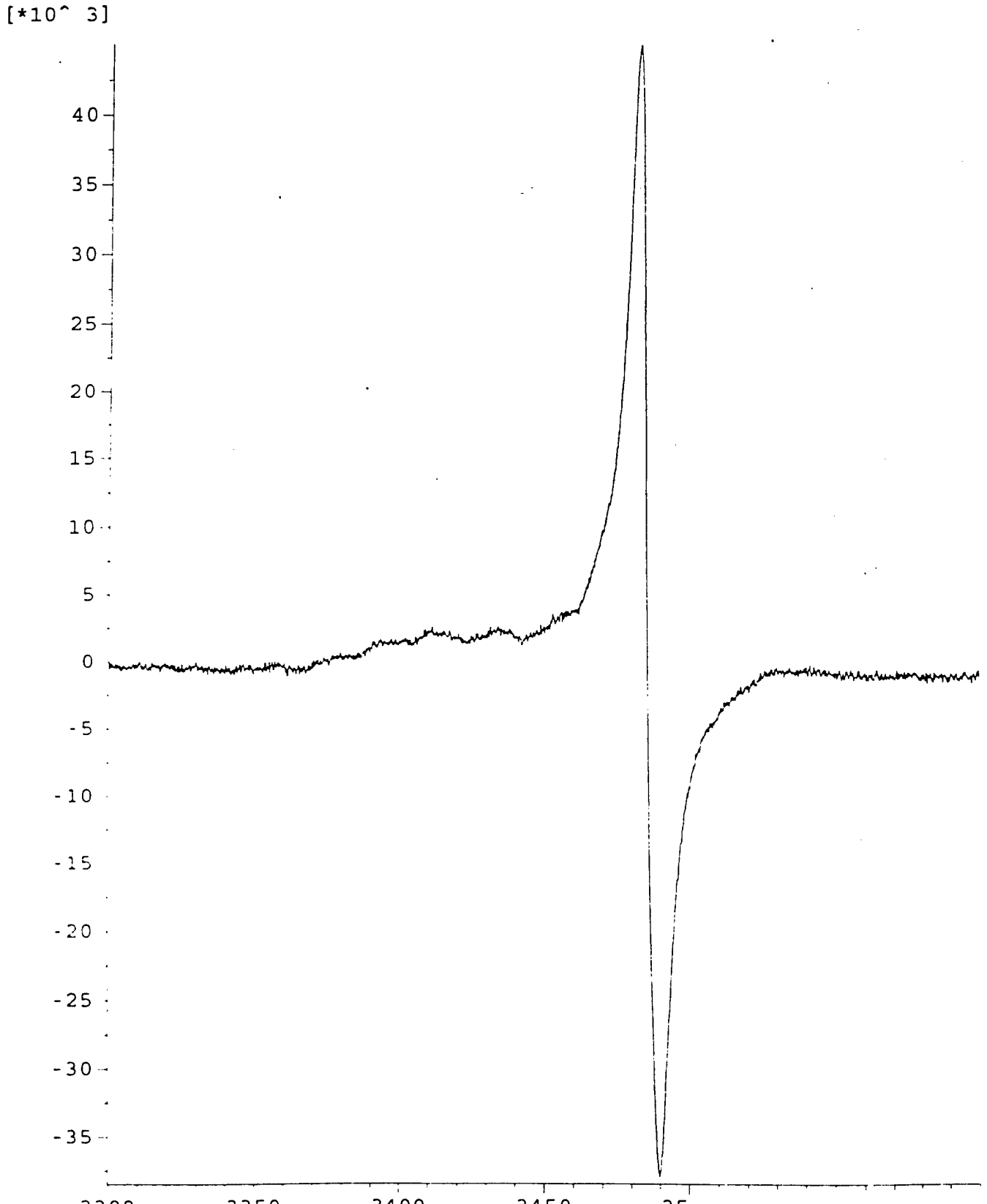

Figure 99
ESR of p-DAT solution
RT

WIN-EPR Acquisition

Date: 03/23/2000 Time: 14:06

FileName: C:\WINDOWS\epr data\oklahoma\032300\Spectrum5.par
Comment: p.dat, 77 K

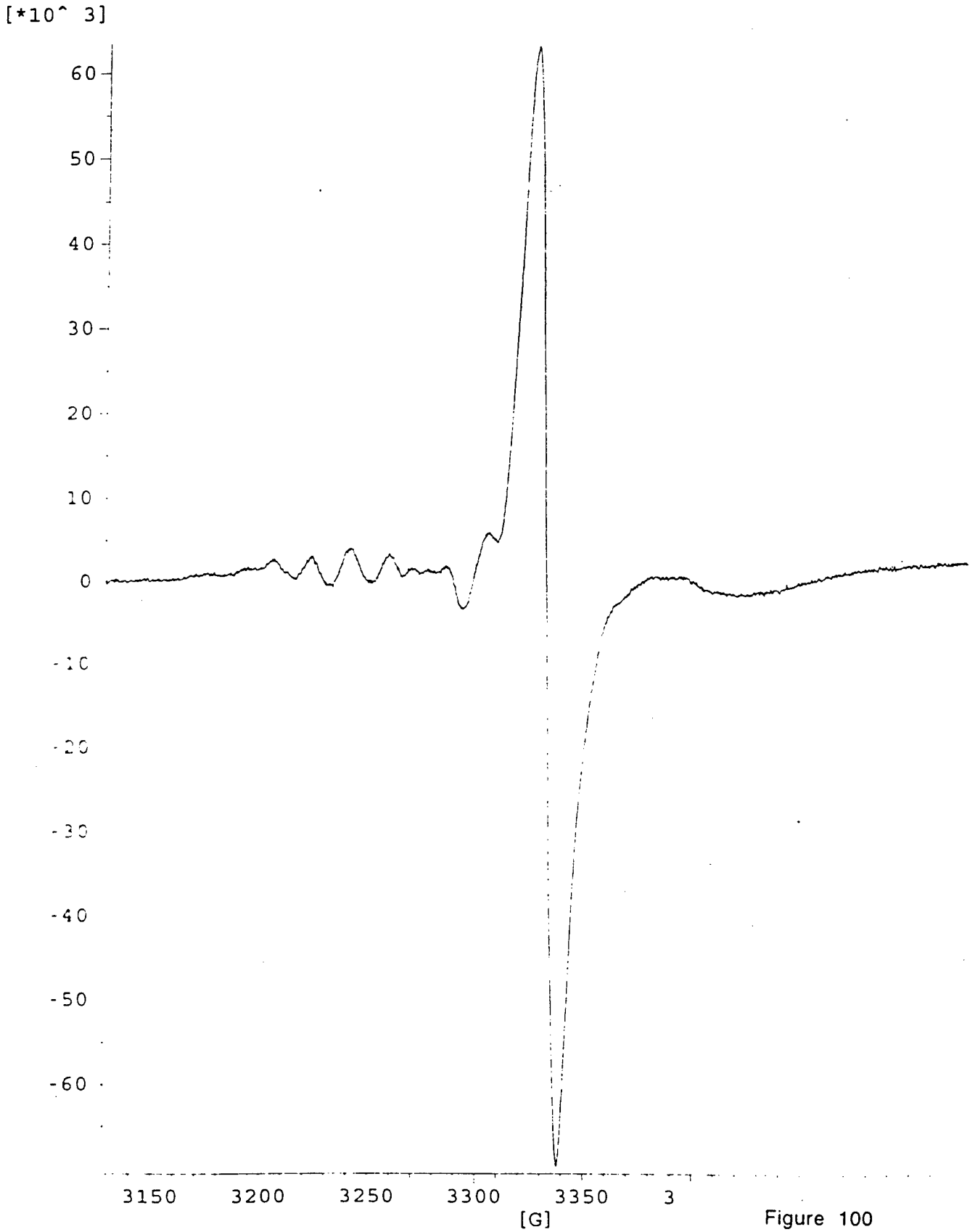

Figure 100
ESR of p-DAT solution
77 K

WIN-EPR Acquisition

Date: 03/24/2000 Time: 13:45

FileName: C:\WINDOWS\epr data\oklahoma\032200\Spectrum8.par
Comment: p.haha, RT

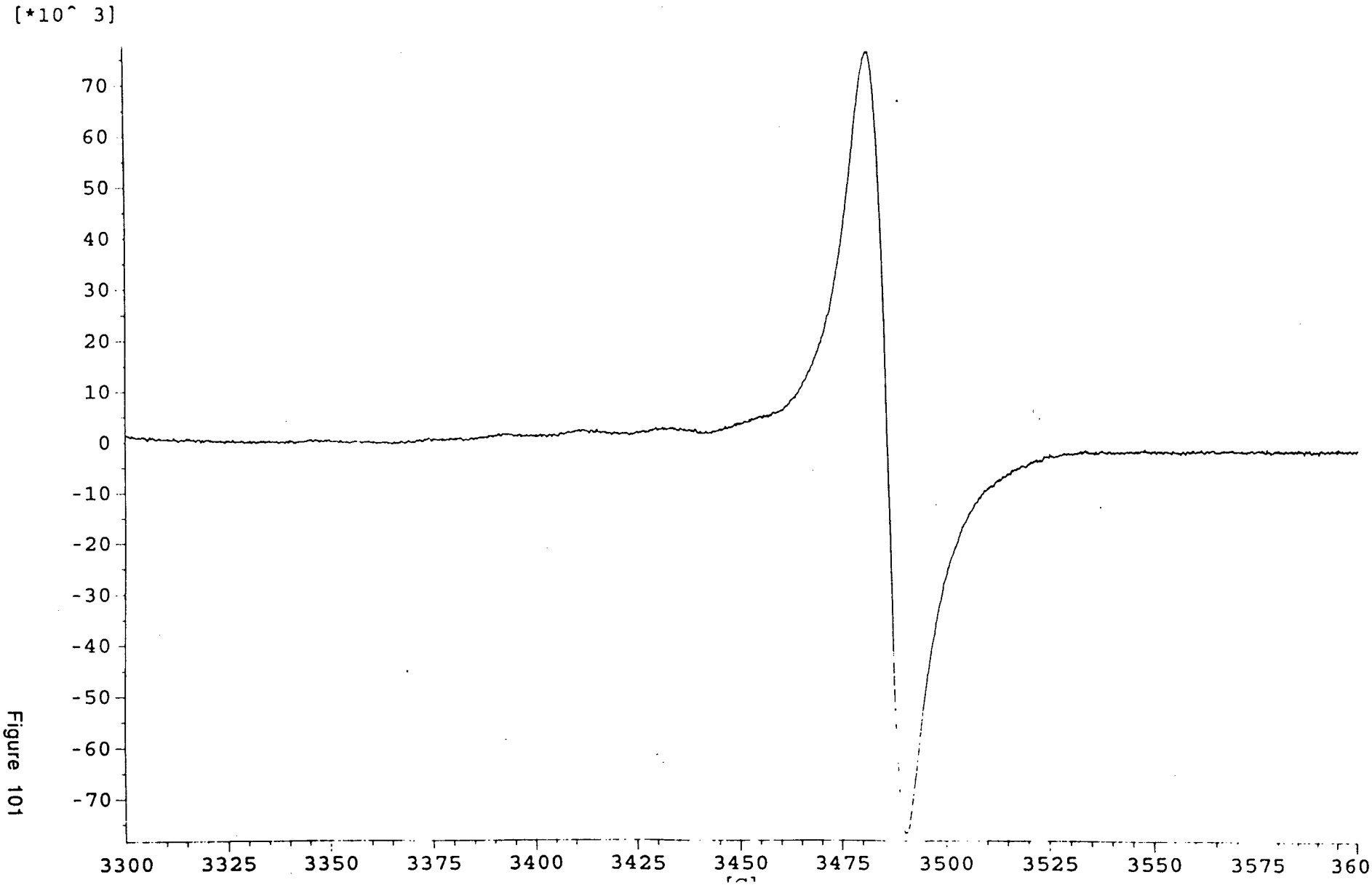

Figure 101
ESR of p-HAHA
RT

wIN-EPR Acquisition

Date: 03/24/2000 Time: 13:46

FileName: C:\WINDOWS\epr data\oklahoma\032200\Spectrum10.par
Comment: p.tyrosine, RT

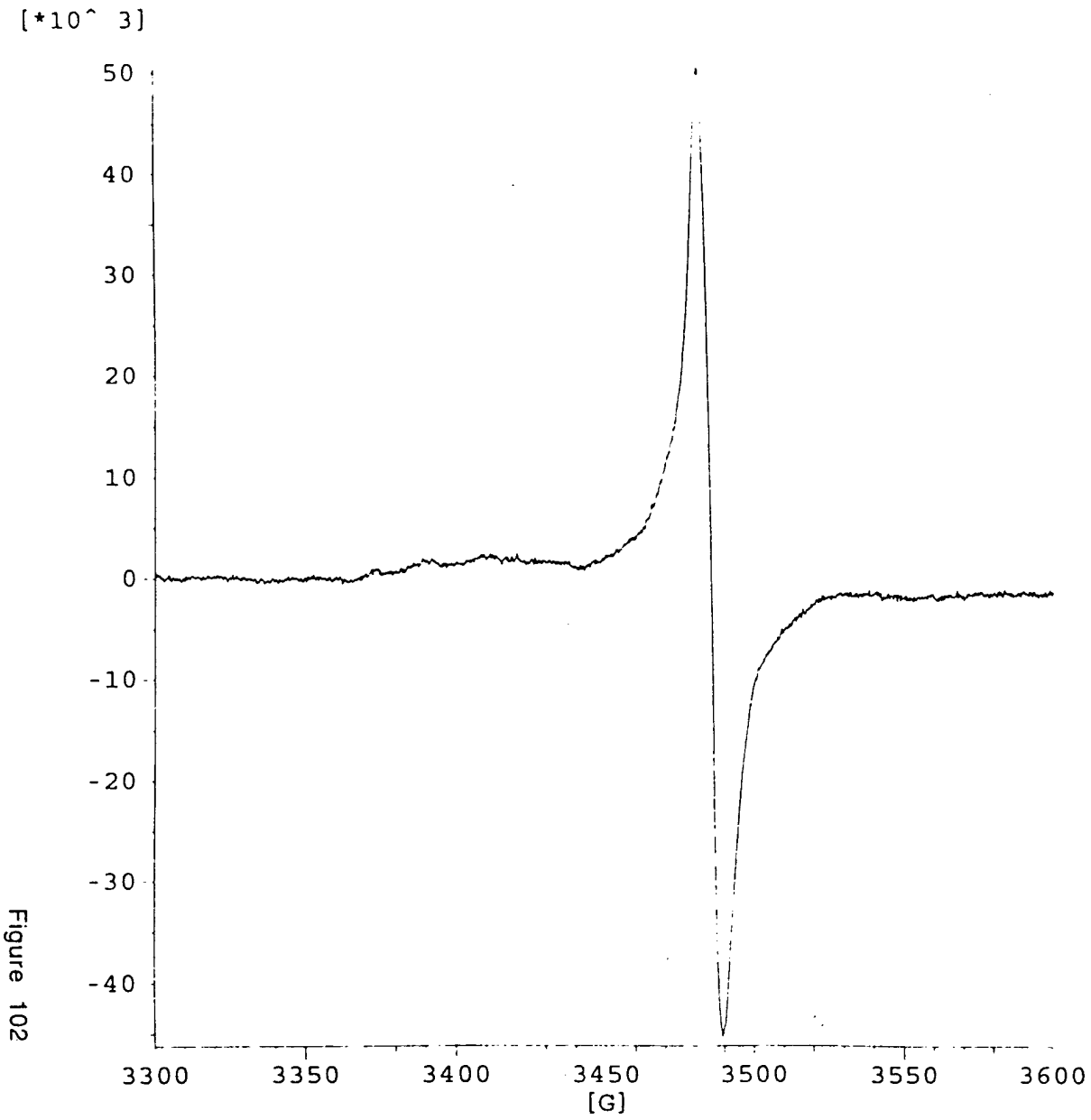

Figure 102
ESR of p-Tyr
Rt

Parameter List

Operator:	SM
Resonator:	c:\...\st8921.cal
Acqu. Date:	03/22/2000
# of Scans:	5

Field

Center Field:	3450.000 G
Sweep Width:	300.000 G
Resolution:	4096 points

Microwave

Frequency:	9.775 GHz
Power:	20.120 mW

Receiver

Receiver Gain:	7.96e+004
Phase:	0.00 deg
Harmonic:	1
Mod. Frequency:	100.00 kHz
Mod. Amplitude:	5.00 G

Signal Channel

Conversion:	40.960 ms
Time Constant:	81.920 ms
Sweep Time:	167.772 s